Laccase catalytic reaction chemistry in relation to enzymatic lignin modicatio

Perna, Valentina

Publication date:
2019

Document Version
Publisher's PDF, also known as Version of record

Laccase catalytic reaction chemistry in relation to enzymatic lignin modification

PhD student:

Valentina Perna

Supervisors:

Professor Anne S. Meyer
Assistant Professor Jane W. Agger

DTU Bioengineering
Department of Biotechnology and Biomedicine

Technical University of Denmark
Department of Biotechnology and Biomedicine
Center of Protein Chemistry and Enzyme Tecnology
Sølofts Plads, building 221,
2800 Kongens Lyngby, Denmark
valper@dtu.dk
www.bioengineering.dtu.dk

Preface

The work presented in this thesis has been conducted during my time as PhD student at the Technical University of Denmark starting at the Department of Chemical and Biochemical Engineering section of Bioprocess Engineering to finish at the Department of Biotechnology and Biomedicine section of Protein Chemistry and Enzyme Technology from December 2015 to May 2019. The project was funded by The Danish Council for Independent Research and by the PhD Program at the Chemical and Biochemical Engineering Department, DTU.

First of all I would like to thank my supervisor Professor Anne Meyer for her enthusiasm about my work, excellent feedbacks and for having always believed in me. A really important thank you goes also to my co-supervisor Assistant Professor Jane Agger who has also always believed me and supporting my ideas. She taught me that there is always the light at the end of the tunnel even in the darkest period. A thank you goes also to Jesper Holck for the interest shown in the project.

I would also to thank Assistant Professor Andreas Baum (DTU Compute) for introducing me to highly complex statistical analysis methods and the good times spent during discussion of the data. Likewise I would like to thank Professor Mogens L. Andersen (Department of Food Science, Copenhagen University) and PostDoc Line Munk for introducing me to Electron Paramagnetic Resonance Spectroscopy. My appreciation goes also to Professor Vincent Eijsink and Lindsay D. Eltis for providing me with LPMOs and bacterial laccase, respectively.

I want to thank all my colleagues at the Section of Protein Chemistry and Enzyme Technology but also to the one at the center of Bioprocess Engineering for sharing good moments together and for creating an enjoyable work environment. Finally I would like to thank Ludovica, Sinja and Sigyn for the good times and lovely moments spent together and to be patient about my poor social life of the last months, my family for being always with me even at long distance and to Sebastian for always supporting me and bringing love in my life.

Lyngby, 01-May-2019 Valentina Perna

Summary

Lignocellulosic biomass is a natural and abundant resource for energy and materials in biorefineries. Lignocellulose is composed typically of 15-30% of lignin, which is a hydrophobic biopolymer built of phenylpropanoid units that act as a waterproof, protective shield in plant cells. Lignin is the least exploited biomass component due to a high degree of polymerization and a complex structure, which makes its degradation difficult. Typically, lignin is burned for energy production in bioprocessing. However considering its complex structure and the fact that it is the only biopolymer exclusively composed of aromatic units, development of an efficient enzymatic processes should be exploited to produce other value-added compounds and thus contribute to valorization of lignin. Laccases have received lots of attention because they are thought to be able to degrade lignin due to their ability to oxidize phenolic compound using atmospheric oxygen as electron acceptor. Laccase modification of lignin has been studied for decades but the mechanisms remain unclear.

The core hypothesis behind this PhD work was to enhance the knowledge of the laccase reaction mechanism and develop new methods to understand the reaction chemistry on small soluble lignin subunits to then progress to laccase reaction on lignin itself.

Ganoderma lucidum laccase was shown in previous study to be able to enhance sugar release during lignocellulose degradation which makes *Ganoderma lucidum* laccase a good candidate for further characterization studies. The development of both an optimization of the recombinant production and of the purification were studied to yield a highly pure enzyme.

Two methods were developed to measure laccase activity and kinetics on small phenolic compounds related to lignin subunits. The methods used LC-MS analysis and Fourier Transform Infrared (FTIR) spectroscopy coupled to Parallel Factor (PARAFAC) analysis. LC-MS was used to measure kinetics on hydroxycinnamic acids and on a dimeric compound to study, first, the specificity of laccase towards the different lignin subunits and, second, the product profiles generated after laccase activation of the substrates. The FTIR-PARAFAC coupled method was used to assess potential differences in the reaction profile of laccases of different origins during

oxidation of different lignin subunits. Both methodologies enabled the development of activity assays on small soluble phenolic compounds and an understanding of the preferred laccase reaction mechanism on theses soluble compounds.

The kinetics of organosolv lignin was also studied by measuring the first product after laccase oxidation of lignin, namely radicals, using Electron Paramagnetic Resonance (EPR) spectroscopy. Laccase kinetic parameters on lignin were compared to the one of the soluble hydroxycinnametes to examine laccase specificity toward lignin. This method also made it possible to study the radical disappearance rate; during laccase oxidation of lignin, radicals were formed by laccase action but at the same time these radicals were quenched due to the highly unstable nature of radicals.

The fate of the radicals was also studied. The activation of oxygen from these radicals was studied by measuring the concentration of hydrogen peroxide during laccase oxidation of organosolv lignin and raw birch wood. The biological role of the laccase-induced hydrogen peroxide production was tested through activation of two lytic polysaccharide monooxygenases (LPMO) reactions, one of which was active on chitin and the other active on cellulose. Both LPMOs could be activated by the levels of hydrogen peroxide produced after laccase oxidation of lignin.

The results obtained in this work showed that a correlation between laccase activation of small soluble compounds cannot be directly translated into laccase action on lignin. Laccase reaction towards soluble substrates was found to be relatively fast and a clear laccase preference towards highly methoxylated compounds, i.e. sinapic acid, was found. Moreover the product profile after laccase oxidation of these soluble substrates was characterized by the presence of oligomeric compounds derived from the starting substrate. Reactions fingerprints, accounting for both substrate depletion and products formation during laccase oxidation of soluble phenolic compounds, were studied with FTIR and they appeared to be dependent on the laccase origin. Laccase kinetics on lignin were determined by measuring the semiquinone radicals formed during laccase oxidation. The radical propagation in lignin after laccase oxidation was slower than the one observed for the hydroxycinnamic acids and therefore possible to be measured. The observed radical formation was a sum of two reaction taking place at the same time, namely the radical formation after laccase oxidation and the spontaneous radical quenching. It appeared that hydrogen peroxide was one possible route for radical propagation of the radicals formed on lignin after laccase oxidation. Hydrogen peroxide formation was induced by laccases and the concentrations produced was high enough to activate lytic polysaccharide monooxygenases reactions, hence suggesting that one role of laccases in lignocellulose degradation could be the controlled formation of hydrogen peroxide in order to activate hydrogen peroxide-dependent enzymes like LPMOs or lignin peroxidases during the initial phase of degradation.

Dansk sammenfatning

Lignocelluloseholdig biomasse er en naturlig og hyppigt forekommende ressource til energi og materialer i biorefinering. Lignocellulose består typisk af 15-30% lignin, som er en hydrofob biopolymer bygget af phenylpropanoid enheder, der virker som et vandtæt beskyttende skjold i planteceller. Lignin er den mindst udnyttede biomassekomponent på grund af en høj grad af polymerisering og en kompleks struktur, hvilket gør dets nedbrydning vanskelig. Typisk brændes lignin til energiproduktion i bioprocessering. I betragtning af dets komplekse struktur og den kendsgerning, at den er den eneste biopolymer udelukkende sammensat af aromatiske enheder, bør der udvikles effektive enzymatiske processer til fremstilling af værdifulde komponenter og således bidrage til at øge værdien af lignin. Laccaser har fået stor opmærksomhed, fordi de menes at være i stand til at nedbryde lignin på grund af deres evne til at oxidere phenolforbindelse ved anvendelse af atmosfærisk oxygen som elektronacceptor. Laccase-modifikation af lignin er blevet undersøgt i årtier, men mekanismerne er stadig uklare.

Formålet med denne afhandling er at forbedre kendskabet til laccase-reaktionsmekanismen og udvikle nye metoder til at forstå kemien bag laccasereaktioner på små opløselige ligninunderenheder for derefter at overføre til laccase-reaktion på selve lignin.

Ganoderma lucidum laccase blev vist i tidligere undersøgelser for at kunne forbedre sukkerfrigivelsen under lignocellulose nedbrydning, hvilket gør *Ganoderma lucidum* laccase en god kandidat til yderligere karakteriseringsundersøgelser. Udviklingen af både en optimering af den rekombinante produktion og rensningen blev undersøgt for at give et meget rent enzym.

To metoder blev udviklet til at måle laccaseaktivitet og kinetik på små phenolforbindelser relateret til ligninunderenheder. Metoderne involverede LC-MS analyse og Fourier Transform Infrared (FTIR) spektroskopi koblet til Parallel Factor (PARAFAC) analyse. LC-MS blev brugt til at måle kinetik på både hydroxycinnamater og på en dimerforbindelse. Først blev specificiteten af laccase over for de forskellige ligningunderenheder bestemt, og derefter blev produktprofilerne for laccaseaktivering af disse substrater undersøgt. Den koblede FTIR-PARAFAC metode blev anvendt til at vurdere potentielle forskelle i reaktionsprofilen af laccaser af forskellig oprindel-

se ud fra deres evne til oxidation af forskellige ligninunderenheder. Begge metoder gjorde det muligt både at udvikle aktivitetsassays til at måle laccaseaktivitet på små opløselige phenoliske komponeneter, og at øge forståelsen for rekationsmekanismen, samt at identificere laccasernes foretrukne substrater.

Kinetikken af organosolv lignin blev også undersøgt ved at måle det første produkt efter laccaseoxidation af lignin, radikaler, ved anvendelse af elektronparamagnetisk resonans (EPR) spektroskopi. Kinetikparametrene for laccaserne på lignin blev sammenlignet med de parametre der blev bestemt ved reaktion med den ene af de opløselige hydroxycinnamater for at undersøge laccasernes specificitet mod lignin. Denne metode gjorde det også muligt at studere radikalernes henfaldssrate. Under laccaseoxidation af lignin blev radikaler dannet, men samtidig henfalder disse radikaler på grund af den meget ustabile karakter af radikaler.

Radikalernes videre skæbne blev også undersøgt. Aktivering af oxygen fra disse radikaler blev undersøgt ved at måle koncentrationen af hydrogenperoxid under laccaseoxidation af organosolv lignin og rå birketræ. Den biologiske rolle af den laccase-inducerede hydrogenperoxidproduktion blev testet ved aktivering af to lytiske polysaccharidmonooxygenaser (LPMO) reaktioner, hvoraf den ene var aktiv på chitin og den anden aktiv på cellulose. Begge enzymer kunne aktiveres af de koncentrationer af hydrogenperoxid der danens evd laccase reaktioner.

Resultaterne opnået i dette arbejde viste, at en korrelation mellem laccaseaktivering af små opløselige forbindelser ikke kan translateres direkte til laccase-virkning på lignin. Laccase-reaktion over for opløselige substrater viste sig at være relativt hurtig, og der blev fundet en klar laccasepræference mod højt methoxylerede forbindelser, dvs. synapinsyre. Endvidere blev produktprofilen efter laccaseoxidation af disse opløselige substrater karakteriseret ved tilstedeværelsen af polymeriserede forbindelser afledt fra udgangssubstratet. Finger printing ved brug af FTIR, der tager højde for både substratforbrug og produktdannelse i løbet af laccaseoxidation af opløselige phenoliske forbindelser, viste sig at være afhængig af, hvilken organisme laccasen oprindeligt kom fra.

Laccase kinetik på lignin blev bestemt ved at måle semiquinonradikalerne dannet under laccaseoxidation. Radikalers propagering i lignin efter laccaseoxidation var langsommere end den, der blev observeret for hydroxycinnaminsyrerne og var derfor mulig at måle. Den observerede radikaldannelse er en sum af to reaktioner, der finder sted på samme tid, nemlig radikaldannelse efter laccaseoxidation og spontan radikal quenching. Tilsyneladende er hydrogenperoxid en mulighed for propagering af de radikaler der dannes i lignin ved laccaseoxidation. Hydrogenperoxiddannelse blev induceret af laccaser, og de fremkomne koncentrationer var høje nok til at aktivere LPMO reaktioner, hvilket tyder på, at en mulig rolle for laccaser ved lignocellulose nedbrydning kunne være den kontrollerede dannelse af hydrogenperoxid til aktivering af hydrogenperoxidafhængige enzymer som LPMO'er eller ligninperoxidaser i den indledende fase af biomassenedbrydning.

List of Publications

This thesis has contributed to the production of four papers:

1. Perna, Valentina; Agger, Jane W.; Holck, Jesper; Meyer, Anne S. Multiple Reaction Monitoring for quantitative laccase kinetics by LC-MS. *Scientific Reports* **8**, 1 (2018).

2. Perna, Valentina; Baum, Andreas; Ernst, Heidi A.; Agger, Jane W.; Meyer, Anne S. Laccase activity measurement by FTIR spectral fingerprinting. *Enzyme and Microbial Technology* **122**, 64-73 (2019).

3. Perna, Valentina; Agger, Jane W.; Andersen, Mogens L.; Holck, Jesper; Meyer, Anne S. Laccase induced lignin radical formation kinetics evaluated by Electron Paramagnetic Resonance spectroscopy. *ACS Sustainable Chemistry & Engineering* (2019). **Under review.**

4. Perna, Valentina; Meyer, Anne S.; Holck, Jesper; Eijsink, Vincent; Agger, Jane W. Laccase oxidation of lignin induces production of H_2O_2. *Green Chemistry*. **Submitted May 2019.**

List of Abbreviations

CBP21	Chitin binding LPMO form *Serratia marcescens*
DP	Degree of polymerization
EPR	Electron Paramagnetic Resonance spectroscopy
FTIR	Fourier Transform Infrared spectroscopy
Gl	Laccase from *Ganoderma lucidum*
LMS	Laccase Mediator System
LPMO	Lytic polysaccharide monooxygenases
Mr	Laccase from *Meithermus ruber*
MRM	Multiple Reaction Monitoring
Mt	Laccase from *Myceliophthora thermophila*
NcLPMO9C	Cellulose binding LPMO form *Neurospora crassa*
PARAFAC	Parallel Factor analysis
PCA	Principal Component Analysis
Slac	Laccase from *Amycolatopsis* sp. 75iv2
Tv	Laccase from *Trametes versicolor*
Tvil	Laccase from *Trametes villosa*

Contents

Chapter 1

Aims and Hypothesis

The overall aim of this thesis was to investigate laccase catalysed reactions on lignin and lignin related compounds. Studying the catalytic reaction of lignin will help to illuminate the biological role of laccase in fungal degradation of lignocellulosic materials.

In order to address this aim three hypotheses were raised:

H1 Based on previous data *Ganoderma lucidum* laccase promotes reaction on lignin in a different way compared to other laccases, which are beneficial for lignocellulose degradation.

H2 Laccase kinetics on individual, soluble lignin building blocks provides information about the laccase specificity towards lignin subunits and whether this specificity and product profile is influenced by the origin of the laccases.

H3 Studying laccase kinetics on lignin provides new clues of the role of laccases during lignin processing in application and degradation in nature.

As follow up from hypothesis H3 a fourth hypothesis was raised:

H4 Laccase catalysed radical formation on lignin induces hydrogen peroxide formation, which is important in the overall redox reactions governing microbial lignocellulose degradation.

In order to test and verify these hypotheses the development of new methodologies become an objective for investigating the roles of laccases both on lignin related compounds and on genuine lignin structures. These methodologies increase understanding of laccase specificity towards

lignin and therefore address the possible role of laccase in delignification processes. Lignin makes up 15-30% of the total lignocellulosic materials. Lignin is the only natural biopolymer composed of aromatics and hence should be exploited to produce biobased products. Studying the laccase reaction mechanism on lignin subunits and lignin itself will give information about the biological role of laccase in nature and the potential role of this enzyme in lignin modification.

Chapter 2

Introduction

2.1 Biomass

Lignocellulosic biomass is mainly composed of three polymeric components, namely cellulose, hemicellulose and lignin. Cellulose and hemicellulose are mainly used in biorefinery, while lignin which constitutes 15-30% of the available carbon source is mainly burned to produce energy.[1,2]

2.1.1 Cellulose

Cellulose is a linear polymer composed by D-glucose monomers linked by β-1,4-glucosidic bonds with a degree of polymerization varying approximately from 500 to 14,000.[4,5] In the plant cell wall, cellulose is found in microfibrils (5-15 nm of diameter) (Figure 2.1). A microfibril consists in 36 cellulose chains with approximately 10,000 D-glucose molecules each.[6,7] Stabilization of the microfibril is achieved by the presence of inter- and intra-molecular hydrogens bonds capable of protecting the cellulose from microbial degradation and penetration by small molecules such as water.[6] The microfibril are built up into macrofibrils and then into fibers with the final scope to give rigidity to the plant cell wall.[8]

2.1.2 Hemicellulose

The cellulose microfibrils are boundles of cellulose chains, and the cellulose microfibrils are interwined between molecular chain of hemicellulose that are linked to lignin via crosslinking and

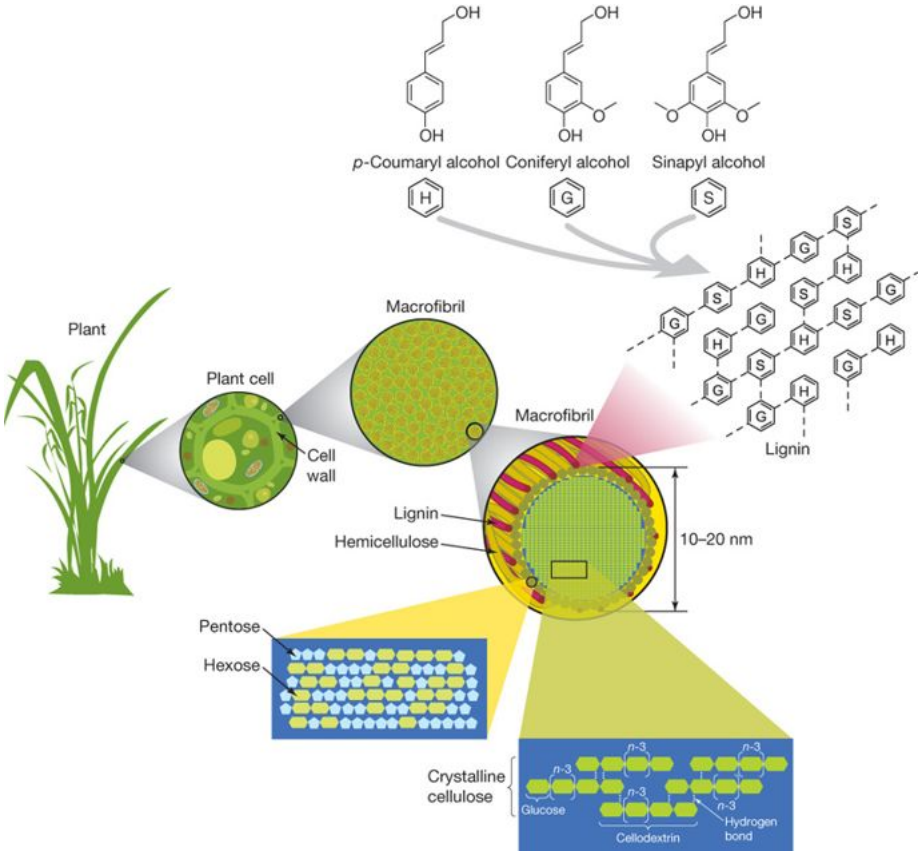

Figure 2.1: Lignocellulosic biomass scheme, adapted from Rubin.[3]

locks the cellulose microfibrils via streches of hydrogen bonding. Hemicellulose is thus bound to cellulose by inter-chain hydrogen bonding and to other hemicelluloses by covalent and hydrogen bonds.[9] Hemicellulose, in contrast to cellulose, is a heterogeneous branched polysaccharide composed mainly by hexoses, D-glucose, D-mannose and D-galactose and pentoses, D-xylose and L-arabinose[10] (Figure 2.1). Hemicellulose is also linked to lignin to form lignin carbohydrate complexes (LCCs).[11–13]

2.1.3 Lignin

Lignin is found in all vascular plants and is involved in essential plant functions, such as water transportation, mechanical strength and defense against pathogens.[14,15] Lignin is a heterogeneous polymer built of three phenylpropanoid precursors (Figure 2.1) known as guaiacyl (G), syringyl (S), and *p*-hydroxyphenyl (H), which are obtained from the coniferyl, sinapyl and *p*-coumaryl alcohol precursors, respectively. The three alcohols are synthetized by the plant, and subsequently activated through the formation of a phenoxy radical by wall-bound peroxidases and hydrogen peroxide.[15,16] Since the phenylpropanoid precursor is a conjugated system, the radical is stabilized by electron delocalization which lead to different activation sites, which

again leads to the formation of a highly complex macromolecule with different linkages.[15,16] The plant origin and growth conditions have an influence on the composition of lignin. The exact composition of lignin may even vary in different cells within the same plant.[17]

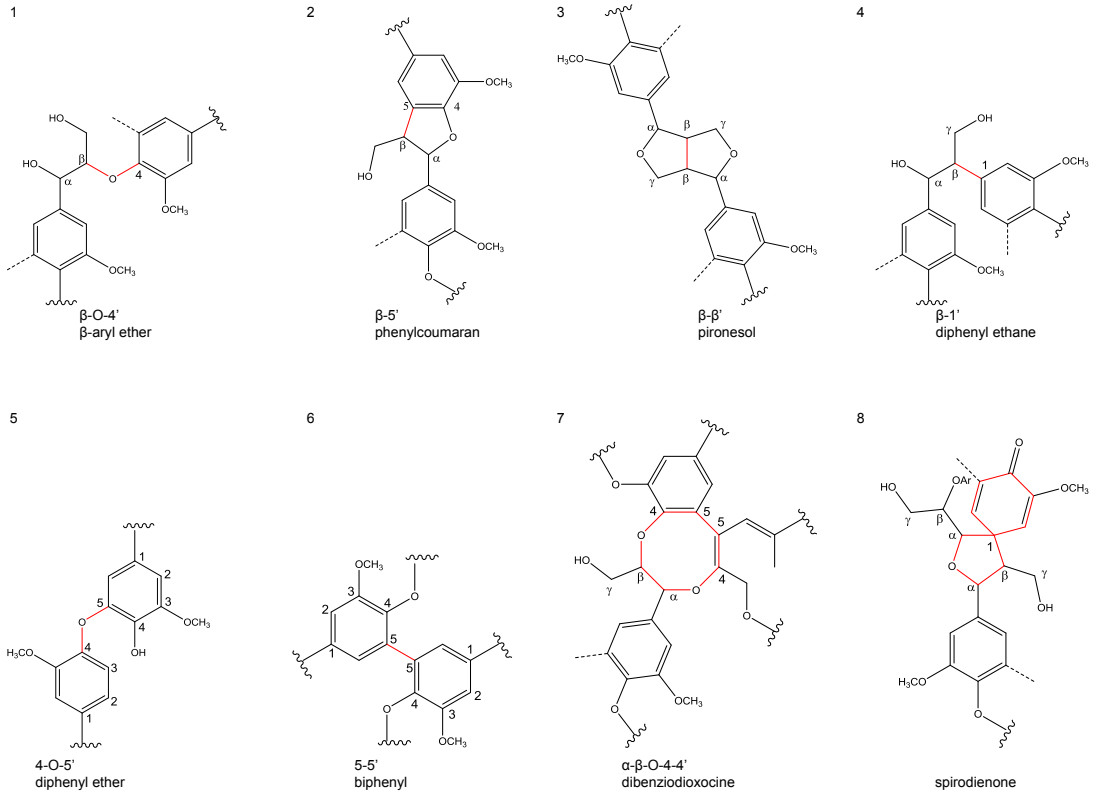

Figure 2.2: Inter-unit linkages in the lignin molecule. The inter-unit linkages formed are highlighted in red.

Lignins are defined according to the ratio between the monomeric units H, G and S.[18] Hardwood (angiosperm - dicot) lignins are mainly composed of G and S units in approximately the same amount, while softwood (gymnosperm) lignins are composed of G units with minor amounts of H units.[19] The presence of S units in hardwood lignin results in a more linear lignin structure compared to softwood lignin.[19] Grass (angiosperm - monocot) lignins contain all three units but the ratio between these varies within the group.[20,21]

Radical propagation in the complex lignin macromolecule formation gives rise to different types of bonds. The most abundant bond is ether β-O-4' (Figure 2.2 1), which is found in all types of lignin (grass, softwood and hardwood) and constitutes 50% of the entire linkages in the lignin molecule.[21,22] The most favorable coupling is in the β position, and therefore other possible types of β-couplings are β-5', β-β' and β-1' (Figure 2.2 2, 3 and 4).[23] Oligomer coupling, i.e. monolignol molecule coupling to an initially formed dimer, may also result in other linkages, such as 4-O-5' and 5-5', which also lead to the branching of lignin (Figure 2.2 5 and 6).[15,23] New types of linkages have been recently discovered, such as spirodienone that is related to

β-1' bonds and dibensodioxocine obtained from 5-5' unit coupled to a third phenylpropanoid monomer (Figure 2.2 7 and 8).[24] Another common linkage type is the C-C bond. When the C-C bond is present in high numbers compared to the ether bonds, lignin is defined as condensed, and is therefore less prone to degradation and more rigid. The C-C bond requires 125-127 kcal/kmol of energy to be broken compared to the ether bond β-O-4' which requires 54-72 kcal/kmol.[25]

The most abundant functional group present in lignin is the hydroxyl group which is found present as phenolic hydroxyl or aliphatic hydroxyl. The phenolic hydroxyl group is the most reactive and comprises 0.2-1 mmol of free hydroxyl per gram of lignin, while the aliphatic hydroxyl group comprises 4 mmol per gram of lignin, corresponding to 80-90% of the subunits in lignin.[26–29] Other types of functional group less frequently present in lignin are carbonyl and methoxy groups.[26]

2.1.3.1 Processed lignin

During separation and physical-chemical processing of biomass, lignin undergoes structural modifications that result in so called technical lignin with different properties from native lignin. Typical technical lignins are by-products from the pulp and paper industry (accounting for 85% of total lignin production)[30,31] and the biorefinery sector, and lignin is currently mainly used to generate energy by incineration. In the pulping process lignin is depolymerized by breakage of the β-O-4' bonds and different types of lignin are obtained kraft lignin, soda lignin, organosolv lignin and lignosulphonate depending on the type of process used.[30] Both kraft lignin and lignosulphonate have high ash and sulphur content which limits the applicability of these lignins, especially for polymer production and fuel blends.[30] On the contrary soda lignin is sulphur free and leaves lignin with a more native structure compared to kraft lignin and lignosulphonate.[30] Organosolv lignin is obtained by separation through solubilization in an organic solvent system, which leads to a less modified lignin, primarily by maintaining β-O-4' bonds in a more intact state.[30] Since all these types of lignin are only by-products and since lignin is the only biopolymer exclusively composed of aromatic units,[2] it should be exploited to produce other value-added compounds, such as chemicals or materials, and thus contribute to developelopment of an overall more efficient process. Technical lignins can exhibit a high degree of condensation due to extensive cleavage of the β-O-4' bonds to obtain a structure more resistant to degradation than native lignin. Therefore, nowadays a new way of thinking is emerging in biomass fractionation, where the focus is to separate lignin first in order to maintain its native structure and the possibilities for exploiting its native chemical properties.[32]

2.2 Fungal enzymatic degradation of biomass

Fungi are the most efficient lignin degraders in nature. Wood degrading fungi colonize dead (and sometimes also living) tree trunks by degrading or modifying the lignocellulose due to extracellular hydrolytic and oxidative enzymes (CAZymes), i.e. cellulolytic, hemicellulolytic and lignin degrading enzymes.[33,34] Degradation and modification is not achieved in the same way by all the different wood degrading fungi, and hence these fungi have traditionally been divided into three groups: white-rot, brown-rot and soft-rot fungi.

Soft-rot ascomycetes attack soft wood to leave a soft, brown residue.[34,35] Soft-rot fungi are able to produce a full range of cellulolytic enzymes, while lignin degradation is not so extensive as that of white-rot fungi because soft-rot fungi are thought to secrete oxidative enzymes to a losser extent than white-rot fungi.[36]

Brown-rot basidiomycetes degrade cellulose and hemicellulose while partially degrading lignin[34] using a combination of enzymatic and non-enzymatic processes, the latter known as the chelator-mediated Fenton system.[37,38] The non-enzymatic processes are needed to degrade lignin because brown-rots fungi do not produce peroxidases. The degradation product has a dark brown color and tends to crack into cubical pieces.[34]

White-rot basidiomycetes are considered to be superior in lignin degradation due to their ability to completely mineralize lignocellulosic material to CO_2 and H_2O and leave a very light almost white, fibrous residue.[34,35,39] Lignin degradation is achieved by the action of a number of oxidoreductases (EC 1), such as lignin peroxidase (EC 1.11.1.14, AA2; Auxiliary Activity[40]), manganese dependent peroxidase (EC 1.11.1.13, AA2) and versatile peroxidase (EC 1.11.1.16, AA2). Laccases (EC 1.10.3.2, AA1) are also thought to participate in lignin degradation. These enzymes non specifically oxidize lignin subunits to produce radicals which shuttle within the large lignin molecule, increasing chemical instability and thus inducing bond cleavage.[41,42] Peroxidases are heme-containing enzymes which oxidize lignin using H_2O_2. Their redox potential is high enough to oxidize non-phenolic units in lignin. Laccases are copper-containing enzymes which use O_2 instead of H_2O_2 to catalyze the oxidation of lignin (further details in Section 2.3). The redox potential of laccase is lower than that of peroxidases and therefore laccase can only attack phenolic lignin subunits (Section 2.3.2). Small molecular weight mediators and other accessory enzymes are also needed for lignin degradation.[33] Among the accessory enzymes are aryl-alcohol oxidases (AA3), glyoxal oxidase and pyranose oxidase (AA3) which enhance the process through peroxide production.[43,44] Even though characterizations of the catalytic properties of single enzymes have been performed, the mechanism for lignin degradation is still not fully understood. Studies have shown that fungi secrete the enzymes in different phases of growth.[45–48] Zhou *et al.*[45] investigated how the enzyme expression varies during the different growth phases of the white-rot basidiomycete *Ganoderma lucidum*. Laccases and peroxidases are the first enzymes to be expressed by the fungus, which means that lignin degradation starts during mycelial growth, i.e. the initial phase of growth.[45–48] Afterwards expression of these enzymes is down regulated and hemicellulases and cellulases are secreted during growth of the

fruit body.[45]

A recent study[49] has suggested that the fungal classification should be changed by introducing a forth class "grey-rot". This proposal arose after 33 fungal genome of brown and white-rot fungi were sequenced and some brown-rot classified fungi were discover to follow a delignification process closer to that of white-rot fungi even in the absence of expressed peroxidases.

2.3 Laccases

Laccase (benzenediol: oxygen oxidoreductases; EC 1.10.3.2; AA1) enzymes are widespread in numerous organisms, such as fungi, plant, bacteria and humans and they belong to the blue multicopper oxidase family.[50–53] Laccases are able to catalyze the oxidation of phenolic compounds using O_2 as final electron acceptor instead of H_2O_2 as used by lignin peroxidases.[52] Therefore laccases are more industrially applicable enzymes because oxygen is freely available in nature. Particular attention has been given to laccase from white-rot basidiomycetes, which are suspected to play a role in lignin degradation[54] even though, as mentioned in Section 2.2, the mechanism of lignin depolymerization is not yet fully understood.

2.3.1 Laccase structure

Fungal laccases are characterized by an amino-acid chain of 520-560 units that correspond to a molecular weight of 60-70 kDa.[52] Fungal laccases are known as blue multicopper oxidase because their active site contains four copper ions. These copper ions are classified in three groups according to their spectroscopic features: type 1 Cu (T1) or blue copper, type 2 Cu (T2) or 'normal' copper, and type 3 Cu (T3) which consists of a pair of antiferromagnetically coupled copper ions (T3αCu and T3βCu)[52] (Figure 2.3). The T1 site is located in a shallow cleft on the surface of the enzyme, whereas the T2 and T3 sites are situated centrally at the interface between two of the structural domains close to each other that form a trinuclear cluster (T2/T3).[52,55] The substrates are consecutively oxidized, i.e. one electron at the time, at the T1 site (Figure 2.3) and the four electrons needed for the reduction of oxygen to water are shuttled to the T2/T3 site along a pathway containing histidine and cysteine residues.

2.3.2 Laccase catalytic cycle

Laccase catalyzes the oxidation of four molecules of phenolic compounds, with the simultaneous reduction of one mole of O_2 to two moles of H_2O (Figure 2.3).[52] The copper T1 is the site responsible of the oxidation of one electron at a time, which is then shuttled intermolecularly to the T2/T3 cluster.[52] In the fully oxidized state, all four copper ions are in oxidation state +2 and bind two OH^- groups (Figure 2.4a); when the four electrons oxidation occurs the laccase is in a

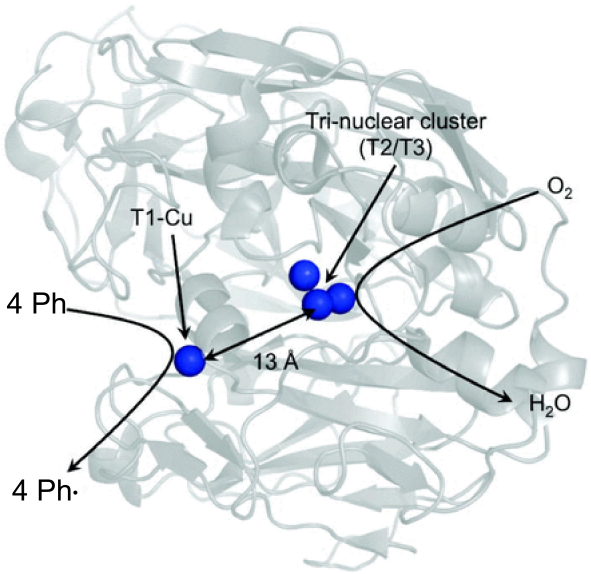

Figure 2.3: *Trametes versicolor* laccase structure. Laccase phenol oxidation is shown. Adapted from Chakraborty and Barton[56].

reduced state with all four copper ions in the +1 state (Figure 2.4b). The amino acids residues positioned close to the catalytic site play an important role in assisting the flow of protons needed for the catalytic reaction.[57] Thus the glutamate residues needs to be protonated while the aspartate residue is deprotonated, which is possible due to the differences in pKa values of the two residues (pKa for aspartate is lower than that of glutamate).[52] At this point the laccase is able to accept O_2 which binds to form a peroxide intermediate (Figure 2.4c). As soon as the fourth electron is transferred from the T1 to the trinuclear site, T1 site returns to its oxidized state, and T2 site loses the strong bond to the peroxide intermediate to form an intermediate + e^- (Figure 2.4d). The glutamate residue positioned at the catalytic site transfers a proton to the peroxide intermediate at the same time another proton is transferred from the water bond at the T2 site to the aspartate residue. The latter transfer reduces the redox potential of the T2 copper site and facilitates a final electron transfer to the peroxide intermediate, which results in a O-O bond cleavage and a fully oxidized native intermediate (Figure 2.4e). When the native intermediate is formed, it can either (1) return to its fully reduced state by accepting four H^+ with the release of two moles of water (Figure 2.4 e->b) or (2) return to its fully oxidized state by accepting two H^+ with the release of one mole of water (Figure 2.4 e->a).[52] Generally, laccase follows the red arrows pathway of Figure 2.4 but will return in its fully oxidized state if there is not enough phenolic substrate.[52,57]

The difference in redox potential between the laccase T1 copper site and the substrate determines the electron transfer rate and is also the reaction rate limiting step.[58,59] The fungal laccase redox potential ranges from $E^0 = 0.44$ V to $E^0 = 0.79$ V vs. Normal Hydrogen Electrode (NHE), depending on the type of fungal origin.[52] Phenols have a redox potential ranging from $E^0 = 0.5$ V to $E^0 = 1$ V vs. NHE depending on both the phenol substitution and the conjugated system.[55,60,61] Laccases reported to have the highest redox potential are those from

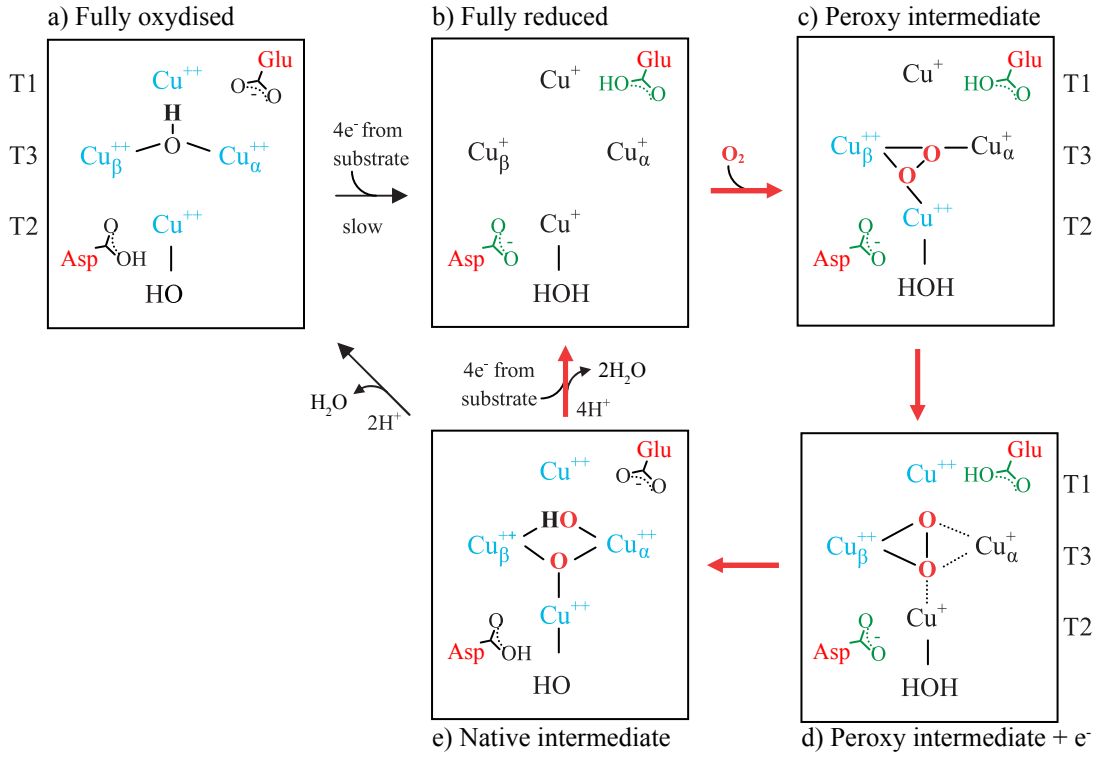

Figure 2.4: Laccase catalytic cycle adapted from Sitarz *et al.*[52] The actual catalytic cycle is shown by the red arrows while the black ones indicate the steps which are not directly part of the catalytic cycle.

white-rot fungi (up to $E^0 = 0.79$ V vs. NHE)[52] and therefore these enzymes show a broader catalytic activity towards phenolics, especially those with high redox potential. High redox potential laccases are not able to oxidize the hydroxyl groups present on the aliphatic chain due to the higher redox potential ($E^0 > 1.3$ V vs. NHE).[62]

Laccase oxidation is influenced by pH because pH can affect both the redox potential of the copper T1 site and the intramolecular transfer of the electron to T2/T3 copper sites, due to the involvement of amino acids in the catalytic cycle.[63] Increasing the pH will decrease the redox potential of the phenolic substrate compared to that of the T1 copper site, which favors the electron rate transfer resulting in a faster reaction. But an increase in pH will also inhibit intramolecular electron transfer from the T1 to the T2/T3 sites due to hydroxide anion binding to the T2/T3 copper ions, which impedes the catalytic cycle.[64]

2.3.3 The role of laccase in lignin depolymerization

The effect of laccase on lignin depolymerization has been studied for many years but is still not completely understood. The action of laccase on lignin will give rise to abstraction of an electron

from a phenolic subunit and lead to formation of a phenoxy radical which make the lignin surface highly unstable.[65] The highly conjugated system found in lignin will stabilize the radicals and result, possibly, in changes in the functional groups, acetylation and demethylation.[66,67] Lignin activation can also result in either grafting of the surface, i.e. low molecular compounds are coupled onto the lignin surface due to a radical-radical coupling reaction, or polymerization.[54,68] While polymerization will increase the average molecular weight of lignin, grafting will result in changes in lignin properties, such as solubilization, or in other physical or chemical properties of the polymer.[54,69]

The ability of laccases to depolymerize lignin has been addressed in many studies, but the indirect estimations sometimes performed led to misleading interpretations. For example studies have shown[70–72] that laccase addition during enzymatic hydrolysis of biomass boosted sugar release. The higher sugar yield measured in these studies[70–72] could be caused by other factors than lignin depolymerization. Laccases may act on potentially inhibitory components of the hydrolytic enzyme, or may interact with the lignin surface and avoid adhesion of cellulolytic enzymes, and both these actions may increase the amount of active hydrolytic enzyme and the sugar yields.[54,73,74] Another example of indirect lignin depolymerization assessment is when laccase was coupled to a mediator in a laccase mediator system (LMS).[75–78] Laccase will oxidize the mediator and the latter will then oxidize the aliphatic subunits present in lignin due to the formation of other radical intermediates.[54] A recent study[79] reported the decrease in molecular weight of a bacterial laccase treated lignocellulosic biomass, indicating lignin bond cleavage. Therefore the possibility that lignin depolymerization by laccase activation could eventually take place cannot be excluded.

2.3.4 Use of laccases in industry

Laccases are receiving industrial attention due to their ability to oxidize soluble phenols using oxygen as final acceptor (Section 2.3.2). This make laccases the perfect candidate for industrial processes. Some of the fields in which laccases could find application are: the food industry, pulp and paper industry, textile industry, nanobiotechnology, cosmetics, synthetic chemistry and soil bioremediation.[80,81]

In the food industry laccase can be used in beer and wine stabilization.[82] Laccases can also be used in the baking field because they are capable of cross-linking biopolymers.[81,83]

In the paper and pulp industry laccases are used in delignification processes. Due to the low laccase redox potential, certain LMS' for bio-bleaching have been developed for wood-pulp[84] but not many have been involved in non-wood pulp used for special papers.[81] Moreover, the ability of laccases to form radicals can be exploited to target the modification of wood fibers for biocomposite production.[81]

In the textile industry laccases are applied in processes related to decolorization of dyes and

textile bleaching.[81]

In nanobiotechnology the ability of laccases to catalyze electron transfer reactions without additional cofactors is used to develop biosensor to detect for example various phenolic compounds, oxygen or azides.[81,85]

Due to high substrate specificity laccases are starting to be used in bioremediation of soil contaminated with polycyclic aromatic hydrocarbons (PAHs) and TNT,[86,87] but also in synthetic chemistry[88] and in cosmetics where laccases are replacing H_2O_2 as oxidizing agents in hair-dyes to give less irritating and easy to handle products.[81,89]

2.4 Expression methods

The industrial attention received by laccases requires the development of some expression systems able to produce laccase at high yields. Different expression methods can be used depending on the application field in which laccases will be used. One approach to obtain active enzymes is by production in a native host.[90] However, fungal strains usually produce different laccase isoforms with similar chemo-physical properties, which leads to difficulties in the purification of single proteins.[91] Laccase production via heterologous expression systems may be another way to increase production yields and simplify the purification steps. If the expression in the native host is not trivial or if the application field, for example the food industry, does not allow enzyme production in the native host, heterologous expression systems can be used. Fungal laccases are expressed in yeasts such as *Pichia pastoris* and *Saccharomices cerevisae*, filamentous fungi such as *Aspergillus* species and *Trichoderma reesei*, plants[80] and recently also bacteria.[92] Bacterial laccases are also receiving important attention because they are more easly expressed compared to fungal laccases. Bacterial laccases are recombinantly expressed in *Escherichia coli* as host microorganism.[80]

In this work it was decided to produce one specific white-rot basidiomycete laccase from *Ganoderma lucidum* recombinantly in *Pichia pastoris*. *Ganoderma lucidum* laccase has been characterized in my research group along with laccases from other basidiomycetes, *Polyporus brumalis*, *Polyporus ciliatus* and *Trametes versicolor*.[93] Sitarz *et al.*[93] showed that by growing the four fungi on a minimal medium supplemented with lignocellulose from sugar cane bagasse, *Ganoderma lucidum* showed the highest laccase activity among the fungal strains tested. Moreover, an increase in sugar release yield was observed by adding the laccase-enriched *Ganoderma lucidum* broth to lignocellulosic biomass along with Cellic^{TM}CTec1.[93] This unique behavior makes *Ganoderma lucidum* laccase a good candidate for further characterization.

2.5 Laccase activity assay

In order to study an enzyme it is important to asses and determine its activity on specific substrates. Yet such activity determination becomes a challenge as far as laccases are concerned. The insolubility and complexity of lignin leads to the necessity of finding substitute soluble substrates to determine laccase activity. The most common way of studying laccase activity is by spectrophotometric methods which assess laccase oxidation of soluble chemical compounds, such as syringaldazine (4-hydroxy-3,5-dimethoxy-benzaldehyde azine), ABTS (2,2'-azino-bis(3-ethylbenzothiazoline-6-sulphonic acid)) and guaicol.[94,95] Laccase oxidation of ABTS is measured at 420 nm and is based on one electron oxidation that results in development of a blue color. The chemical structure of ABTS could allow a second oxidation, but it is not yet completely understood whether laccases are able to catalyze the abstraction of this second electron.[96] Laccase oxidation of syringaldazine causes oxidation of two electrons per substrate molecule in order to produce the quinone characterized by a pink color measurable at 530 nm.[97] Laccase oxidation of guaicol forms a dimeric quinone (3,3'-dimethoxy-4,4'-biphenoquinone) because of the reaction between two phenoxy radicals, and this coupling reaction gives rise to an amber colored product measurable at 470 nm.[98] Oxidized ABTS is labile towards external oxidizing agents, i.e. light, and the oxidized syringaldazine product tends to precipitate even at low concentrations[99]; these drawbacks have given rise to misinterpretations of laccase activity in such assays. So though these assays can be used to screen laccase activity, they resemble lignin poorly and hence a direct estimation of laccase activity on lignin cannot be performed. In contrast, determination of laccase activity on guaiacol resembles the natural activity of the enzyme on the guaiacol units in lignin, but due to its toxicity even guaiacol is not the best substrate for determination of laccase activity.

Chapter 3

Recombinant production and purification of *Ganoderma lucidum* laccase

This chapter focuses on the production and purification of *Ganoderma lucidum* (Gl) laccase and it addresses the following hypothesis and objectives:

H1 Based on previous data *Ganoderma lucidum* laccase promotes reaction on lignin in a different way compared to other laccases, which are beneficial for lignocellulose degradation.

Obj1 To develop an optimized fermentation protocol to enhance Gl laccase expression and an optimized purification protocol to obtain a highly pure Gl laccase.

Laccase from the white-rot basidiomycete *Ganoderma lucidum* has previously been characterized in my group and was found to be able to enhance cellulose catalyzed lignocellulosic degradation when combined with Cellic^{TM}CTec1.[70,93] In order to characterize Gl laccase behavior it was necessary to produce Gl laccase in high yield and with high purity, and hence both the optimization of the production system and the purification were studied.

3.1 Protein production optimization

Protein production was performed using the yeast *Pichia pastoris* as the recombinant expression system. The easy handling of the cells, fast and facile manipulation of the genes, inexpensive

cultivation media and rapid growth rate are some of the advantages obtained in using yeast cells as a recombinant enzyme production technique. Recombinant laccase production in yeast has been widely studied, and very broad ranges of laccase volumetric activities (0.034 - 380,000 U/L based on ABTS)[100,101] and laccase yields (2 – 130 mg/L)[102–104] have been reported. The highest *Trametes versicolor* laccase yield reported in *P. pastoris* is 140,000 U/L (130 mg/L).[103]

Improvement in laccase expression in yeast can be achieved by controlling both the copy number level,[105–108] i.e. via gene construct optimization, and the optimal yeast cultivation production,[109,110] i.e. via optimization of the fermentation parameters.

Recombinant gene construct

Selection of the optimal Secretion Signal Sequence In the native fungal host laccases are secreted due to the N-terminal sequence prepropeptide which allows the enzyme to be transported outside the cell. For recombinant expression, the ability to have the laccase expressed extracellularly is an advantage in the recovery of the protein itself, and the native signal peptide can also be recognized by some production hosts. A native signal peptide has been used in the production of some laccases in yeast, including laccase from *Fome lignosus*,[105] *Physisporinus rivulosus*,[106] *Pycnoporus cinnabarinus*,[111] *Trametes versicolor*[109] and *Ganoderma lucidum*[108]. It is also possible to use a yeast native signal peptide, and the one used the most is the *S. cerevisiae* α-mating factor, also known as the α-factor. Unfortunately, there is no a standard rule for whether the native or the α-factor signal peptide is the best signal sequence. Different results are reported in literature; for example, for the production of laccase from *Pycnoporus cinnabarinus*,[111] no differences in laccase yields were achieved by comparing the recombinant expression with native and α-factor signal peptide. In the case of laccase from *Physisporinus rivulosus*[106] the gene containing the yeast α-factor yielded a laccase with higher activity compared to the same gene with the native signal peptide. In the case of laccase from *Fome lignosus*,[105] the opposite was achieved with the clone with the native signal peptide exhibiting higher laccase activity compared to the clone with the α-factor.

Codon optimization Due to the differences in codon usage between filamentous fungi and yeast, a codon optimization of the protein of interest gene for yeast might be necessary. Yeast and fungi do not use the same DNA triplets to code for an amino acid. Therefore the fungi DNA triplets need to be exchanged for those of the yeast in order to improve the protein gene translation and hence its production in yeast. Several studies have shown higher laccase yield after gene codon optimization, and some examples are laccases from *Coprinus cinereus*,[112] *Ganoderma lucidum*[113] and *Pleurotus ostreatus*.[113]

Fermentation parameters

Copper concentration Due to the fact that laccase contains copper inside its structure (Section 2.3.1), a source of copper such as $CuSO_4$ must be present in the cultivation media. Copper is a yeast growth inhibitor[114] and thus it is necessary to find a compromise in the copper concentration that results in the correct laccase folding but has the least effect on growth. Copper concentration was studied in the range of 0.1-0.5 mM[102,110] for *Pichia pastoris*, and reached 6 mM for the recombinant production of *M. thermophila* laccase in *S. cerevisiae*.[115] It is not possible to define a standard optimal copper concentration; concentration varies according to the *P. pastoris* strain and the type of laccase.[102,105,110] For example, in the case of the recombinant expression of *Trametes versicolor* laccase in *P. pastoris* X-33, the optimal copper concentration was found to be 0.5 mM,[110] whereas if the *Trametes versicolor* laccase was expressed in *P. pastoris* GS115 and KM71, the optimal copper concentration was found to be 0.2 mM.[109]

pH Another parameter affecting laccase production is the pH of the cultivation medium. During yeast growth the pH tends to drop to pH$<$3 which affects the activity of the secreted laccase, and therefore the cultivation media has to be buffered. Li *et al.*[110] showed how the initial media pH in shake flask fermentation can influence *Trametes versicolor* laccase activity. The optimal growth pH was found to be 7 and approximately 40% of the laccase activity was lost even by decreasing the pH to 6.[110]

Fermentation temperature Temperature plays an important role in heterologous protein production. Optimal growth temperature and optimal expression temperature may not be the same. Several studies have shown that lowering the expression temperature increases laccase expression and results in higher stability of the laccase, avoidance of incorrect enzyme folding and release of proteases from dead cells in the cultivation medium.[102] Unfortunately there are also no standard rules for the temperature optimum: *Fome lignosus* laccase was produced in *P. pastoris* at 20°C, showing 1.5 fold higher activity compared to growth at 30°C,[105] but a *Pycnoporus sanguineus* laccase in *P. pastoris* showed a 2.2 fold higher activity at 30°C compared to 20°C.[116]

Fermentation time The expression time before the protein is recovered is also a key parameter for recombinant enzyme production, and this time depends on the fermentation type, i.e. shake flasks or lab-bench fermenter. The optimal cultivation time in shake flasks was found to be between 72 and 386 h,[102,110] while in the case of lab-fermenters the optimal time was between 144 and 192 h.[102,117]

3.2 Protein purification optimization

Several purification methods can be applied depending on the properties of the enzyme. In general, when recombinant enzymatic production is performed, the preferred purification method is affinity chromatography. The most used affinity tags are His- and Strep-tags. Other techniques to purify enzymes are ion exchange, hydrophobic interaction and size exclusion chromatography.[118]

Recombinant laccase purification from yeast expression has mainly been performed with ion exchange chromatography (one or more steps) followed by size exclusion chromatography.[119] Affinity chromatography using His-tag was also studied[120] for laccase purification and a purification fold of approximately 4.5 obtained. This strategy is not often used due to the nickel based matrix used for purification. In order for the His-tag to bind to the column, the nickel column has to be charged using salts.[121] If all the nickel sites are not saturated, the copper present in the laccase could bind to the column and eventually be extracted from the enzyme, thus rendering the enzyme inactive.

3.3 Materials and Methods

3.3.1 Recombinant production of *Ganoderma lucidum* laccase

Laccase from *Ganoderma lucidum* (Gl) was expressed in *Pichia pastoris* X-33. The gene encoding Gl laccase has been characterized previously by Sitarz *et al.*[70] and the constructs were delivered in pPICZalphaA vector. Chemically competent *Escherichia coli* DH5α was prepared using Mix & Go E. coli Transformation Kit (Zymo Research, Irvine USA) and transformed with plasmid DNA. Clones containing the heterologous plasmid were selected on low salt LB-medium containing 25 μg/mL Zeocin as a selective marker. Recombinant plasmid was purified with QIAprep Spin Miniprep Kit (Qiagen, Germany) following the manufacturer's instructions. The plasmid was linearized with MssI and transformed into *P. pastoris* by electroporation according to the manual of the EasySelect Pichia expression kit (Invitrogen). Positive clones were selected on YPD plates containing 100 μg/mL Zeocin and screened on ABTS plates as described below (Section 3.3.2). Protein expression was verified in small scale fermentation in BMGY and BMMY media with methanol induction according to the user manual from Invitrogen with the addition of 0.7 mM of $CuSO_4$ to BMMY. 5 L fermentation was afterwards performed according to Silva *et al.*[122] The total time for the fermentation process was 112 h. Laccase enriched fermentation broth was recovered by centrifugation at 5300 xg 5°C for 1 h and the supernatant was subjected to sterile filtration and concentrated by ultrafiltration, using a cross-flow bioreactor system with a 10 kDa cutoff membrane (Millipore, Sartorius, Denmark), as described by Silva et al.[122] The enzyme aliquots were stored at -80°C.

Different gene construct parameters were tested in order to find the optimal construct leading to the highest laccase activity. First, differences were tested in recombinant expression of the wild type and the codon optimized for *P. pastoris* Gl laccase encoding gene with yeast α-factor signal peptide. The genes were transformed in both *P. pastoris* X-33 and SMD1168H, wild type and protease-free *P. pastoris* strains, respectively. The wild type gene was also cloned in *P. pastoris* X-33 using the native signal peptide instead of the yeast α-factor in the presence or absence of a His-tag. Comparisons between laccase expressions were performed in shake flasks and the activity levels achieved after five days fermentation are measured using ABTS activity assay.

At the fermentation level some parameters such as temperature, copper concentration, pH and oxygen content were optimized.

3.3.2 ABTS screening plates for $CuSO_4$ concentration and temperature optimum

ABTS screening plates were prepared by adding 0.2 mM ABTS and 1% methanol to the minimum BMMH agar media. Differences in laccase yield production were studied by preparing plates with different $CuSO_4$ concentrations ranging from 0.2 to 1 mM incubated at 30°C. Plates containing 0.7 mM $CuSO_4$ (which was found to be the $CuSO_4$ concentration leading to the highest Gl laccase yield) were incubated at 15, 20, 25, 28 and 30°C to determine the growth temperature leading to the highest laccase yield. Positive *Pichia pastoris* clones were picked from YPD plates containing 100 μg/mL Zeocin and dissolved in 1 mL liquid YPD media. 10 μL of the dissolved clone was pipetted on the ABTS screening plate and incubated for 7 days. Additional 1% methanol was added each day to the plate lid to induce Gl laccase production. Colonies producing laccase showed a green halo around the colony, and the intensity of this halo was used to determine the optimal parameters, i.e. $CuSO_4$ concentration and growth temperature.

3.3.3 Copper saturation

Copper (I) saturation of Gl laccase was performed by adding 1, 3 and 6 mg/mL of solid CuCl to 1 mL fermentation broth. The saturation was performed in a thermomixer at 25°C and 1250 rpm. Laccase activity was followed over time for 5 hours. Removal of excess copper was done on a PD10 column (GE Healthcare) following the manufacturer's instructions, using 25 mM sodium acetate buffer pH 5 as buffer exchange solution. The eluted protein was up-concentrated using Vivaspin 6 MWCO 20 kDa (Sartorius, Denmark).

3.3.4 Purification of Gl laccase

3.3.4.1 Affinity chromatography

His-tag Gl laccase was purified by affinity chromatography on an IMAC-column (HisTrap HP 5 mL column, GE Healthcare) using an Äkta Purifier 100 (GE Healthcare, Uppsala Sweden). Fermentation broth was diluted 2 times in 3x binding buffer (120 mM EPPS (pH 7.4), 1.5 M NaCl, 72 mM imidazole), filtered and applied to the column operated at 3 mL/min. Protein was eluted with a gradient from 0 to 100% elution buffer (40 mM EPPS (pH 7.4), 0.5 M NaCl, 0.5 M imidazole) over 12 min in 1 mL fractions. All the fractions were screened using ABTS assay and fraction showing activity were assessed in SDS-gel and pooled.

Profinity-tag Gl laccase was purified following the manufacturer's instructions (Profinity eXact Tag, BioRad, Denmark). Due to Gl laccase inhibition towards sodium fluoride, the elution buffer used was 0.1 M sodium phosphate and 0.1 M sodium nitrite at pH 7.2. The elution was performed at 4°C by incubating the column overnight. All the fractions were screened using ABTS assay and fraction showing activity were assessed in SDS-gel and pooled.

3.3.4.2 Anion exchange chromatography

Untagged Gl laccase was purified by anion exchange on both a weak anion exchange column (DEAE FF 1 mL, GE Healthcare) and a strong anion exchange column (HiTrap Q 5 mL, GE Healthcare) using an Äkta Purifier 100 (GE Healthcare, Uppsala Sweden). Fermentation broth was diluted 20 times in binding buffer (50 mM sodium acetate, pH 5.5) and eluted with a linear gradient (20 CV) in elution buffer (50 mM sodium acetate, 1 M NaCl, pH 5.5). All the fractions were screened using ABTS assay and fraction showing activity were assessed in SDS-gel and pooled. For HiTrap purification different buffer capacities were studied ranging from 50 mM to 2.5 mM sodium acetate pH 5.5. Different pH values under coditions of optimized buffer capacity were also tested: pH 5.5 and pH 6 in 12.5 mM sodium acetate buffer and pH 6, pH 6.5, pH 7 and pH 8 in 12.5 mM Tris-HCl buffer. In all cases the purification was optimized using a step gradient elution with step elution buffer concentrations ranging from 13 and 22%.

3.3.4.3 Size exclusion chromatography

After anion exchange chromatography, 200 μL (containing approximately 0.3 mg of total protein concentration) of the purified sample were loaded into a high resolution size exclusion column (Superdex 200 Increase 10/300 GL, GE Healthcare) equilibrated with 50 mM sodium acetate pH 5.5 buffer and 150 mM of NaCl. All the fractions were screened using ABTS assay and fraction showing activity were assessed in SDS-gel and pooled.

3.3.5 Laccase activity assay with ABTS

Activity of laccase was assessed by monitoring the oxidation of ABTS (2,2'-azino-bis(3-ethylbenzothiazoline-6-sulphonic acid) at 420 nm ($\epsilon = 3.9 \times 10^4$ M^{-1} cm^{-1}). The assay reaction mixture contained 1 mM ABTS, 25 mM sodium acetate pH 5.0 and an appropriate amount of enzyme. ABTS oxidation was monitored at 25°C for 10 minutes. Enzyme activity was expressed in units with one International Unit (U) being defined as the amount of enzyme required to catalyze the conversion of 1 μmol of substrate (ABTS) per minute under the assay reaction conditions.

3.3.6 Endo-H treatment for Gl laccase deglycosylation

Deglycosylation of Gl laccase was performed using Endo-H_f kit (New England Biolab, Herlev, Denmark) according to the manufacturer's instructions. The reaction was incubated at 37°C for 24 h to achieve full deglycosylation of the laccase.

3.3.7 PAGE gels

SDS–PAGE was performed with 7.5% - 12% precast polyacrilamide gel (MiniProtean TGX, BioRad, Denmark) using as a protein ladder a Precision Plus Protein Standard Unstained (BioRad, Denmark) running alongside. Native-PAGE was performed under the same conditions as the SDS-PAGE without the protein denaturation step (5 min 90°C) and using a stained protein marker (Precision Plus Protein Standard Dual Color, BioRad, Denmark). The gels were run in Tris/Glycine/SDS Buffer (BioRad, Denmark) at 150 V and 3 A for an hour and stained for 3 hours in Bio-Safe Coomassie stain (BioRad, Denmark).

ABTS stained Native-PAGE was carried out under the same conditions as the Native page using a different staining procedure. The gel was stained in darkness with 25 mM sodium acetate buffer pH 5 and 0.1 mM ABTS for 30 min. The bands showing laccase activity reacted to ABTS by developing a blue-green color.

3.3.8 Statistics

One-way ANOVA using Tukey's test with a pooled standard deviation for determination of statistical significance on the activity data was made in RStudio (RStudio Inc., Boston, USA). Statistical significance was established at $p \leq 0.05$.

3.4 Results and Discussions

3.4.1 Optimization of the Gl laccase gene construct

High laccase activity (0.065 U/mL) was found in the codon optimized gene cloned in X-33. The codon optimized gene expressed in SMD1168H yielded only half of the laccase activity compared with the codon optimized X-33 (Table 3.1). A similar behavior was found in the case of the wild type gene. Wild type gene expressed in X-33 yielded to 0.033 U/mL, while the wild type gene expressed in SMD1168H gave the lowest laccase activity 0.023 U/mL (Table 3.1).

The highest laccase activity (0.17 U/mL) was found in the construct encoding Gl with the native signal peptide and wild type gene in the presence of His-tag, and exhibited a 2.6 fold higher activity compared to the codon optimized gene in X-33 (Table 3.1). On the contrary, the construct encoding for a non-tagged version produced the same level of laccase activity as the wild type gene with α-factor (Table 3.1).

Table 3.1: Recombinant production of Gl laccase in *Pichia pastoris*. Comparison between laccase activity on ABTS measured after 5 days shake flask fermentation using different gene construct are reported.

		Signal sequence	Protein concentration[1] mg/mL	Activity[2] U/mL
Wild type	X-33	α-factor	0.83	0.033 ± 0.002 ^{b,y}
	SMD1168H	α-factor	0.83	0.023 ± 0.001 ^{c}
	X-33	native, no tag	-	0.032 ± 0.003 ^{y}
	X-33	native, His-tag	-	0.170 ± 0.009 ^{x}
Codon optimized	X-33	α-factor	1.37	0.065 ± 0.004 ^{a}
	SMD1168H	α-factor	1.41	0.031 ± 0.001 ^{bc}

Standard deviations are shown and significant difference ($p \leq 0.05$) of activity for the clones with α-factor are shown as superscripted letters (a-c), significance difference ($p \leq 0.05$) of activity for the wild type gene cloned in X-33 are shown as superscripted letters (x-y).
[1] Protein concentration was determined using BSA assay.
[2] Laccase activity was measured using ABTS assay.

3.4.2 Optimization of the fermentation parameters

The absence of a standard procedure for producing laccases led to the necessity of optimizing each single laccase fermentation and thus also different fermentation parameters. Therefore copper concentration, expression temperature, fermentation broth pH, expression time and oxygen availability were all tested in order to increase both Gl laccase activity and yield.

Optimization of expression temperature and copper concentration were performed using ABTS screening plates. Five different copper concentrations ranging from 0.2 to 1 mM were tested and analyzed after 4 days of induction. The optimal copper concentration was selected by

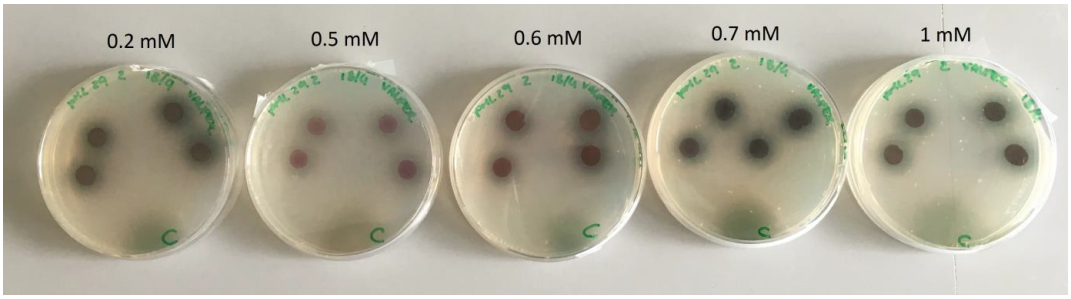

Figure 3.1: Gl laccase expression at different copper concentrations using ABTS screening plates. Optimal copper concentration was found at 0.7 mM.

inspecting the halo intensity around the colonies, and the optimum was found at 0.7 mM of $CuSO_4$ (Figure 3.1). The same screening method was used to find the optimum expression temperature. Five different expression temperatures were tested, namely 15, 20, 25, 28 and 30°C, while maintaining the copper concentration constant at 0.7 mM. In this case too the optimal temperature was selected by examining the halo intensity around the colonies and the highest laccase expression was found at 20°C. These optimized values were applied in the 5L fermenter set-up which increased the activity by a factor 2.2 (F248, Table 3.2) compared to F233 which was run with the non-optimized conditions: 0.2 mM $CuSO_4$ and 20°C (Table 3.2). The pML29 clone used for producing F248 was frozen to be able to repeat the fermentation but unfortunately poor levels of activity (0.2-1.3 U/mL) were obtained by using the same starting colony. The low laccase activity level was solved by preparing fresh *P. pastoris* transformant prior each fermentation. The complexity of the laccase gene presumably resulted in loss of the gene from the *P. pastoris* cells and hence lower laccase activity was obtained. The requirement of performing a new transformation every time prior to fermentation meant that each fermentation was started with a different *P. pastoris* colony which also led to differences in the capability to express laccase. Therefore in order to be able to optimize the fermentation parameters two fermentation were always started in parallel from the same colony.

The effect of pH on fermentation was studied with the limitation of the buffer capacity used in our fermentation set-up, which did not allow increasing the pH to higher than 6. Therefore two parallel fermentations were started, one running at pH 6 (F256, Table 3.2) and the other at the standard pH 5 (F255 Table 3.2), while maintaining all other fermentation parameters constant. The increase in pH did not show increase in activity, i.e. F255 and F256 showed the same level of volumetric activity equal to 1.8 U/mL (Table 3.2).

Fermentation time can also help in increasing laccase activity,[102] and therefore fermentations were run for 8 days instead of the standard 5 days. The longer fermentation time might lead to death of some *P. pastoris* cells, which could release into the fermentation broth proteases that could eventually degrade laccase. In order to decrease the chances of protease degradation of laccase, Gl laccase was cloned in *P. pastoris* SMD1168H (clone OLAF, Table 3.2), a protease free strain. Half of F259 (Table 3.2) was harvested after 5 days and the other half was run for three additional days. Even though the activity of F259 after 8 days of fermentation was 10

Table 3.2: Recombinant production of Gl laccase in *Pichia pastoris*. Laccase activity on ABTS measured after 5 L fermentation are reported.

Name	Clone	Protein concentration[1] mg/mL	Activity[2] U/mL	Note
F233	pML29[3]	23.7	1.3 ± 0.03 [c]	0.2 mM $CuSO_4$, 20°C, pH 5
F248	pML29[3]	26.5	2.9 ± 0.3 [a]	0.7 mM $CuSO_4$, 20°C, pH 5
F255	pML29[3]	21.9	1.8 ± 0.02 [b]	0.7 mM $CuSO_4$, 20°C, pH5
F256	pML29[3]	18.9	1.8 ± 0.1 [b]	0.7 mM $CuSO_4$, 20°C, pH6
F259	OLAF[4]	11.8	0.16	0.7 mM $CuSO_4$, 20°C, pH5, 5 days fermentation
		15.6	1.2 ± 0.02 [c]	0.7 mM $CuSO_4$, 20°C, pH5, 8 days fermentation
F265	OLAF[4]	35.2	2.9 ± 0.1 [a]	0.7 mM $CuSO_4$, 20°C, pH5, 8 days fermentation
F266	OLAF[4]	21.1	0.7	0.7 mM $CuSO_4$, 20°C, pH5, 5 days fermentation, P_{O_2}=5%
		32.9	2.1± 0.05 [b]	0.7 mM $CuSO_4$, 20°C, pH5, 8 days fermentation, P_{O_2}=5%
F278	SVEN[5]	25.6	1.4 ± 0.2 [c]	0.2 mM $CuSO_4$, 20°C, pH5

[1] Protein concentration was determined using BSA assay.
[2] Laccase activity was measured using ABTS assay (Section 3.3.5).
[3] pML29 defines the non-tagged wild type Gl laccase gene using pPICZA as expression vector and yeast α-factor as signal peptide cloned in *P. pastoris* X-33 strain.
[4] OLAF defines the non-tagged codon optimized for *P. pastoris* Gl laccase gene using pJexpress912 as expression vector and yeast α-factor as signal peptide cloned in *P. pastoris* SMD1168H strain (protease free).
[5] SVEN defines the His-tagged wild type Gl laccase gene using pPICZA as expression vector and yeast native signal peptide cloned in *P. pastoris* X-33 strain.

times higher than the activity after 5 days (Table 3.2), the same activity level to that of F248 was reached (Table 3.2) which was produced with *P. pastoris* X-33 in 5 days.

Oxygen limitation has been shown by Brander *et al.*[123] to improve the production of a bacterial laccase in *Escherichia coli*. With that knowledge in mind, fermentation F266 (Table 3.2) was performed at a lower oxygen partial pressure (P_{O_2}=5%) compared to the standard protocol (P_{O_2}>20%) to see whether oxygen limitation could also lead to an increase in laccase yield in recombinant production in yeast. The final laccase activity of F266 run for 8 days fermentation at P_{O_2}=5% was lower (2.1 U/mL) than the activity of F265 (2.9 U/mL) run at the standard oxygen level. Therefore recombinant laccase production in yeast was not boosted by oxygen depletion but instead it was lowered.

After the optimization of the gene construct (Section 3.4.1), the Gl laccase construct which expressed best was the one encoding for the wild type gene with native signal peptide (Table 3.1). Thus a 5 L fermentation was performed to try to obtain high laccase yield. Unfortunately the fermentation activity yielded only 1.4 U/mL (F278, Table 3.2), which was only 10 times higher than the activity after shake flask fermentation (0.17 U/mL, Table 3.1). One possible

explanation for the low activity level could be found in the low copper concentration (0.2 mM of $CuSO_4$) of the fermentation media.

3.4.3 Copper saturation

The complexity of the laccase structure containing four moles of copper caused stress in the *P. pastoris* cells, which as mention before led to the need to prepare new transformants prior to fermentation. It was also thought that laccase could eventually not be secreted by the cells. Therefore the biomass recovered from the fermenter was lysed, screened for laccase activity with ABTS and loaded onto SDS-PAGE, but neither laccase activity nor a laccase band were found.

Another problem resulting from the cell stress could be miss-incorporation of the copper into the laccase structure. While it is not possible to reconstruct the laccase activity if the copper in the T2/T3 site is missing, the copper in the T1 site is easily reconstructable. Buck *et al.*[124] showed that simply by adding 6 mg/mL of solid CuCl in the laccase broth, the T1Cu was reconstructed and the enzyme recovered all its activity. Therefore, using a similar set-up, 1, 3 and 6 mg/mL of solid CuCl was added to Gl laccase fermentation broth and the activity was monitored for 5 hours, but in our case the Gl laccase activity did not increase.

3.4.4 Gl laccase purification

Purification of Gl laccase was studied using two strategies: affinity chromatography and anion exchange chromatography.

3.4.4.1 Affinity chromatography

Two types of affinity chromatography were studied: His-tag and Profinity-tag purification.

Profinity-tag purification gives rise to a tag free protein beneficial for avoiding negative interaction of the tag with the protein. The mutated serine protease present in the chromatographic resin interacts with the Profinity tag. Then, after addition of azide or fluoride atoms, the tag is cleaved from the protein and the target protein is released by the column resin in its native form. In the experiment, Gl laccase was inhibited both by azide and fluoride atoms and therefore sodium nitrite was used as cleaving agent. Low activity was detected after shake flask fermentation, i.e. laccase activity was found at 0.0082 and 0.0048 U/mL for X-33 and SMD1168H, respectively. Profinity-tag purification was tested anyway but unfortunately laccase activity was not detected after protein elution.

Gl laccase was also produced using His-tag (F278) and therefore His-tag affinity chromatography

was performed. Unfortunately, also in this case no purification was achieved and laccase activity was found only in the flow through of the column. In order to test if the His-tag was present on the enzyme, the laccase was run in a Western blot which did not show the presence of the His-tag. Our guess was that the His-tag was not located outside of the enzyme structure but was embedded in the laccase structure and hence of no use for protein purification.

3.4.4.2 Anion exchange chromatography

Gl laccase purification was tested both with weak and with strong anion exchanger. Trial tests on weak anion exchanger showed poor laccase activity recovery and hence the optimization of the purification was performed on the strong anion exchanger. The theoretical Gl laccase isoelectric point (pI) is around pI 4.92 and hence 50 mM sodium acetate buffer pH 5.5 was selected at first as elution buffer. Unfortunately the recovered activity was only 1.2% of the total Gl laccase activity loaded in the column. In order to improve the recovered laccase activity, the buffer capacity effect was studied by testing the buffer concentration in the range 50 - 5 mM. The highest recovered activity equal to 33% was found by decreasing the buffer capacity to 12.5 mM.

The elution buffer pH was also varied from 5.5 to 8 while maintaining the buffer capacity constant at 12.5 mM to test if the recovered laccase activity could be increased. Since sodium acetate buffer could not reach pH 8 the elution buffer was changed to Tris-HCl buffer, under the assumiption that the optimized buffer capacity (12.5 mM) was also optimal for the Tris-HCl buffer. By increasing pH the amount of recovered laccase activity increased from 33% to 85%, for 12.5 mM sodium acetate pH 5.5 and 12.5 mM Tris-HCl pH 8, respectively (Figure 3.2 a and b).

The anion exchange purification step alone did not yield to a pure laccase (Figure 3.2a) and hence a size exclusion purification was added after anion exchange.

From the size exclusion, at first glance, a better protein separation was obtained, but unfortunately laccase activity was not found under a single peak (Figure 3.2 c insets). The inability to completely define a laccase peak resulted in a poor degree of purification, and the low protein concentration of the purified samples (Figure 3.3a) made it not possible to see protein bands on SDS-gel. Even though the protein concentration was low, laccase bands appeared at the expected molecular weight (around 100 kDa) by performing an ABTS activity staining of the gel. *P. pastoris* tends to heavily glycosylate heterogeneous proteins,[105,125–127] which results in Gl laccase showing higher molecular weight, in this case approximately 100 kDa, compared to the native Gl laccase molecular weight of approximately 54.5 kDa[70] (Figure 3.3b). The band showing laccase activity was sent for peptide sequencing which confirmed that it was Gl laccase.

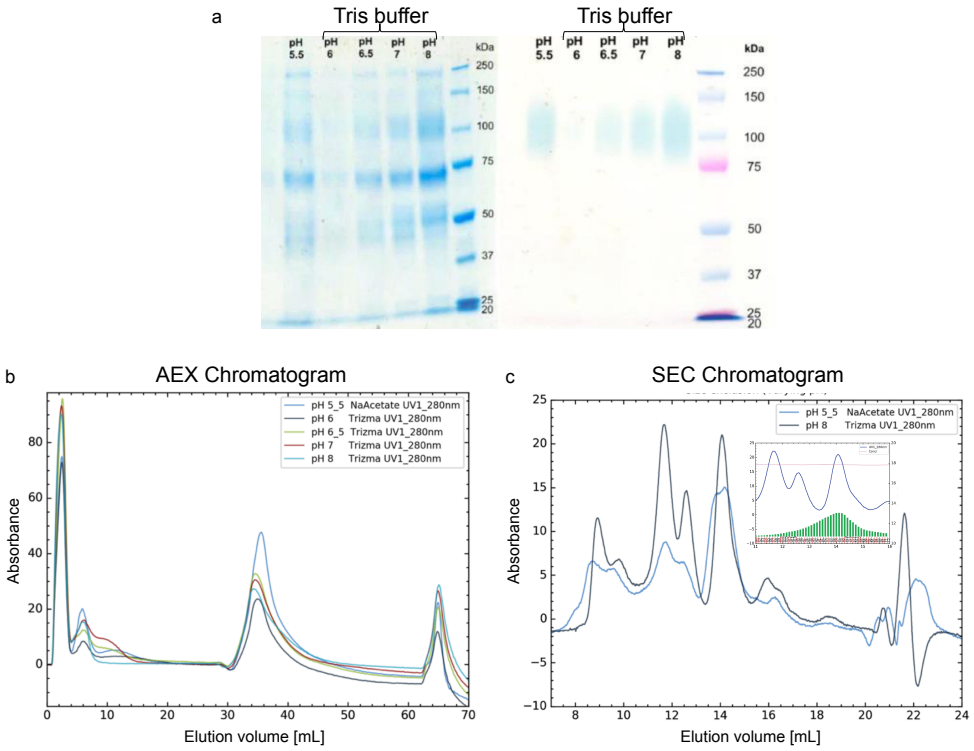

Figure 3.2: Two steps purification of Gl laccase. a) SDS-PAGE and ABTS Native gel after anion exchange chromatography at different elution buffer pH. b) Anion exchange (AEX) chromatograms at different elution buffer pH. c) Size exclusion (SEC) chromatograms at two different elution buffer at two different pH. The insert shows the fraction (in green) showing laccase activity.

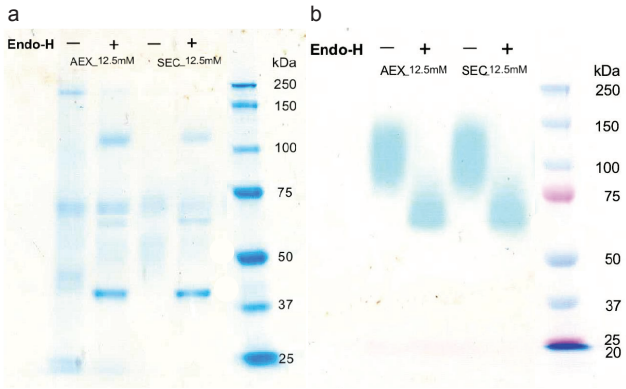

Figure 3.3: Endo-H treatment after the two purification steps of Gl laccase. a) SDS-PAGE after anion exchange (AEX) and size exclusion (SEC) with (+) and without (-) Endo-H. b) ABTS Native gel after anion exchange (AEX) and size exclusion (SEC) with (+) and without (-) Endo-H.

3.5 Conclusions

Optimization of the recombinant production of *Ganoderma lucidum* laccase in *Pichia pastoris* was attempted by studying the effect of changes in the gene construction, fermentation parameters and copper saturation after laccase expression. Investigation of the Gl laccase production in shake flasks led to a 2.6 fold increase in laccase activity when the α-factor signal peptide was replaced with the Gl native signal sequence. This increase in activity was unfortunately not achieved in scaling up the fermentation in a 5 L fermenter. A major problem that arose during laccase production was that the Gl laccase gene caused stress to and gene loss by the yeast cells. This effect meant that it was necessary to prepare fresh new *P. pastoris* transformant prior to each fermentation. The low laccase activities obtained in the different fermentation strategies allows the conclusion that *P. pastoris* is not the best host for the production of *Ganoderma lucidum* laccase. Other hosts should be taken into account, such as *Aspergillus* sp., which could hopefully give rise to higher laccase yield and laccase activity.

The purification was not a trivial factor either. The optimization of the elution buffer pH to 8 in the anion exchange chromatography allowed a significant increase in the recovered laccase activity, but even after size exclusion it was impossible to obtain a pure Gl laccase. Again the reasons for this result could be due to the stress that the laccase gene caused to the host, which may lead to laccase with different degrees of glycosylation and miss-folded protein and to low concentration of the expressed laccase. Therefore a change of expression host will also be beneficial from the purification point of view.

Despite the inability to obtain a pure *Ganoderma lucidum* laccase and thus to either support or dismiss hypothesis H1, enough laccase activity was present for this particular laccase to be included in the following characterization studies. To overcome differences in laccases purities, enzyme loadings were expressed as activity rather than on a mol basis.

Chapter 4

Development of new laccase activity assays

This chapter focuses on the development of two new methods for measuring laccase activity (Paper 1 and Paper 2) and addresses the following hypothesis and objectives:

H2 Laccase kinetics on individual, soluble lignin building blocks provides information about the laccase specificity towards lignin subunits and whether this specificity and product profile is influenced by the origin of the laccases.

Obj2 To assess laccase activity in real time with a highly sensitive and accurate method using LC-MS on small phenolic compounds and a dimeric OH-dilignol compound.

Obj3 To investigate whether laccase kinetic rates and catalytic efficiencies of laccases depend on the substitution on the phenolic ring and/or the molecular structure beyond the phenolic moiety.

Obj4 To examine whether reaction pattern on small phenolic compounds obtained from FTIR spectral evolution can be used to distinguish or group together laccases from different origins.

The commonly used laccase activity assays rely on spectrophotometric methods which measure the change in UV adsorption of a product produced or a substrate consumed during laccase reaction. As introduced in Section 2.5, the most used spectrophotometric laccase activity assays are ABTS and syringaldazine which have structures very different from that of lignin and which therefore cannot be used for drawing a direct comparison to laccase activity on

lignin. We have therefore developed two quantitative assays for laccase activity using the LC-MS system (Paper 1) and FTIR (Paper 2) with compounds related to lignin as substrates, namely sinapic, ferulic, *p*-coumaric acid and OH-dilignol for the LC-MS assay and sinapic acid, sinapic aldehyde, sinapyl, coniferyl and *p*-coumaryl alcohol for the FTIR assay (Figure 4.1).

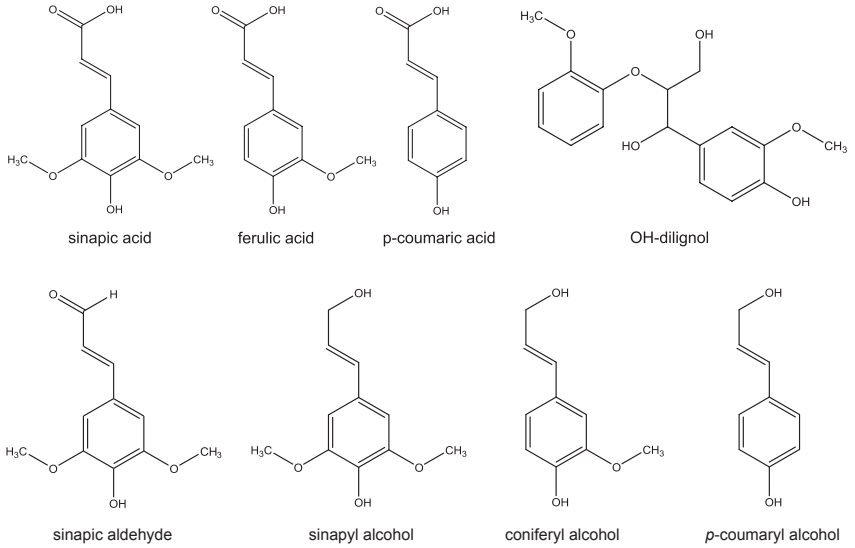

Figure 4.1: Structure of the substrates used in the LC-MS and FTIR studies

4.1 Laccase activity measured by LC-MS (Paper 1)

Two major drawbacks can be identified when using spectrophotometric measurement for quantification of enzymatic activity. One drawback is related to the general characteristics of substances to be able to adsorb light, which can give rise to misleading measurement if the enzyme analyzed is not pure. The second drawback in the specific case of laccase is related to the not so well known products formed during reaction. LC-MS is mostly used as a qualitative tool to determine the mass of the compounds in the analyzed mixture, but it is also receiving increasing attention as quantitative tool. In the proteomics field, quantification is achieved by running the LC-MS in Multiple Reaction Monitoring (MRM) mode.[128] MRM identifies and quantifies specific fragment ions deriving from a known precursor list of parent masses and this offers several advantages such as high specificity, and low susceptibility to interfering compounds found in biological samples.[129,130] LC-MS was employed as a quantitative method to monitor substrate depletion during laccase oxidation of phenolic compounds by running the MS in MRM mode, which detected selectively a specific precursor mass, i.e. the specific m/z of the substrate and its specific fragmentation. In addition, the MS was also run in full scan to obtain the product profile during the continued radical coupling reaction. Two enzymes were used in this study: the benchmark *Trametes versicolor* (Tv) laccase and *Ganoderma lucidum* (Gl) laccase produced in-house. Due to the different purity level of the two laccases the only

way to be sure of dosing the same amount of active enzyme was to dose them at the same level of syringaldazine units. In this work the Gl and Tv laccase oxidation kinetics and product profiles of four different substrates were studied: sinapic acid, ferulic acid, *p*-coumaric acid and OH-dilignol (Figure 4.1).

4.1.1 Michaelis-Menten kinetics

Laccase reaction was initiated in the LC-MS autosampler and two μL of the reaction sample were injected into the column every six minutes (Figure 4.2). Substrate depletions were quantified to a molar concentration using the specific standard curve depending on the substrate analyzed.

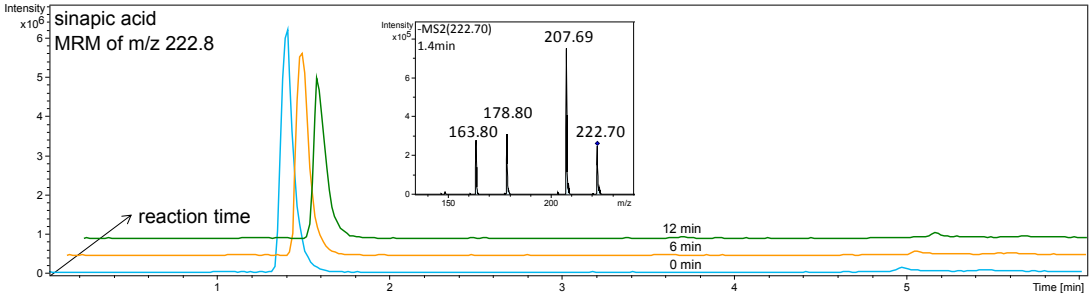

Figure 4.2: Laccase oxidation evolution profile for sinapic acid using MRM analysis for substrate quantification. Chromatograms of three reaction times: 0 minutes (blue), 6 minutes (orange) and 12 minutes (green). Inset shows MS/MS of the peaks. Observation of the ions was performed as $[M\text{-}H]^-$.

Initial rates were determined by measuring the amount of substrate consumed in 12 minutes reaction for the different substrate concentration. By plotting these initial rates vs. the initial substrate concentration, Michaelis-Menten curves were obtained for both enzymes and all substrates; examples of Michaelis-Menten curves for Gl laccase oxidation of ferulic acid and OH-dilignol are shown in Figure 4.3.

Kinetic parameters were determined (Table 4.1) for both Gl and Tv laccase. Due to differences in purity of the two enzymes and hence the lack of the value of active laccase concentration in the sample used, the common enzymatic parameters known as k_{cat} and k_{cat}/K_m could not be determined. Two new enzymatic parameters were defined as apparent specific activity: the amount of substrate that is converted by the enzyme in one second, representing k_{cat}/K_m, and apparent catalytic efficiency: the number of oxidation cycles that the enzyme is capable of in one second, representing k_{cat}, both of them having at the denominator the amount of syringaldazine units which has to be intended as a measure of the active laccase concentration in the sample. While differences between kinetic parameters between enzymes were not present, the K_m values varied according to the phenolic substitution (Table 4.1). K_m resulted to be the least for the double methoxylated sinapic acid and the highest for the non methoxylated *p*-coumaric acid in accordance with previous studies.[131–133] K_m values directly influence the apparent catalytic efficiency values (Table 4.1). The lower the K_m values, the higher is the apparent catalytic

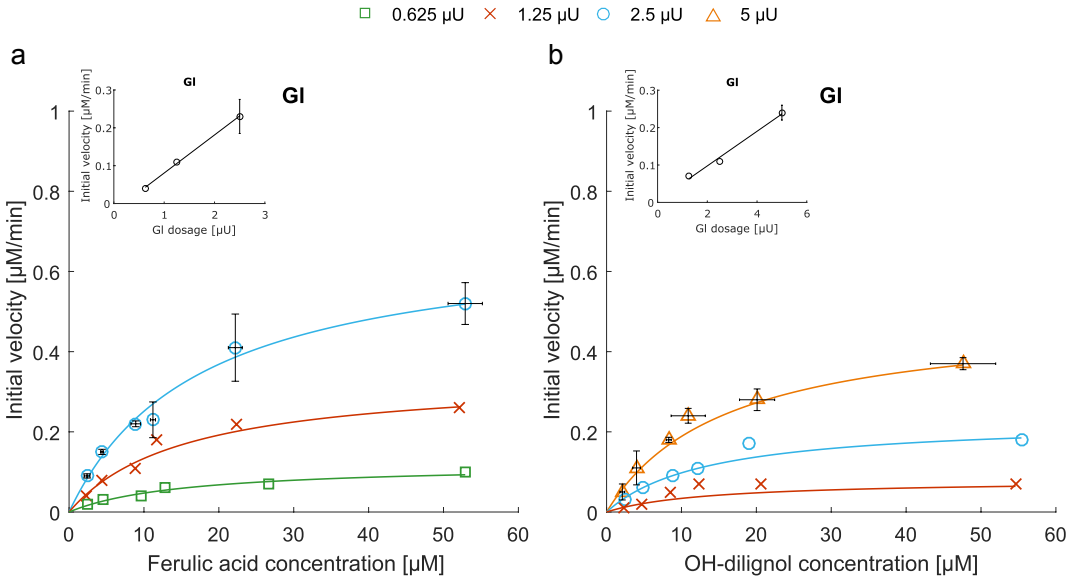

Figure 4.3: Michaelis-Menten curves for Gl laccase on ferulic acid (a) and OH-dilignol (b). Three different enzyme dosages (in syringaldazine assay units) are shown: for ferulic acid (a): 0.625 μU (green open square), 1.25 μU (red cross) and 2.5 μU (blue open circle). For OH-dilignol (b): 1.25 μU (red cross), 2.5 μU (blue open circle) and 5 μU (orange open triangle). Dose response at 10 μM substrate concentration are shown in the insets. For the highest enzyme dose standard deviations are shown.

efficiency and thus the enzyme is capable of performing a higher number of oxidation cycle per second. In contrast, OH-dilignol showed a K_m value close to that of sinapic and ferulic acid, but the apparent specific activity value was approximately 6 times lower than with sinapic acid. While the 'dimeric' molecule of OH-dilignol did not affect the affinity of the enzyme towards it, the apparent specific activity was approximately 2 to 4 times lower for OH-dilignol.

4.1.2 Definition of a new laccase activity assay

One of the prerequisites of having a good activity assay method is to ensure a dose response relation, which means that the activity measured at a specific substrate concentration and the enzyme dose result in a linear response. Initial rates obtained at 10 μM substrate concentration were plotted vs. the enzyme dose and a clear linear behavior was obtained with correlation factors $R^2 \geq 0.97$ for both Tv and Gl laccase on all four different substrates (Figure 4.3 insets).

Starting the reaction in the LC-MS auto-sampler had the advantage of allowing fast and real time measurements which therefore only negligibly affected the reaction volume and substrate quantification. In addition only 2 μL of sample were withdrawn from the reaction mixture without affecting the reaction volume and hence substrate quantification. The reaction was stopped immediately when the mobile phase was met at pH 2 after injection into the column so as to avoid any kind of user handling of the sample.

Table 4.1: K_m, V_{max}, apparent specific activity and apparent catalytic efficiency for hydroxycinnamic acids and OH-dilignol.

		Tv		Gl	
Sinapic acid	V_{max} [μM/min]	1.15	$\pm$ 0.07^{x}	1.06	$\pm$ 0.03^{x}
	K_m [μM]	12.13	$\pm$ 2.23^{b,x}	12.11	$\pm$ 0.46^{b,x}
	Apparent specific activity [nM/μU·s]	8.32	$\pm$ 0.47^{a,x}	6.97	$\pm$ 0.22^{a,x}
	Apparent catalytic efficiency [1/μU·s]	565.6	$\pm$ 102.15^{a,x}	550.8	$\pm$ 36.3^{a,x}
Ferulic acid	V_{max} [μM/min]	1.14	$\pm$ 0.10^{x}	0.82	$\pm$ 0.07^{y}
	K_m [μM]	17.17	$\pm$ 4.99^{b,x}	17.84	$\pm$ 0.93^{b,x}
	Apparent specific activity [nM/μU·s]	6.66	$\pm$ 0.59^{a,x}	4.55	$\pm$ 0.45^{b,y}
	Apparent catalytic efficiency [1/μU·s]	280.0	$\pm$ 64.2^{b,x}	284.8	$\pm$ 33.7^{b,x}
p-coumaric acid	V_{max} [μM/min]	6.73	$\pm$ 0.40^{x}	7.31	$\pm$ 0.55^{x}
	K_m [μM]	130.27	$\pm$ 2.56^{a,x}	271.04	$\pm$ 5.25^{a,y}
	Apparent specific activity [nM/μU·s]	0.51	$\pm$ 0.03^{b,x}	0.55	$\pm$ 0.04^{d,x}
	Apparent catalytic efficiency [1/μU·s]	3.92	$\pm$ 0.27^{c,x}	2.05	$\pm$ 0.17^{c,y}
OH-dilignol	V_{max} [μM/min]	0.39	$\pm$ 0.03^{x}	0.46	$\pm$ 0.03^{x}
	K_m [μM]	12.89	$\pm$ 3.68^{b,x}	11.76	$\pm$ 2.61^{b,x}
	Apparent specific activity [nM/μU·s]	1.43	$\pm$ 0.09^{c,x}	1.70	$\pm$ 0.09^{c,x}
	Apparent catalytic efficiency [1/μU·s]	84.9	$\pm$ 20.5^{d,x}	106.1	$\pm$ 20.8^{d,x}

Standard deviations are shown and significant difference ($p \leq 0.05$) of K_m, apparent specific activity and apparent catalytic efficiency column-wise are shown as superscripted letters (a-d), significance difference ($p \leq 0.05$) of K_m, V_{max}, apparent specific activity and apparent catalytic efficiency row-wise are shown as superscripted letters (x-y).

Another positive aspect of the methodology is related to the sensitivity level reached; it was indeed possible to reach substrate concentrations in the sub-pmol range 3 fold lower than with the common UV activity assays which measure substrate concentration in the nmol scale.[134] It was the choice to quantify substrate depletion in MRM mode which helped to increase the sensitivity of the measure and reach a lower limit of substrate detection of 0.04 pmol.

The differences in enzyme purity were not an issue in the quantification of the initial rates, thus a method was obtained that can be used with a certain degree of laccase impurity.

A drawback in the assay is related to the necessity of having samples and standards sharing similar conditions. In cases where the differences between standards and samples are too large quantification problems can be experienced. Differences between standards and samples could be caused for example by ion suppression referred to a reduced detector response obtained by impurities in the samples. The ion suppression effect can be eliminated by applying pure and simple reaction mixtures with little ionic strength thereby keeping the total number of ions low.

Therefore a new activity assay was developed measuring laccase oxidation of 10 μM of sinapic acid. New activity values for all the laccase used in this thesis were determined and compared to the common syringaldazine activity assay (Table 4.2). Laccase activity on sinapic acid was found to be 118-135 times higher compared to syringaldazine activity for all the laccases, hence confirming that sinapic acid is a better substrate than syringaldazine for screening laccase activity.

Table 4.2: Comparison between laccase activity measured with syringaldazine and sinapic acid for all the laccase studied in the thesis.

Name	Activity [mU]				Paper
	Syringaldazine[1]		Sinapic acid[2]		
Gl	11	± 1	1,500	± 12	Paper 1, 2, 3 and 4
Tv	1.1	± 0.01	134	± 10	Paper 1, 2, 3 and 4
Tvil	260	± 15	33,540	± 115	Paper 2
Mr	0.19	± 0.04	25	± 1.7	Paper 2
Mt	8,400	± 72	991,200	± 280	Paper 3 and 4
Slac	5.50	± 0.1	653	± 16	Paper 4

[1] Activity established on syringaldazine 25 mM sodium acetate pH 5 and 25°C.
[2] Activity established on sinapic acid 12.5 mM sodium acetate pH 5 and 30°C.

4.1.3 Product profile

Product profiling of laccase oxidation of hydroxycinnamates was performed by running the LC-MS in full scan mode in order to detect the entire range of product precursor m/z masses present in the ongoing reaction. The main products obtained after laccase reaction were identified as dimer and trimer of the starting substrate by the value of their m/z but also products with the loss of m/z 44 describing the loss of a carboxylic group (Figure 4.4a). Peaks with the same masses m/z were identified, as for example peak 3 and 4 in Figure 4.4a which indicated that different isomers of the same product were formed. One product structure was identified by Lacki *et al.*[135] in the case of sinapic acid dimer to be dehydrodisinapic lactone, and hence it is highly possible that one of the two products below peak 3 and 4 is the one found by Lacki.[135] The formation of dimers is preferred in *ortho* and *para* position and therefore the complexity of the product profile increased with the decrease of methoxylation on the phenolic ring (Figure 4.4). For OH-dilignol the dimeric product only was found, and the absence of saturation in its structure (Figure 4.1) confined the radical to the phenolic ring thus allowing only one 5-5' linkages.[15]

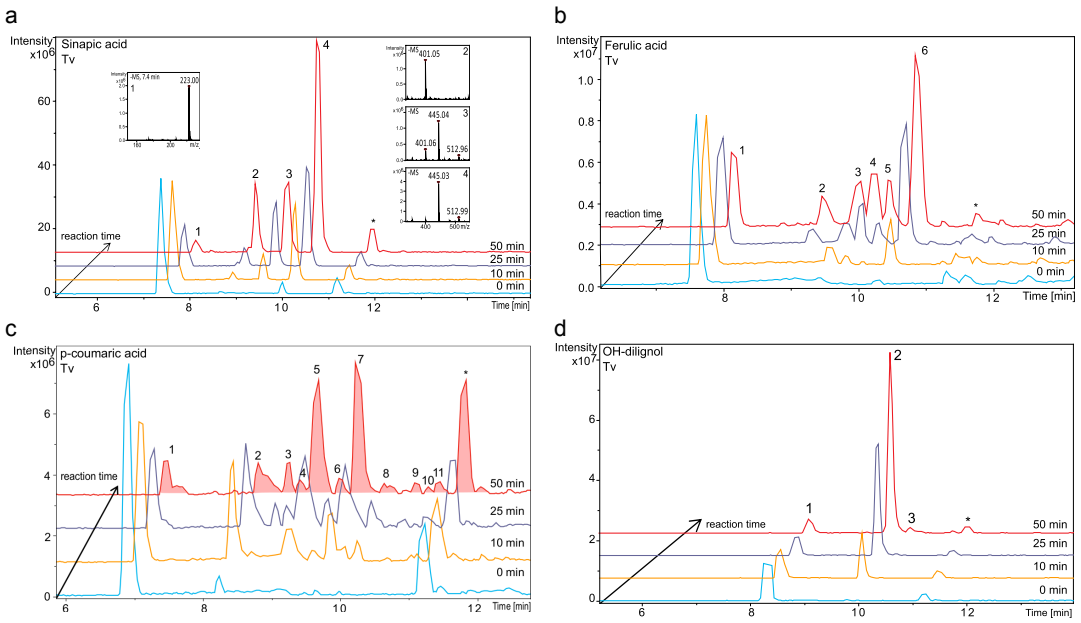

Figure 4.4: Tv laccase oxidation evolution profiles for hydroxycinnamic acids and OH-dilignol: oxidation of sinapic acid (a); oxidation of ferulic acid (b); oxidation of *p*-coumaric acid (c) and oxidation of OH-dilignol (d). Chromatograms at different reaction times are shown: 0 minutes (light blue), 10 minutes (yellow), 25 minutes (violet) and 50 minutes (red). Please note that the intensity scale may differ between chromatograms and is adjusted to give optimal display of figures. (a) includes an example of the MS spectra corresponding to each peak, all ions are observed as $[M\text{-}H]^-$.

4.2 Laccase reaction fingerprinting with FTIR coupled to PARAFAC (Paper 2)

It is common to monitor substrate depletion or product formation in order to measure enzyme activity. There is a methodology that is able to take into account both substrate depletion and product formation at the same time, which has been thoroughly investigated by Baum *et al.*[136–138] and other research groups.[139,140] This new method combines Fourier Transform Infrared spectroscopy (FTIR) with multiway Parallel Factor Analysis (PARAFAC).

FTIR When conventional spectroscopy is used, the sample is irradiated with a monochromatic light beam, i.e. only a single wavelength passes through the sample. Infrared (IR) spectroscopy measures the interaction of electromagnetic light from the infra-red region (780 - 300,000 μm) with inter-atomic covalent bonds and the intermolecular bonding of a sample. When the infra-red radiation passes through a sample, an infra-red spectrum is obtained which determines the fraction of the incident radiation that is adsorbed at a particular energy. IR is used to identify molecules. The adsorption occurs when the frequency of the IR equals the vibrational frequency of a bond or of a collection of bonds.[141] In order to obtain a more complete screening of the sample more quickly, it is necessary to irradiate the sample with different frequencies at the same time, and this can be achieved by Fourier Transform Infrared spec-

troscopy (FTIR). FTIR works by irradiating the sample with a light beam containing several frequencies at once and measures how much of that beam is adsorbed by the sample. The typical instrument used to measured FTIR spectra is called a Michelson Interferometer. The light from the radiation source is adjusted and directed to a beam splitter (Figure 4.5a). In an ideal interferometer 50% of the light is refracted towards the stationary mirror while the other 50% is transmitted towards the moving mirror (Figure 4.5a red arrows). The light is reflected back by the two mirrors to the beam splitter (Figure 4.5a green arrows). The interference of radiation between these two beams gives rise to an interferogram which passes through the sample and is detected by a detector. In order to change the interference between the two light beams, the optical path difference has to be varied, and this is achieved by varying the distance between the moving mirror and the beam splitter (Figure 4.5a).[141] When λ_s equals λ_m (Figure 4.5b) a constructive interference is obtained, whereas if λ_s equals $1/2\ \lambda_m$ (Figure 4.5c) the interference is destructive. The raw data obtained in the detector (light absorption for each mirror position) need to undergo a computer processing using the Fourier Transformant to convert them to the desired result, i.e. absorbance value for each wavelength.

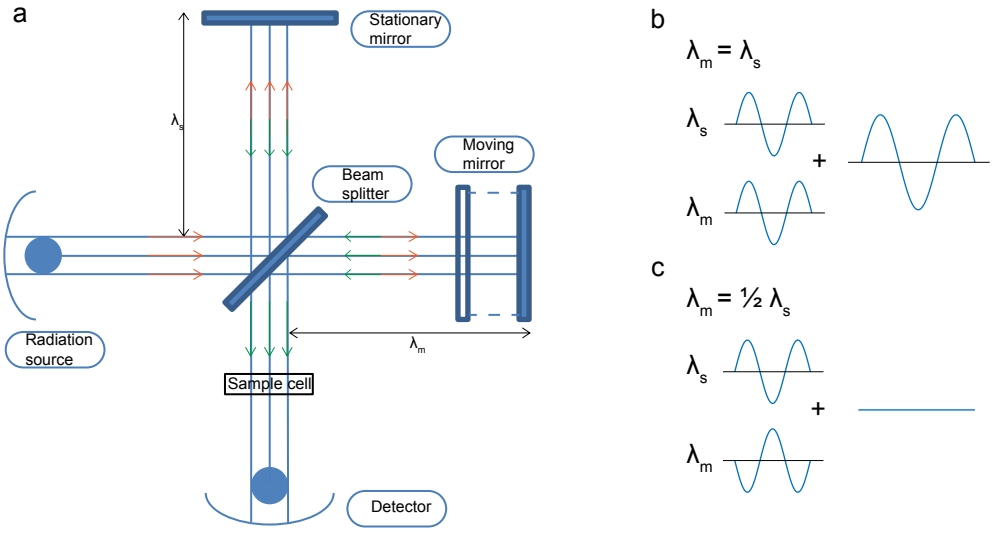

Figure 4.5: Schematic representation of a Michelson Interferometer. (a) The red arrows indicate the radiation which comes from the radiation source, passes through the beam splitter and reaches the two mirrors, stationary and moving. The green arrows indicate the reflected radiation from the two mirrors back to beam splitter which reaches the sample cell. λ_s is the distance between the beam splitter and stationary mirror and λ_m is the distance between the beam splitter and the moving mirror. The two extreme radiations obtainable are showed in (b) constructive interference and (c) destructive interference.

PARAFAC Parallel Factor Analysis (PARAFAC) is a chemometric (statistical) tool used to analyze a multiway dataset, i.e. a three dimensional dataset.[142] PARAFAC decomposes a tensor, which can be understood as a generalization of matrices of higher orders; for example a two-way tensor can be represented as a matrix, while a three-way tensor can be understood as a 'data cube' (Figure 4.6 tensor X), into loadings and scores in a suitable sub-space (Figure 4.6 matrix A, B and C). PARAFAC is an unsupervised tensor decomposition, i.e. it does not

have 'knowledge' of the physical meaning of the data analyzed (for instance enzyme dosages). In this way it has the ability to find common profiles and/or patterns present in all samples and to perform a fitting where all those common profiles are taken into account simultaneously, resulting in an unique solution.[143] The unique solution is obtained through an iterative process and is achieved when the right number of components give a good linearity (R^2) (Figure 4.6 calibration curve) and when a core consistency diagnostics number known as the CORCONDIA number is applied. Figure 4.6 is an example of a single component PARAFAC decomposition into one set of single matrices A, B and C (Figure 4.6). Matrix A or spectral mode loadings contains the fingerprints of the enzymatic system that is completely enzyme dosage independent; matrix B or time mode loading contains the spectral number as a function of enzyme dosage and is time dependent; and matrix C or scores describes the projections of the spectral changes in A in relation to enzyme dosage in B. If a high correlation is obtained, the spectral mode loadings (Figure 4.6 matrix A) represent the true enzymatic oxidation pattern.[136] In some cases the solution cannot be found using one single component and more than one are needed. This is mainly the case when some other events take place during the monitored reaction, for example product precipitation. The CORCONDIA number describes the maximum number of components necessary for the PARAFAC model to fully describe the dataset; this nuber should be as close to 100% as possible yet not lower than 90%.[144]

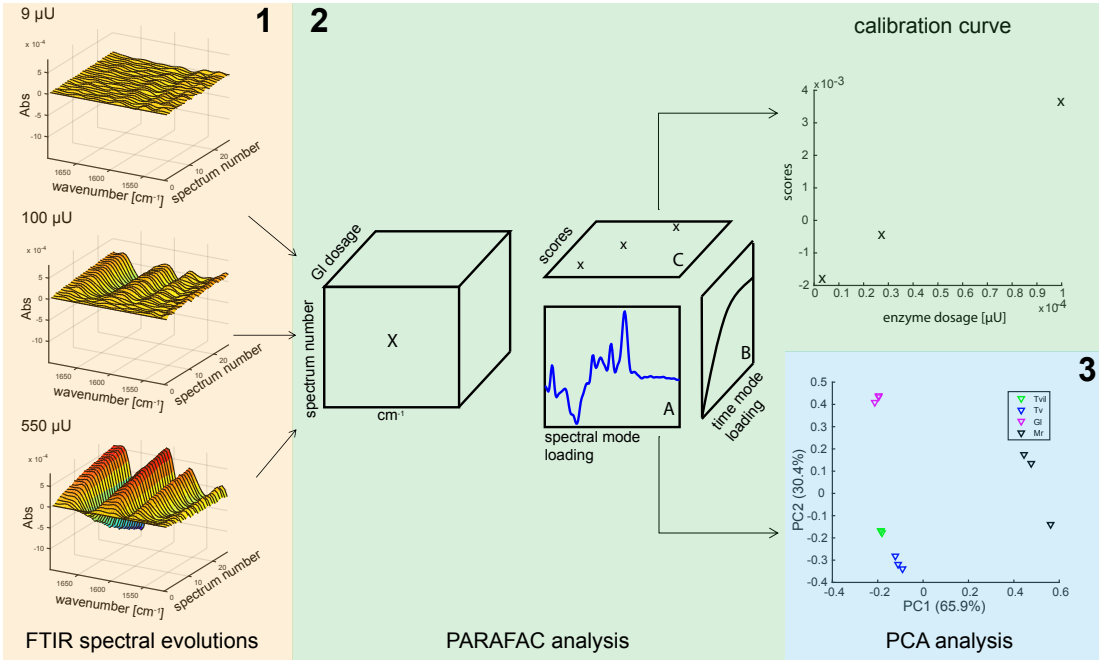

Figure 4.6: Schematic representation of FTIR spectra and chemometric analysis. A three step approach is shown: 1. Evolution profiles for three different Gl laccase dosages obtained by FTIR (orange background), 2. PARAFAC decomposition (green background) and 3. PCA analysis (blue background). Evolution profiles are stacked in order to form the tensor X. PARAFAC decomposition of tensor X into loadings and score matrices is illustrated in this example by using one component. The two loading matrices are A; spectral mode loading, B; time mode loadings and matrix C represents scores. PARAFAC scores (matrix C) are plotted vs. the enzyme dosage to obtain calibration curves. PARAFAC spectral mode loadings (matrix A) from several PARAFAC models (each replicate analysis) are combined using PCA to perform spectral pattern recognition and hence enzyme similarity clustering.

PCA Principal Component Analysis (PCA) is a statistical analysis which simplifies multidimensional datasets into fewer dimensional representations emphasizing differences in the dataset.[145] PCA decomposes the dataset in loadings and scores, where the loadings are the orthogonal projection in space describing the maximum variance in the data and the scores are a measure of the abundancy of the loadings in the reduced space, hence the scores are used to compare samples between each other. The projections describing the maximum variance are called Principal Components (PC), and usually a small number of these PCs are needed to describe the major variance in a dataset.[145]

The methodology of Baum *et al.*,[137] was used in this study to assay laccase activity on the simple phenolic compounds: sinapic acid, sinapic aldehyde, sinapyl, coniferyl and *p*-coumaryl alcohol (Figure 4.1). Additionally, we used PCA to compare reaction pathways for four laccases of different origin, namely three fungal laccases from *Trametes versicolor* (Tv), *Trametes villosa* (Tvil) and *Ganoderma lucidum* (Gl) and one bacterial laccase from *Meiothermus ruber* (Mr) in order to find common or different patterns in the evolution profiles.

4.2.1 Evolution profiles and calibration curve determination

Laccase oxidation of five different substrates was initiated by addition of the enzyme and injected into the FTIR instrument that measured the reaction IR spectra for 30 minutes continuously to obtain the so-called evolution profiles (Figure 4.7).

Each laccase substrate oxidation is characterized by a specific evolution profile (Figure 4.7A) that depict the spectral changes evolving over time, which are most likely related to bending and stretching of the unsaturated aromatic or aliphatic C-C bonds.[146] Both a control experiment measuring the evolution profile without the addition of the enzyme and a dose response experiment were performed to be sure that the changes measured were due only to enzyme activity (Figure 4.7B). A clear increase in the signal was detected by increasing the enzyme dosage (Figure 4.7B). However in order to assess mathematically whether these increases followed a linear patter, the spectral evolution profiles were analyzed with PARAFAC.

PARAFAC analysis was performed for the four laccases on the five different substrates. In all cases a linear correlation between score and enzyme dosage was found with a correlation factor $R^2 \geq 0.83$. The calibration curves obtained are a measure of laccase activity on each specific compound, taking into account both substrate depletion and product formation, and hence, describe the reaction in all its complexity and provide a more specialized activity assay. Due to the unsupervised property of PARAFAC, the calibration curves can show either positive or negative slopes which do not have any physical/chemical meaning,[137] i.e. the sign is not related to product formation or substrate depletion.

In the majority of the PARAFAC analyses the decompositions were performed with one component, but in a few cases two components were necessary to yield a valid model. D_2O was

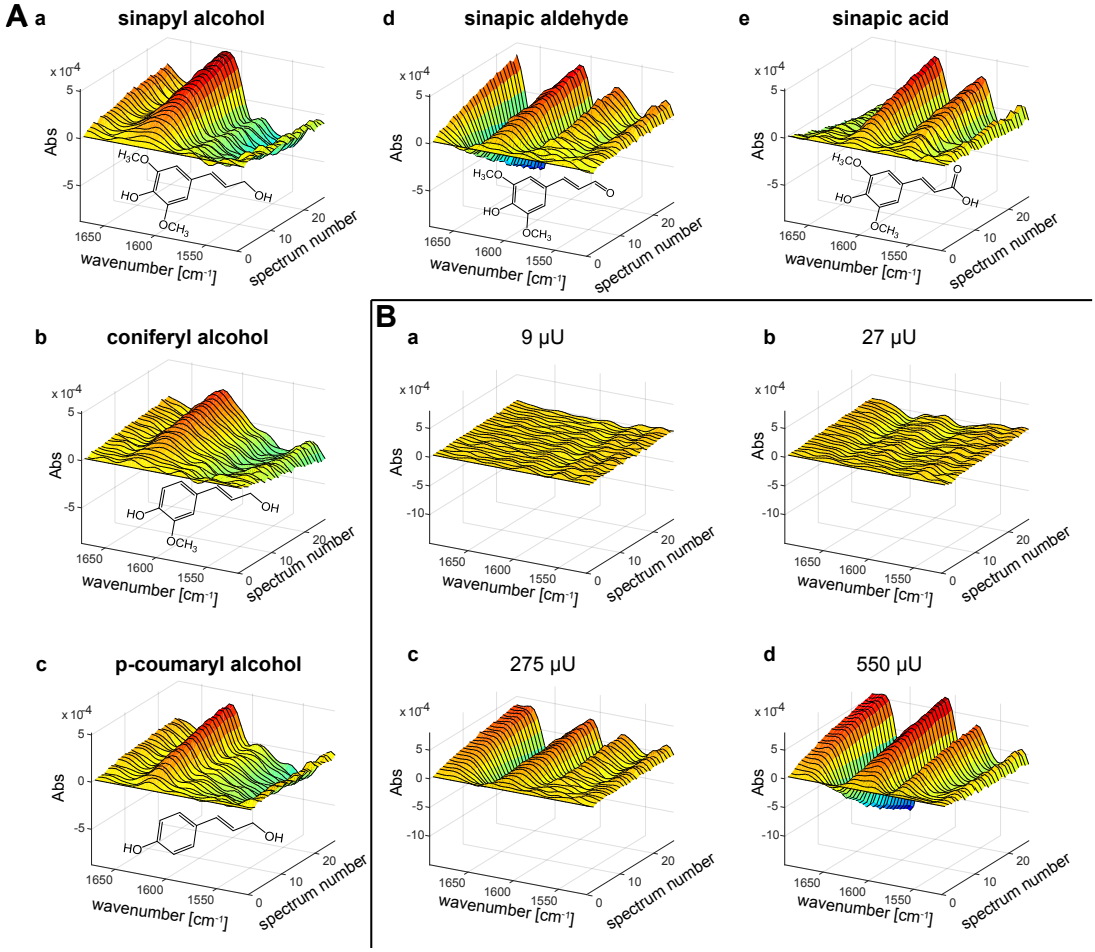

Figure 4.7: Examples of FTIR evolution profiles of laccase oxidation of different substrates. Panel A shows the evolution profiles of oxidation of 9 mM of sinapyl alcohol (a), coniferyl alcohol (b), *p*-coumaryl alcohol (c), sinapic aldehyde (d) and sinapic acid (e) using 275 μU (U expressed as syingaldazine units) of Gl laccase. Panel B shows the evolution profiles of the laccase oxidation of sinapic aldehyde at four different dose of Gl laccase: 9μU (a), 27μU (b), 275μU (c) and 550μU (d).

used to remove H-O bands of water in the mid infra-red region in order to be able to monitor the reaction changes during laccase oxidation of the small soluble phenols. If an exchange of H^+ with deuterium in D_2O occurred, the proton exchange effect will be superimposed on the true laccase reaction and therefore a second component is needed to separate the two effects.[139]

4.2.2 How to compare evolution profiles from different laccase

The evolution profiles obtained from the FTIR can be understood as laccase specific reaction fingerprints. The methodology was used to compare laccases from different origins, i.e. the three fungal laccase Gl, Tv and Tvil and one bacterial laccase Mr, and understand whether or not they were acting equally on the same substrate. The analysis to achieve this understanding was not straight forward and different pathways were studied.

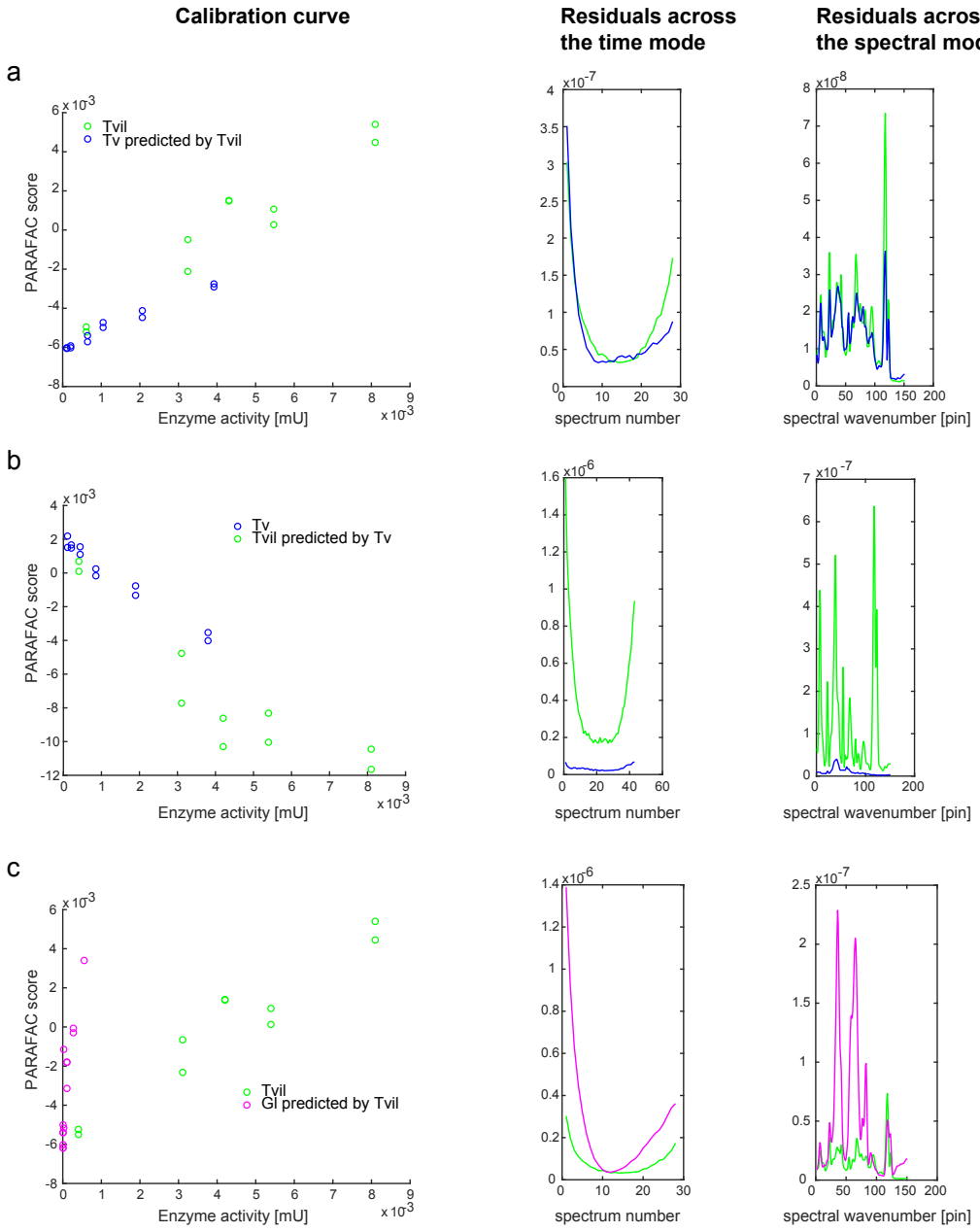

Figure 4.8: Prediction of laccase behavior on sinapic acid using a second laccase. Calibration curves, residual across the time and spectral mode are shown. (a) Prediction of Tv evolution profile using Tvil laccase, (b) prediction of Tvil evolution profile using Tv laccase and (c) prediction of Gl evolution profile using Tvil laccase.

4.2.2.1 Prediction of laccase behavior

The first approach to asses if two laccases acted equally on the same substrate was to predict the evolution profile of one laccase using a second one. Three parameters were studied in order

to explain differences or equality, namely calibration curves, residuals across the time mode, and residuals across the spectral mode. The two latter parameters are used as measure on how the predicted laccase behavior fits the behavior of the laccase used for the prediction. The more similar the evolution profiles of the enzymes are, the closer are the residuals, which in turn results in two calibration curves with the same slope. Some examples of this approach are shown in Figure 4.8 in the case of sinapic acid oxidation.

When the prediction of Tv laccase evolution profile was done using Tvil laccase (Figure 4.8a), similarity between the enzymes was found. If the opposite was performed instead, i.e. the Tvil laccase evolution profile was predicted by Tv (Figure 4.8b), neither the residuals across the time mode nor residuals across the spectral mode lay on top of one another. Since the previous analysis showed a similarity between Tv and Tvil, the same result was expected in the opposite case also. It was hypothesized that the differences obtained in the second analysis were due to the different range of enzyme activity used in the experiment. Tvil was dosed at higher syringaldazine dosages compared to Tv, and hence when Tvil was predicted by Tv laccase (Figure 4.8b) the data were extrapolated which led to the difference in the final result. When Tv was predicted by Tvil laccase instead, almost all the dosage range used for Tv fell within the Tvil dosage range (Figure 4.8a). Therefore Gl laccase evolution was modelled with Tvil to verify the extrapolation limitation of the analysis (Figure 4.8c). In this case also, due to differences in laccase dosage range, Gl behavior was extrapolated from the calibration curve of Tvil laccase. With this type of analysis it was not possible to estimate whether the difference seen was due to laccase origin or were due only to bias from the different activity levels used. Therefore a better approach to compare laccase had to be considered.

4.2.2.2 Spectral mode loadings comparison

The different activity ranges used in this study did not allow easy comparison between the laccases and therefore an activity independent strategy was adopted. Another output of PARAFAC analysis is spectral mode loading. If the calibration curve has a high linearity level ($R^2 \geq 0.8$) spectral mode loading give a laccase dose independent representation of the overall reaction fingerprint on a specific substrate. Since the R^2 requirement was verified for all calibration curves, comparisons between laccases from different origins were performed using the spectral mode loadings (Figure 4.9a). Even though it was possible to see similarities or differences between laccases on sinapic aldehyde by plotting the spectral mode loadings for the different enzymes (Figure 4.9a), a more detailed analysis to assess precisely the relatedness between enzymes was performed using PCA analysis (Figure 4.9 b, c and d). The closer the points in the PCA plot are to each other, the more the laccases are related. Figure 4.9 shows three examples of PCA plots from which different information can be obtained. For example, in the case of sinapic aldehyde, PC1 appears to separate the fungal laccases Gl, Tv and Tvil from the bacterial Mr, while PC2 appears to discriminate between the fungal laccases; the *Trametes* sp. Tv and Tvil laccases had similar reaction fingerprints while that of Gl laccase was different (Figure 4.9b). In the case of sinapic acid, all laccases regardless of origin had a similar reaction fingerprint

since all the laccase points are clustered together (Figure 4.9c).

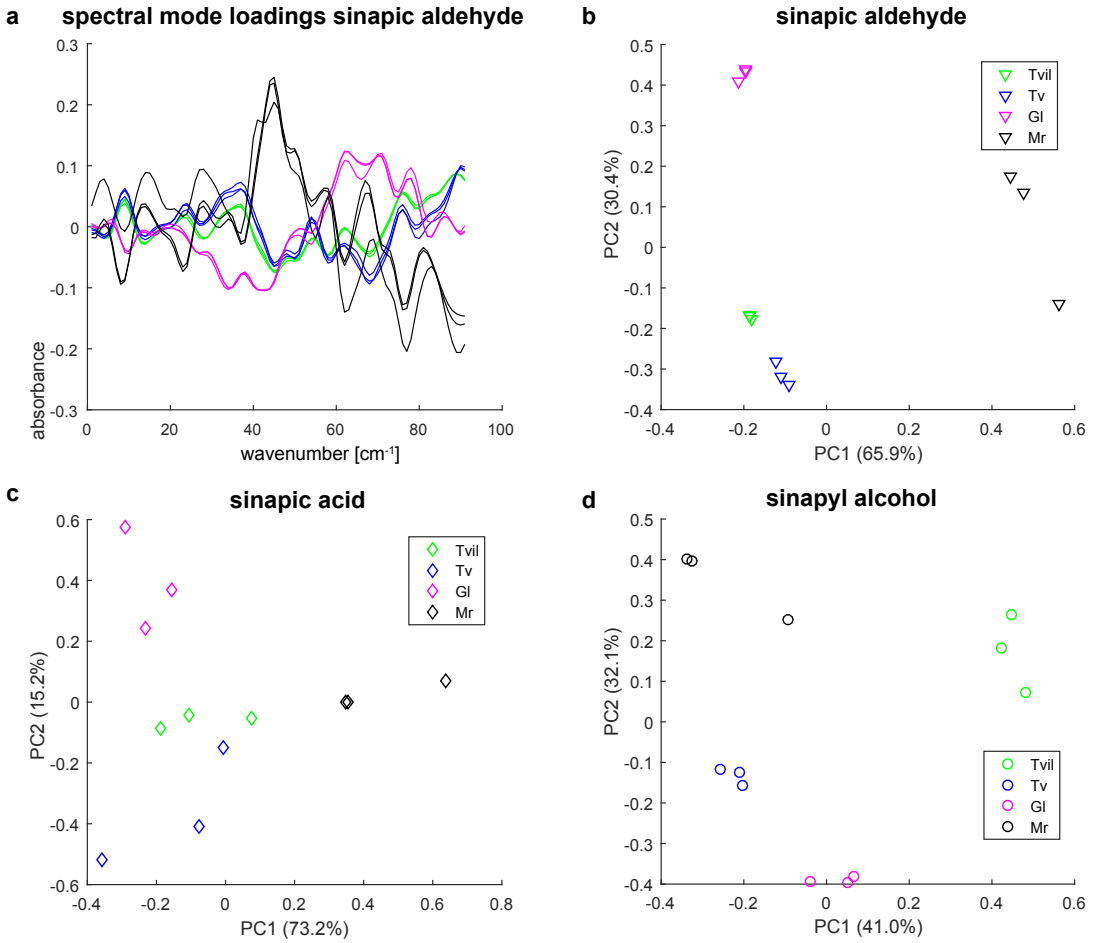

Figure 4.9: Spectral mode loadings and PCA analysis of the PARAFAC loadings. Spectral mode loadings from PARAFAC analysis of sinapic aldehyde (a) are shown for each of the four laccases. For each substrate sinapic aldehyde (b), sinapic acid (c), sinapyl alcohol (d) Principal Component 2 (PC2) was plotted vs. Principal Component 1 (PC1) in order to show relatedness between enzymes. In each plot the percentage of variance explanation of the two PCs are reported in brackets. In all plots Tvil laccase is shown in green, Tv laccase is shown in blue, Gl laccase is shown in magenta and Mr laccase is shown in black.

In the last case of sinapyl alcohol oxidation, all laccases appeared to have a specific reaction fingerprint, and even the two laccases from the *Trametes* sp., Tv and Tvil, were found to have two different reaction evolutions (Figure 4.9d). Another level of knowledge can also be obtained from PCA analysis in that the technique enables us to know which wavenumber ranges are responsible for the major differences between the laccases. Even though it is important to know where these differences are, the methodology cannot directly relate the wavenumber range to a chemical interpretation of the changes. It is known[52,147] that fungal and bacterial laccases have different structures and redox potentials, and such difference may explain the differences observed between the Mr laccase and all the fungal laccases. Alternatively, the differences observed between the fungal laccases, especially between laccasses of Gl and the *Trametes* sp., may be due to structural differences and capability to extract and shuttle the electrons in the

enzyme structure, which result in differences in oxidation rates.

It has been shown before that laccase activity can be quantified using calibration curves. However, due to the differences measured, an unique calibration curve for determination of laccase activity on a specific compound cannot be performed, which is a limitation of the methodology.

4.3 Conclusions

The data in these two studies (Paper 1 and Paper 2) verified hypothesis H2; two new methods for screening laccase activity on simple soluble phenolic compounds were studied using two different techniques and results showed that a clear laccase specificity and affinity exist within the different lignin subunits.

LC-MS allows fast real time measurements quantifying laccase activity by monitoring substrate depletion. Moreover, LC-MS can give information about the product profile after substrate oxidation by laccase. Kinetic measurements and product profiles were performed for two fungal laccases, Gl and Tv laccase, and no differences were obtained between the two enzymes either, in terms of kinetic parameters or of resulting oxidation products.

FTIR combined with PARAFAC analysis can be also used for laccase activity determination by means of calibration curves. The activity is measured taking into account both substrate depletion and product formation and constitute a methodology capable of describing the laccase reaction in its all complexity. Spectral evolution profiles were also used to assess whether or not laccase origin could result in differences in the reaction fingerprints. The enzyme dose independent PARAFAC output spectral mode loadings were analyzed using PCA to obtain a mapping plot which made it possible to see differences in spectral evolution pathways based on laccase origin. The bacterial laccase Mr appeared always to have a different reaction fingerprint to the fungal laccases, and in general Gl laccase also showed some differences compared to the *Trametes* sp. Tv and Tvil.

The differences between enzymes measured in FTIR can appear to go against the results obtained in the LC-MS study where no differences in both the kinetic parameters and product profiles of the Gl and Tv laccases were obtained, but that is not the case. FTIR measures all the changes in wavenumber taking place during the evolution of the reaction, and also takes account of unstable reaction intermediates and radicals,[148] while LC-MS mainly measures the final products masses after radical coupling. Therefore the differences seen in the evolution of the reaction of Gl and Tv laccase in FTIR may be due to structural differences. The latter could lead to different abilities in extracting and shuttling the electrons in the enzyme structure with the result that different oxidation rates are obtained and intermediates are formed. Even if the final point seen in LC-MS is the same for Gl and Tv laccase, they may differ in how that point was reached.

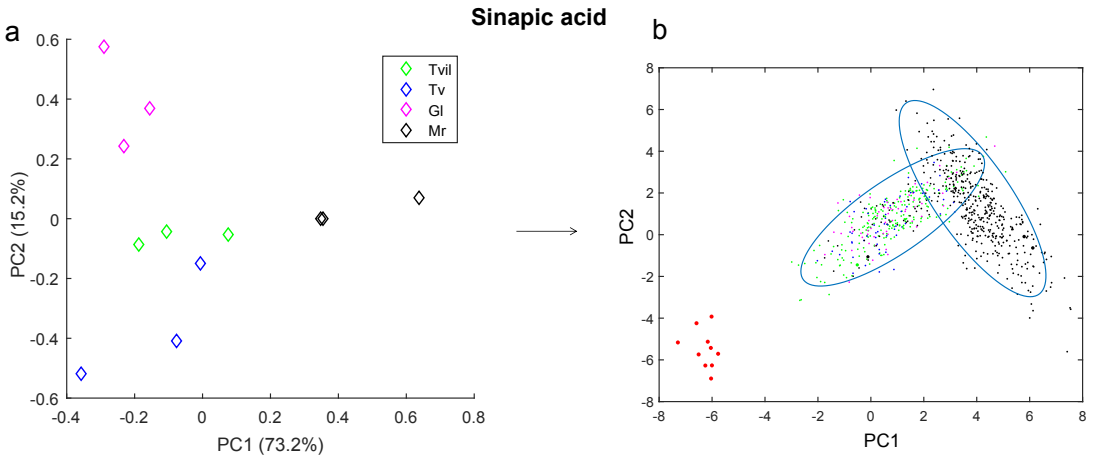

Figure 4.10: High throughput analysis of protein engineered clones expressing laccase. Red points in the right hand plot are showing outstanding mutants with different behavior compared to the reference system. The plot on the right hand side is a simulation illustrating a prediction (it does not show genuine experimental data).

The high affinity of Gl and Tv laccase to sinapic acid obtained from the kinetic parameter in the LC-MS assay (Paper 1) and the lower level of differences level in terms of evolution profiles observed in the FTIR assay (Paper 2) make sinapic acid the best candidate for screening laccase activity. While LC-MS would give information on laccase activity, the FTIR measurements could be used in protein engineering for screening different mutants and highlighting outstanding mutants with distinctive activity (Figure 4.10). Potentially FTIR could be applied to a large set of data (Figure 4.10 b). After definition of a reference system, i.e. obtained by assessing more replicates of Tv, Tvil, Gl and Mr laccase, FTIR could offer the advantage of identifying unknown odd-behaving laccases (Figure 4.10b red dots) without prior knowledge of reaction mechanisms; the distinctive laccases could then be analyzed with conventional techniques, such as LC-MS or NMR, to address specifically the origins of the differences observed.

Chapter 5

Laccase kinetics on lignin measured by EPR

This chapter focuses on the determination of laccase kinetics measured on lignin (Paper 3) and addresses the following hypothesis and objectives:

H3 Studying laccase kinetics on lignin provides new clues of the role of laccases during lignin processing in application and degradation in nature.

Obj5 To study laccase kinetic on lignin quantitatively using Electron Paramagnetic Resonance (EPR) spectroscopy.

Obj6 To investigate whether laccase kinetic parameters on lignin differ from the kinetic parameters on the small soluble compounds obtained in Paper 1

Assessing laccase kinetics and activity on small soluble phenolic compounds, as in Chapter 4, describes laccase activity better than the traditional methods due to the use of more lignin-related compounds, but does not really assay and quantify the real laccase oxidation on lignin. Munk *et al.*[149] developed a laccase activity assay that measures the first laccase product after oxidation of lignin, namely the radicals, using Electron Paramagnetic Resonance (EPR) spectroscopy.

Species with unpaired electrons can be studied by EPR because these electrons can move between their two spin states when an external magnetic field is applied.[150,151] EPR monitors the net energy absorption caused by the electron shift of energy state, i.e. the electrons are

found in a lower resting energy state and when the magnetic field is applied they tend to move to the higher state level.[150] This adsorption energy is converted into a spectrum which is specific for each compound. The spectrum characteristics are related to the radical structure and are influenced by the radical quantity, environmental conditions and hyperfine interaction with neighboring nuclei.[152] The simplest spectrum is obtained for a single radical and is described by only one line, i.e. only one peak. In the presence of more radicals, the spin interaction with the nearby nuclear spins gives rise to hyperfine splittings and therefore EPR spectra with more than one line.[150,151] An example of a multiple line spectrum is the stable nitroxyl radical TEMPO (2,2,6,6-tetramethyl-1- piperidinyloxy), which consists of three symmetrical peaks due to the mobility of the NO• radical in the solution (Figure 5.1 1).

An intrinsic correlation known as the g-value exists between the unpaired electrons and the magnetic field in EPR. The g-value can be interpreted as being similar to the chemical shift values in NMR and is thus a unique identifier for a given paramagnetic species.[151,152] The g-value depends on the chemical environment, i.e. molecular arrangement. For organic molecules the g-value is small and close to the g-value of a free electron ($g \sim 2.0023$), whereas the g-value is large in transition metals (for Fe^{3+} in rubredoxin $g = 4.32$).[151]

EPR spectroscopy can be used to measure radicals in lignin.[153–155] Due to the high complexity of the lignin molecule, quinone radicals are present in the lignin molecule also prior to laccase oxidation (Figure 5.1 4 red line).[153–155] Even if the chemical structure of the semiquinone radicals are different, they share the same overall g-value which results in a single line spectrum (Figure 5.14).[156,157]

The real time formation of the first laccase product on lignin, i.e. semiquinone radicals, can be measured and quantified using the stable TEMPO radical as standard (Figure 5.1 1, 2 and 3). TEMPO radicals are a suitable quantitative standard for lignin because they share the same overall g-value, hence the EPR lignin spectrum (Figure 5.1 4) lies on same magnetic field as the middle peak of TEMPO (Figure 5.1 1). After measuring the EPR spectra of different concentrations of TEMPO (Figure 5.1 1), a double integration of the EPR spectra (Figure 5.1 2) is done to correlate the area below the spectrum to a TEMPO radical concentration and obtaining a standard curve (Figure 5.1 3). During laccase oxidation of lignin the concentration of radicals increases obtaining a broader spectrum (Figure 5.1 4 blue line) is obtained compared to the lignin background (Figure 5.1 4 red line). Radical quantification during laccase reaction is determined by subtraction of the lignin blank from the reaction spectrum (Figure 5.1 4 yellow line) and hence the double integration is performed on the resulting spectrum (Figure 5.1 5). The area obtained underneath the peak is then correlated with the TEMPO radical concentration using the calibration curve. This technique was used to quantify radical formation on organosolv lignin during its oxidation by three different laccases namely *Ganoderma lucidum*(Gl), *Trametes versicolor* (Tv) and *Myceliophthora thermophila* (Mt) laccase.

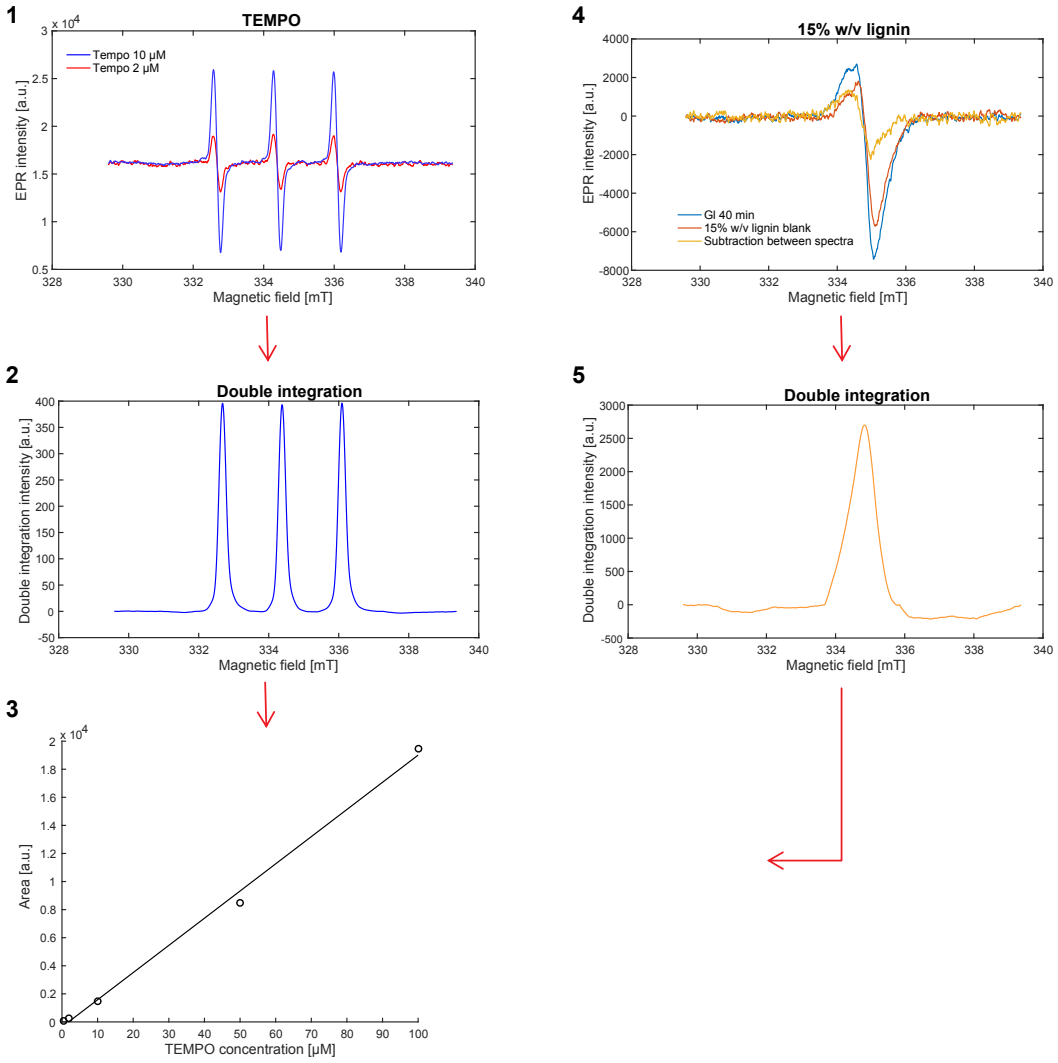

Figure 5.1: Schematic representation of the EPR technique and data analysis. 1) Typical three line EPR spectra of 10 μM (blue) and 2 μM (red) TEMPO. 2) Double integration of the TEMPO spectrum. 3) TEMPO calibration curve. The areas obtained in 2) are plotted vs. the TEMPO concentrations. 4) EPR spectrum of Gl laccase 15 minutes reaction (blue) with 15% w/v lignin, EPR spectrum of the blank 15% w/v lignin (red) and the resulted EPR spectrum after subtraction of the blank from the reaction spectrum (yellow). 5) Double integration of the subtracted spectrum in 4). The area below the peak is then converted to a radical concentration by employing the TEMPO calibration curve in 3).

5.1 Kinetics

Radical formation was monitored for Tv, Gl and Mt laccase at different organosolv lignin concentrations and initial radical formation rates were determined after 30 minutes of reaction. By plotting these initial rates against lignin concentration converted into a phenolic concentration obtained from P-NMR analysis,[158,159] Michaelis-Menten kinetics were fitted for all three laccases (Figure 5.2a). The enzymes were dosed based on the syringaldazine units due to differences in purity of the laccases and hence apparent specific activities and apparent catalytic efficiencies were determined. The three laccases showed different behavior towards organosolv lignin (Table 5.1). Even though Tv laccase was the fastest enzyme, Gl laccase showed the highest affinity to organosolv lignin, with an apparent catalytic efficiency = $3.03 \cdot 10^{-4}$ 1/U·s, followed by the Tv laccase, while Mt laccase showed the lowest apparent catalytic efficiency = $0.53 \cdot 10^{-4}$ 1/U·s (Table 5.1).

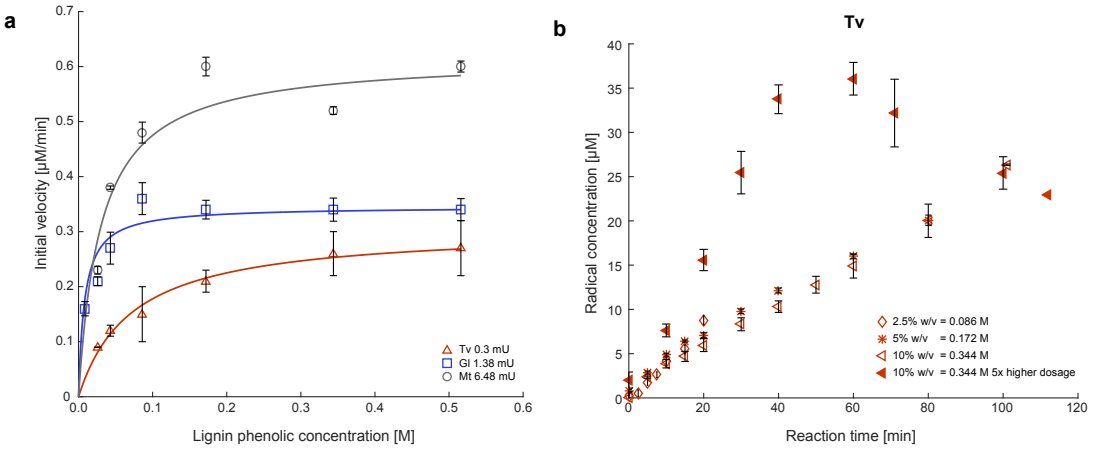

Figure 5.2: Michaelis-Menten curves for Tv, Gl and Mt laccases (a) and radical formation at different lignin phenol concentrations for Tv laccase (b). (a) Tv (red triangle), Gl (blue square) and Mt (grey circle) kinetic curves are shown. Phenol concentration determined based on phenol content in lignin. (b) radical formation vs. extended reaction times at different lignin concentrations: 2.5% w/v, diamond; 5% w/v, star and 10% w/v, left-pointing triangle, are shown. Tv laccase dosed 0.3 mU and Tv laccase dosed five times higher on 10% w/v lignin (1.5 mU). Standard deviations are also shown.

Gl and Tv laccase kinetic parameters can be compared directly with the kinetic parameters of the small soluble phenols obtained in Chapter 4 Section 4.1.1 (Table 5.1). The K_m values for sinapic acid are three orders of magnitude higher than K_m obtained for lignin. In addition, due to the low enzyme dosage used in the LC-MS study compared to the laccase dosage for lignin oxidation, the apparent catalytic efficiency of sinapic acid is twelve orders of magnitude higher than that of lignin (Table 5.1). It is therefore clear that laccases in general work better and faster on small soluble phenols than on the insoluble lignin substrate. One explanation could be that the high complexity of the lignin structure hinders the accessibility of phenols to laccase oxidation. This would mean that the amount of phenols that laccase can react with is lower than the theoretical amount, which results in slower kinetics compared to the soluble

compounds where all the phenol are accessible for laccase oxidation.

Table 5.1: K_m, V_{max}, apparent specific activity and apparent catalytic efficiency for hydroxycinnamic acids and OH-dilignol.

		Mt	Gl	Tv
Lignin	V_{max} [μM/min]	0.62 ± 0.01	0.36 ± 0.03	0.30 ± 0.04
	K_m [mM]	30.1 ± 0.7^{y}	$15.3 \pm 3.7^{b,z}$	$73.0 \pm 5.9^{b,x}$
	Apparent specific activity [μM/U·s]	1.59 ± 0.02^{z}	$4.52 \pm 0.14^{b,y}$	$16.8 \pm 2.2^{b,x}$
	Apparent catalytic efficiency [1/U·s]	$0.53{\cdot}10^{-4} \pm 0.02{\cdot}10^{-4\,y}$	$3.03{\cdot}10^{-4} \pm 0.65{\cdot}10^{-4\,b,x}$	$2.42{\cdot}10^{-4} \pm 0.56{\cdot}10^{-4\,b,x}$
Sinapic acid	V_{max} [μM/min]		1.06 ± 0.03^{x}	1.15 ± 0.07^{x}
	K_m [mM]		$12{,}110 \pm 460^{a,x}$	$12{,}130 \pm 2230^{a,x}$
	Apparent specific activity [μM/U·s]		$6{,}970 \pm 220^{a,x}$	$8{,}320 \pm 470^{a,x}$
	Apparent catalytic efficiency [1/U·s]		$5.5{\cdot}10^{8} \pm 0.4{\cdot}10^{8\,a,x}$	$5.7{\cdot}10^{8} \pm 1.0{\cdot}10^{8\,a,x}$

Standard deviations are shown and significant difference ($p \leq 0.05$) of K_m, apparent specific activity and apparent catalytic efficiency column-wise only for Tv and Gl laccase are shown as superscripted letters (a-b), significance difference ($p \leq 0.05$) of K_m, V_{max} (only for sinapic acid), apparent specific activity and apparent catalytic efficiency row-wise are shown as superscripted letters (x-z).

5.2 Radical evolution

Radical formation at longer reaction times was monitored, and a plateau in radical concentration was found for all enzymes and all lignin concentrations, followed by a decrease in radical concentration. This plateau was dependent on lignin concentration and enzyme dosage; i.e. when dosage of Tv laccase was increased five times, the radical plateau was found after 60 minutes, while with the lower enzyme dosage, the plateau was not reached even after 100 minutes (Figure 5.2b). A test was made to find out whether the plateau was caused by enzyme inactivation or substrate depletion. While addition of extra enzyme during reaction had no effect, the addition of extra substrate resulted in an increase in radical concentration, confirming that not all the phenols present in lignin are accessible for laccase oxidation. Since radicals are unstable species they tend to stabilize themselves by quenching.[160] Therefore the disappearance of radicals was assessed by inactivating the laccases during reaction at different times and following the decrease in radical concentration over time (Figure 5.3a). Radical quenching happened very fast following an apparent first order reaction initially, and then slowed down and reached a steady level of radicals (Figure 5.3a). The first and faster radical disappearance is most likely due to quenching of the radicals (Figure 5.3c1), while the second slower part could be due to consecutive radical reactions taking place as electron transfer reactions (Figure 5.3c2). The latter reactions are less thermodynamically favored due to the higher stability of the species and hence would give rise to a much slower reaction.[161]

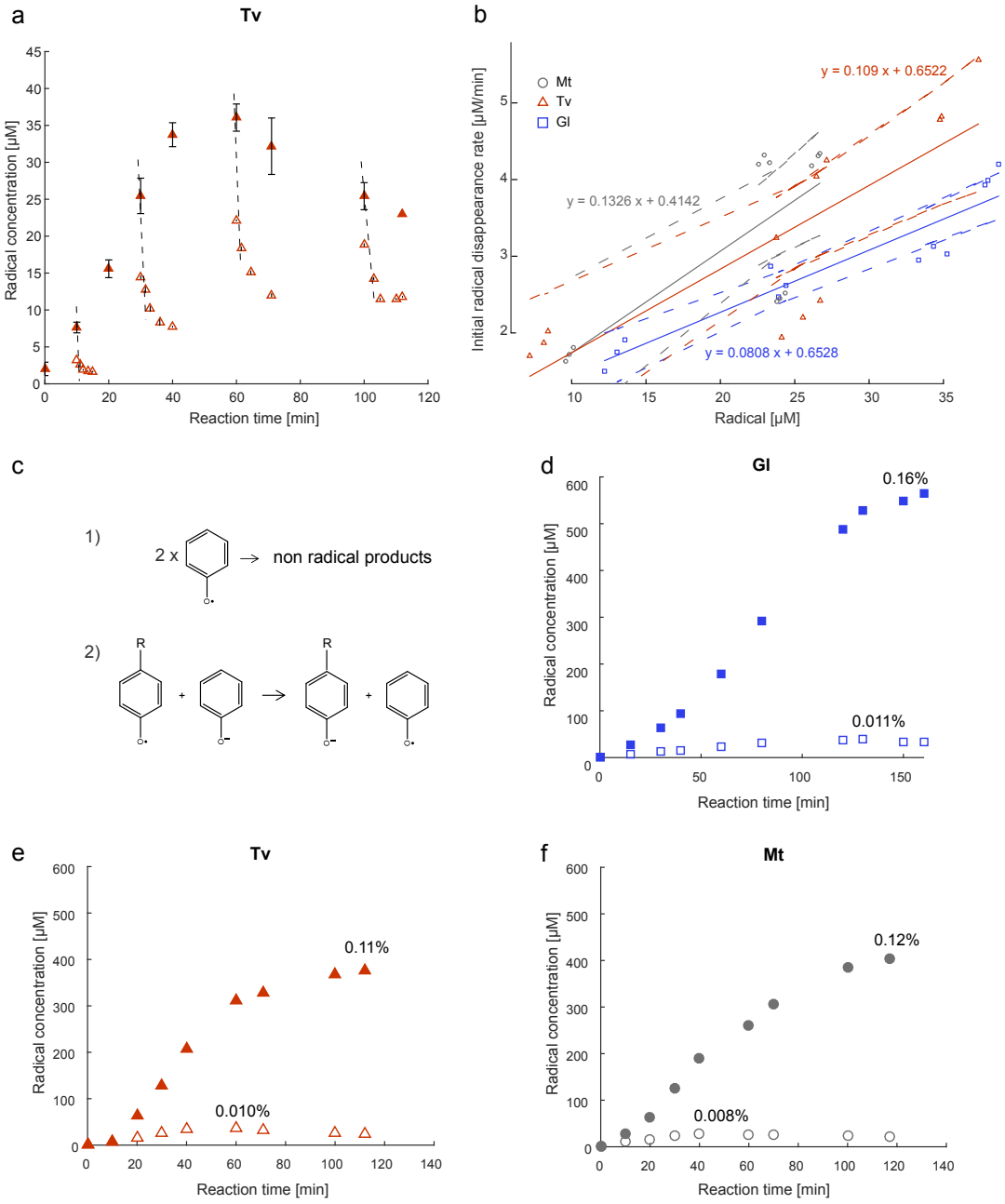

Figure 5.3: Radical disappearance (a), radical disappearance rate (b), possible radical reaction happening during disappearance (c), and theoretical radical formation (d, e, f). (a) The reaction of Tv laccase with 10% w/v lignin was followed over time and the enzyme was inactivated at different time point (10, 30, 60 and 100 min) with NaN_3 (red open triangle). The black dashed lines indicate the initial radical disappearance rates and the close red triangle show the reaction without enzyme inactivation. (b) Radical disappearance rate vs. the radical concentration before enzyme inactivation for the three laccase: Gl, blue square; Mt, grey circle and Tv, red triangle. 95% confidence intervals (Gl, blue dotted line; Mt, grey dotted line and Tv, red dotted line) and linear correlations between disappearance rate and radical concentration (Gl, blue line; Mt, grey line and Tv, red line) show that the decay rates are essentially the same and following on average the equation $y = 0.1075\ x + 0.5731$. (c) Two possible reaction pathways taken by the radical during quenching (1) and electron transfer reaction (2). (d, e, f) Comparison between EPR measured radical concentration (open markers) and theoretical radical concentration (close markers) for Gl (d), Tv (e) and Mt (d) laccase. In all plots the conversion values at the maximum level of radical concentration are shown.

The initial radical disappearance rate was determined after 2 minutes from inactivation, i.e. when the disappearance was still in the first order reaction, and then plotted vs. the radical concentration prior to inactivation (Figure 5.3b). The overlapping of the 95% confidence intervals plotted for all enzymes in Figure 5.3b indicated, as expected, the independence of the radical disappearance from the enzyme origin and hence being only a chemical driven reaction. The radical concentration measured with EPR has to be understood as a sum of two opposite reactions related to radical formation after laccase oxidation of lignin and to the spontaneous quenching of the radicals. In the first part of the reaction, the radical concentration is dominated by laccase catalysed formation of radicals. When the substrate becomes limiting, a plateau in the formation rate is reached, and afterwards quenching of radicals is the dominating reaction, hence leading to a decrease in radical concentration. The coexistence of these two reactions affects the kinetic parameters determined in Table 5.1 which should be considered apparent.

5.3 Theoretical radical formation during laccase oxidation of lignin

A theoretical radical concentration of laccase oxidation of lignin might eventually be extrapolated based on the radical decay rates determined in Figure 5.3b. The linear fitting obtained by plotting the initial radical rate vs. the radical concentration (Figure 5.3b) could be used to determine the disappearance rate at all the data points at which radicals have been measured during reaction and adding this concentration to the EPR measured radicals, the theoretical radical concentration for each laccase was extrapolated (Figure 5.3 d, e and f). In the theoretical enzymatic radical formation, the concentration of radicals continued to increase as opposed to the measured concentration, for all three enzymes (Figure 5.3 d, e and f) up to a maximum level. This maximum in radical concentration was found at the same reaction time as the plateau in the radical measured by EPR. It is worth noticing that while the radical concentration at which this decrease happened for Tv and Mt laccase is equal to 350 μM, radical concentration is much higher and equal to 500 μM for the Gl laccase. Nothing is known about the Gl laccase structure but maybe it is capable of accessing more phenoxyl moieties than the other two laccases, as was also shown by the lower K_m i.e. higher affinity, determined after kinetic measurements (Table 5.1).

Substrate conversion was determined by dividing the maximum radical concentration measured by EPR during laccase oxidation of lignin by the total amount of phenols present in the specific lignin concentration, i.e. considering that the oxidation of one phenol results in the formation of one radical. The conversion values obtained for the radical concentration measured by EPR are low and around 0.010% (Figure 5.3 d, e and f) for the oxidation of 10% w/v lignin. The conversion values obtained from the theoretical curves are one order of magnitude higher and the maximum level obtained is for Gl laccase and equal to 0.16% (Figure 5.3d). Even though the radical quenching effect was not considered in this theoretical calculation, the conversion remained low, indicating that only a small portion of the phenol in lignin is accessible for laccase

oxidation.

5.4 Conclusions

EPR is a unique methodology which allows the study of the first laccase product, i.e. the radical, directly in the ongoing reaction without changing the properties of the sample, for example through solubilization or pyrolysis. EPR was used to determine the kinetic parameters of three different laccases. The kinetics of the three laccases differed and by comparing the apparent catalytic efficiency found for lignin to that of sinapic acid, a difference of twelve orders of magnitude was found, which showed a clear laccase preference towards soluble substrates. Radical concentration was used to estimate the total conversion of phenols to investigate how many lignin phenols were oxidized to radicals, and only 0.011% of the total phenols in the 10% w/v organosolv lignin phenols were detected as radicals. Little is known about the actual structure of the organosolv lignin used. It is possible that not all the phenols present in the structure were actually accessible for laccase oxidation. The finding that the theoretical radical conversion was only one order of magnitude higher (0.16%) supports the possibility.

We thought that using pure lignin derived from raw biomass would have showed an increase in laccase reactivity because of the less condensed lignin structure and the more natural substrate. Therefore an attempt was made to measure the radical formation of raw birch wood with EPR. The biomass contained trace amount of manganese[162] (Figure 5.4) which completely masks the phenoxy radical spectrum and therefore kinetics on natural biomass could not be performed in this study.

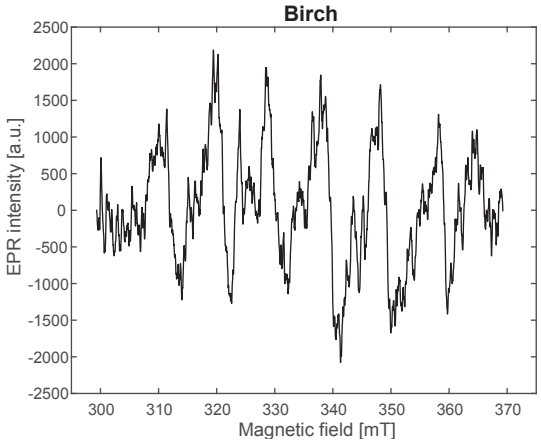

Figure 5.4: EPR spectrum of raw birch biomass.

EPR was also used to assess why the radical concentration reached a plateau followed by a decrease. At each time point two reactions take place at the same time: radical formation due to laccase oxidation of lignin, and radical disappearance due to radical quenching or secondary reaction of the radicals. From a chemical point of view, among the quenching types of reaction,

it is possible to find polymerization, depolymerization, grafting or modification of the lignin.[54] Laccase has always been defined as one of the enzymes involved in the depolymerization of lignin which is also sometimes able to enhance sugar release during enzymatic hydrolysis.[70,79] In the LC-MS study (Section 4.1) it was shown how easily laccase can activate soluble phenols which would then polymerize. Moreover, the comparison between the kinetic parameters on the small soluble phenols and on lignin lead to the conclusion that the affinity of laccases for lignin is much lower than their affinity for soluble phenols. These results verified hypothesis H3 and could raise the question as to whether lignin is the "real" laccase substrate. At the same time it is known that laccases are among the first enzymes secreted by fungi during delignification processes.[45–48] If the laccase gene is knocked out from the fungal genome, the fungi loses the ability to grow on lignin,[163] which implies that laccases play an important role during delignification processes. Some other questions can be raised, such as *are laccases necessary to start some processes that then activate other lignocellulosic enzymes?* And *why are so many unstable reactive species formed on the lignin structure?* The second question in particular was used to hypothesize whether the radical produced during laccase oxidation of lignin can eventually activate the oxygen present in the system to peroxyl radicals that can react further to form hydrogen peroxide.

Other enzymes present in the fungal genome are able to reduce O_2 to H_2O_2. These enzymes are known as oxidases: glucose oxidases, alcohol oxidases, aryl-alcohol oxidases and pyranose oxidase (AA3) and vanillyl-alcohol oxidases (AA4). Oxidases can act on glucose or on monomeric lignin compounds[44] and therefore are not active in the first part of the delignification process. Therefore if laccase can induce H_2O_2 formation in small concentrations but in a localized position and time, H_2O_2 will be available for other H_2O_2 dependent lignocellulosic enzymes, such as peroxidases, or eventually also LPMOs[164,165] and thus effective biomass degradation may be initiated.

Chapter 6

Do laccases produce H_2O_2?

This chapter focuses on the oxygen activation after lignin oxidation by laccase (Paper 4) and it addresses the following hypothesis and objectives:

H4 Laccase catalysed radical formation on lignin induces hydrogen peroxide formation, which is important in the overall redox reactions governing microbial lignocellulose degradation.

Obj7 To investigate whether laccase induced formation of H_2O_2 is independent on the origin of the laccase.

Obj8 To assess whether the H_2O_2 induced by laccase oxidation of lignin can be used to activate LPMO reactions.

Lignin oxidation by laccases might result in the formation of reactive oxygen species after oxygen activation and hence it was investigated if hydrogen peroxide was an endpoint of reaction for lignin radicals. The H_2O_2 formation was measured after oxidation of raw birch wood and organosolv lignin for four laccases from different origins: one fungal laccase from the ascomycetes family *Myceliophthora thermophila* (Mt), two fungal laccase from the basidiomycetes family *Ganoderma lucidum* (Gl) and *Trametes versicolor* (Tv) and a bacterial laccase from *Amycolatopsis* sp. 75iv2 (Slac).[79]

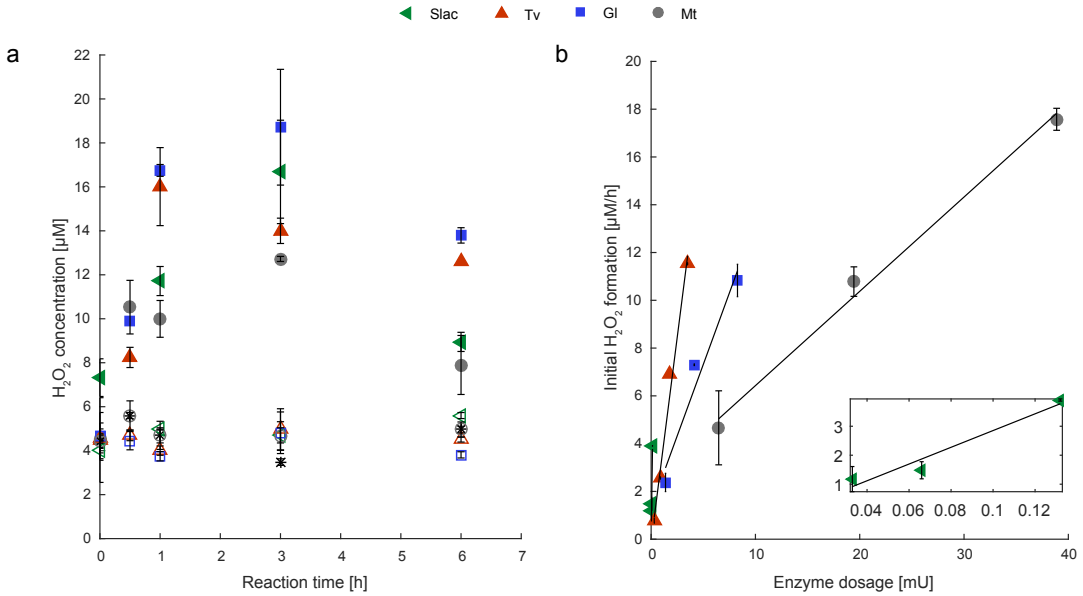

Figure 6.1: (a) H_2O_2 formation after laccase treatment of 5% DM birch by four different laccases. H_2O_2 concentration vs. reaction time for four laccases: 0.132 mU Slac (green close left-pointed triangle), 3.5 mU Tv (red close triangle), 8.28 mU Gl (blue close square) and 19.44 mU Mt (grey closed circle). H_2O_2 concentration from the birch substrate alone (black star) as well as the H_2O_2 concentration measured after incubation with heat inactivated laccase (open symbols) are shown. (b) Initial rate of H_2O_2 formation as a function of enzyme dosage on 5% DM birch for all four laccases. Symbols for each enzyme are equivalent to symbols in plot (a).

6.1 H_2O_2 formation on real biomass

H_2O_2 formation after laccases oxidation of raw birch biomass was followed for 6 hours for the four different laccase Gl, Tv, Mt and Slac (Figure 6.1a). For all four laccases H_2O_2 concentration increased in the first hour up to 10-17 μM (Figure 6.1a), after which the concentration of H_2O_2 started to decrease. Following radical concentration by EPR measurements (Figure 5.2b) showed that the radicals pursued the same progress curve, reaching a plateau followed by a decrease. Even though EPR measurements were performed on organosolv lignin and not on birch wood, it appears likely that the same events occurs for birch wood. So the stagnation and even decrease in radical concentration will eventually stop the formation of H_2O_2. The actual decrease in H_2O_2 observed in the experiment with birch wood, might also be related to decomposition by trace amounts of manganese (Figure 5.4) which could lead to Fenton reaction, i.e. hydrogen peroxide disproportionation into OH^- and $HO^\bullet$.[166,167]

The four different laccases were dosed at different syringaldazine units in order to obtain a relatively similar concentration of H_2O_2 after one hour of reaction. While Slac was not included in the EPR study on lignin kinetics, the other three laccases, Gl, Tv and Mt laccase, showed different affinities towards organosolv lignin. Therefore there would be no surprise if their affinities were also different towards the raw birch. Differences in laccase kinetics on lignin may

be reflected in the formation of H_2O_2. Birch biomass has a background concentration of H_2O_2 (Figure 6.1a) most likely due the radical background found in lignin (Figure 5.1 4 red line), and this level of H_2O_2 was not affected by the presence of heat inactivated laccase, showing that it was indeed the laccases inducing H_2O_2 formation (Figure 6.1a). In addition a dose response experiment was performed to verify that the measured H_2O_2 was obtained in the presence of laccase only (Figure 6.1b). Initial H_2O_2 rates determined after one hour reaction were plotted vs. laccase dosages and resulted in a clear linearity ($R^2 \geq 0.96$) for all four enzymes (Figure 6.1b).

H_2O_2 concentration was also measured after one hour laccase reaction with organosolv lignin (Table 6.1). Considering that the laccase reaction was performed on 10% w/v of organosolv lignin the H_2O_2 concentration measure after one hour is only slightly higher than the one measured for raw birch biomass where the lignin content is approximately 20% of the DM,[168] resulting in approximately 1% w/v in the laccase reactions. This result means that natural lignin is more easy to oxidize than the organosolv lignin that might contain some degree of condensation in the lignin structure.

Table 6.1: H_2O_2 formation after 1 hour laccase oxidation of organosolv lignin. H_2O_2 concentration stated as an average of triplicate determinations. The lowest row shows the inherent background level of H_2O_2 present in the organosolv lignin.

Laccase	$H_2O_2[\mu M]$
Mt	20.8 ± 4.4
Tv	26.1 ± 0.6
Gl	19.6 ± 1.8
Slac	19.0 ± 0.2
Organosolv lignin	5.28 ± 0.5

6.2 H_2O_2 formation mechanism

If the formation of H_2O_2 after laccase oxidation of lignin is achieved by oxygen activation, several can be the routes that the reactive oxygen species could follow to form H_2O_2:[165,169]

1. Oxygen can first undergo a reduction to a superoxide radical and then it can be further reduced to H_2O_2 either spontaneously, enzymatically or by small organic reductants.[165]
   $O_2 \xrightarrow{e^-} O_2^{-\bullet} \xrightarrow{e^- + 2H^+} H_2O_2$

2. Oxygen can directly undergo a two-electron reduction to H_2O_2[165]
   $O_2 \xrightarrow{2e^- + 2H^+} H_2O_2$

3. Two moles of peroxyl radicals can react to form a mole of H_2O_2 and a mole of oxygen[169]
   $2HO_2^{\bullet} \longrightarrow H_2O_2 + O_2$

4. Peroxyl radicals can extract the hydrogen from a lignin sub-molecule to form H_2O_2 and an activated lignin subunit[169,170]

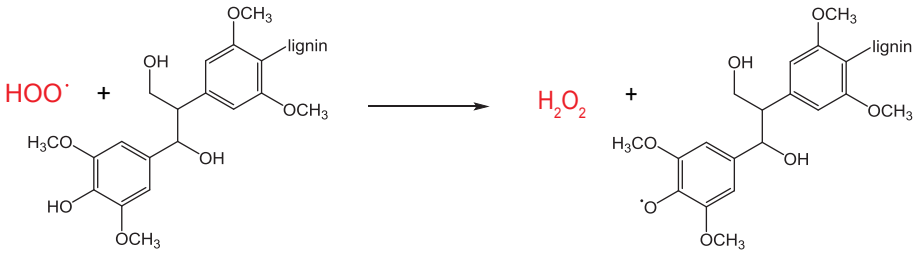

Ii is difficult to describe the entire complexity of the radical system created after laccase action on lignin and therefore it is not possible to know exactly which of the pathway towards H_2O_2 is taking place and it is also possible that more than one mechanism acts at the same time. A possible oxygen activation pathway was presented by Valgimigli *et al.*[169] (Figure 6.2) which shows how the addition of oxygen to a semiquinone radical could lead to the formation of a hydroperoxyl radical. The lignin moiety (Figure 6.2 1) is oxidized by the laccase into a semiquinone radical (Figure 6.2 2). The radical can then shuttle in the aromatic ring due to resonance stabilization (Figure 6.2 3). If an oxygen molecule is present in the surroundings, it can be added to the lignin moieties. This addition happens in the *para* position to yield a peroxyl radical stabilized by the formation of an intramolecular H-bond (Figure 6.2 4).[169] The oxygen addition creates instability in the lignin moiety which then releases the hydroperoxyl radical into the system (Figure 6.2 5),[169] leaving the lignin moiety with an unsaturated bond on the aliphatic chain (Figure 6.2 5).

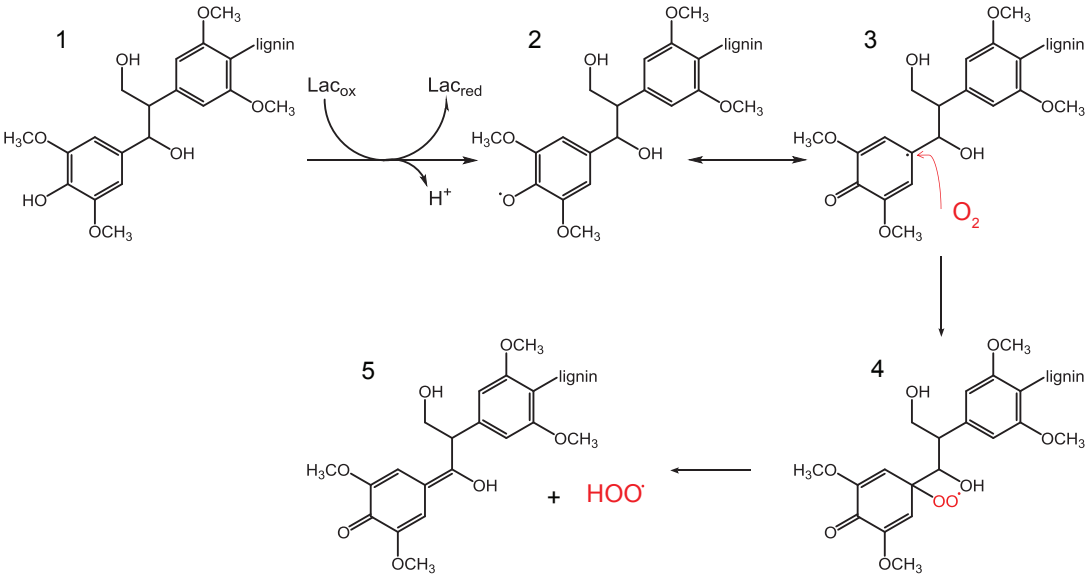

Figure 6.2: Possible formation of H_2O_2 by direct addition of oxygen into the lignin moiety and spontaneous elimination of peroxyl radical.

6.3 Coupled laccase-LPMO reaction

The enzymes currently known to be able to use H_2O_2 as a substrate are lignin peroxidases and LPMO.[164] Due to the difficulties in analyzing products from peroxidases, i.e. lignin depolymerization, we chose to study whether the H_2O_2 level induced by laccase oxidation of lignin was enough to activate LPMO reaction. Two different oxidation reactions were studied: a chitin active LPMO from the bacteria *Serratia marcescens* (CBP21) and a cellulose active LPMO from the fungus *Neurospora crassa* (NcLPMO9C). The first was chosen to completely decouple the two systems, i.e. to study only H_2O_2 LPMO activation, while the second was chosen to investigate whether the mechanism could actually take place in the natural system. CBP21 will oxidize β-chitin at the C1 position and shows a preference for products with an even number DP: DP4, DP6 and so forth, while NcLPMO9C will oxidize cellulose (PASC) at the C4 position to form preferentially short oxidized cello-oligosaccharide: DP2 and DP3 (Figure 6.3). The LPMO reaction can start in the presence of a reductant such as ascorbic acid, which will reduce O_2 to H_2O_2, or in the direct presence of H_2O_2. LPMO activities on both β-chitin and PASC were tested using 2 mM and 1 mM of ascorbic acid for CBP21 and NcLPMO9C, respectively, with these conditions defined as standard LPMO reactions. The LPMO structure contains one copper atom at the 2+ state, which has to be reduced to the 1+ state in order to have LPMO activation. Once the reduction is achieved, the enzyme will continue to react until the substrate is no longer present in the reaction system.[171] Therefore when LPMOs are reacting with H_2O_2 at least an equimolar concentration of reductant has to be present in the reaction. The lowest H_2O_2 concentration obtained in the laccase reaction was found at around 12.5μM. Thus the activation of both CBP21 and NcLPMO9C was tested in the presence of 12.5μM H_2O_2 and 2 μM and 50 μM of ascorbic acid, for CBP21 and NcLPMO9C, respectively.

6.3.1 Activation of CBP21

The main idea was to show LPMO activation with the hydrogen peroxide formed after laccase oxidation. The initial attempt was to perform a one pot reaction, i.e. laccase reactions on lignin and CBP21 reaction on chitin conducted simultaneously. There were two major limitations in trying to combine the two reaction namely, different temperature and pH optima for the LPMO and the laccases. Laccases in general work better at acidic pH, approximately around 5, and at room temperature, while optimal condition for CBP21 to work are at pH 8 and 50°C. In order to optimize the H_2O_2 formation, the reactions were run as close as possible to the laccase optimum, while CBP21 reaction worked at a slower rate. After 24 h incubation no β-chitin products were detected in the reaction supernatant.

The two reactions were run separately to decrease the complexity of the system. Laccase reactions on both 10% w/v organosolv lignin and 5% DM birch were run for one hour, i.e. the reaction time giving the maximum concentration of H_2O_2 (Figure 6.1a), followed by supernatant recovery and laccase heat inactivation steps. The recovered supernatant was added to

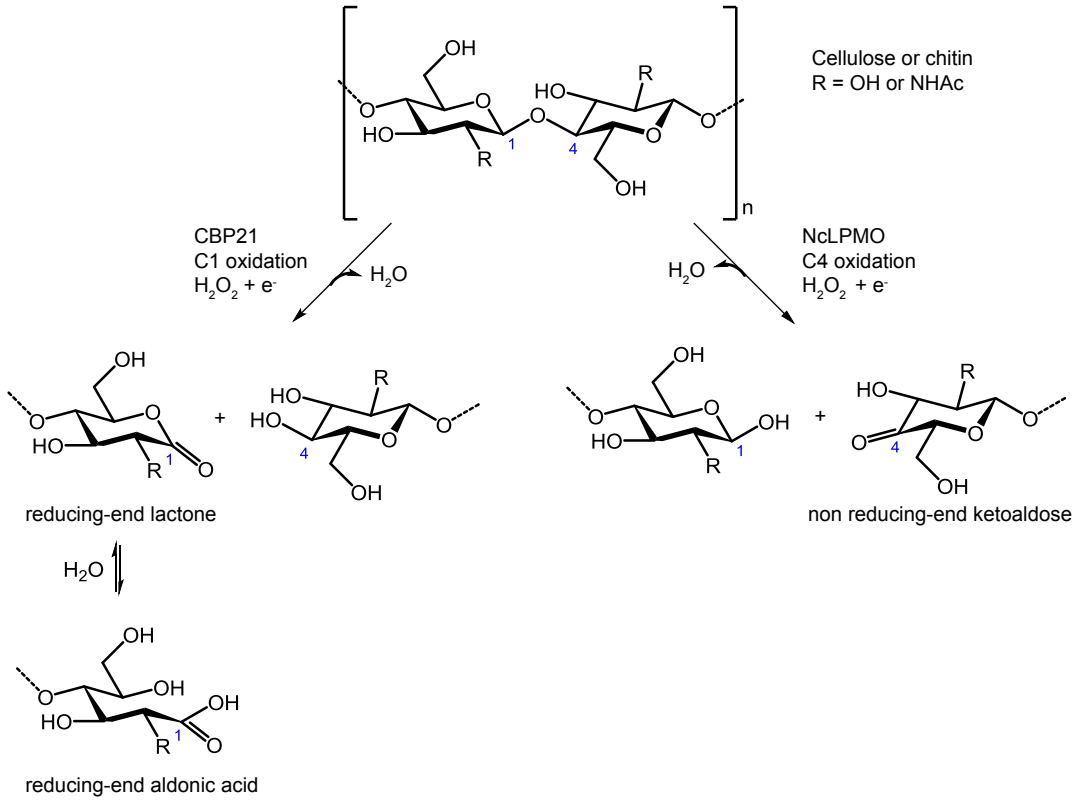

Figure 6.3: LPMO reaction mechanism on cellulose and β-chitin for NcLPMO9C and CBP21, respectively.

the CBP21 reaction, but even in this case β-chitin oxidation products were not detected after 24 hours. Additional H_2O_2 was added to the CBP21 reaction with laccase supernatant to study possible inhibition from the activated laccase lignin supernatant, but also in this case no products were detected. CBP21 most likely underwent inhibition due to the presence of small phenolic compounds released from lignin. Hence a phenolic removal from the laccase treated supernatant was performed (Figure 6.4 a) and when the cleaned supernatant was added to the CBP21 reaction, β-chitin oxidation products were obtained for both birch biomass and organosolv lignin (Figure 6.5). The products obtained from the laccase activated organosolv lignin supernatants were characterized by LC-MS as DP3, DP4, DP5 and DP6 β-chitin oligomers for all enzymes (Figure 6.5a). In the case of birch biomass only DP3 and DP4 were detected. Even though the H_2O_2 concentrations obtained on birch were close to those obtained on organosolv lignin, the extent of reaction was lower (Figure 6.5). Most probably the cleaning step of the supernatant was not efficient enough and some trace of inhibitors were retained in the system. These inhibitors could have caused enzyme inhibition or favored H_2O_2 decomposition and thus resulted in a system with less substrate for the LMPO (Figure 6.5b). Only Gl laccase supernatant did not show formation of DP5 and DP6. Gl laccase was the laccase with the lowest level of purification and therefore side endo-chitinase activity from the *Pichia pastoris* fermentation was tested. The enzyme preparation was added to DP6 N-acetylglucosamine, i.e. chitin oligomer, which was completely degraded after 72 h into products. Even though the

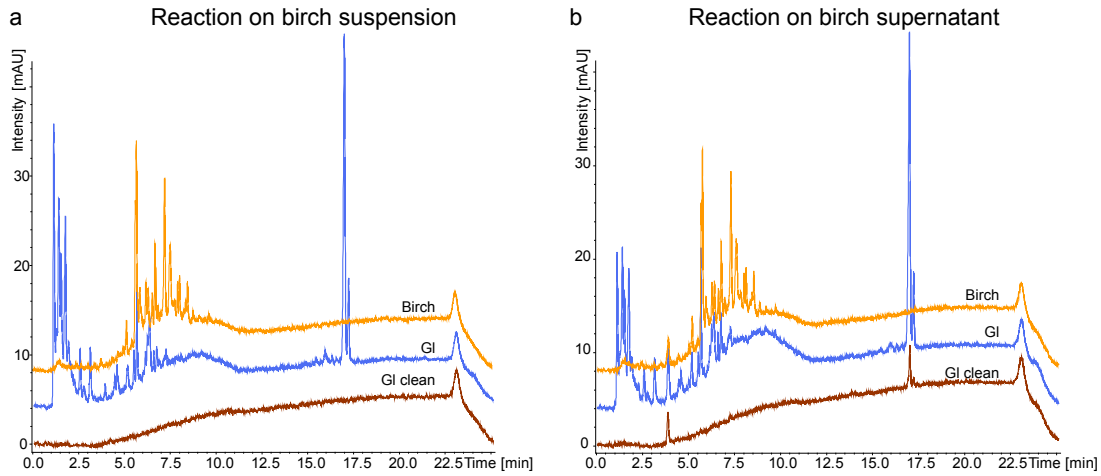

Figure 6.4: LC-UV at 280 nm profiles before and after Gl laccase 1h reaction on 5% DM birch suspension and after phenolic removal step (a). Phenolic profiles before and after Gl laccase 1h reaction on the supernatants of 5% DM birch, i.e. without solid suspension, before and after phenolic removal step (b).

supernatant after laccase oxidation of lignin was subjected to heat inactivation, maybe the step had not been long enough to completely inactivate the chitinase.

Different controls were performed to be absolutely sure that the β-chitin oxidation observed was due to the laccase induced H_2O_2, and none of these controls showed any CBP21 activation. An important control test was performed to investigate whether the H_2O_2 concentration measured in the reaction supernatant was due to the presence of the lignin or not. Both 5% DM birch and 10% w/v organosolv lignin were incubated overnight to solubilize possible compounds, especially phenolic compounds, present in the lignin. Laccases were added to the recovered supernatants from the overnight incubation and allowed to react for one hour. H_2O_2 was measured after the reaction and no difference was found compared with the H_2O_2 concentration prior to laccase reaction; i.e. the measured H_2O_2 was equal to the background H_2O_2 concentration observed in organosolv lignin and birch biomass, indicating that H_2O_2 formation is dependent on the presence of insoluble lignin. These supernatants were analyzed for phenolic profile and showed almost identical 280 nm UV signal profile to the profile obtained for laccase reaction on lignin (Figure 6.4 b), and the addition of these supernatants to the CBP21 reaction did not show oxidation products.

Another way to confirm that CBP21 activation was due to H_2O_2 was to perform the reaction in anaerobic conditions. The development of the reaction relies on the presence of oxygen which can be reduced to H_2O_2 by the ascorbic acid. If oxygen is not present the reaction will not develop, on the contrary if H_2O_2 is present in the system the enzyme will also work under anaerobic conditions. CBP21 was activated by the laccase activated supernatant under anaerobic conditions, confirming again that laccase induces H_2O_2 formation.

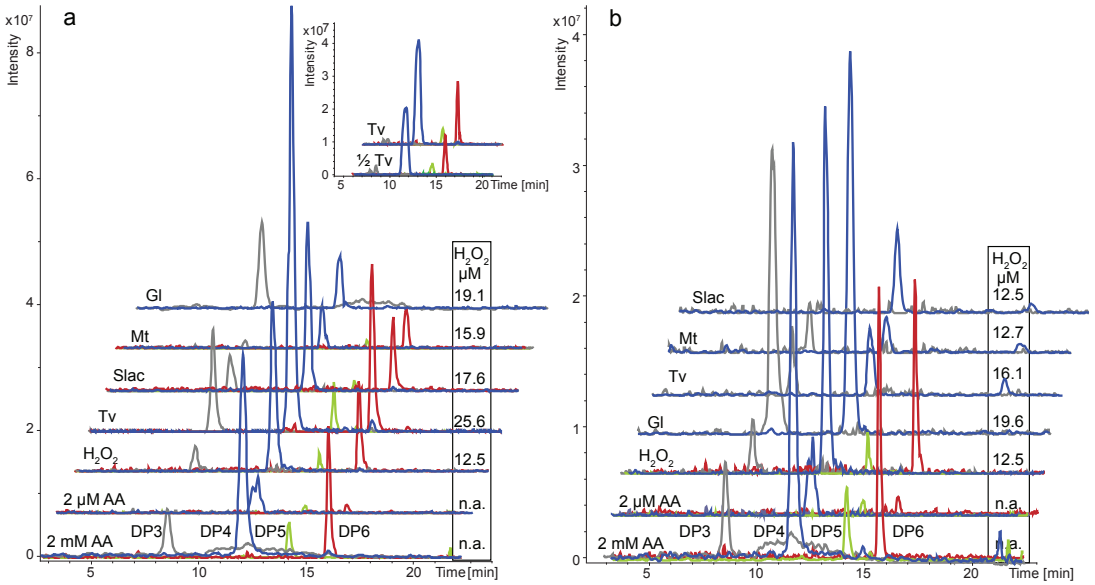

Figure 6.5: Chromatograms of β-chitin oxidation products obtained after CBP21 reaction with laccase activated lignin supernatant of organosolv lignin (a) and birch biomass (b). Three main products were detected and characterized by their masses m/z as DP3 (grey), DP4 (blue), DP5 (green) and DP6 (red). The H_2O_2 concentration is reported on the column on the left hand side of each plot. (a) H_2O_2 dose response is shown in the inset. Supernatant of 1 h reaction of Tv laccase with organosolv lignin was added to CBP21 reaction in two amounts: 150 μL supernatant and 150 μL water (1/2 Tv) and 300 μL supernatant (Tv).

6.3.2 Activation of NcLPMO9C

A more biologically related system was studied to couple the laccase reaction to a cellulose active LPMO and the same set of experiments as done for CBP21 reaction were performed. The one-pot reaction was tested but in this case also PASC oxidized products were not detected and hence the NcLPMO9C activation was studied by decoupling the two reactions. As with CBP21, NcLPMO9C appeared to be inhibited by the laccase activated supernatant prior to the phenolics removal step. Good activation was obtained with the supernatant from organosolv lignin, while birch biomass supernatant did not give rise to extended activation (Figure 6.6).

It is known that LPMOs can use phenolic compounds as reductant instead of ascorbic acid.[172,173] A recent study[174] showed how small phenolic compound released from lignin after a laccase mediator system could activate the LPMO fraction contained in Cellic^{TM}CTec2. The results obtained here showed exactly the opposite, both CBP21 and NcLPMO9C showed some inhibition in the presence of the laccase supernatant before the phenolic cleaning step.

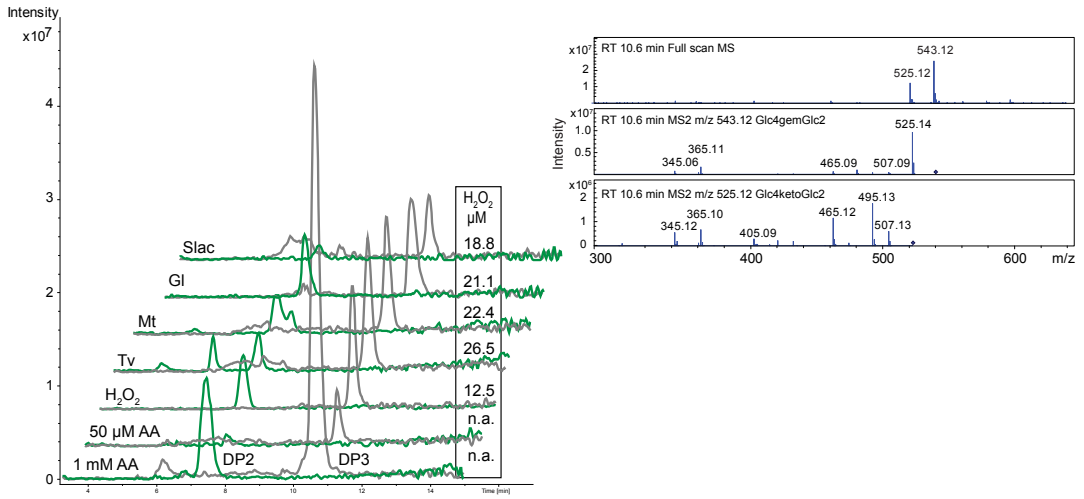

Figure 6.6: Chromatograms of PASC oxidation products obtained after NcLPMO9C reaction with laccase activated lignin supernatant of organosolv lignin. Two main products were detected and characterized by their masses m/z as DP2(green) and DP3 (grey). The H_2O_2 concentration is reported on the column on the left hand side of each plot. Mass spectra on the right hand side the chromatogram show the major peaks appearing at retention time 10.6 min in full scan mode, corresponding to grey trace (DP3), and show m/z 543.12 and 525.12, which correspond to the sodium adducts of the gemdiol and ketone of the trimeric oxidation product, respectively. MS2 fragmentation spectra of m/z 543.12 and 525.12 are shown below the full scan spectrum.

6.4 Conclusions

This study verified the hypothesis H4 that laccase activation of lignin induces the formation of H_2O_2. Laccase from different origins were tested and all showed H_2O_2 formation with differences in the H_2O_2 formation rate. One important result of the study was that H_2O_2 concentration was measured on unpretreated raw birch biomass which confirmed that this phenomenon can also happen in nature. The activation of two LPMO was studied to explore the biological role of H_2O_2 concentration. Both LPMOs were activated only after a phenolic removal step. The presence of some compounds, i.e. phenols in the supernatant directly after laccase oxidation of lignin, strongly inhibited the LMPO reactions. The products formed after addition of the laccase activated lignin supernatant were in agreement with the products formed in the standard control LPMO reaction using only ascorbic acid as reductant. Anaerobic as well as several other control experiments were performed and verified that LPMO activation was due to the H_2O_2 in the laccase supernatant.

The discovery of H_2O_2 as the true LPMO substrate was made only recently.[164] This finding and the discovery that laccase can induce the formation of H_2O_2 when reacting with lignin can explain the beneficial effect of addition of laccase on a cellulolytic enzymes cocktail, which leads to enhancement of released sugar yield, as shown in the work of Sitarz *et al.*[93] and thus verifying hypothesis H1.

Chapter 7

Discussions and Perspectives

The present work has focused on exploring laccase catalytic reaction chemistry in order to understand the biological effect of laccase during biomass degradation.

One of the first objectives of this work was to optimize fermentation and purification procedures to obtain *Ganoderma lucidum* (Gl) laccase. The recombinant production of Gl laccase in *Pichia pastoris* was not successfull. Laccase production in yeast can be performed even at high yield,[103] but this type of recombinant production was not suitable for this specific Gl laccase case. In order to improve laccase expression and remove some of the challenges encountered during the production in yeast, laccase expression might be investigated in higher eukaryote organisms, i.e. using either the native fungal strain or a fungal host. For example, white-rot laccases have been produced recombinantly in different filamentous fungi from *Aspergillus* species: *A. oryzae*,[175] *A. nidulans*,[176] *A. niger*,[119,177–181] *A. sojae*,[182] and in *Trichoderma reesei*,[183,184] and *Penicillium canescens*,[185] and show both higher volumetric laccase activity (on the base of ABTS) in the range of 592 - 774,000 U/L[180,186] and laccase yield in the range of 8 - 920 mg/L.[182,183] compared to laccase recovered from yeast production. Glycosylation, a characteristic of the yeast recombinant expression, might also be avoided by using higher fungi as the recombinant expression hosts. The removal of glycosylation can be beneficial for the laccase properties, such as thermostability and resistance to high concentrations of organic solvents.[59,187–189] The advantage of using yeast is the easy fermentation protocol which is in contrast to the complex filamentous fungi fermentation due to the morphological complexity of the fungi charachterized by different structural forms during the life cycle.[190] Complexity of the purification procedure will also be affected by using fungi as the recombinant expression system. Fungi are characterized by the production of several isoenzymes[191] which share almost the same physical properties, such as pI, which may render the purification step more complicated.[192]

One way to overcome this issue could be to express a His-tagged Gl laccase in the fungal expression system. But laccase purification with His-Tag is not without complication either. The nickel column used for His-Tag purification can chelate the copper contained in the laccase structure or the copper could bind to the column and result in inactive laccase. However, it has been shown previously[120] that laccase His-tag purification can be achieved. If it is possible to obtain a Gl laccase enzyme with a useful His-tag, it would be worth investigating whether protein loss due to inactivation or binding to the nickel column in the His-tag purification would be of relatively less importance compared to the potential high purity of the protein and fast purification system that may be achieved.

Characterization and comparison of enzymes have always been performed by means of activity assays. Therefore seeking the best methods to assess laccase activity using compounds resembling lignin or lignin itself has inspired the work of several groups and was also one of the objectives of this work. An example of a new colorimetric assay was developed by Pardo *et al.*[134] using soluble compounds such as sinapic acid, acetosyringone and syringaldehyde and monitoring their oxidation at 512, 520 and 370 nm, respectively. The assay developed by Pardo *et al.*[134] assess laccase in a more lignin related way but does not give additional information on the product profile after laccase activation of the substrate. The LC-MS method developed in this study combines the measurement of laccase kinetics and activity on the monomeric subunits of lignin, i.e. hydroxycinnamic acids, to describe which products are formed after laccase reaction. Classical spectrophotometric methods rely only on the measurement at one specific wavelength. Therefore the presence of interfering compounds in the enzyme preparation, especially when using unpurified enzyme, could potentially give rise to some misleading activity measurements. Both the LC-MS and the FTIR methods developed in this study are independent of enzyme purity: the low degree of purity of Gl laccase and thus the fermentation broth compounds did not affect the measurements. In the LC-MS assay the substrate mass only is followed over time, and therefore laccase action of the specific compound is captured by the analysis. Compounds coming from the fermentation broth might potentially have a significant effect on the analysis if the standards and the samples do not share similar conditions. In the FTIR-PARAFAC coupled method the sample is screened at more than one wavenumber. If a superimposition of two effects are taking place, such as a laccase reaction and response from the fermentation broth, the PARAFAC model would need an additional decomposing component in order to be valid: one describing the real laccase evolution profile and the other accounting for the fermentation broth interference.

The LC-MS and FTIR methods developed are good, and easy available screening tools for laccase activity which can potentially be used in any lab, but they can only detect laccase activity on soluble compounds that do not have the same complexity and properties as lignin. Activity measurements on lignin have already been performed by some studies. Tonin *et al.*[193] developed a new colorimetric spectrophotometric assay using technical lignin. This new activity assay measures the absorbance at 450-508 nm of 2,4-dinitrophenylhydrasine which reacts with the carbonyl groups released after the action of lignin degrading enzyme on lignin. While peroxidase activity with Tonin's method can be estimated, laccase activity is dependent on

the presence of ABTS as mediator and hence it is not possible to measure the natural laccase action on lignin. Alternatively, the method developed by Munk *et al.*[149] detects natural laccase action on lignin measuring on-line radical formation on lignin. This method was used in this work to study laccase kinetics on organosolv lignin. The kinetic parameters obtained for lignin were significantly different from those determined on soluble hydroxycinnamates, probably due to limitation of laccase to access the phenols in the lignin structure. Moreover the sum of two effects: laccase oxidation and radical quenching, is always present, which results in an underestimation of the kinetic parameters.

The LC-MS study showed that both Tv and Gl laccase kinetics were higher on sinapic acid compared to those of ferulic acid and *p*-coumaric acid. It could be of interest to study whether this preference towards S-units is also observed on lignin itself. For such a study deep characterization of the lignin structure and unit ratio has to be performed. Measuring radical formation by EPR on different types of lignin containing different ratio between S, G and H units could potentially show whether the laccases act preferentially on certain types of lignin structure. The difference in reaction evolution profiles on small phenolic compounds depending on the laccase origin was studied with FTIR. It could be interesting to measure laccase reaction fingerprints on lignin by FITR to see whether the evolution profiles of lignin are also dependent on the laccase origin as in the case of small phenolic compounds found in this study. Evolution profiles on lignin could provide a picture of the overall reaction by capturing reaction intermediates and radicals.

Another way to study laccase activity could be by measuring consumption of oxygen, the second laccase substrate. One high throughput method to measure oxygen consumption in solution was studied by Hommes *et al.*[194] who measured oxygen consumption during laccase oxidation of 2,6-dimethoxyphenol. Direct correlation between oxygen consumed and phenol oxidation was shown to be valid in Hommes's work.[194] Coupling oxygen measurements to lignin oxidation could potentially improve the knowledge about laccase reaction mechanism and would be an interesting experiment to perform. However, we did show that some of the radicals that laccases produce on the lignin molecule can react with the oxygen itself, activating it with the final formation of H_2O_2. If H_2O_2 is formed it means that some of the free oxygen in the system has been used for H_2O_2 generation and not by the laccase reaction itself. It is therefore important to be aware of other oxygen consuming reactions in the system otherwise the amount of consumed oxygen will be misinterpreted. The oxygen will be a combination of oxygen consumed during laccase reaction and that converted into H_2O_2.

The very slow reactions of laccases towards lignin compared to the small phenolic compounds are not hard to imagine; lignin is an insoluble polymer characterized by a complex structure. Therefore if the real substrate of laccase is lignin there should be a reason for this process to procede so slowly. Fungal degradation of lignin in nature does not occur in hours but will take weeks or even months,[45] therefore some reactions may be performed at a slow rate. The reaction system during fungal biomass degradation is highly complex and is controlled by enzymes which create an overall redox potential that cannot be harmful to the fungus itself. The

purpose of laccase in nature is still not clear. It is known from the laccase reaction mechanism that water is released in the system. The LC-MS study showed that for small soluble phenols polymerization preferentially takes place after substrate activation by laccases. Finally, we have shown that the activation of native (unpretreated) wood lignin by laccases can induce sufficient H_2O_2 formation to activate LMPO reactions. Whether the purpose of laccase is to produce a small and localized amount of H_2O_2 to allow other enzymes to start their reaction, or it is to remove phenolic inhibition after peroxidase activity by polymerization of the small phenols or to produce water in the system or it is a combination of the three is difficult to address, but the enzyme is definitely needed by the fungal microorganism to grow on wood/lignocellulose and hence its function is important in the first part of the fungal growth.

In conclusion the work performed elucidated some of the laccase reaction preferences and mechanisms which in turn has increased the understanding of laccase specificity towards lignin subunits and the possible biological role of laccase in nature. Laccase oxidation on small phenolic compounds results in polymeric structures of the starting substrate and laccase affinity towards these small phenols depends on the substitution on the phenolic ring, the higher the number of methoxylation on the phenolic ring, the higher the laccase affinity. In addition it has been shown that the laccase action on these small phenols depends on the origin of the laccase itself. These findings verified hypothesis H2.

Laccase activation on lignin was slower than the activity on small phenols and furthermore a two reactions system was taking place when studying lignin activation by laccase: both the formation and the disappearance of radical happened at the same time. Trying to address the quenching of the radicals after laccase oxidation of lignin helped to increase the knowledges about the laccase potentiality in the natural system. Laccase formation of radicals can induce the activation of oxygen to H_2O_2 which was produced in sufficient amounts to activate H_2O_2 dependent enzymes such as LPMOs, hence supporting hypotheses H3 and H4. The LPMO activation due to laccase induced production of H_2O_2 after oxidation of lignin, and thus the boosting of lignobiomass degradation allowed also to confirm hypothesis H1 with the exception that the beneficial lignocellulose degradation was observed for all the laccases studied and was not confined to *Gnoderma lucidum* laccase. In addition the H_2O_2 levels were measured after activation of natural unpretreated birch wood which showed only slightly lower H_2O_2 concentrations than those measured on organosolv lignin even though the reaction on organosolv lignin contained ten times more lignin than in the birch wood reaction. Lignin present in the natural biomass appeared more accessible to laccase oxidation most likely due to the lower degree of condensation of the lignin structure. The development of processes able to maintain the natural lignin structure as intact as possible could be of exceptional importance in further studies of the real catalytic function of laccases in nature. Future in vitro studies of laccases could focus on slowly increasing the complexity of the system and thereby mimick the natural degradation situation step by step. First step could be to study whether the amount of H_2O_2 induced by the laccase oxidation on lignin is in sufficient amounts to activate peroxidases. If the latter is successful peroxidases would start to depolymerize lignin and hence as second step oxidases could be included in the system. The oxidases will oxidize the small phenolic moieties

derived from the peroxidases depolymerization of lignin producing more H_2O_2 which will boost the peroxidases reaction. The presence of oxidases will at the same time reduce the soluble substrate available for laccase oxidation and hence it could be possible to study how the extent of polymerization due to laccase action is reduced. Finally, increasing even more the complexity could be done by adding LPMOs and hydrolytic enzymes and hopefully understand the overall delignification process.

Bibliography

[1] Crestini, C., Crucianelli, M., Orlandi, M. & Saladino, R. Oxidative strategies in lignin chemistry: A new environmental friendly approach for the functionalisation of lignin and lignocellulosic fibers. *Catal. Today* **156**, 8–22 (2010).

[2] Ragauskas, A. J. *et al.* Lignin valorization: Improving lignin processing in the biorefinery. *Sci.* **344** (2014).

[3] Rubin, E. M. Genomics of cellulosic biofuels. *Nat.* **454**, 841–845 (2008).

[4] Gardner, K. H. & Blackwell, J. The structure of native cellulose. *Biopolym.* **13**, 1975–2001 (1974).

[5] Mohnen, D., Bar-Peled, M. & Somerville, C. Cell Wall Polysaccharide Synthesis. In *Biomass Recalcitrance*, 94–187 (Blackwell Publishing Ltd., Oxford, UK, 2009).

[6] Lynd, L. R., Weimer, P. J., van Zyl, W. H. & Pretorius, I. S. Microbial cellulose utilization: Fundamentals and biotechnology. *Microbiol. Mol. Biol. Rev.* **66**, 506–577 (2002).

[7] Klemm, D., Heublein, B., Fink, H.-P. & Bohn, A. Cellulose: Fascinating biopolymer and sustainable raw material. *Angewandte Chemie Int. Ed.* **44**, 3358–3393 (2005).

[8] Sjöström, E. *Wood chemistry : fundamentals and applications* (Academic Press, 1993).

[9] Decker, S. R., Siika-Aho, M. & Viikari, L. Enzymatic Depolymerization of Plant Cell Wall Hemicelluloses. In *Biomass Recalcitrance*, 352–373 (Blackwell Publishing Ltd., Oxford, UK, 2008).

[10] Scheller, H. V. & Ulvskov, P. Hemicelluloses. *Annu. Rev. Plant Biol.* **61**, 263–289 (2010).

[11] Imamura, T., Watanabe, T., Kuwahara, M. & Koshijima, T. Ester linkages between lignin and glucuronic acid in lignin-carbohydrate complexes from *Fagus crenata*. *Phytochem.* **37**, 1165–73 (1994).

[12] Du, X., Gellerstedt, G. & Li, J. Universal fractionation of lignin-carbohydrate complexes (LCCs) from lignocellulosic biomass: an example using spruce wood. *The Plant J.* **74**, 328–338 (2013).

[13] Watanabe, T., Ohnishi, J., Yamasaki, Y., Kaizu, S. & Koshijima, T. Binding-site analysis of the ether linkages between lignin and hemicelluloses in lignin-carbohydrate complexes by ddq-oxidation. *Agric. Biol. Chem.* **53**, 2233–2252 (1989).

[14] Vanholme, R., Demedts, B., Morreel, K., Ralph, J. & Boerjan, W. Lignin biosynthesis and structure. *Plant Physiol.* **153**, 895–905 (2010).

[15] Ralph, J. *et al.* Lignins: Natural polymers from oxidative coupling of 4-hydroxyphenyl-propanoids. *Phytochem. Rev.* **3**, 29–60 (2004).

[16] Hatfield, R. & Vermerris, W. Lignin formation in plants. the dilemma of linkage specificity. *Plant Physiol.* **126**, 1351–1357 (2001).

[17] Moura, J. C. M. S., Bonine, C. A. V., de Oliveira Fernandes Viana, J., Dornelas, M. C. & Mazzafera, P. Abiotic and Biotic Stresses and Changes in the Lignin Content and Composition in Plants. *J. Integr. Plant Biol.* **52**, 360–376 (2010).

[18] Djikanović, D. *et al.* Structural Differences Between Lignin Model Polymers Synthesized from Various Monomers. *J. Polym. Environ.* **20**, 607–617 (2012).

[19] Espiñeira, J. M. *et al.* Distribution of lignin monomers and the evolution of lignification among lower plants. *Plant Biol.* **13**, 59–68 (2011).

[20] del Río, J. C. *et al.* Structural Characterization of Wheat Straw Lignin as Revealed by Analytical Pyrolysis, 2D-NMR, and Reductive Cleavage Methods. *J. Agric. Food Chem.* **60**, 5922–5935 (2012).

[21] Buranov, A. U. & Mazza, G. Lignin in straw of herbaceous crops. *Ind. Crop. Prod.* **28**, 237–259 (2008).

[22] Zakzeski, J., Bruijnincx, P. C. A., Jongerius, A. L. & Weckhuysen, B. M. The Catalytic Valorization of Lignin for the Production of Renewable Chemicals. *Chem. Rev.* **110**, 3552–3599 (2010).

[23] Ralph, J., Brunow, G. & Boerjan, W. Lignins. In *Encyclopedia of Life Sciences* (John Wiley & Sons, Ltd, Chichester, UK, 2007).

[24] Crestini, C., Melone, F., Sette, M. & Saladino, R. Milled Wood Lignin: A Linear Oligomer. *Biomacromolecules* **12**, 3928–3935 (2011).

[25] Parthasarathi, R., Romero, R. A., Redondo, A. & Gnanakaran, S. Theoretical Study of the Remarkably Diverse Linkages in Lignin. *The J. Phys. Chem. Lett.* **2**, 2660–2666 (2011).

[26] Brunow, G. & Lundquist, K. Functional groups and bonding patterns in lignin (including the lignin-carbohydrate complexes). *Lignin lignans: advances chemistry* 267–299 (2010).

[27] Pu, Y., Cao, S. & Ragauskas, A. J. Application of quantitative 31P NMR in biomass lignin and biofuel precursors characterization. *Energy & Environ. Sci.* **4**, 3154 (2011).

[28] Schoemaker, H. E., Harvey, P. J., Bowen, R. M. & Palmer, J. M. On the mechanism of enzymatic lignin breakdown. Tech. Rep. 1, Central Laboratory DSM, PO Box 18, NL-6160 IUD Geleen, The Netherlands (1985).

[29] Lai, Y.-Z. Determination of Phenolic Hydroxyl Groups. In *Methods in Lignin Chemistry.*, 423–434 (Springer, Berlin, Heidelberg, 1992).

[30] Vishtal, A. G. & Kraslawski, A. Challenges in industrial applications of technical lignins. *BioResources* **6**, 3547–3568 (2011).

[31] Faruk, O., Sain, M., Haghdan, S., Renneckar, S. & Smith, G. D. Sources of Lignin. *Lignin Polym. Compos.* 1–11 (2016).

[32] Renders, T., Van den Bosch, S., Koelewijn, S.-F., Schutyser, W. & Sels, B. F. Lignin-first biomass fractionation: the advent of active stabilisation strategies. *Energy & Environ. Sci.* **10**, 1551–1557 (2017).

[33] Liers, C., Arnstadt, T., Ullrich, R. & Hofrichter, M. Patterns of lignin degradation and oxidative enzyme secretion by different wood- and litter-colonizing basidiomycetes and ascomycetes grown on beech-wood. *FEMS Microbiol. Ecol.* **78**, 91–102 (2011).

[34] Hatakka, A. & Hammel, K. E. Fungal Biodegradation of Lignocelluloses. In *Industrial Applications*, 319–340 (Springer Berlin Heidelberg, Berlin, Heidelberg, 2011).

[35] Carlile, M. J. M. J., Watkinson, S. C. & Gooday, G. W. *The fungi* (Academic Press, 2001).

[36] Cragg, S. M. *et al.* Lignocellulose degradation mechanisms across the Tree of Life. *Curr. Opin. Chem. Biol.* **29**, 108–119 (2015).

[37] Goodell, B. Brown-Rot Fungal Degradation of Wood: Our Evolving View. Tech. Rep., Wood Science and Technology Department, University of Maine, Orono (2003).

[38] Goodell, B. *et al.* Modification of the nanostructure of lignocellulose cell walls via a non-enzymatic lignocellulose deconstruction system in brown rot wood-decay fungi. *Biotechnol. for biofuels* **10**, 179 (2017).

[39] Kirk, T. & Cullen, D. Enzymology and molecular genetics of wood degradation by white-rot fungi (1998).

[40] Levasseur, A., Drula, E., Lombard, V., Coutinho, P. M. & Henrissat, B. Expansion of the enzymatic repertoire of the CAZy database to integrate auxiliary redox enzymes. *Biotechnol. for Biofuels* **6**, 41 (2013).

[41] Kirk, T. K. & Farrell, R. L. Enzymatic "Combustion": The Microbial Degradation of Lignin. *Annu. Rev. Microbiol.* **41**, 465–501 (1987).

[42] Martínez, Á. T., Ruiz-Dueñas, F. J., Martínez, M. J., del Río, J. C. & Gutiérrez, A. Enzymatic delignification of plant cell wall: from nature to mill. *Curr. Opin. Biotechnol.* **20**, 348–357 (2009).

[43] Ruiz-Dueñas, F. J. & Martínez, Á. T. Microbial degradation of lignin: how a bulky recalcitrant polymer is efficiently recycled in nature and how we can take advantage of this. *Microb. Biotechnol.* **2**, 164–177 (2009).

[44] Martínez, A. T. *et al.* Biodegradation of lignocellulosics: microbial, chemical, and enzymatic aspects of the fungal attack of lignin. *Int. microbiology : official journal Span. Soc. for Microbiol.* **8**, 195–204 (2005).

[45] Zhou, S. *et al.* Investigation of lignocellulolytic enzymes during different growth phases of *Ganoderma lucidum* strain G0119 using genomic, transcriptomic and secretomic analyses. *PLOS ONE* **13**, 1–20 (2018).

[46] Lechner, B. & Papinutti, V. Production of lignocellulosic enzymes during growth and fruiting of the edible fungus *Lentinus tigrinus* on wheat straw. *Process. Biochem.* **41**, 594–598 (2006).

[47] Ohga, S. & Royse, D. J. Transcriptional regulation of laccase and cellulase genes during growth and fruiting of *Lentinula edodes* on supplemented sawdust. *FEMS Microbiol. Lett.* **201**, 111–115 (2001).

[48] Elisashvili, V., Kachlishvili, E. & Penninckx, M. Lignocellulolytic enzymes profile during growth and fruiting of *Pleurotus ostreatus* on wheat straw and tree leaves. *Acta Microbiol. et Immunol. Hungarica* **55**, 157–168 (2008).

[49] Riley, R. *et al.* Extensive sampling of basidiomycete genomes demonstrates inadequacy of the white-rot/brown-rot paradigm for wood decay fungi. *Proc. Natl. Acad. Sci.* **111**, 9923–9928 (2014).

[50] Virk, A. P., Sharma, P. & Capalash, N. Use of laccase in pulp and paper industry. *Biotechnol. Prog.* **28**, 21–32 (2012).

[51] Mate, D. M. & Alcalde, M. Laccase: a multi-purpose biocatalyst at the forefront of biotechnology. *Microb. Biotechnol.* 1457–1467 (2017).

[52] Sitarz, A. K., Mikkelsen, J. D. & Meyer, A. S. Structure, functionality and tuning up of laccases for lignocellulose and other industrial applications. *Critical Rev. Biotechnol.* **36**, 70–86 (2016).

[53] Lahiri, A., Hedl, M., Yan, J. & Abraham, C. Human LACC1 increases innate receptor-induced responses and a LACC1 disease-risk variant modulates these outcomes. *Nat. Commun.* **8** (2017).

[54] Munk, L., Sitarz, A. K., Kalyani, D. C., Mikkelsen, J. D. & Meyer, A. S. Can laccases catalyze bond cleavage in lignin? *Biotechnol. Adv.* **33**, 13–24 (2015).

[55] Giardina, P. *et al.* Laccases: a never-ending story. *Cell. Mol. Life Sci.* **67**, 369–385 (2010).

[56] Chakraborty, D. & Barton, S. C. Influence of Mediator Redox Potential on Fuel Sensitivity of Mediated Laccase Oxygen Reduction Electrodes. *J. The Electrochem. Soc.* B440–B447 (2011).

[57] Augustine, A. J., Quintanar, L., Stoj, C. S., Kosman, D. J. & Solomon, E. I. Spectroscopic and kinetic studies of perturbed trinuclear copper clusters: the role of protons in reductive cleavage of the O-O bond in the multicopper oxidase Fet3p. *J. Am. Chem. Soc.* **129**, 13118–26 (2007).

[58] Xu, F. *et al.* A study of a series of recombinant fungal laccases and bilirubin oxidase that exhibit significant differences in redox potential, substrate specificity, and stability. *Biochimica et biophysica acta* **1292**, 303–11 (1996).

[59] Maté, D. *et al.* Laboratory Evolution of High-Redox Potential Laccases. *Chem. & Biol.* **17**, 1030–1041 (2010).

[60] Steenken, S. & Neta, P. One-electron redox potentials of phenols. Hydroxy- and aminophenols and related compounds of biological interest. *The J. Phys. Chem.* **86**, 3661–3667 (1982).

[61] Tadesse, M. A., D'Annibale, A., Galli, C., Gentili, P. & Sergi, F. An assessment of the relative contributions of redox and steric issues to laccase specificity towards putative substrates. *Org. & Biomol. Chem.* **6**, 868–878 (2008).

[62] D'Acunzo, F., Galli, C., Gentili, P. & Sergi, F. Mechanistic and steric issues in the oxidation of phenolic and non-phenolic compounds by laccase or laccase-mediator systems, the case of bifunctional substrates. *New J. Chem.* **30**, 583–591 (2006).

[63] Cannatelli, M. D. & Ragauskas, A. J. Two Decades of Laccases: Advancing Sustainability in the Chemical Industry. *The Chem. Rec.* **17**, 122–140 (2017).

[64] Xu, F. Effects of redox potential and hydroxide inhibition on the pH activity profile of fungal laccases. *The J. biological chemistry* **272**, 924–8 (1997).

[65] Suurnäkki, A. *et al.* Factors affecting the activation of pulps with laccase. *Enzym. Microb. Technol.* **46**, 153–158 (2010).

[66] Crestini, C., Jurasek, L. & Argyropoulos, D. S. On the Mechanism of the Laccase–Mediator System in the Oxidation of Lignin. *Chem. - A Eur. J.* **9**, 5371–5378 (2003).

[67] Gutiérrez, A. *et al.* Demonstration of laccase-based removal of lignin from wood and non-wood plant feedstocks. *Bioresour. Technol.* **119**, 114–122 (2012).

[68] Barneto, A. G., Aracri, E., Andreu, G. & Vidal, T. Investigating the structure–effect relationships of various natural phenols used as laccase mediators in the biobleaching of kenaf and sisal pulps. *Bioresour. Technol.* **112**, 327–335 (2012).

[69] Moldes, D., Díaz, M., Tzanov, T. & Vidal, T. Comparative study of the efficiency of synthetic and natural mediators in laccase-assisted bleaching of eucalyptus kraft pulp. *Bioresour. Technol.* **99**, 7959–7965 (2008).

[70] Sitarz, A. K., Mikkelsen, J. D., Meyer, A. S. & Lezyk, M. J. A novel laccase from *Ganoderma Lucidum* capable of enhancing enzymatic degradation of lignocellulolytic biomass (2014). Also registered as: WO2013EP68836, EP20120183917; WO2014041030; C12N9/00.

[71] Kalyani, D. *et al.* Characterization of a novel laccase from the isolated *Coltricia perennis* and its application to detoxification of biomass. *Process. Biochem.* **47**, 671–678 (2012).

[72] Chen, Q., Marshall, M. N., Geib, S. M., Tien, M. & Richard, T. L. Effects of laccase on lignin depolymerization and enzymatic hydrolysis of ensiled corn stover. *Bioresour. Technol.* **117**, 186–192 (2012).

[73] Palonen, H. & Viikari, L. Role of oxidative enzymatic treatments on enzymatic hydrolysis of softwood. *Biotechnol. Bioeng.* **86**, 550–557 (2004).

[74] Moilanen, U., Kellock, M., Galkin, S. & Viikari, L. The laccase-catalyzed modification of lignin for enzymatic hydrolysis. *Enzym. Microb. Technol.* **49**, 492–498 (2011).

[75] Eggert, C., Temp, U., Dean, J. F. & Eriksson, K. E. A fungal metabolite mediates degradation of non-phenolic lignin structures and synthetic lignin by laccase. *FEBS letters* **391**, 144–8 (1996).

[76] Bourbonnais, R., Paice, M. G., Reid, I. D., Lanthier, P. & Yaguchi, M. Lignin oxidation by laccase isozymes from *Trametes versicolor* and role of the mediator 2,2'-azinobis(3-ethylbenzthiazoline-6-sulfonate) in kraft lignin depolymerization. *Appl. environmental microbiology* **61**, 1876–80 (1995).

[77] Longe, L. F. *et al.* Importance of Mediators for Lignin Degradation by Fungal Laccase. *ACS Sustain. Chem. & Eng.* **6**, 10097–10107 (2018).

[78] Hämäläinen, V. *et al.* Enzymatic Processes to Unlock the Lignin Value. *Front. Bioeng. Biotechnol.* **6**, 20 (2018).

[79] Singh, R. *et al.* Enhanced delignification of steam-pretreated poplar by a bacterial laccase. *Sci. Reports* **7**, 42121 (2017).

[80] Antošová, Z. & Sychrová, H. Yeast Hosts for the Production of Recombinant Laccases: A Review. *Mol. Biotechnol.* **58**, 93–116 (2016).

[81] Rodríguez Couto, S. & Luis Toca Herrera, J. Research review paper industrial and biotechnological applications of laccases: A review. *Biotechnol. Adv.* **24**, 500–513 (2006).

[82] Osma, J. F., Toca-Herrera, J. L. & Rodríguez-Couto, S. Uses of Laccases in the Food Industry. *Enzym. Res.* **2010** (2010).

[83] Flander, L. *et al.* Effects of Laccase and Xylanase on the Chemical and Rheological Properties of Oat and Wheat Doughs. *J. Agric. Food Chem.* **56**, 5732–5742 (2008).

[84] Crestini, C. & Argyropoulos, D. S. The early oxidative biodegradation steps of residual kraft lignin models with laccase. *Bioorganic & medicinal chemistry* **6**, 2161–9 (1998).

[85] Roy, J. J., Abraham, T. E., Abhijith, K. S., Kumar, P. V. S. & Thakur, M. S. Biosensor for the determination of phenols based on cross-linked enzyme crystals (CLEC) of laccase. *Biosens. & bioelectronics* **21**, 206–11 (2005).

[86] Viswanath, B., Rajesh, B., Janardhan, A., Kumar, A. P. & Narasimha, G. Fungal laccases and their applications in bioremediation. *Enzym. research* **2014**, 163242 (2014).

[87] Durán, N. & Esposito, E. Potential applications of oxidative enzymes and phenoloxidase-like compounds in wastewater and soil treatment: a review. *Appl. Catal. B: Environ.* **28**, 83–99 (2000).

[88] Witayakran, S. & Ragauskas, A. Synthetic Applications of Laccase in Green Chemistry. *Adv. Synth. & Catal.* **351**, 1187–1209 (2009).

[89] Mate, D. M. & Alcalde, M. Laccase: a multi-purpose biocatalyst at the forefront of biotechnology. *Microb. biotechnology* **10**, 1457–1467 (2017).

[90] Majeau, J.-A., Brar, S. K. & Tyagi, R. D. Laccases for removal of recalcitrant and emerging pollutants. *Bioresour. Technol.* **101**, 2331 – 2350 (2010).

[91] Riva, S. Laccases: blue enzymes for green chemistry. *Trends Biotechnol.* **24**, 219 – 226 (2006).

[92] Grandes-Blanco, A. I. *et al.* Heterologous Expression of Laccase (LACP83) of *Pleurotus ostreatus*. *BioResources* **12**, 3211–3221 (2017).

[93] Sitarz, A. K., Mikkelsen, J. D., Højrup, P. & Meyer, A. S. Identification of a laccase from *Ganoderma lucidum* CBS 229.93 having potential for enhancing cellulase catalyzed lignocellulose degradation. *Enzym. Microb. Technol.* **53**, 378–385 (2013).

[94] Johannes, C. & Majcherczyk, A. Laccase activity tests and laccase inhibitors. *J. biotechnology* **78**, 193–9 (2000).

[95] Tinoco, R., Pickard, M. A. & Vazquez-Duhalt, R. Kinetic differences of purified laccases from six *Pleurotus ostreatus* strains. *Lett. applied microbiology* **32**, 331–5 (2001).

[96] Cantarella, G., Galli, C. & Gentili, P. Free radical versus electron-transfer routes of oxidation of hydrocarbons by laccase/mediator systems: Catalytic or stoichiometric procedures. *J. Mol. Catal. B: Enzym.* **22**, 135–144 (2003).

[97] Thurston, C. F. The structure and function of fungal laccases. *Microbiol.* **140**, 19–26 (1994).

[98] Doerge, D. R., Divi, R. L. & Churchwell, M. I. Identification of the colored guaiacol oxidation product produced by peroxidases. *Anal. Biochem.* **250**, 10 – 17 (1997).

[99] Setti, L., Giuliani, S., Spinozzi, G. & Pifferi, P. G. Laccase catalyzed-oxidative coupling of 3-methyl -benzothiazolinone hydrazone and methoxyphenols. *Enzym. Microb. Technol.* **25**, 285–289 (1999).

[100] Necochea, R. *et al.* Phylogenetic and biochemical characterisation of a recombinant laccase from *Trametes versicolor*. *FEMS Microbiol. Lett.* **244**, 235–241 (2005).

[101] Nishibori, N., Masaki, K., Tsuchioka, H., Fujii, T. & Iefuji, H. Comparison of laccase production levels in *Pichia pastoris* and *Cryptococcus* sp. S-2. *J. Biosci. Bioeng.* **115**, 394–399 (2013).

[102] Hong, F., Meinander, N. Q. & Jönsson, L. J. Fermentation strategies for improved heterologous expression of laccase in*Pichia pastoris*. *Biotechnol. Bioeng.* 438–449 (2002).

[103] Hong, Y. *et al.* Expression of a laccase cdna from *Trametes* sp. ah28-2 in *Pichia pastoris* and mutagenesis of transformants by nitrogen ion implantation. *FEMS Microbiol. Lett.* **258**, 96–101 (2006).

[104] Camarero, S. *et al.* Engineering platforms for directed evolution of Laccase from *Pycnoporus cinnabarinus*. *Appl. environmental microbiology* **78**, 1370–84 (2012).

[105] Liu, W., Chao, Y., Liu, S., Bao, H. & Qian, S. Molecular cloning and characterization of a laccase gene from the basidiomycete *Fome lignosus* and expression in *Pichia pastoris*. *Appl. Microbiol. Biotechnol.* **63**, 174–181 (2003).

[106] Hildén, K. *et al.* Heterologous expression and structural characterization of two low pH laccases from a biopulping white-rot fungus *Physisporinus rivulosus*. *Appl. Microbiol. Biotechnol.* **97** (2013).

[107] You, L. F. *et al.* Molecular cloning of a laccase gene from *Ganoderma lucidum* and heterologous expression in *Pichia pastoris*. *J. Basic Microbiol.* **54**, 134–141 (2014).

[108] Joo, S. S. *et al.* Molecular cloning and expression of a laccase from *Ganoderma lucidum*, and its antioxidative properties. *Mol. And Cells* **25**, 112–118 (2008).

[109] O'Callaghan, J., O'Brien, M., McClean, K. & Dobson, A. Optimisation of the expression of a *Trametes versicolor* laccase gene in *Pichia pastoris*. *J. Ind. Microbiol. Biotechnol.* **29**, 55–59 (2002).

[110] Li, Q. *et al.* Overexpression and characterization of laccase from *Trametes versicolor* in *Pichia pastoris*. *Appl. Biochem. Microbiol.* **50**, 140–147 (2014).

[111] Otterbein, L., Record, E., Longhi, S., Asther, M. & Moukha, S. Molecular cloning of the cdna encoding laccase from *Pycnoporus cinnabarinus* i937 and expression in *Pichiapastoris*. *Eur. J. Biochem.* **267**, 1619–1625 (2000).

[112] Lin, Y. *et al.* Purification and characterization of a novel laccase from *Coprinus cinereus* and decolorization of different chemically dyes. *Mol. Biol. Reports* **40**, 1487–1494 (2013).

[113] Rivera-Hoyos, C. M. *et al.* Computational Analysis and Low-Scale Constitutive Expression of Laccases Synthetic Genes GlLCC1 from *Ganoderma lucidum* and POXA 1B from *Pleurotus ostreatus* in *Pichia pastoris*. *PLOS ONE* **10**, e0116524 (2015).

[114] Dönmez, G. & Aksu, Z. The effect of copper(II) ions on the growth and bioaccumulation properties of some yeasts. *Process. Biochem.* **35**, 135–142 (1999).

[115] Alcalde, M. *et al.* Screening Mutant Libraries of Fungal Laccases in the Presence of Organic Solvents. *J. Biomol. Screen.* 624–631 (2005).

[116] Lu, L. *et al.* Production and synthetic dyes decolourization capacity of a recombinant laccase from *Pichia pastoris*. *J. Appl. Microbiol.* **107**, 1149–1156 (2009).

[117] Liu, H. *et al.* Overexpression of a Novel Thermostable and Chloride-Tolerant Laccase from *Thermus thermophilus* SG0.5JP17-16 in *Pichia pastoris* and Its Application in Synthetic Dye Decolorization. *PLOS ONE* **10**, e0119833 (2015).

[118] Healthcare, G. E. & Sciences, L. Recombinant protein purification, principles and methods. *GE* 1 – 308 (2012).

[119] Bohlin, C., Jönsson, L. J., Roth, R. & van Zyl, W. H. Heterologous expression of *Trametes versicolor* laccase in *Pichia pastoris* and *Aspergillus niger*. In *Twenty-Seventh Symposium on Biotechnology for Fuels and Chemicals*, 195–214 (Humana Press, Totowa, NJ, 2006).

[120] Tian, Y.-S., Xu, H., Peng, R.-H., Yao, Q.-H. & Wang, R.-T. Heterologous expression and characterization of laccase 2 from Coprinopsis cinerea capable of decolourizing different recalcitrant dyes. *Biotechnol. biotechnological equipment* **28**, 248–258 (2014).

[121] Bioscience, A. Purification of (His) 6-tagged proteins using HiTrap Chelating HP columns charged with different metal ions. Tech. Rep., Amersham Bioscience (2002).

[122] Silva, I. R., Larsen, D. M., Meyer, A. S. & Mikkelsen, J. D. Identification, expression, and characterization of a novel bacterial RGI Lyase enzyme for the production of bio-functional fibers. *Enzym. Microb. Technol.* **49**, 160–166 (2011).

[123] Brander, S. ., Mikkelsen, J. D. & Kepp, K. P. Characterization of an Alkali-and Halide-Resistant Laccase Expressed in *E. coli*: CotA from *Bacillus clausii*. *Cit.* (2014).

[124] Bukh, C. & Bjerrum, M. J. The reversible depletion and reconstitution of a copper ion in *Coprinus cinereus* laccase followed by spectroscopic techniques. *J. Inorg. Biochem.* **104**, 1029–1037 (2010).

[125] Sigoillot, C. *et al.* Comparison of different fungal enzymes for bleaching high-quality paper pulps. *J. Biotechnol.* **115**, 333–343 (2005).

[126] Rodgers, C. J. *et al.* Designer laccases: a vogue for high-potential fungal enzymes? *Trends Biotechnol.* **28**, 63–72 (2010).

[127] Maestre-Reyna, M. *et al.* Structural and Functional Roles of Glycosylation in Fungal Laccase from *Lentinus* sp. *PLOS ONE* **10**, e0120601 (2015).

[128] Cox, J. & Mann, M. Quantitative, High-Resolution Proteomics for Data-Driven Systems Biology. *Annu. Rev. Biochem.* **80**, 273–299 (2011).

[129] Kuzyk, M. A., Parker, C. E., Domanski, D. & Borchers, C. H. Development of MRM-Based Assays for the Absolute Quantitation of Plasma Proteins. In *Methods in molecular biology (Clifton, N.J.)*, vol. 1023, 53–82 (Springer, 2013).

[130] Anderson, L. & Hunter, C. L. Quantitative Mass Spectrometric Multiple Reaction Monitoring Assays for Major Plasma Proteins. *Mol. & Cell. Proteomics* **5**, 573–588 (2006).

[131] Shleev, S. *et al.* Comparison of physico-chemical characteristics of four laccases from different basidiomycetes. *Biochimie* **86**, 693 – 703 (2004).

[132] Camarero, S., Ibarra, D., Martínez, M. J. & Martínez, A. T. Lignin-derived compounds as efficient laccase mediators for decolorization of different types of recalcitrant dyes. *Appl. environmental microbiology* **71**, 1775–84 (2005).

[133] Camarero, S. *et al.* *p*-hydroxycinnamic acids as natural mediators for laccase oxidation of recalcitrant compounds. *Environ. Sci. & Technol.* **42**, 6703–6709 (2008).

[134] Pardo, I., Chanagá, X., Vicente, A., Alcalde, M. & Camarero, S. New colorimetric screening assays for the directed evolution of fungal laccases to improve the conversion of plant biomass. *BMC Biotechnol.* **13**, 90 (2013).

[135] Lacki, K. & Duvnjak, Z. Transformation of 3,5-dimethoxy,4-hydroxy cinnamic acid by polyphenol oxidase from the fungus *Trametes versicolor*: Product elucidation studies. *Biotechnol. Bioeng.* **57**, 694–703 (1998).

[136] Baum, A. *et al.* Enzyme activity measurement via spectral evolution profiling and PARAFAC. *Anal. Chimica Acta* **778**, 1–8 (2013).

[137] Baum, A., Hansen, P. W., Meyer, A. S. & Mikkelsen, J. D. Simultaneous measurement of two enzyme activities using infrared spectroscopy: A comparative evaluation of PARAFAC, TUCKER and N-PLS modeling. *Anal. Chimica Acta* **790**, 14–23 (2013).

[138] Baum, A., Hansen, P. W., Nørgaard, L., Sørensen, J. & Mikkelsen, J. D. Rapid quantification of casein in skim milk using Fourier transform infrared spectroscopy, enzymatic perturbation, and multiway partial least squares regression: Monitoring chymosin at work. *J. dairy science* **99**, 6071–6079 (2016).

[139] Karmali, K., Karmali, A., Teixeira, A. & Curto, M. M. Assay for glucose oxidase from *Aspergillus niger* and *Penicillium amagasakiense* by Fourier transform infrared spectroscopy. *Anal. Biochem.* **333**, 320–327 (2004).

[140] Pacheco, R., Karmali, A., Serralheiro, M. & Haris, P. Application of Fourier transform infrared spectroscopy for monitoring hydrolysis and synthesis reactions catalyzed by a recombinant amidase. *Anal. Biochem.* **346**, 49–58 (2005).

[141] Stuart, B. H. *Infrared spectroscopy: Fundamentls and Applications Analytical Techniques* (John Wiley & Sona, Ltd, 2004).

[142] Kiers, H. A. L. Some procedures for displaying results from three-way methods. *J. Chemom.* **14**, 151–170 (2000).

[143] Tutorial, T. P. & Bro, R. Chemometrics and intelligent laboratory systems. *Chemomemcs Intell. Lab. Syst.* **38**, 149–171 (1997).

[144] Bro, R. & Kiers, H. A. L. A new efficient method for determining the number of components in PARAFAC models. *J. Chemom.* **17**, 274–286 (2003).

[145] Altman, N. & Krzywinski, M. Points of Significance: Clustering. *Nat. Methods* **14**, 545–546 (2017).

[146] Glagovich, N. IR Absorptions for Representative Functional Groups (2007).

[147] Alcalde, M. *Laccases: Biological Functions, Molecular Structure and Industrial Applications*, 461–476 (Springer Netherlands, Dordrecht, 2007).

[148] Berthomieu, C. & Boussac, A. FTIR and EPR study of radicals of aromatic amino acids 4-methylimidazole and phenol generated by UV irradiation. *Biospectroscopy* **1**, 187–206 (1995).

[149] Munk, L., Andersen, M. L. & Meyer, A. S. Direct rate assessment of laccase catalysed radical formation in lignin by electron paramagnetic resonance spectroscopy. *Enzym. Microb. Technol.* **106**, 88–96 (2017).

[150] Khulbe, K., Ismail, A. & Matsuura, T. Electron Paramagnetic Resonance (EPR) Spectroscopy. *Membr. Charact.* 47–68 (2017).

[151] Roessler, M. M. & Salvadori, E. Principles and applications of EPR spectroscopy in the chemical sciences. *2534 / Chem. Soc. Rev* **47**, 2534 (2018).

[152] Gerson, F. & Huber, W. *Electron spin resonance spectroscopy of organic radicals* (Wiley-VCH, 2003).

[153] Steelink, C. & Hansen, R. E. A solid phenoxy radical from disyringylmethane–a model for lignin radicals. *Tetrahedron Lett.* **7**, 105–111 (1966).

[154] Steelink, C. Free radical studies of lignin, lignin degradation products and soil humic acids. *Geochimica et Cosmochimica Acta* **28**, 1615–1622 (1964).

[155] Rex, R. W. Electron Paramagnetic Resonance Studies of Stable Free Radicals in Lignins and Humic Acids. *Nat.* 1185–1186 (1960).

[156] Bährle, C., Nick, T. U., Bennati, M., Jeschke, G. & Vogel, F. High-Field Electron Paramagnetic Resonance and Density Functional Theory Study of Stable Organic Radicals in Lignin: Influence of the Extraction Process, Botanical Origin, and Protonation Reactions on the Radical g Tensor. *The J. Phys. Chem. A* **119**, 6475–6482 (2015).

[157] Patil, S. V. & Argyropoulos, D. S. Stable Organic Radicals in Lignin: A Review. *ChemSusChem* **10**, 3284–3303 (2017).

[158] Podschun, J., Saake, B. & Lehnen, R. Reactivity enhancement of organosolv lignin by phenolation for improved bio-based thermosets. *Eur. Polym. J.* **67**, 1–11 (2015).

[159] Granata, A. & Argyropoulos, D. S. 2-Chloro-4,4,5,5-tetramethyl-1,3,2-dioxaphospholane, a Reagent for the Accurate Determination of the Uncondensed and Condensed Phenolic Moieties in Lignins. *J. Agric. Food Chem.* **43**, 1538–1544 (1995).

[160] Samanta, A. *et al.* Quenching of Excited Doublet States of Organic Radicals by Stable Radicals. *J. Phys. Chem* **93**, 3651–3656 (1989).

[161] Sawada, H. Chapter 3. Thermodynamics of Radical Polymerization. *J. Macromol. Sci. Part C: Polym. Rev.* **3**, 357–386 (1969).

[162] Romanowski, S. M. d. M. *et al.* Synthesis, characterization, EPR spectroelectrochemistry studies and theoretical calculations of manganese(II) complexes with the ligands H3bpeten and H3bnbpeten. *J. Braz. Chem. Soc.* **21**, 842–850 (2010).

[163] Jin, W. *et al.* Importance of a Laccase Gene (Lcc1) in the Development of *Ganoderma tsugae*. *Int. journal molecular sciences* **19** (2018).

[164] Bissaro, B. *et al.* Oxidative cleavage of polysaccharides by monocopper enzymes depends on H2O2. *Nat. Chem. Biol.* **13**, 1123–1128 (2017).

[165] Bissaro, B., Várnai, A., Røhr, Å. K. & Eijsink, V. G. H. Oxidoreductases and Reactive Oxygen Species in Conversion of Lignocellulosic Biomass. *Microbiol. molecular biology reviews : MMBR* **82**, e00029–18 (2018).

[166] Nguyen, X. S., Ngo, K. D., Nguyen, X. S. & Ngo, K. D. The Role of Metal-Doped into Magnetite Catalysts for the Photo-Fenton Degradation of Organic Pollutants. *J. Surf. Eng. Mater. Adv. Technol.* **08**, 1–14 (2018).

[167] Barbusiński, K. Fenton reaction: controversity concerning the chemistry. *Ecol. chemistry engineering* **16**, 347–358 (2009).

[168] Mosbech, C., Holck, J., Meyer, A. S. & Agger, J. W. The natural catalytic function of CuGE glucuronoyl esterase in hydrolysis of genuine lignin–carbohydrate complexes from birch. *Biotechnol. for Biofuels* **11**, 71 (2018).

[169] Valgimigli, L. *et al.* The unusual reaction of semiquinone radicals with molecular oxygen. *J. Org. Chem.* **73**, 1830–1841 (2008).

[170] Kapich, A. N., Jensen, K. A. & Hammel, K. E. Peroxyl radicals are potential agents of lignin biodegradation. *FEBS Lett.* **461**, 115 – 119 (1999).

[171] Forsberg, Z. *et al.* Structural determinants of bacterial lytic polysaccharide monooxygenase functionality. *J. Biol. Chem.* **293**, 1397–1412 (2018).

[172] Kracher, D., Andlar, M., Furtmüller, P. G. & Ludwig, R. Active-site copper reduction promotes substrate binding of fungal lytic polysaccharide monooxygenase and reduces stability. *The J. biological chemistry* **293**, 1676–1687 (2018).

[173] Breslmayr, E. *et al.* A fast and sensitive activity assay for lytic polysaccharide monooxygenase. *Biotechnol. for Biofuels* **11**, 79 (2018).

[174] Brenelli, L., Squina, F. M., Felby, C. & Cannella, D. Laccase-derived lignin compounds boost cellulose oxidative enzymes AA9. *Biotechnol. for Biofuels* **11** (2018).

[175] Yaver, D. S. *et al.* Purification, characterization, molecular cloning, and expression of two laccase genes from the white rot basidiomycete *Trametes villosa*. *Appl. environmental microbiology* **62**, 834–41 (1996).

[176] Larrondo, L. F., Avila, M., Salas, L., Cullen, D. & Vicuña, R. Heterologous expression of laccase cDNA from *Ceriporiopsis subvermispora* yields copper-activated apoprotein and complex isoform patterns. *Microbiol.* **149**, 1177–1182 (2003).

[177] Benghazi, L. *et al.* Production of the *Phanerochaete flavido-alba* laccase in *Aspergillus niger* for synthetic dyes decolorization and biotransformation. *World J. Microbiol. Biotechnol.* **30**, 201–211 (2014).

[178] Tamayo-Ramos, J. A. *et al.* Enhanced production of *Aspergillus niger* laccase-like multicopper oxidases through mRNA optimization of the glucoamylase expression system. *Biotechnol. Bioeng.* **110**, 543–551 (2013).

[179] Tamayo Ramos, J. A., Barends, S., Verhaert, R. M. & de Graaff, L. H. The *Aspergillus niger* multicopper oxidase family: analysis and overexpression of laccase-like encoding genes. *Microb. Cell Factories* **10**, 78 (2011).

[180] Téllez-Jurado, A., Arana-Cuenca, A., González Becerra, A., Viniegra-González, G. & Loera, O. Expression of a heterologous laccase by *Aspergillus niger* cultured by solid-state and submerged fermentations. *Enzym. Microb. Technol.* **38**, 665–669 (2006).

[181] Wang, Y. *et al.* Isolation of four pepsin-like protease genes from *Aspergillus niger* and analysis of the effect of disruptions on heterologous laccase expression. *Fungal Genet. Biol.* **45**, 17–27 (2008).

[182] Hatamoto, O., Sekine, H., Nakano, E. & Abe, K. Cloning and Expression of a cDNA Encoding the Laccase from *Schizophyllum commune*. *Biosci. Biotechnol. Biochem.* **63**, 58–64 (1999).

[183] Kiiskinen, L.-L. *et al.* Expression of *Melanocarpus albomyces* laccase in *Trichoderma reesei* and characterization of the purified enzyme. *Microbiol.* **150**, 3065–3074 (2004).

[184] Zhang, J. *et al.* Improved biomass saccharification by *Trichoderma reesei* through heterologous expression of lacA gene from *Trametes* sp. AH28-2. *J. Biosci. Bioeng.* **113**, 697–703 (2012).

[185] Abyanova, A. R. *et al.* A heterologous production of the *Trametes hirsuta* laccase in the fungus *Penicillium canescens*. *Appl. Biochem. Microbiol.* **46**, 313–317 (2010).

[186] Yaver, D. S. *et al.* Molecular characterization of laccase genes from the basidiomycete *Coprinus cinereus* and heterologous expression of the laccase lcc1. *Appl. environmental microbiology* **65**, 4943–8 (1999).

[187] Pardo, I. & Camarero, S. Laccase engineering by rational and evolutionary design. *Cell. Mol. Life Sci.* **72**, 897–910 (2015).

[188] Pardo, I. *et al.* A highly stable laccase obtained by swapping the second cupredoxin domain. *Sci. Reports* **8**, 15669 (2018).

[189] Zumárraga, M. *et al.* In Vitro Evolution of a Fungal Laccase in High Concentrations of Organic Cosolvents. *Chem. & Biol.* **14**, 1052–1064 (2007).

[190] Gembloux, P., Delvigne, F., Musoni, M. & Bahama, J.-B. *Biotechnology, agronomy, society and environment: BASE* (Bibliothéque de la Faculté, 1997).

[191] Minussi, R. *et al.* Purification, characterization and application of laccase from *Trametes versicolor* for colour and phenolic removal of olive mill wastewater in the presence of 1-hydroxybenzotriazole. *Afr. J. Biotechnol.* **6** (2002).

[192] Kumar, A. *et al.* Gel-Based Purification and Biochemical Study of Laccase Isozymes from *Ganoderma* sp. and Its Role in Enhanced Cotton Callogenesis. *Front. microbiology* **8**, 674 (2017).

[193] Tonin, F., Vignali, E., Pollegioni, L., D'Arrigo, P. & Rosini, E. A novel, simple screening method for investigating the properties of lignin oxidative activity. *Enzym. Microb. Technol.* **96**, 143–150 (2017).

[194] Hommes, G., Gasser, C. A., Ammann, E. M. & Corvini, P. F. X. Determination of oxidoreductase activity using a high-throughput microplate respiratory measurement. *Anal. Chem.* **85**, 283–291 (2013).

Papers

Paper 1

Multiple Reaction Monitoring for quantitative laccase kinetics by LC-MS

SCIENTIFIC REPORTS

OPEN

Multiple Reaction Monitoring for quantitative laccase kinetics by LC-MS

Received: 16 January 2018
Accepted: 9 May 2018
Published online: 25 May 2018

Valentina Perna, Jane W. Agger, Jesper Holck & Anne S. Meyer

Laccases (EC 1.10.3.2) are enzymes known for their ability to catalyse the oxidation of phenolic compounds using molecular oxygen as the final electron acceptor. Lignin is a natural phenylpropanoids biopolymer whose degradation in nature is thought to be aided by enzymatic oxidation by laccases. Laccase activity is often measured spectrophotometrically on compounds such as syringaldazine and ABTS which poorly relate to lignin. We employed natural phenolic hydroxycinnamates having different degree of methoxylations, *p*-coumaric, ferulic and sinapic acid, and a lignin model OH-dilignol compound as substrates to assess enzyme kinetics by HPLC-MS on two fungal laccases *Trametes versicolor* laccase, Tv and *Ganoderma lucidum* laccase, Gl. The method allowed accurate kinetic measurements and detailed insight into the product profiles of both laccases. Both Tv and Gl laccase are active on the hydroxycinnammates and show a preference for substrate with methoxylations. Product profiles were dominated by the presence of dimeric and trimeric species already after 10 minutes of reaction and similar profiles were obtained with the two laccases. This new HPLC-MS method is highly suitable and accurate as a new method for assaying laccase activity on genuine phenolic substrates, as well as a tool for examining laccase oxidation product profiles.

Lignin is a natural plant biopolymer composed of aromatic units in the form of phenylpropanoids, i.e. p-hydroxyphenyl (H), guaiacyl (G), and syringyl (S)[1]. Lignin is present at levels of 20–50% by weight in lignocellulosic materials. Along with cellulosic biomass refining, the attention on exploiting lignin for sustainable production of new materials or for recovering valuable aromatic compounds has recently risen significantly[2]. Degradation of lignin in nature is thought to be achieved by means of enzymes such as peroxidases and laccases produced by different organisms. Laccases (benzenediol: oxygen oxidoreductases; EC 1.10.3.2) are blue multi-copper oxidoreductase enzymes produced ubiquitously by fungi, plants and bacteria (and even humans)[3,4] currently receiving particular attention because they catalyse the oxidation of phenolic compounds similar to subunits in lignin using only molecular oxygen as final electron acceptor[5]. The overall reaction cycle involves the oxidation of four moles of phenolic substrate with the simultaneous reduction of one mole of O_2 to two moles of H_2O[6,7]. As a result of the enzyme catalysed phenol oxidation, phenoxy radicals are generated in lignin. In turn, the phenoxy radicals react further via different non-enzymatic reactions such as radical polymerization, depolymerization, grafting and modification of functional groups[5,8–10].

Often laccase activity is determined by monitoring the oxidation of chemical compounds such as syringaldazine (4-hydroxy-3,5-dimethoxy-benzaldehyde azine) and ABTS (2,2′-azino-bis(3-ethylbenzothiazoline-6-sulphonic acid)) by changes in UV absorbance. Since syringaldazine and ABTS are poorly related to lignin, the use of them provide insufficient information about the actual oxidative kinetics of laccase on true natural phenols and "lignin-like" phenolic structures. Another drawback of using these substrates is that the oxidation products formed after laccase oxidation tend to precipitate quickly even at modest concentrations[11] creating an unstable assay with the risk of measuring wrong enzyme activity values. Pardo *et al.*[12,13] developed a new colorimetric assay method using "lignin-like" compounds including sinapic acid and 2,6-dimethoxyphenol, where the oxidation was followed spectrophotometrically. The substrates chosen are highly relevant but spectrophotometric analysis only allows sensitivity in the nmol range[12] and provides little insight into the possible products formed during the laccase catalysed oxidation.

Center for BioProcess Engineering, Department of Chemical and Biochemical Engineering, Technical University of Denmark, Kgs, Lyngby, 2800, Denmark. Correspondence and requests for materials should be addressed to J.W.A. (email: jaag@kt.dtu.dk)

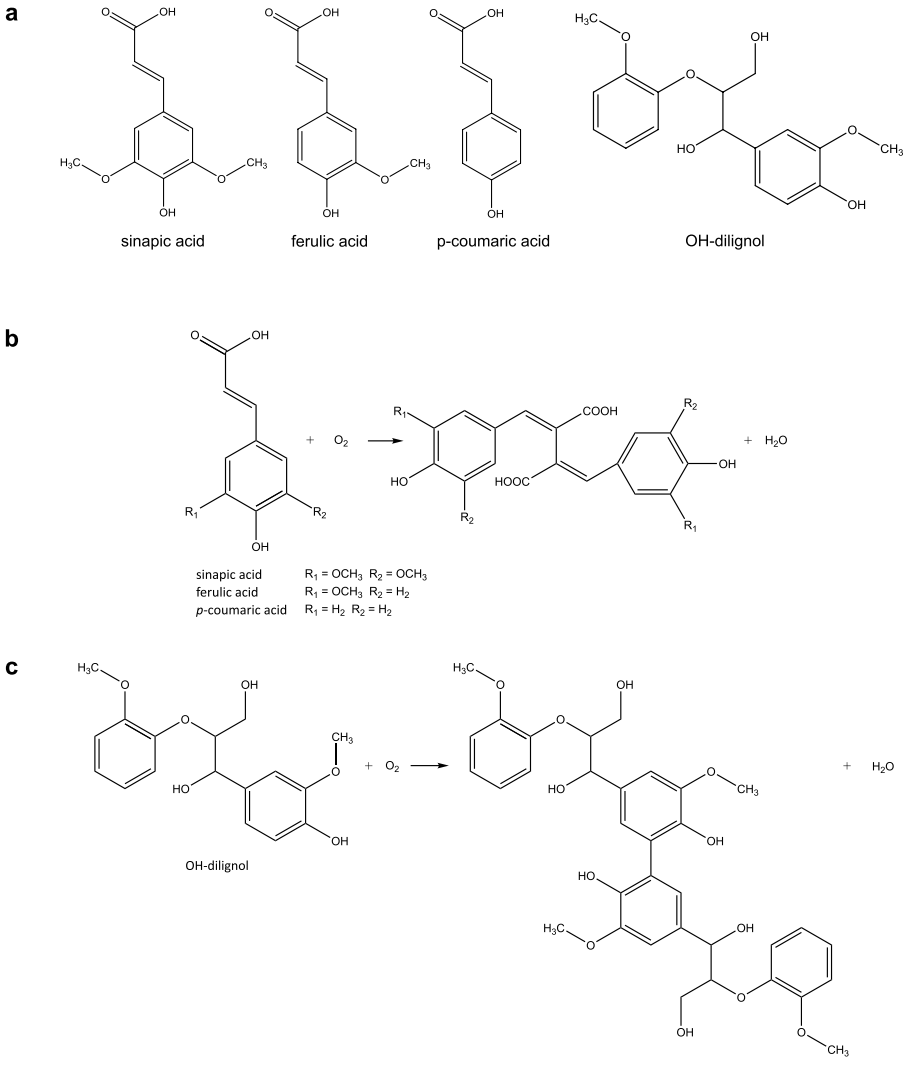

Figure 1. Hydroxycinnamic acid and OH-dilignol structures (**a**). Possible concept for product formation after laccase oxidation: dimer formation from the hydroxycinnamic acids (**b**) and from the OH-dilignol (**c**).

HPLC-MS analysis allows for direct monitoring of product formation and quantitative assessment of kinetics. The direct monitoring of the reaction in real time not only give information about the substrate oxidation but also provide insight into the products formed during the continued radical reactions, including e.g. various isomeric and polymeric compounds. HPLC-MS is receiving increasing attention as a quantitative tool and particularly within the field of proteomics the quantitative use of Multiple Reaction Monitoring is widespread[14]. Multiple Reaction Monitoring is based on identification and quantification of specific fragment ions from a predetermined precursor list of parent masses and offers several advantages including high level of specificity, high sensitivity and low susceptibility to interfering compounds[15,16]. The latter is particularly important in biological samples with highly complex matrices.

The objective of the present work was to develop a real time, highly sensitive and accurate methodology based on HPLC-MS to assess laccase activity on monomeric phenolics and a dimeric OH-lignol-compound and specifically assess whether the kinetic rates and catalytic efficiencies of laccases depend on the substitutions on the phenolic ring structure and/or on the molecular structure as a whole beyond the monomeric phenol moiety. The work performed was driven by the hypothesis that laccases may have different reaction kinetics on different hydroxycinnamates and that accurate and sensitive analysis might reveal such differences. We hypothesized that a methodology based on HPLC-MS analysis can be used to describe laccase oxidized reactions to a higher detail than what has been common practice both with respect to quantitative measures and product description. In this scenario Multiple Reaction Monitoring quantification by HPLC-MS is feasible because the reactions are well-defined consisting of known starting components.

Three different hydroxycinnamic acids (sinapic acid, ferulic acid and *p*-coumaric acid) and an OH-dilignol (Fig. 1 panel a) were used to assess the action of two different white-rot fungal laccases: laccase from *Trametes versicolor* (Tv) and laccase from *Ganoderma lucidum* (Gl). The Tv laccase is a widely studied high redox potential laccase, whereas the Gl laccase represents a newer laccase, we have found to work particularly well in relation

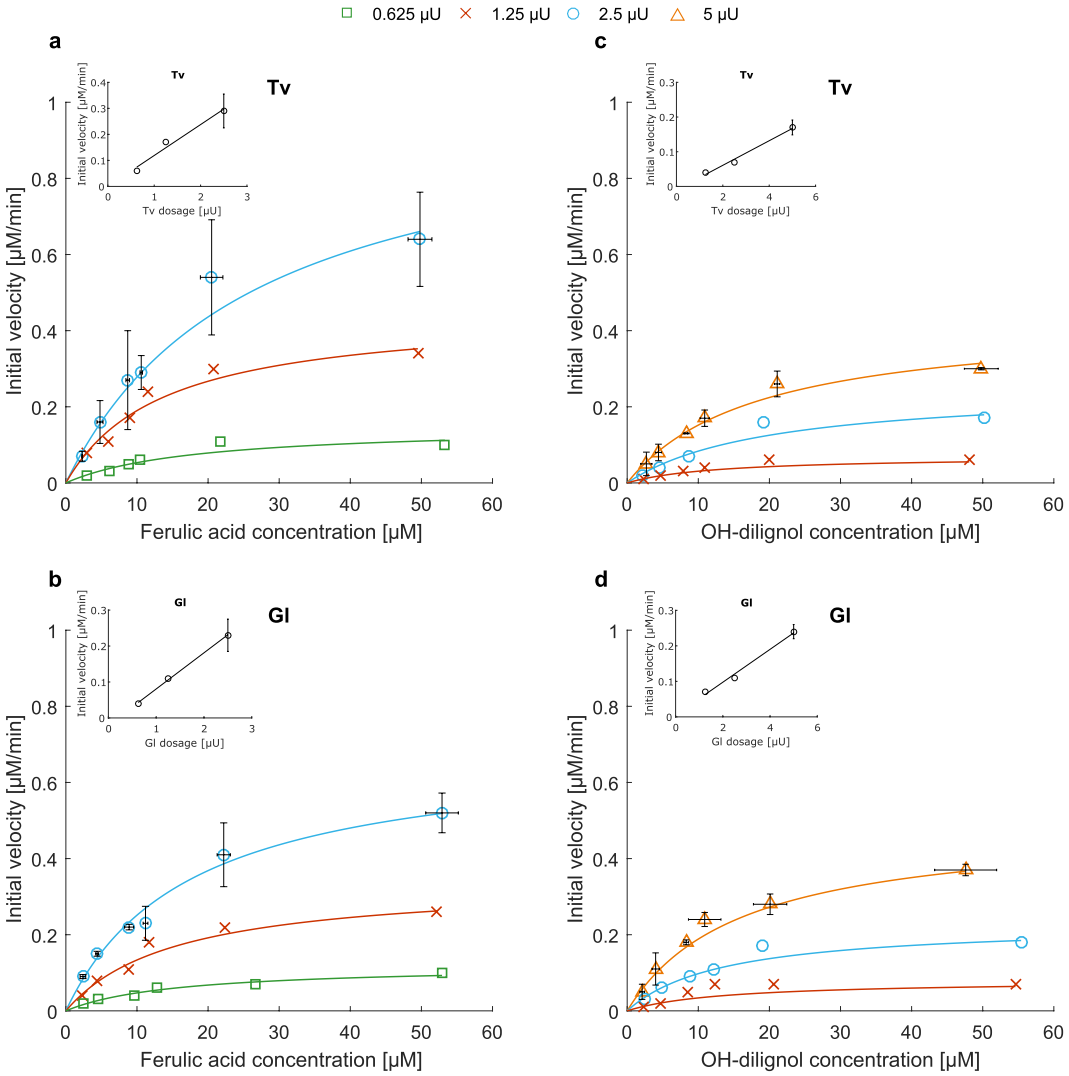

Figure 2. Michaelis-Menten curves for Tv and Gl laccase on ferulic acid (**a**,**b**) and OH-dilignol (**c**,**d**). Three different enzyme dosages (in syringaldazine assay units) are shown: for ferulic acid (**a**,**b**): 0.625 μU (green open square), 1.25 μU (red cross) and 2.5 μU (blue open circle). For OH-dilignol (**c**,**d**): 1.25 μU (red cross), 2.5 μU (blue open circle) and 5 μU (orange open triangle). Dose response at 10 μM substrate concentration is shown in the inset. For the highest enzyme dose standard deviations are shown.

to enhancing cellulose catalysed lignocellulosic degradation[17]. From the type of the reactions monitored in this study, it is expected that oxidation products will primarily be dimeric and possibly similar to the structures in Fig. 1 panel b and c.

Results

Kinetics. LC-MS was used to determined kinetics for *Trametes versicolor* (Tv) and *Ganoderma lucidum* (Gl) laccase on lignin model compounds: sinapic acid, ferulic acid, *p*-coumaric acid and OH-dilignol. Kinetics were determined as an on-line measurement of substrate depletion and these results moreover confirm that LC-MS analysis is a highly relevant methodology for describing enzyme kinetics. In order to overcome differences in enzyme purity between the Tv and Gl laccase the enzyme loading in the kinetic measurements was based on dosing equal levels of each enzyme's activity on syringaldazine. In this way the dosage of active enzyme protein was uniform in all experiments allowing for direct comparison between the kinetic rates of the enzymes on the particular phenolic substrates. This approach for dosing is commonly used in enzyme work[12,18–21] and represents another strategy for standardizing enzyme loading within a set of experiments in comparison to loading by protein concentration. As exemplified by ferulic acid and OH-dilignol (Fig. 2) there was a clear dose response effect for both enzymes where the initial rate increased perfectly proportionally with the increase in enzyme concentration on both substrates (Fig. 2 inserts). Equivalent results were obtained with both enzymes for the enzyme kinetics on sinapic acid and *p*-coumaric acid (Supplementary Fig. S1).

For both enzymes the K_m on the *p*-coumaric acid was significantly higher than the one for ferulic and sinapic acid, although no statistical significance could be discerned, the K_m values tended to decrease with the

		Tv	Gl
Sinapic acid	V_{max} [μM/min]	1.15 ± 0.07^{x}	1.06 ± 0.03^{x}
	K_m [μM]	$12.13 \pm 2.23^{b,x}$	$12.11 \pm 0.46^{b,x}$
Ferulic acid	V_{max} [μM/min]	1.14 ± 0.10^{x}	0.82 ± 0.07^{y}
	K_m [μM]	$17.17 \pm 4.99^{b,x}$	$17.84 \pm 0.93^{b,x}$
p-coumaric acid	V_{max} [μM/min]	6.73 ± 0.40^{x}	7.31 ± 0.55^{x}
	K_m [μM]	$130.27 \pm 2.56^{a,x}$	$271.04 \pm 5.25^{a,y}$
OH-dilignol	V_{max} [μM/min]	0.39 ± 0.03^{x}	0.46 ± 0.03^{x}
	K_m [μM]	$12.89 \pm 3.68^{b,x}$	$11.76 \pm 2.61^{b,x}$

Table 1. K_m and V_{max} for hydroxycinnamic acids and OH-dilignol. The enzymes were dosed at equal levels of syringaldazine activity. Standard deviations are shown and significant difference ($p \leq 0.05$) of K_m column-wise are shown as superscripted letters (a-b), significance difference ($p \leq 0.05$) of K_m and V_{max} row-wise are shown as superscripted letters (x−y).

		Tv	Gl
Sinapic acid	Apparent specific activity [nM/μU · s]	$8.32 \pm 0.47^{a,x}$	$6.97 \pm 0.22^{a,x}$
	Apparent catalytic efficiency [1/μU · s]	$565.6 \pm 102.15^{a,x}$	$550.8 \pm 36.3^{a,x}$
Ferulic acid	Apparent specific activity [nM/μU · s]	$6.66 \pm 0.59^{a,x}$	$4.55 \pm 0.45^{b,y}$
	Apparent catalytic efficiency [1/μU · s]	$280.0 \pm 64.2^{b,x}$	$284.8 \pm 33.7^{b,x}$
p-coumaric acid	Apparent specific activity [nM/μU · s]	$0.51 \pm 0.03^{b,x}$	$0.55 \pm 0.04^{d,x}$
	Apparent catalytic efficiency [1/μU · s]	$3.92 \pm 0.27^{c,x}$	$2.05 \pm 0.17^{c,y}$
OH-dilignol	Apparent specific activity [nM/μU · s]	$1.43 \pm 0.09^{c,x}$	$1.70 \pm 0.09^{c,x}$
	Apparent catalytic efficiency [1/μU · s]	$84.9 \pm 20.5^{d,x}$	$106.1 \pm 20.8^{d,x}$

Table 2. Apparent specific activity and apparent catalytic efficiency for hydroxycinnamic acids and OH-dilignol. Apparent specific activity is defined as the amount of substrate that is converted by the enzyme in one second, the apparent catalytic efficiency is the number of oxidation cycles that the enzyme is capable of in one second. The enzymes were dosed at equal levels of syringaldazine activity. Standard deviations are shown and significant difference ($p \leq 0.05$) of apparent specific activity and apparent catalytic efficiency column-wise are shown as superscripted letters (a–d), significance difference ($p \leq 0.05$) of apparent specific activity and apparent catalytic efficiency row-wise are shown as superscripted letters (x–y).

methoxylation (Table 1). The order of K_m on the hydroxycinnamates is in complete agreement with previous studies[19,22,23]. V_{max} is enzyme dosage dependent and should therefore only be compared between enzymes and both Tv and Gl showed the same overall maximum velocity on all the substrates except for ferulic acid where Tv laccase was slightly faster. Apparent specific activity is standardized with the enzyme dosage and allows comparison between substrates, confirming that the degree of methoxylation is affecting the enzyme activity (Table 2). The apparent catalytic efficiency is the number of oxidation cycles that the enzyme is capable of. The catalytic efficiency also demonstrates the influence of methoxylations where ferulic acid and sinapic acid show 2 to 3 order of magnitude higher apparent catalytic efficiency values than *p*-coumaric acid (Table 2). The poor catalytic efficiency obtained with both enzymes on *p*-coumaric acid is also a direct consequence of the high K_m value towards this substrate (Tables 1 and 2).

OH-dilignol was chosen based on its similar structure to subunits in lignin and the fact that it represents a dimer. The K_m value for both enzymes towards this substrate was the same as the K_m values for the methoxylated hydroxycinnamates sinapic and ferulic acid, confirming that the presence of methoxylation is apparently of higher importance for the enzyme affinity than the remaining molecular structure. Despite similar affinities between the methoxylated hydroxycinnamate and OH-dilignol the apparent specific activity was approximately 2 to 4 times lower for the OH-dilignol and this was also reflected in the apparent catalytic efficiency (Table 2).

Reaction evolution profiles. The HPLC-MS methodology provides an insight into the products generated as a result of laccase driven substrate oxidation (Fig. 3). When looking into the product profiles generated during laccase oxidation of the hydroxycinnamates and OH-dilignol, it was observed that both enzymes generated similar products on each substrates (Fig. 3), although the oxidation of *p*-coumaric acid and OH-dilignol catalysed by the Gl laccase resulted in a few more peaks than those obtained with Tv laccase catalysis (Fig. 3 panel e, f, g and h).

The primary products detected were in agreement with the masses of dimers and trimers of the corresponding substrates but also compounds with loss of 44 were formed which could represent the loss of a carboxyl group. One example of the formation of such compounds is the reaction from sinapic acid (Fig. 3 panel a) where the MS spectra of products show two different isomers of dimer formation (peak 3 and 4) and two dimeric products presumably lacking a carboxylic group (peak 2 and 3). The work by Lackii *et al.*[24] reports that the predominant coupling among sinapic acid radicals is the $\beta-\beta'$ coupling having a dehydrodisinapic lactone as main product.

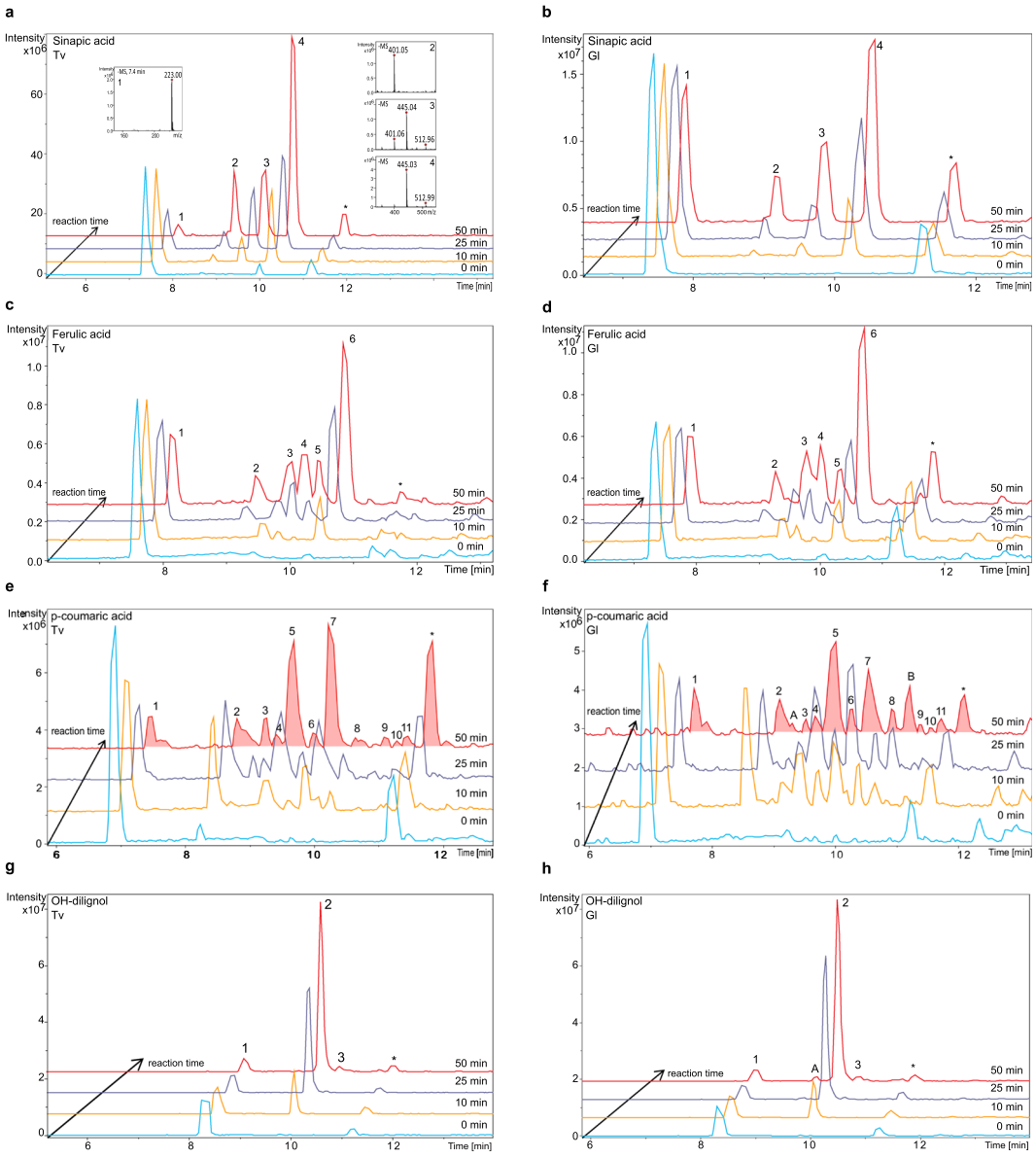

Figure 3. Laccase oxidation evolution profiles for hydroxycinnamic acids and OH-dilignol: oxidation of sinapic acid with Tv and Gl laccase (**a**,**b**); oxidation of ferulic acid with Tv and Gl laccase (**c**,**d**); oxidation of *p*-coumaric acid with Tv and Gl laccase (**e**,**f**) and oxidation of OH-dilignol with Tv and Gl laccase (**g**,**h**). Chromatograms at different reaction times are shown: 0 minutes (light blue), 10 minutes (yellow), 25 minutes (violet) and 50 minutes (red). Please note that the intensity scale may differ between chromatograms and is adjusted to give optimal display of figures. Panel a includes an example of the MS spectra corresponding to each peak, all ions are observed as $[M-H]^-$. All other MS and MS/MS spectra are found in Supplementary Figs S2–S11. Oxidation reaction products are numbered according to substrate and are therefore comparable between enzymes.

In accordance to that ferulic acid radicals may also have a $\beta-\beta'$ coupling obtaining a dehydrodiferulic acid lactone[25,26]. Suggested product structures can be found in Supplementary Figs S12–S15.

Reaction products are a result of (non-enzyme catalysed) chemical reactions between radicals formed by laccase oxidation and hence several conformations are possible. The data obtained show that such reactions may also lead to further random modification like decarboxylation. It appears that dimeric products occur early, and that decarboxylation may follow instantaneously (Fig. 3 panel a, b, c and d). At a later stage (after 25 minutes) in the reaction also trimeric and tetrameric products occurred (for *p*-coumaric acid in particular), some which might be further modified by decarboxylation. In the evolution of reaction products from *p*-coumaric acid oxidation certain products decrease in intensity after 50 minutes incubation (Fig. 3 panel e and f for peak number 2, 4, 6 and 8) and this may be a result of either compound instability or because the products react further with newly formed radicals from the laccase catalysis. The method does not allow the distinction between the two possibilities.

Laccase oxidation of OH-dilignol results in only two product peaks (Fig. 3 panel g and h), both dimeric after 50 minutes incubation and neither of these products are prone to decarboxylation. Furthermore, in order to fit the observed product masses, the OH-dilignol structure only allows dimeric compounds to form via the benzyl ring and this limits the number of possible isomers (Supplementary Fig. S15). Product profiles for the hydroxycinnamates are much more complex compared to the profile for OH-dilignol (Fig. 3) and the complexity increase with the decrease in methoxy groups on the aromatic ring. The methoxy groups may cause sterical hindrance during radical driven propagation and therefore less products are formed after reaction on sinapic acid compared to *p*-coumaric acid.

Discussion

OH-dilignol was chosen based on its similar structure to hydroxycinammates and higher degree of polymerization in order to have a substrate mimicking lignin. Despite the similar values of K_m (Table 1) the V_{max} was lower causing the apparent specific laccase activity for OH-dilignol (Table 2) to be lower than on the hydroxycinnamates. This difference could be related to resonance stabilization where the OH-dilignol might be capable of forming a more stable radical than the hydroxycinnamates[27]. Due to a lack in conjugated double bonds between the phenoxyl groups and the rest of the molecule the radical stays longer on the phenoxyl group before it reacts further. The analytical method does not allow the observation of radical formation and hence does not allow for interpretation of oxidation until the radical has reacted to deplete the substrate. On that notion it could be speculated that the laccases are equally efficient in oxidizing the OH-dilignol as they are in oxidizing the methoxylated hydroxycinnamates. The reaction of OH-dilignol with laccase showed only two isomers of the dimer (Fig. 3 panel g and h and Supplementary Figs S10 and S11) as a result of the lack of conjugation. The formation of the dimers is most likely linked via the 5−5′ position because there is a preference for formation linked in the *ortho* or *para* position which in this case only allows for 5−5′ linkage[26] (possible structures are reported in Supplementary Fig. S15). These linkage preferences also explain why the complexity of the product profiles increased with the decrease in methoxylation on the aromatic ring. The higher the number of methoxylated groups, the higher the stereo-chemical hindrance and hence less products are formed.

Importantly, increasing number of methoxylations on the substrate molecule resulted in higher affinity by the laccases. For both Tv and Gl laccases the enzyme's affinity follows sinapic acid $\geq$ ferulic acid $>$ *p*-coumaric acid (Table 1), which is in accordance with hydroxycinnamates antioxidant power and other studies[19,28]. The preference for oxidizing the methoxylated substrates was not only seen with these simple monomeric molecules but was also found in pretreated lignocellulosic materials[29].

The two different enzymes, Tv and Gl laccase, were applied at two different degrees of purity. The HPLC-MS showed that it was possible to monitor and quantify reaction parameters for both enzymes despite the differences in purity, concentration and potentially interfering compounds. In order to overcome the differences in purity and to allow direct comparison between the two enzymes the laccase activity was measured on syringaldazine and used to dose the two enzymes at the same level. The normalization against syringaldazine eliminated any differences in protein concentration and hence dosages could be based on addition of a fixed amount of activity rather than a fixed protein concentration. In this way a direct comparison between the two different enzymes was possible.

In order to obtain reliable quantification by LC-MS comparable conditions between calibration standards and unknown samples should be met. In this work, similar conditions were achieved by applying pure and simple reaction mixtures with little ionic strength thereby keeping the total number of ions low. In situation where differences between samples and calibration standards become too large the quantitative approach may not apply. Hence, an individual evaluation should be conducted in each situation before engaging in a new setup and there may be scenarios where the LC-MS methodology is not applicable.

Our results showed that the HPLC-MS can be used as a highly suitable assay for studying laccase activity and it has several advantages compared to more traditional methods based on change in UV absorbance[12,19,30]. The HPLC-MS allows fast (few minutes retention time), online analysis in real time, meaning that the reaction is monitored while it proceeds with minimal disturbance. A negligible amount of sample volume (2 μL) is drawn from the reaction at any given time point and the enzyme reaction is immediately quenched when the sample is injected into the flow path (mobile phase, pH 2). This type of analysis is also highly descriptive of the reaction both in terms of product profiling with mass detection and also in relation to maintaining the integrity of the sample when no artifacts are introduced by extensive sample handling such as heat inactivation. HPLC-MS also offers high sensitivity with enzyme concentrations in μU scale and substrate concentration in sub-pmol scale compared to UV signals reported in the nmol scale[12]. Comparison between MS (in Multiple Reaction Monitoring-mode) and UV signals directly measured in this work showed that the lower limit for substrate detection is approximately 0.04 pmol on the MS versus approximately 2 pmol in UV signal. One of the explanations for this high sensitivity is low levels of noise on the MS in Multiple Reaction Monitoring-mode. With respect to assay specificity the method allows to distinguish laccase from peroxidase activity because the latter requires an additional co-substrate in the form of H_2O_2. Polyphenol oxidase may also respond in this type of assay and in case of doubt substrates more specific for polyphenol oxidase might need to be included.

The original hypothesis that laccases have different reaction kinetics on the three lignin units has been investigated and the work shows that laccases indeed have different preferences for oxidizing structures that resemble lignin - the low solubility of lignin and the apparent dependency of laccase kinetics of the availability of reactive phenol-hydroxyls in larger lignin structure is a separate issue[18]. This work also shows that hydroxycinnamates are reliable models for lignin-derived phenols and smaller lignin polymeric moieties and that the hydroxycinnamates are excellent candidates as model substrates for laccases.

Methods

Materials. Sinapic acid, ferulic acid, *p*-coumaric acid and all the chemicals used in the work were purchased from Sigma-Aldrich (Steinheim, Germany). OH-dilignol was a kind gift from Prof. Dr. Carsten Bolm, Institute of Organic Chemistry in RWTH Aachen University. Laccase from *Trametes versicolor* (Tv) was purchased from Sigma-Aldrich (Steinheim, Germany) and the *Ganoderma lucidum* (Gl) laccase was produced in house using *Pichia pastoris* as heterogeneous expression system. The construct containing the gene encoding Gl (pML α-LacGL1) was produced similar to previous work[17], however in this work an enzyme without His-tag was used. A 5 L scale production of recombinant laccase in *P. pastoris* was performed according to Silva *et al.*[31]. In order to improve enzyme's stability the methanol Fed-Batch phase was carried out at 20 °C. The total time for the fermentation process was 112 h. Laccase enriched fermentation broth was recovered by centrifugation at 5300 × g 5 °C for 1 h and the supernatant was subjected to sterile filtration and concentrated by ultrafiltration, using a cross-flow bioreactor system with a 10 kDa cutoff membrane (Millipore, Sartorius, Denmark), as described by Silva *et al.*[31]. The enzyme aliquots were stored at −80 °C with the addition of 20% (w/v) glycerol. In the present work Gl laccase was used directly after concentration of the fermentation supernatant. No further purification steps were performed.

Laccase activity assay. Activity of laccase was assessed by monitoring the oxidation of syringaldazine (SGA) at 530 nm ($\varepsilon = 6.5 \times 10^4\,M^{-1}\,cm^{-1}$). The assay reaction mixture contained 25 μM syringaldazine, 10% ethanol, 25 mM sodium acetate pH 5.0 and a proper amount of enzyme. Syringaldazine oxidation was monitored at 25 °C for 20 minutes. Enzyme activity was expressed in units: one International Unit (U) was defined as the amount of enzyme required to catalyse the conversion of 1 μmol of substrate (syringaldazine) per minute under the assay reaction conditions. SGA activity was used in this work as measure of enzyme dose to overcome the differences in enzyme purity. Therefore Tv and Gl laccases were dosed on the same value of SGA activity in the HPLC-MS reactions diluting them in 12.5 mM sodium acetate buffer pH 5.

HPLC-MS screening method. Laccase oxidation of sinapic acid, ferulic acid, *p*-coumaric acid and OH-dilignol and formation of products were assessed using liquid chromatography and mass spectroscopy (HPLC-MS). The reaction mixture (reaction volume of 500 μL) contained 50 μM of substrate in 12.5 mM sodium acetate buffer pH 5 and an appropriate dose of enzyme depending on the substrate analysed, i.e. 2.5 μU for sinapic acid and ferulic acid, 220 μU for *p*-coumaric acid and 5 μU for OH-dilignol (where needed the enzymes were diluted in 12.5 mM sodium acetate buffer pH 5). The samples were incubated in the HPLC autosampler at 30 °C. Two μL of reaction mixture were injected onto a Hypersil Gold Phenyl column (150 mm × 2.1 mm; 3 μm, Thermo Fisher Scientific, Waltham, MA, USA). The chromatography was performed on a Dionex UltiMate 3000 UPLC (Thermo Fischer Scientific, Sunnyvale, CA, USA) at 0.4 mL min^{-1} at 40 °C with a three-eluent system with eluent A 0.1% formic acid in water, eluent B acetonitrile and eluent C water. The elution was performed as follow (time indicated in min): 0, 10% A 0% B 90% C; 0–15, linear gradient to 10% A 90% B 0% C; 15–20, isocratic 10% A 90% B 0% C; 20–25, isocratic 10% A 0% B 90% C. The HPLC was connected to an ESI-iontrap (model Amazon SL from Bruker Daltonics, Bremen, Germany) and the electrospray was operated in negative ultra scan mode using a target mass of 300 *m/z* for the three acid and a target mass of 400 *m/z* for OH-dilignol. A scan range from 50 to 2200 *m/z* was selected and capillary voltage at 4.5 kV, end plate offset 0.5 kV, nebulizer pressure at 3.0 bar, dry gas flow at 12.0 L min^{-1}, and dry gas temperature at 280 °C were used.

HPLC-MS kinetic method. Laccase kinetic on sinapic acid, ferulic acid, *p*-coumaric acid and OH-dilignol was assayed with liquid chromatography and mass spectroscopy (HPLC-MS) with a set-up similar to the one described above, however with minor adjustments to accommodate short time intervals between sampling. The reaction (reaction volume of 500 μL) was performed using different concentrations of the substrate ranging from 2 μM to 50 μM, 12.5 mM sodium acetate buffer pH 5 and three different dosage of enzyme: 0.625, 1.25 and 2.5 μU for sinapic acid and ferulic acid; 55, 110 and 220 μU for *p*-coumaric acid; and 1.25, 2.5 and 5 μU for OH-dilignol (where needed the enzymes were diluted in 12.5 mM sodium acetate buffer pH 5). Two μL of the reaction mixture were injected onto a Hypersil Gold Phenyl column. For reaction performed at 2 and 4 μM substrate concentration, 5 μL sample were injected to have sufficient signal intensity. This was taken into account during quantification. The chromatography was performed at 0.4 mL min^{-1} at 40 °C on a three-eluent system with eluent A 0.1% formic acid in water, eluent B acetonitrile and eluent C water. The elution profile was performed as follow (time indicated in min): 0–1.5, isocratic 10% A, 30% B 60% C; 1.5–4, step gradient to 10% A 90% B 0%; 4–6, isocratic 10% A, 30% B 60% C. The HPLC was connected to an ESI-iontrap and the electrospray was operated in negative ultra scan with Multiple Reaction Monitoring (MRM) mode using a target mass of 200 *m/z* for the acids and of 300 *m/z* for OH-dilignol. MRM mode was chosen to selectively follow only substrate depletion. MRM ion precursor were chosen according to the $[M-H]^-$ value for the different substrates assayed, i.e. *m/z* 222.83, *m/z* 192.74, *m/z* 162.79 and *m/z* 319.10, for sinapic acid, ferulic acid, *p*-coumaric acid and OH-dilignol respectively. 100% amplitude for reaction was selected in order to have fragmentation of the ion precursor examined. Capillary voltage at 4.5 kV, end plate offset 0.5 kV, nebulizer pressure at 3.0 bar, dry gas flow at 12.0 L min^{-1}, and dry gas temperature at 280 °C were used. Standards of each substrate at different concentration, ranging from 1 to 100 μM were also analysed as external standards with the same method for calibration.

Quantification. Quantification of the precursor ion was performed using Bruker Compass QuantAnalysis software (Bruker Daltonik GmbH), defining an individual method for each substrate. All ions were observed as $[M-H]^-$. Sinapic acid quantification was performed by defining an Extracted Ion Chromatogram (EIC) on MSn of *m/z* 222.8, masses *m/z* 222.75, *m/z* 207.72, *m/z* 178.75 and *m/z* 163.78 with a width of ± 0.5, retention time 1.4 min with a window of 0.2 min. Ferulic acid quantification was performed by defining an EIC on MSn of *m/z* 192.7, masses *m/z* 192.72, *m/z* 177.71, *m/z* 148.80 and *m/z* 133.85 with a width of ± 0.5, retention time

1.4 min with a window of 0.2 min. *p*-coumaric acid quantification was performed by defining an EIC on MSn of *m/z* 162.8, masses *m/z* 162.79 and *m/z* 119.00 with a width of ± 0.5, retention time 1.4 min with a window of 0.2 min. OH-dilignol quantification was performed by defining an EIC on MSn of *m/z* 319.1, masses *m/z* 319.10, *m/z* 270.75 and *m/z* 194.77 with a width of ± 0.5, retention time 1.7 min with a window of 0.2 min. In all the cases peak detection was done using algorithm version 2.1, S/N threshold 1, area threshold 0.1, intensity threshold 0.1, skim ratio 0.1 and smoothing width 1. Calibration curve was performed using 9 levels of concentrations and fitting the data with a quadratic curve (see Supplementary Figs S16 and S17 to see how the different masses were chosen and how the standard curves looked).

Kinetic parameters determination. Kinetic parameters V_{max} and K_m were obtained using Hane linearization of the Michaelis-Menten curve for all the different enzyme dosages assessed. Apparent specific activity was determined by normalizing V_{max} over the highest value of enzyme dosage used. The normalization was performed using 2.5 μU for sinapic acid and ferulic acid, 220 μU for *p*-coumaric acid and 5 μU for OH-dilignol. Apparent catalytic activity was determined by dividing the apparent specific activity by K_m.

Statistical analysis. One-way ANOVA for determination of statistical significance was made in Minitab 18 (Minitab Inc., State College, PA, USA) using Tukey's test with a pooled standard deviation. Statistical significance was established at $p \leq 0.05$.

References

1. Gellerstedt, G. & Henriksson, G. Chapter 9 - lignins: Major sources, structure and properties. In Belgacem, M. N. & Gandini, A. (eds.) *Monomers, Polymers and Composites from Renewable Resources*, 201–224 (Elsevier, Amsterdam 2008).
2. Ragauskas, A. J. *et al*. Lignin valorization: Improving lignin processing in the biorefinery. *Sci*. **344** (2014).
3. Virk, A. P., Sharma, P. & Capalash, N. Use of laccase in pulp and paper industry. *Biotechnol. Prog.* **28**, 21–32 (2012).
4. Lahiri, A., Hedl, M., Yan, J. & Abraham, C. Human LACC1 increases innate receptor-induced responses and a LACC1 disease-risk variant modulates these outcomes. *Nat. Commun*. **8** (2017).
5. Munk, L., Sitarz, A. K., Kalyani, D. C., Mikkelsen, J. D. & Meyer, A. S. Can laccases catalyze bond cleavage in lignin? *Biotechnol. Adv.* **33**, 13–24 (2015).
6. Sitarz, A. K., Mikkelsen, J. D. & Meyer, A. S. Structure, functionality and tuning up of laccases for lignocellulose and other industrial applications. *Critical Rev. Biotechnol.* **36**, 70–86 (2016).
7. Jones, S. M. & Solomon, E. I. Electron transfer and reaction mechanism of laccases. *Cell. Mol. Life Sci.* **72**, 869–883 (2015).
8. Mai, C., Schormann, W., Hüttermann, A., Kappl, R. & Hüttermann, J. The influence of laccase on the chemo-enzymatic synthesis of lignin graft-copolymers. *Enzym Microb. Technol.* **30**, 66–72 (2002).
9. Kudanga, T., Nyanhongo, G. S., Guebitz, G. M. & Burton, S. Potential applications of laccase-mediated coupling and grafting reactions: A review. *Enzym Microb. Technol.* **48**, 195–208 (2011).
10. Widsten, P. & Kandelbauer, A. Laccase applications in the forest products industry: A review. *Enzym Microb. Technol.* **42**, 293–307 (2008).
11. Setti, L., Giuliani, S., Spinozzi, G. & Pifferi, P. G. Laccase catalyzed-oxidative coupling of 3-methyl 2-benzothiazolinone hydrazone and methoxyphenols. *Enzym Microb. Technol.* **25**, 285–289 (1999).
12. Pardo, I., Chanagá, X., Vicente, A. I., Alcalde, M. & Camarero, S. New colorimetric screening assays for the directed evolution of fungal laccases to improve the conversion of plant biomass. *BMC Biotechnol.* **13**, 90 (2013).
13. Pardo, I. *et al*. Re-designing the substrate binding pocket of laccase for enhanced oxidation of sinapic acid. *Catal. Sci. Technol.* **6**, 3900–3910 (2016).
14. Cox, J. & Mann, M. Quantitative, high-resolution proteomics for data-driven systems biology. *Annu. Rev. Biochem.* **80**, 273–299 (2011).
15. Anderson, L. & Hunter, C. L. Quantitative mass spectrometric multiple reaction monitoring assays for major plasma proteins. *Mol. Cell. Proteomics* **5**, 573–588 (2006).
16. Kuzyk, M. A., Parker, C. E., Domanski, D. & Borchers, C. H. Development of mrm-based assays for the absolute quantitation of plasma proteins. In Bäckvall, H. & Lehtiö, J. (eds) *The Low Molecular Weight Proteome: Methods and Protocols*, 53–82 (Springer New York, New York, NY 2013).
17. Sitarz, A., Mikkelsen, J., Meyer, A. & Lezyk, M. A novel laccase from ganoderma lucidum capable of enhancing enzymatic degradation of lignocellulolytic biomass (2014).
18. Munk, L., Andersen, M. L. & Meyer, A. S. Direct rate assessment of laccase catalysed radical formation in lignin by electron paramagnetic resonance spectroscopy. *Enzym Microb. Technol.* **106**, 88–96 (2017).
19. Camarero, S. *et al*. p-hydroxycinnamic acids as natural mediators for laccase oxidation of recalcitrant compounds. *Environ. Sci. & Technol.* **42**, 6703–6709 (2008).
20. Zeuner, B. *et al*. Dependency of the hydrogen bonding capacity of the solvent anion on the thermal stability of feruloyl esterases in ionic liquid systems. *Green Chem.* **13**, 1550–1557 (2011).
21. Payne, C. M. *et al*. Fungal Cellulases. *Chem. Rev.* **115**, 1308–1448 (2015).
22. Shleev, S. *et al*. Comparison of physico-chemical characteristics of four laccases from different basidiomycetes. *Biochimie* **86**, 693–703 (2004).
23. Camarero, S., Ibarra, D., Martínez, M. J. & Martínez, A. T. Lignin-derived compounds as efficient laccase mediators for decolorization of different types of recalcitrant dyes. *Appl.environmental microbiology* **71**, 1775–84 (2005).
24. Lacki, K. & Duvnjak, Z. Transformation of 3,5-dimethoxy,4-hydroxy cinnamic acid by polyphenol oxidase from the fungusTrametes versicolor: Product elucidation studies. *Biotechnol. Bioeng.* **57**, 694–703 (1998).
25. Carunchio, F., Crescenzi, C., Girelli, A. M., Messina, A. & Tarola, A. M. Oxidation of ferulic acid by laccase: identification of the products and inhibitory effects of some dipeptides. *Talanta* **55**, 189–200 (2001).
26. Ralph, J. *et al*. Lignins: Natural polymers from oxidative coupling of 4-hydroxyphenyl- propanoids. *Phytochem. Rev.* **3**, 29–60 (2004).
27. Önnerud, H., Zhang, L., Gellerstedt, G. & Henriksson, G. Polymerization of monolignols by redox shuttle–mediated enzymatic oxidation. *The Plant Cell* **14**, 1953–1962 (2002).
28. Takahama, U. Oxidation of hydroxycinnamic acid and hydroxycinnamyl alcohol derivatives by laccase and peroxidase. interactions among p-hydroxyphenyl, guaiacyl and syringyl groups during the oxidation reactions. *Physiol. Plantarum* **93**, 61–68 (1995).
29. Singh, R. *et al*. Enhanced delignification of steam-pretreated poplar by a bacterial laccase. *Sci. Reports* **7**, 42121 (2017).
30. Koschorreck, K. *et al*. Cloning and characterization of a new laccase from Bacillus licheniformis catalyzing dimerization of phenolic acids. *Appl. Microbiol. Biotechnol.* **79**, 217–224 (2008).
31. Silva, I. R., Larsen, D. M., Meyer, A. S. & Mikkelsen, J. D. Identification, expression, and characterization of a novel bacterial rgi lyase enzyme for the production of bio-functional fibers. *Enzyme Microb. Technol.* **49**, 160–166 (2011).

Acknowledgements
This study was supported by The Danish Council for Independent Research (Project ref. DFF-4184-00355) and by the PhD Program at Dept. of Chemical and Biochemical Engineering, DTU.

Author Contributions
V.P. conducted the experiments and analysed the results, V.P. and J.W.A. wrote the manuscript and interpreted the results. All authors participated in the conceptual development of the idea, reviewed and accepted the manuscript.

Additional Information
Supplementary information accompanies this paper at https://doi.org/10.1038/s41598-018-26523-0.

Competing Interests: The authors declare no competing interests.

Publisher's note: Springer Nature remains neutral with regard to jurisdictional claims in published maps and institutional affiliations.

Multiple Reaction Monitoring for quantitative laccase kinetics by LC-MS / Supplementary information

Valentina Perna[1], **Jane W. Agger**[1,*], **Jesper Holck**[1], **and Anne S. Meyer**[1]

[1]Center for BioProcess Engineering, Department of Chemical and Biochemical Engineering, Technical University of Denmark, Kgs. Lyngby, 2800, Denmark
[*]jaag@kt.dtu.dk

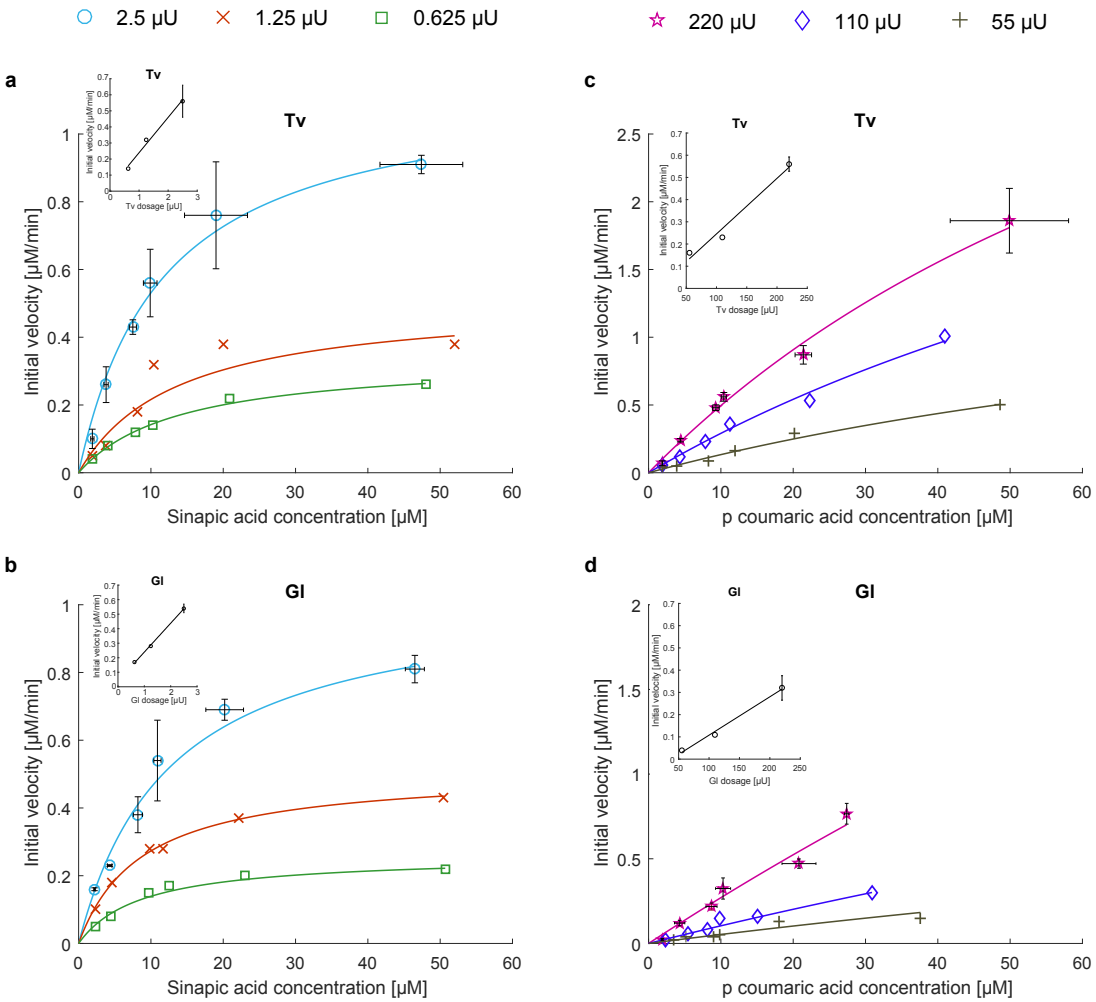

Figure S1. Michaelis-Menten curves for *Trametes versicolor* and *Ganoderma lucidum* laccase on sinapic acid (a, b) and *p*-coumaric acid (c, d). Three different enzyme dosages are shown: for sinapic acid (a, b): 0.625 μU (green open square), 1.25 μU (red cross) and 2.5 μU (blue open circle). For *p*-coumaric acid (c, d): 55 μU (grey cross), 110 μU (dark blue open diamond) and 220 μU (purple open star). Dose response at 10 μM substrate concentration is shown in the inset. For the highest enzyme dose standard deviation are shown. Y-axis is optimized in order to have a optimal view of the curves.

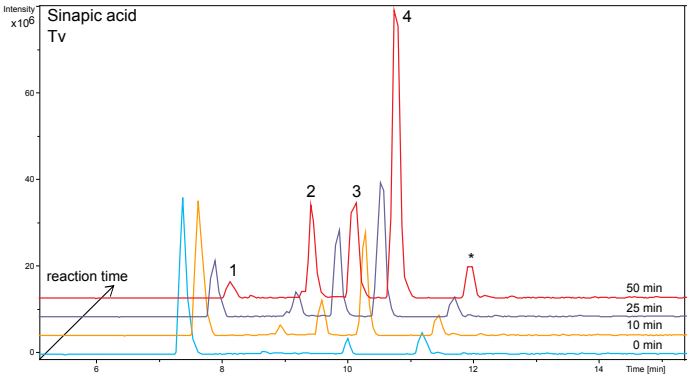
Intensity
x10^6
Sinapic acid
Tv
reaction time
1
2
3
4
*
50 min
25 min
10 min
0 min
Time [min]


Intensity
x10^6
Peak 1
-MS, 7.4min
223.00
290.94

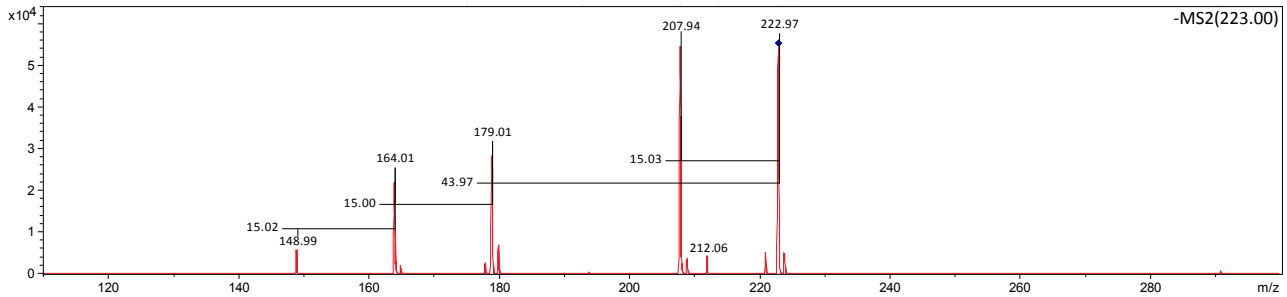
x10^4
-MS2(223.00)
207.94
222.97
179.01
164.01
15.03
43.97
15.00
15.02
148.99
212.06
m/z

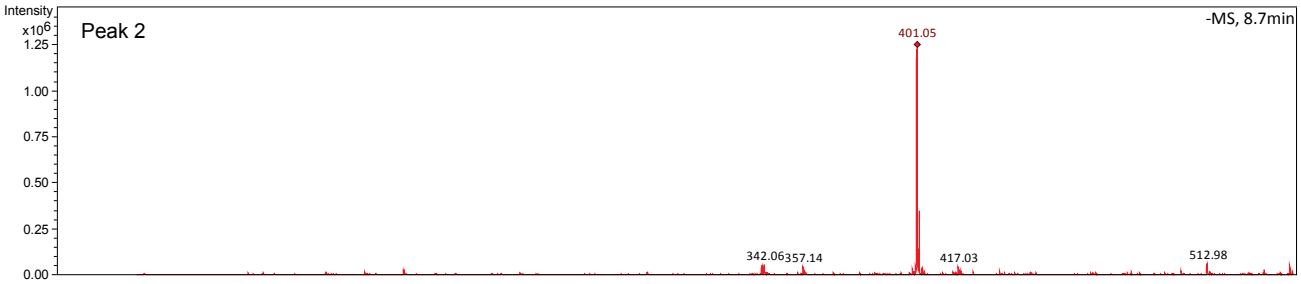
Intensity
x10^6
Peak 2
-MS, 8.7min
401.05
342.06
357.14
417.03
512.98

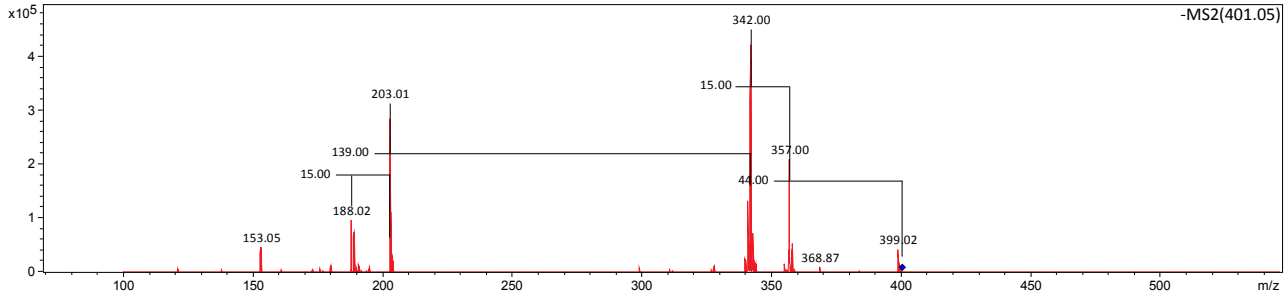
x10^5
-MS2(401.05)
342.00
15.00
203.01
139.00
357.00
15.00
44.00
188.02
153.05
399.02
368.87
m/z

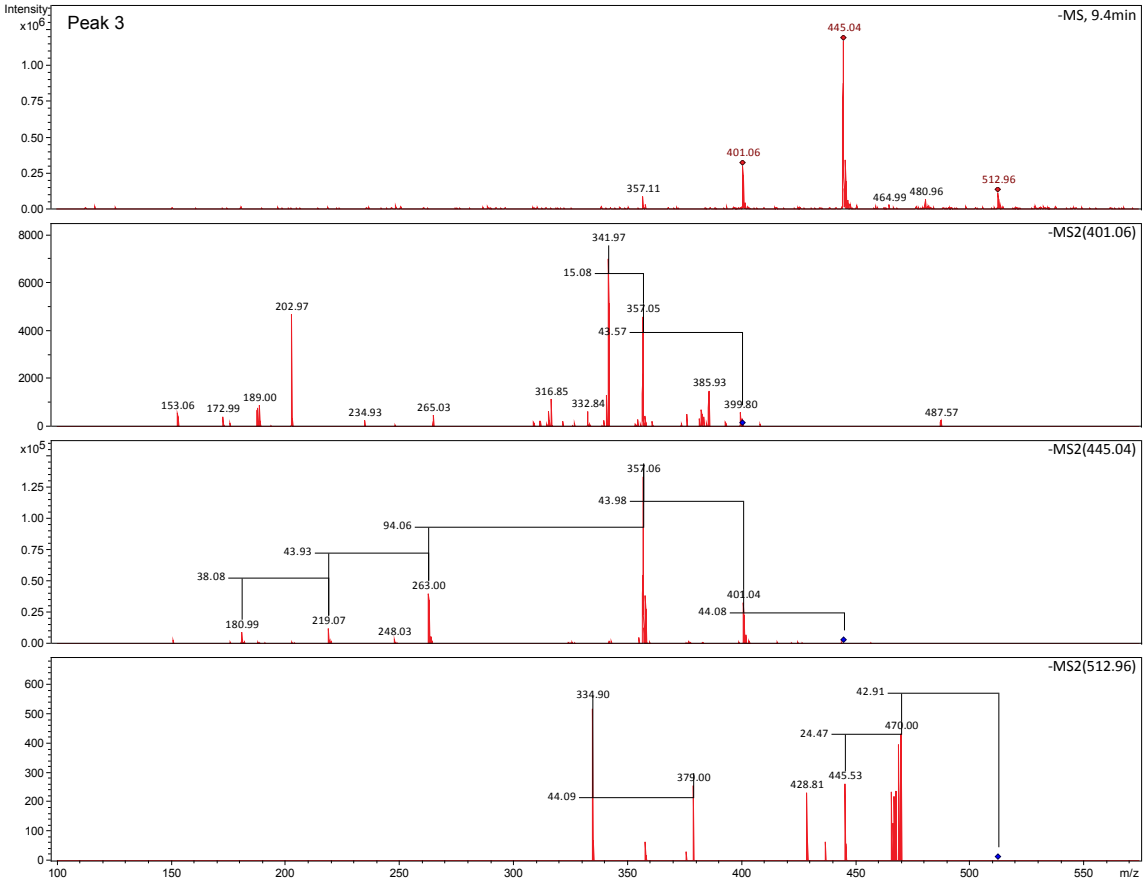
Peak 3
-MS, 9.4min
445.04
401.06
357.11
512.96
464.99
480.96
-MS2(401.06)
341.97
15.08
357.05
43.57
202.97
385.93
316.85
332.84
153.06
172.99
189.00
234.93
265.03
399.80
487.57
-MS2(445.04)
357.06
43.98
94.06
43.93
38.08
263.00
401.04
44.08
180.99
219.07
248.03
-MS2(512.96)
334.90
42.91
470.00
24.47
379.00
445.53
428.81
44.09
m/z

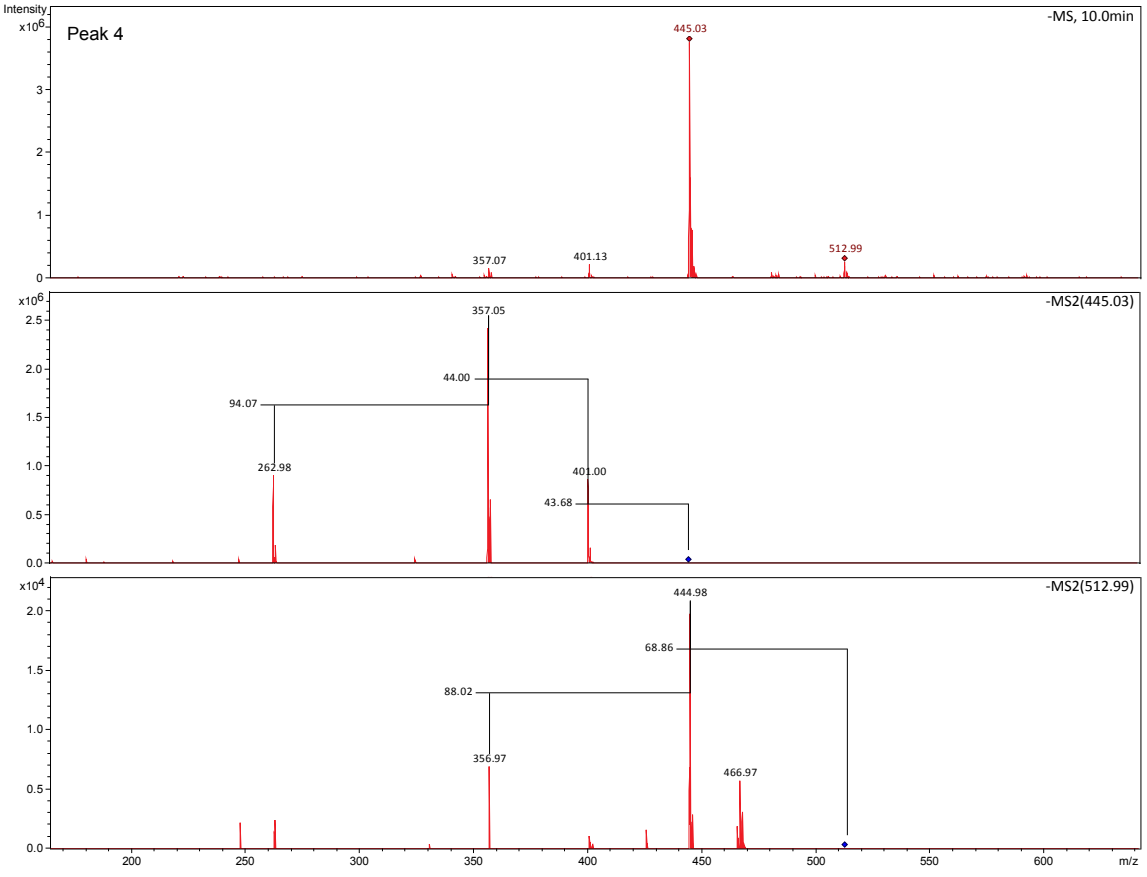
Peak 4
-MS, 10.0min
445.03
357.07
401.13
512.99
-MS2(445.03)
357.05
44.00
94.07
262.98
401.00
43.68
-MS2(512.99)
444.98
68.86
88.02
356.97
466.97
m/z

Figure S2. Evolution profile of sinapic acid oxidation by *Trametes versicolor* laccase. LC chromatograms at different reaction times are shown: 0 minutes (light blue), 10 minutes (yellow), 25 minutes (violet) and 50 minutes (red). MS and MS/MS spectra for each peak are also shown. All ions are observed as $[M-H]^-$. As reaction time is increasing substrate peak (peak 1) is decreasing in intensity, while product peaks (peak 2, 3 and 4) are increasing in intensity, meaning that the substrate is being consumed and the products formed. Major losses during fragmentation are indicated on the MS/MS spectra when relevant. Product peaks are not always characterized by one single mass, but two or more different compounds can be found in each peak. Whether it is a result of co-elution of two or more different products or chemical degradation has not be investigated. Sinapic acid *m/z* 223 elutes at a retention time (RT) of 7.4 min (peak 1). Three products can be distinguished already after 10 minutes of reaction. Two isomers of the dimer *m/z* 445.05 are eluting at RT 9.4 and 10 min (peak 3 and 4). A sodium formate adduct (+ 68) of the dimer can be also found in peak 3 and 4 characterized by *m/z* 513. Peak 2 RT 8.7 min is characterized by *m/z* 401.05 which correspond to a dimer with the loss of 44, most likely the loss of a carboxilic group. Peak * RT 11.3 min, containing *m/z* 293.13 and *m/z* 361.13, where the latter is a sodium formate adduct of *m/z* 293.13, was also found by Petrucci *et al.*[1] (corresponding MS spectra is shown in Supplementary Figure S10). It is, most likely, an impurity of LC-MS eluent system since it is present also in the blank run. Suggested chemical structure for the major products are shown in Supplementary Figure S12.

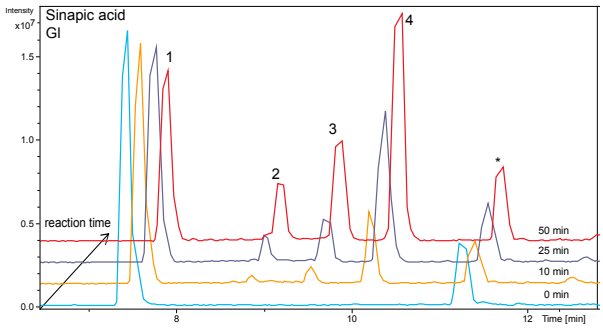
Intensity
x10^7
Sinapic acid
Gl
1
2
3
4
*
reaction time
50 min
25 min
10 min
0 min
Time [min]

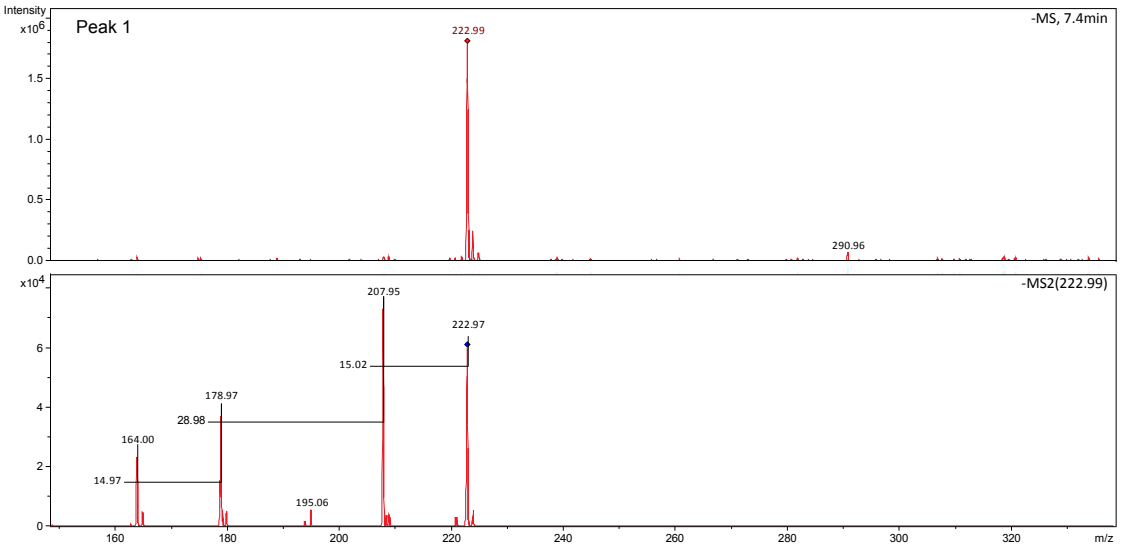
Intensity
x10^6
Peak 1
-MS, 7.4min
222.99
290.96
x10^4
-MS2(222.99)
207.95
222.97
15.02
178.97
28.98
164.00
14.97
195.06
m/z

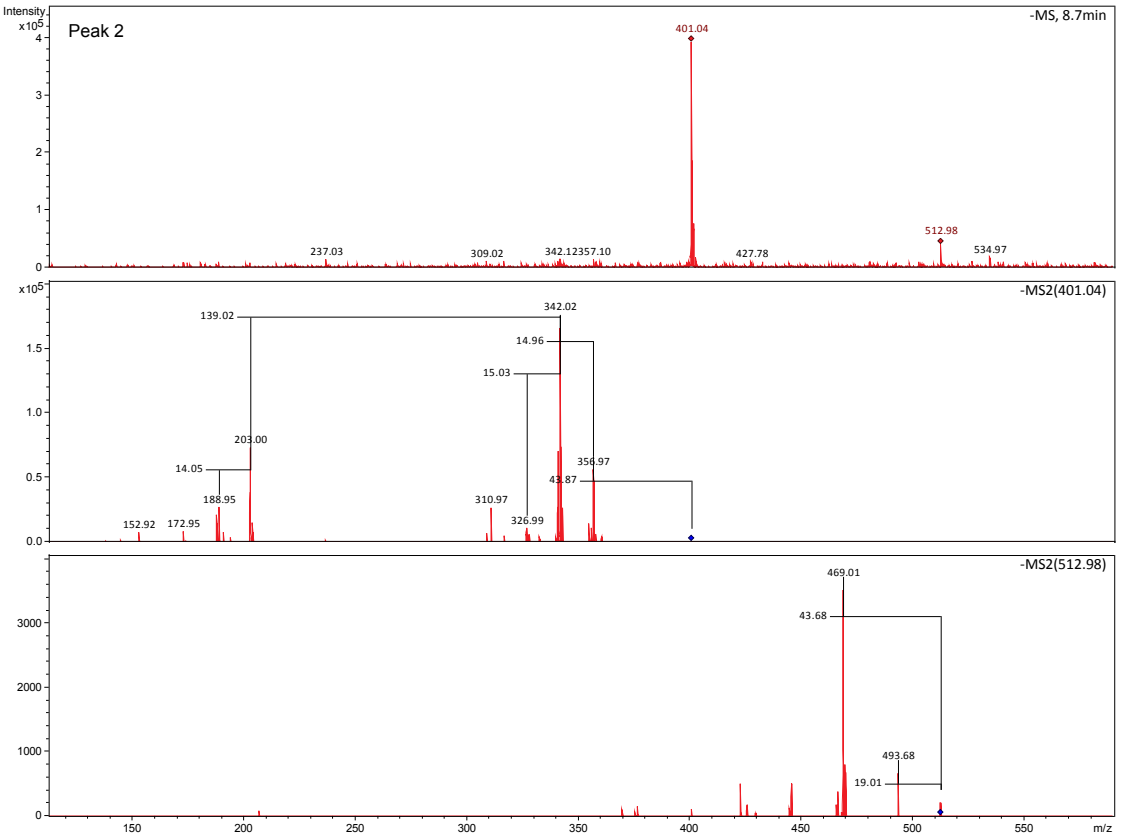
Intensity
x10^5
Peak 2
-MS, 8.7min
401.04
237.03
309.02
342.12357.10
427.78
512.98
534.97
x10^5
-MS2(401.04)
342.02
139.02
14.96
15.03
203.00
14.05
356.97
43.87
188.95
310.97
152.92
172.95
326.99
-MS2(512.98)
469.01
43.68
493.68
19.01
m/z

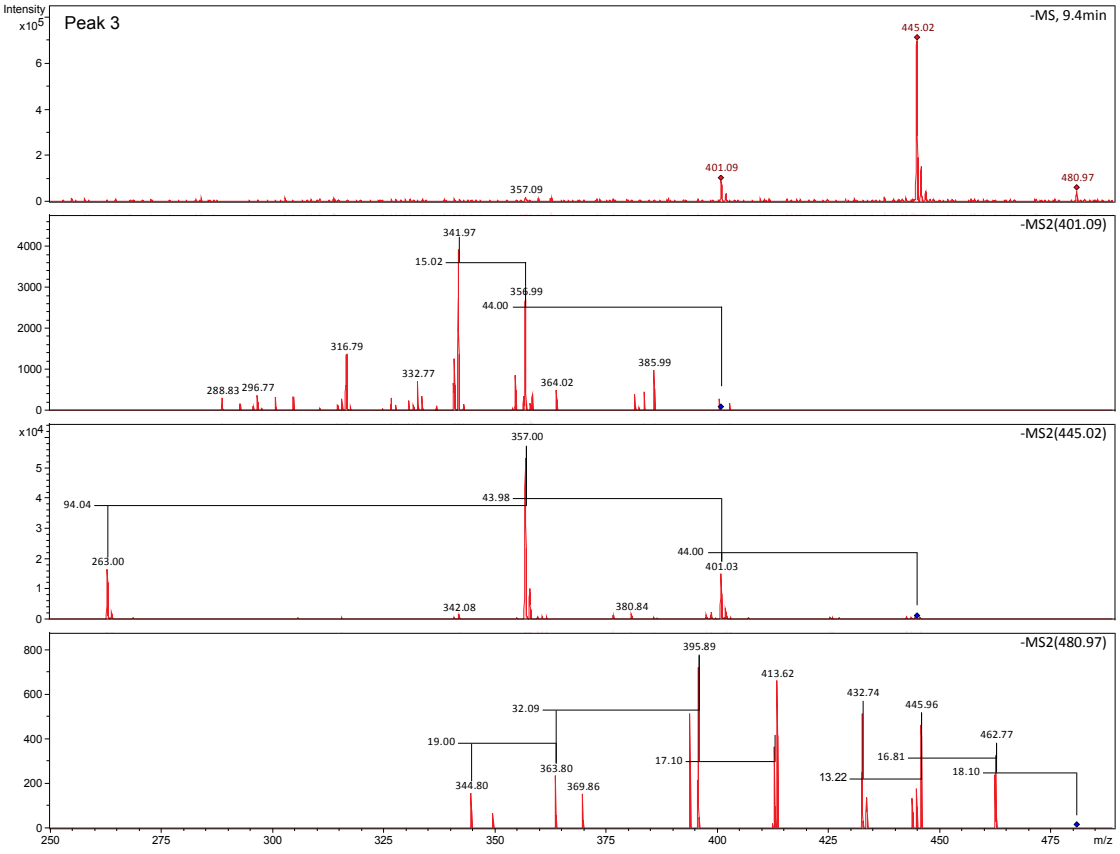
Intensity
x10^5
Peak 3
-MS, 9.4min
445.02
401.09
480.97
357.09
-MS2(401.09)
341.97
15.02
356.99
44.00
316.79
385.99
332.77
364.02
288.83
296.77
x10^4
-MS2(445.02)
357.00
43.98
94.04
263.00
44.00
401.03
342.08
380.84
-MS2(480.97)
395.89
413.62
432.74
445.96
462.77
32.09
19.00
16.81
17.10
13.22
18.10
363.80
344.80
369.86
250
275
300
325
350
375
400
425
450
475
m/z

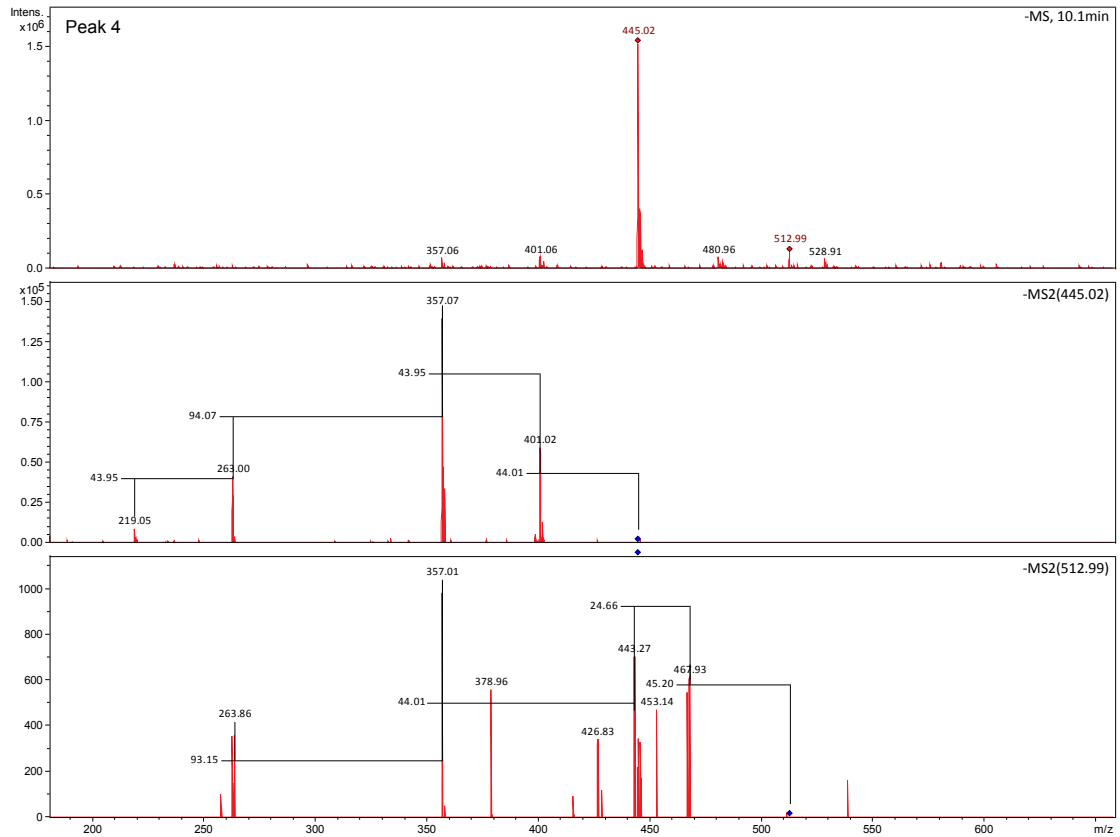
Intens.
x10^6
Peak 4
-MS, 10.1min
445.02
357.06
401.06
480.96
512.99
528.91
x10^5
-MS2(445.02)
357.07
43.95
94.07
401.02
263.00
44.01
43.95
219.05
-MS2(512.99)
357.01
24.66
443.27
467.93
45.20
378.96
44.01
453.14
263.86
426.83
93.15
200
250
300
350
400
450
500
550
600
m/z

Figure S4. Evolution profile of sinapic acid oxidation by *Ganoderma lucidum* laccase. LC chromatograms at different reaction times are shown: 0 minutes (light blue), 10 minutes (yellow), 25 minutes (violet) and 50 minutes (red). MS and MS/MS spectra for each peak are also shown. All ions are observed as $[M-H]^-$. As reaction time is increasing substrate peak (peak 1) is decreasing in intensity, while product peaks (peak 2, 3 and 4) are increasing in intensity, meaning that the substrate is being consumed and the products formed. Major losses during fragmentation are indicated on the MS/MS spectra when relevant. Product peaks are not always characterized by one single mass, but two or more different compound can be found in each peak. Whether it is a result of co-elution of two or more different product or chemical degradation has not be investigated. Sinapic acid *m/z* 223 elutes from the chromatographic column at a retention time (RT) 7.4 min (peak 1). Three product can be distinguished already after 10 minutes of reaction. Two isomers of the dimer *m/z* 445.05 are eluted at RT 9.4 and 10 min (peak 3 and 4). Three isomers of the decarboxylated dimer (loss of 44) characterized by *m/z* 401.06 are found in peak 2, 3 and 4. A sodium formate adduct (+ 68) of the dimer can be also found in peak 2 and 4 characterized by *m/z* 513. Peak 3 contains masses that could not be immediately resolved to a proposed structure. Peak * RT 11.3 min, containing *m/z* 293.13 and *m/z* 361.13, where the latter is a sodium formate adduct of *m/z* 293.13, was also found by Petrucci *et al.*[1] (corresponding MS spectra is shown in Supplementary Figure S11). It is, most likely, an impurity of LC-MS eluent system since it is present also in the blank run. Suggested chemical structure for the major products are shown in Supplementary Figure S12.

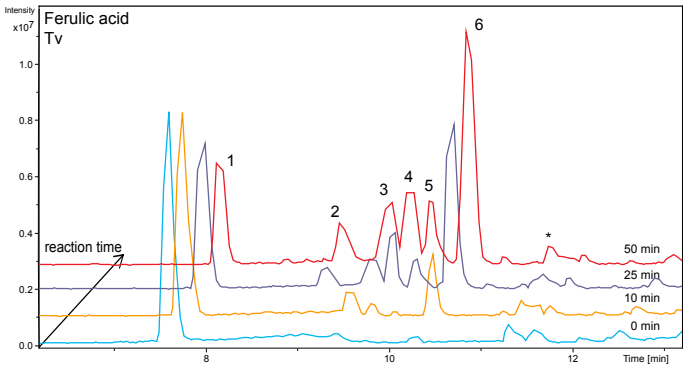
Intensity
x10^7
Ferulic acid
Tv
1
2
3
4
5
6
*
reaction time
50 min
25 min
10 min
0 min
Time [min]

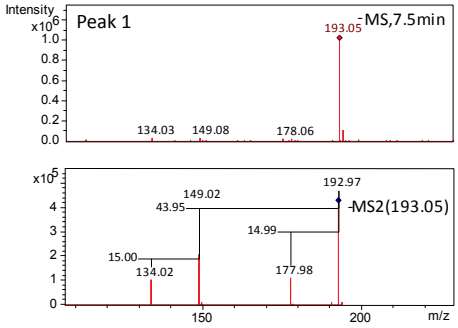
Intensity
x10^6
Peak 1
-MS,7.5min
193.05
134.03
149.08
178.06
x10^5
192.97
149.02
43.95
-MS2(193.05)
14.99
15.00
134.02
177.98
150
200
m/z

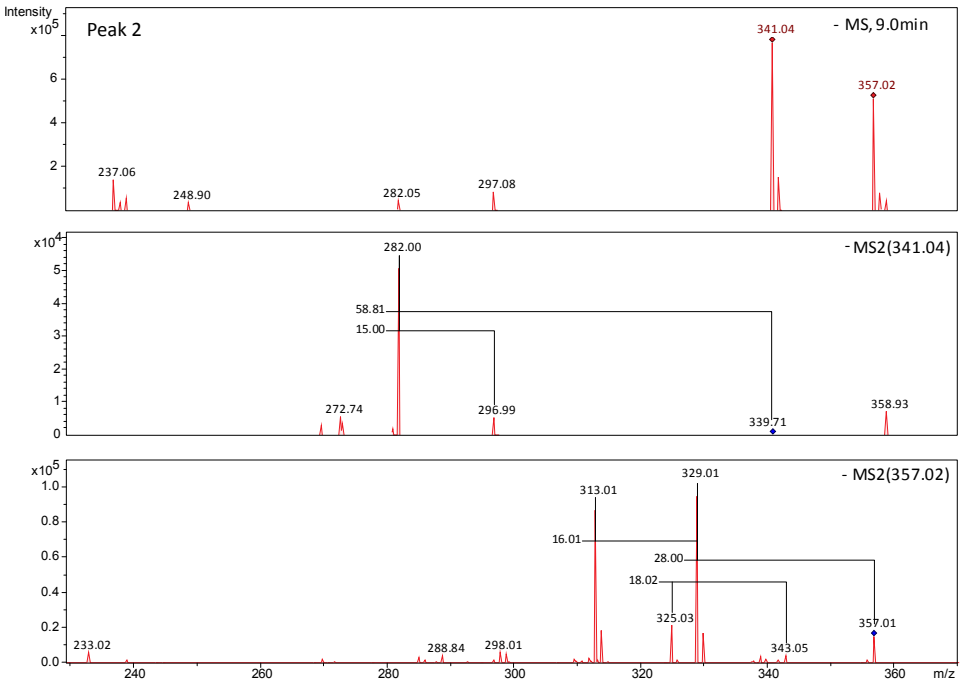
Intensity
x10^5
Peak 2
- MS, 9.0min
341.04
357.02
237.06
248.90
282.05
297.08
x10^4
282.00
- MS2(341.04)
58.81
15.00
272.74
296.99
339.71
358.93
x10^5
329.01
313.01
- MS2(357.02)
16.01
28.00
18.02
325.03
357.01
233.02
288.84
298.01
343.05
240
260
280
300
320
340
360
m/z

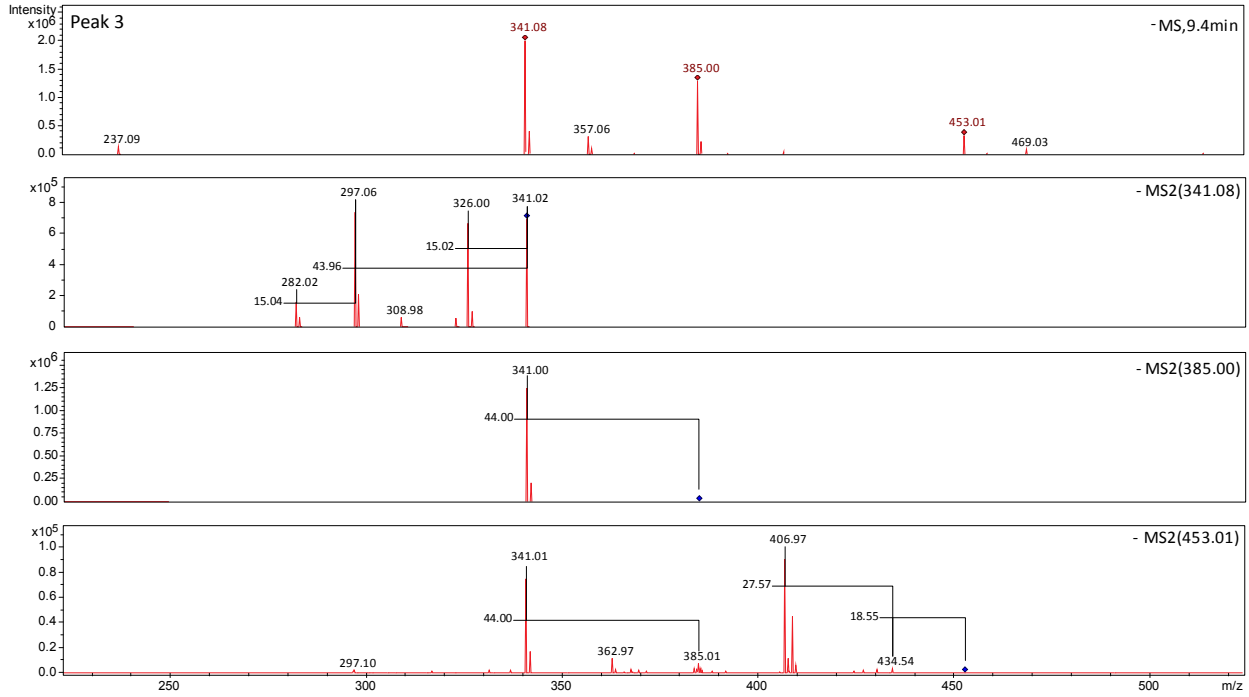
Intensity
Peak 3
- MS,9.4min
341.08
385.00
357.06
453.01
237.09
469.03
- MS2(341.08)
297.06
326.00
341.02
15.02
43.96
282.02
15.04
308.98
- MS2(385.00)
341.00
44.00
- MS2(453.01)
406.97
341.01
27.57
44.00
18.55
362.97
385.01
297.10
434.54
m/z

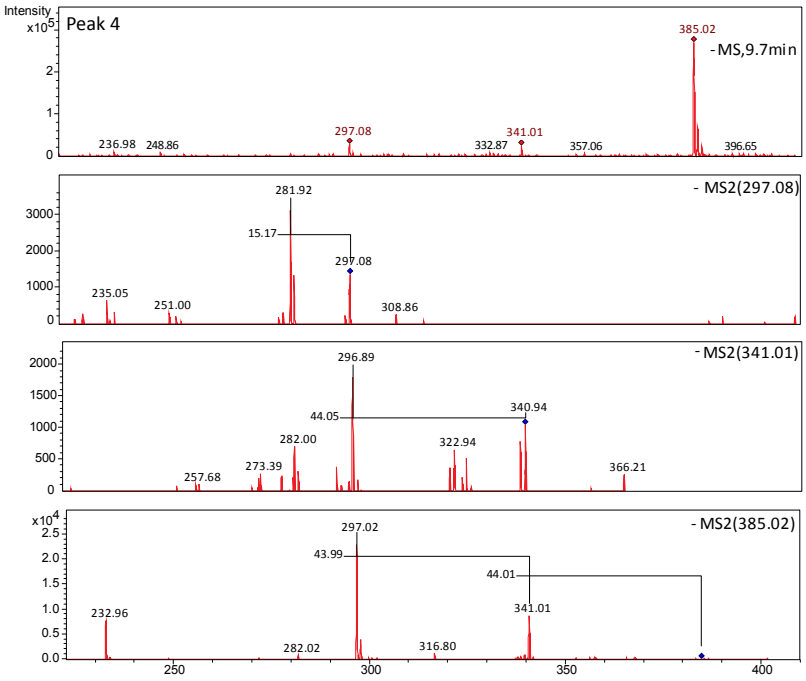
Intensity
Peak 4
385.02
- MS,9.7min
297.08
341.01
236.98
248.86
332.87
357.06
396.65
- MS2(297.08)
281.92
15.17
297.08
235.05
251.00
308.86
- MS2(341.01)
296.89
44.05
340.94
282.00
322.94
273.39
257.68
366.21
- MS2(385.02)
297.02
43.99
44.01
341.01
232.96
282.02
316.80

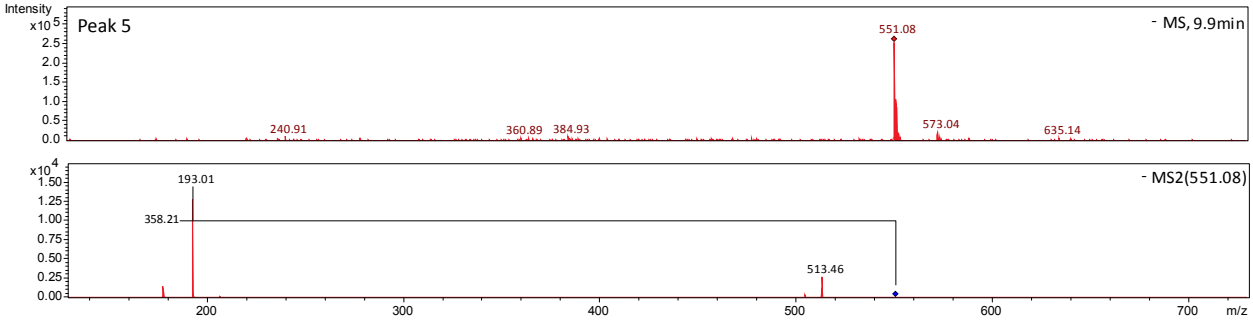
Intensity
Peak 5
- MS, 9.9min
551.08
240.91
360.89
384.93
573.04
635.14
- MS2(551.08)
193.01
358.21
513.46
m/z

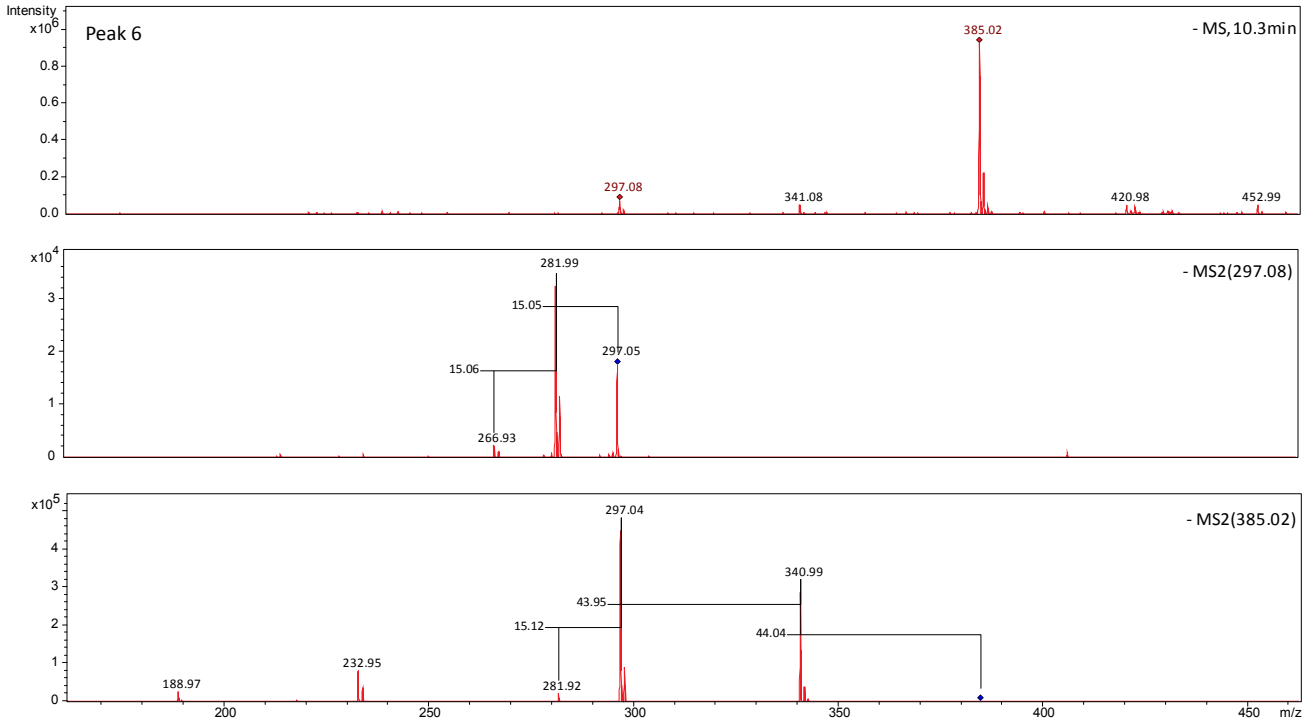

Figure S6. Evolution profile of ferulic acid oxidation by *Trametes versicolor* laccase. LC chromatograms at different reaction times are shown: 0 minutes (light blue), 10 minutes (yellow), 25 minutes (violet) and 50 minutes (red). MS and MS/MS spectra for each peak are also shown. All ions are observed as $[M-H]^-$. As reaction time is increasing substrate peak (peak 1) is decreasing in intensity, while product peaks (peaks 2-6) are increasing in intensity, meaning that the substrate is being consumed and the products formed. Major losses during fragmentation are indicated on the MS/MS spectra when relevant. Product peaks are not always characterized by one single mass, but two or more different ones elute at the same time. Whether it is a result of co-elution of two or more different product or chemical degradation has not be investigated. Ferulic acid is identified with the *m/z* 192.99 and a retention time (RT) of 7.6 min. After 10 minutes reaction time four different product peaks are present with RT 9.4, 9.7, 9.9 and 10.3 (peak 3, 4, 5 and 6), while a fifth product peak is appearing after 25 minutes at RT 8.9 min (peak 2). Three different isomers of ferulic acid dimer are present in peak 3, 4 and 6 characterized by *m/z* 385.02. The decarboxylated dimer *m/z* 341.06 (characterized by the loss of 44) is also present in three different isomeric forms (peak 2, 3 and 4). Peak 2 and 6 also contain, a compound with *m/z* 297.08 corresponding to a double decarboxylated dimer. A sodium formate adduct of the dimer can be found in peak 3 characterized by *m/z* 453. Peak 2 and 5 contain masses that could not be immediately resolved to a proposed structure. Peak * RT 11.3 min, containing *m/z* 293.13 and *m/z* 361.13, where the latter is a sodium formate adduct of *m/z* 293.13, was also found by Petrucci *et al.*[1] (corresponding MS spectra is shown in Supplementary Figure S10). It is, most likely, an impurity of LC-MS eluent system since it is present also in the blank run. Suggested chemical structure for the major products are shown in Supplementary Figure S13.

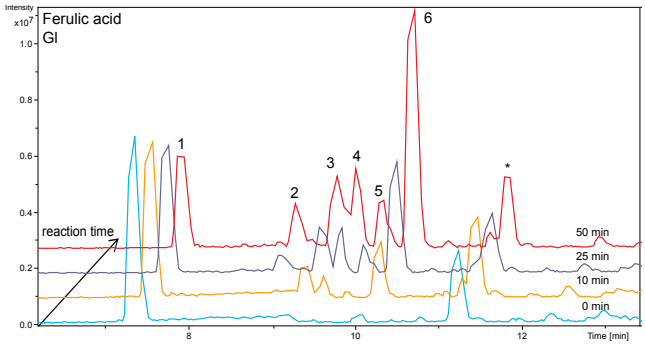
Ferulic acid
GI
reaction time
50 min
25 min
10 min
0 min
Time [min]

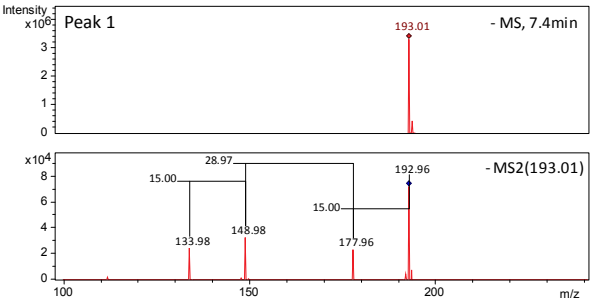
Peak 1
- MS, 7.4min
193.01
- MS2(193.01)
28.97
15.00
192.96
15.00
148.98
133.98
177.96
m/z

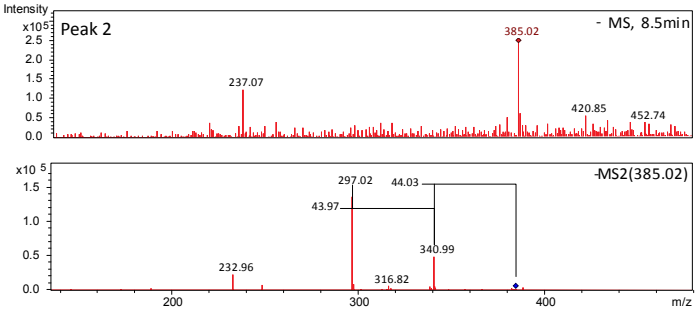
Peak 2
- MS, 8.5min
385.02
237.07
420.85
452.74
-MS2(385.02)
297.02
44.03
43.97
340.99
232.96
316.82
m/z

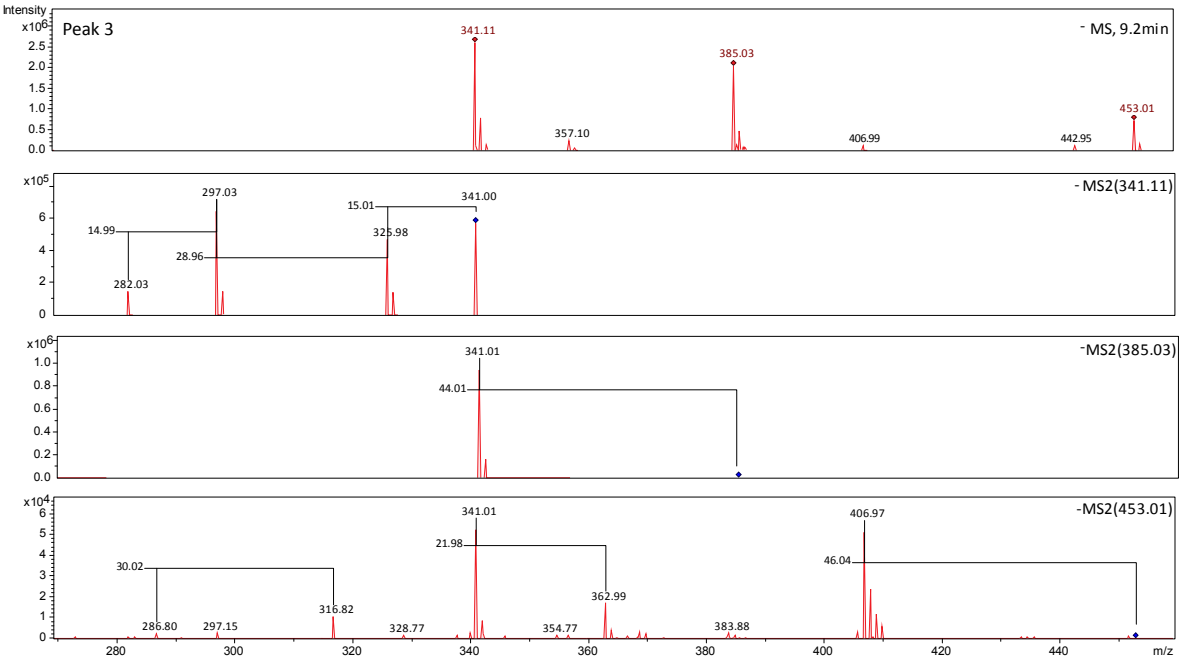
Peak 3
- MS, 9.2min
341.11
385.03
453.01
357.10
406.99
442.95
- MS2(341.11)
297.03
15.01
341.00
14.99
325.98
28.96
282.03
-MS2(385.03)
341.01
44.01
-MS2(453.01)
341.01
406.97
21.98
46.04
30.02
362.99
316.82
286.80
297.15
328.77
354.77
383.88
m/z

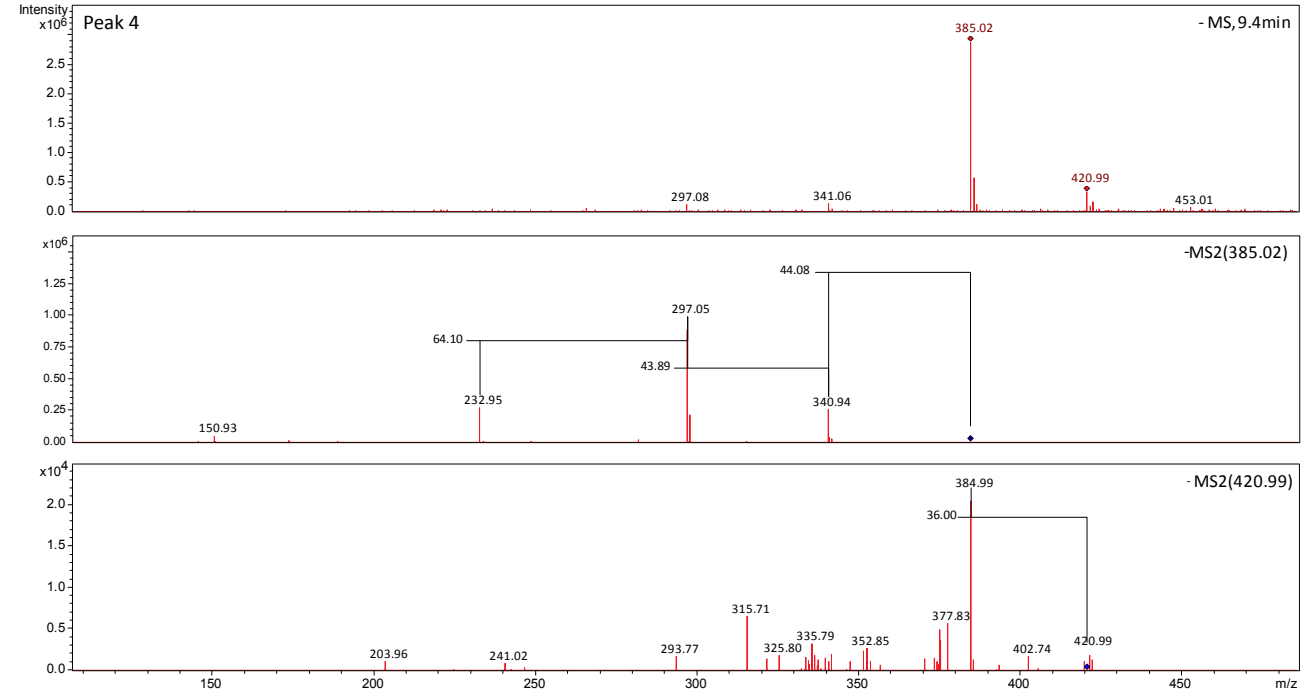
Intensity
Peak 4
- MS, 9.4min
385.02
420.99
297.08
341.06
453.01
-MS2(385.02)
44.08
297.05
64.10
43.89
232.95
340.94
150.93
- MS2(420.99)
384.99
36.00
315.71
377.83
335.79
352.85
325.80
293.77
203.96
241.02
402.74
420.99
m/z

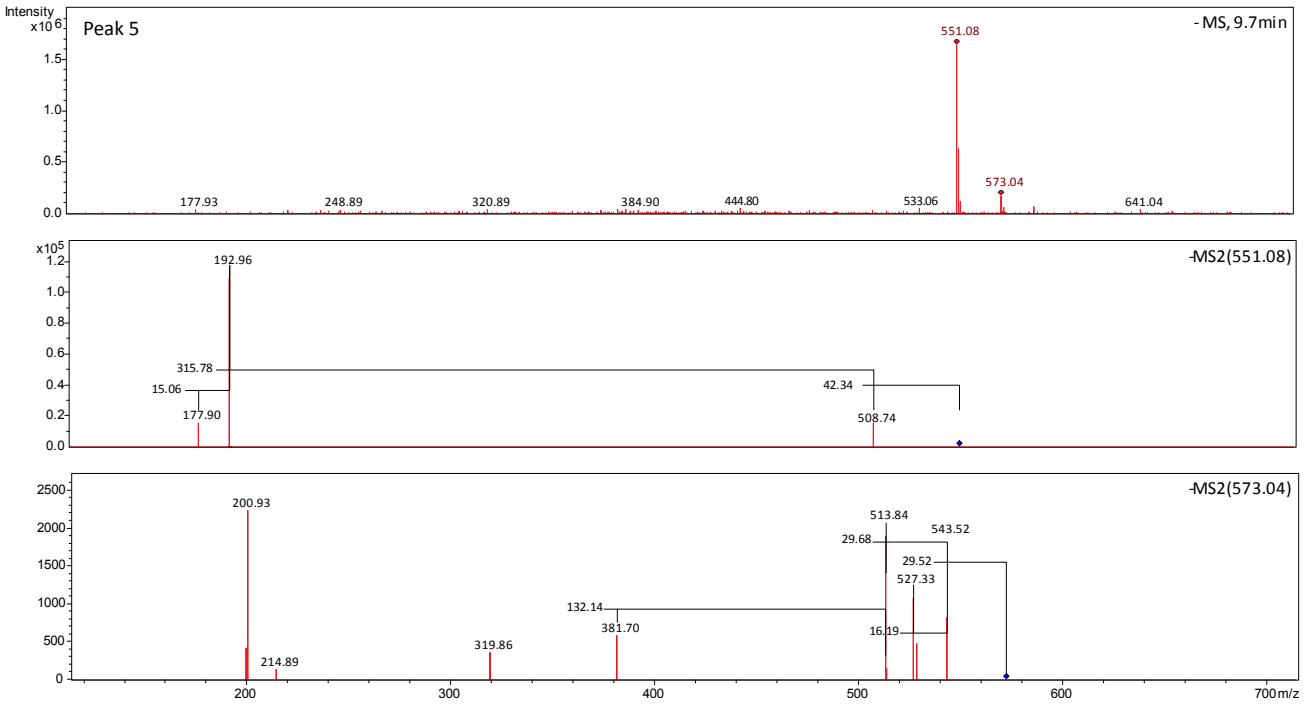
Intensity
Peak 5
- MS, 9.7min
551.08
573.04
177.93
248.89
320.89
384.90
444.80
533.06
641.04
-MS2(551.08)
192.96
315.78
15.06
42.34
177.90
508.74
-MS2(573.04)
200.93
513.84
543.52
29.68
29.52
527.33
132.14
381.70
16.19
319.86
214.89
m/z

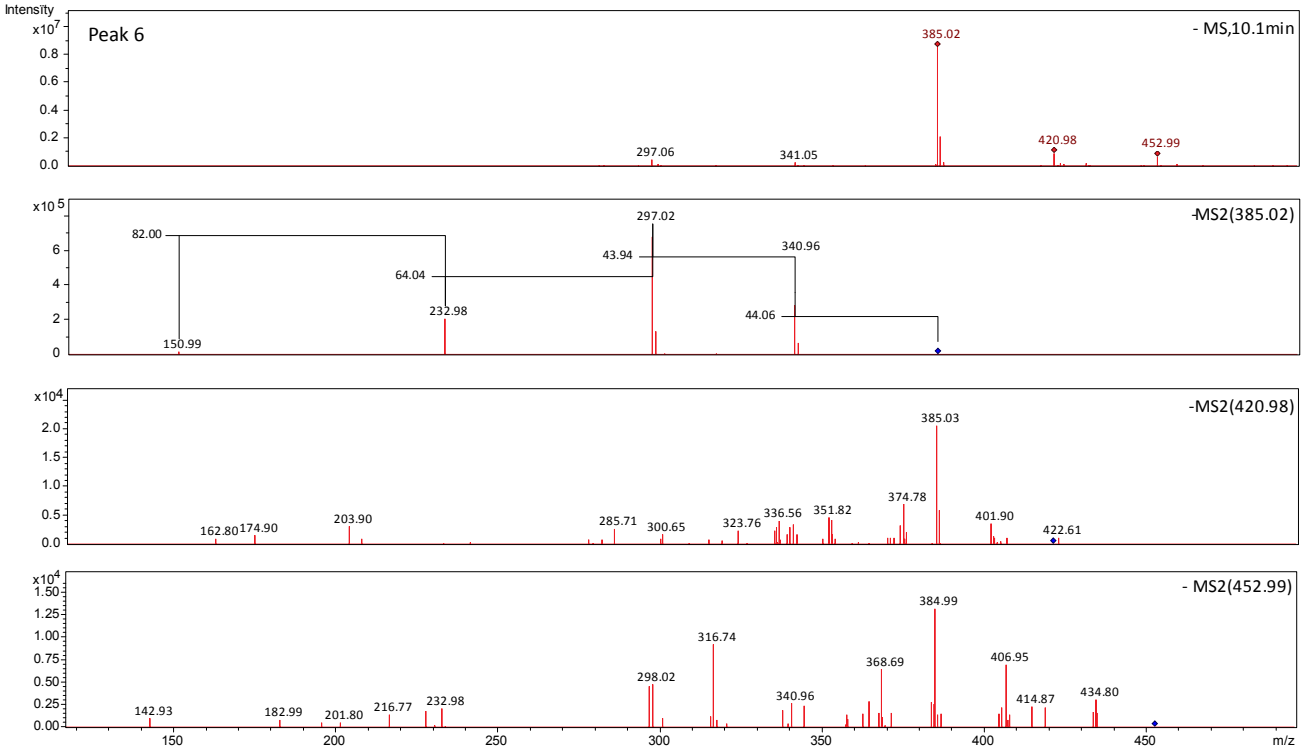

Figure S7. Evolution profile of ferulic acid oxidation by *Ganoderma lucidum* laccase. LC chromatograms at different reaction times are shown: 0 minutes (light blue), 10 minutes (yellow), 25 minutes (violet) and 50 minutes (red). MS and MS/MS spectra for each peak are also shown. All ions are observed as $[M-H]^-$. As reaction time is increasing substrate peak (peak 1) is decreasing in intensity, while product peaks (peaks 2-6) are increasing in intensity, meaning that the substrate is being consumed and the products formed. Major losses during fragmentation are indicated on the MS/MS spectra when relevant. Product peaks are not always characterized by one single mass, but two or more different ones elute at the same time. Whether it is a result of co-elution of two or more different product or chemical degradation has not be investigated. Ferulic acid is identified with the *m/z* 192.99 and a retention time (RT) of 7.6 min. After 10 minutes reaction time four different product peaks are present with RT 9.4, 9.7, 9.9 and 10.3 (peak 3, 4, 5 and 6), while a fifth product peak is appearing after 25 minutes at RT 8.9 min (peak 2). Three different isomers of ferulic acid dimer are present in peak 3, 4 and 6 characterized by *m/z* 385.02. The decarboxylated dimer *m/z* 341.06 (characterized by the loss of 44) is present in two different isomeric forms (peak 2 and 3). Sodium formate adducts of the dimer can be found under peak 3 and 6 characterized by *m/z* 453. Peak 2, 4, 5 and 6 contain masses that could not be immediately resolved to a proposed structure. Peak * RT 11.3 min, containing *m/z* 293.13 and *m/z* 361.13, where the latter is a sodium formate adduct of *m/z* 293.13, was also found by Petrucci *et al.*[1] (corresponding MS spectra is shown in Supplementary Figure S11). It is, most likely, an impurity of LC-MS eluent system since it is present also in the blank run. Suggested chemical structure for the major products are shown in Supplementary Figure S13.

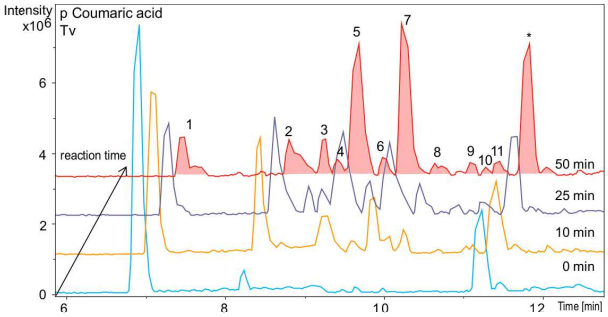
Intensity
x10^6
p Coumaric acid
Tv
reaction time
50 min
25 min
10 min
0 min
Time [min]

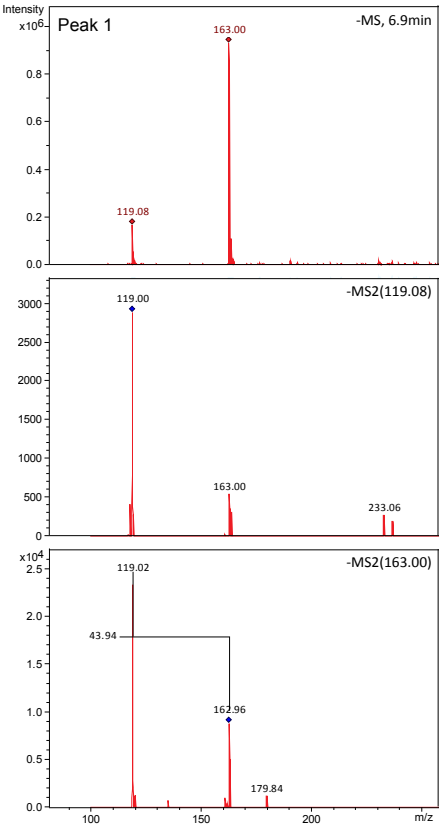
Peak 1
-MS, 6.9min
163.00
119.08
-MS2(119.08)
119.00
163.00
233.06
-MS2(163.00)
119.02
43.94
162.96
179.84
m/z

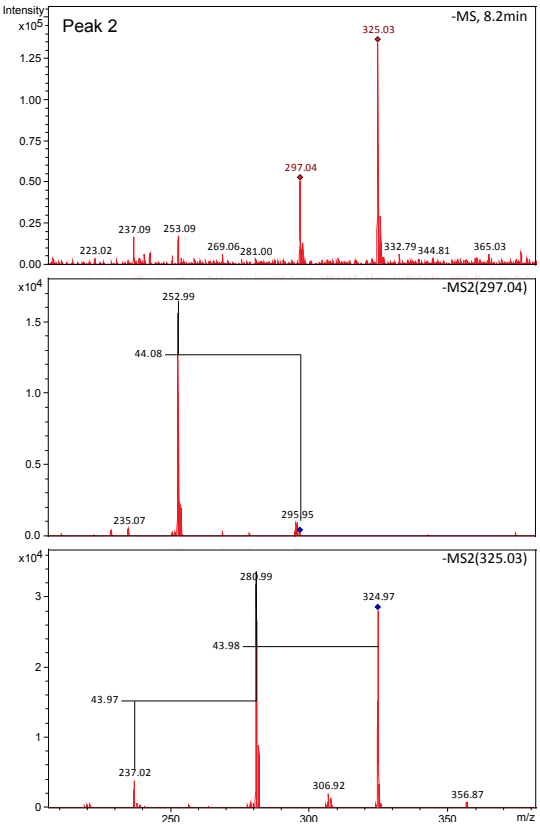
Peak 2
-MS, 8.2min
325.03
297.04
237.09
253.09
223.02
269.06
281.00
332.79
344.81
365.03
-MS2(297.04)
252.99
44.08
235.07
295.95
-MS2(325.03)
280.99
324.97
43.98
43.97
237.02
306.92
356.87
m/z

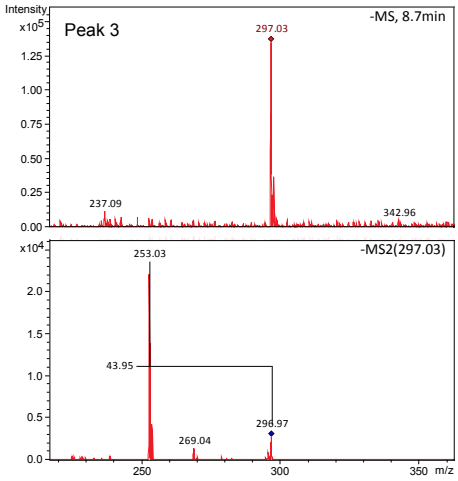
Peak 3
-MS, 8.7min
297.03
237.09
342.96
-MS2(297.03)
253.03
43.95
296.97
269.04
m/z

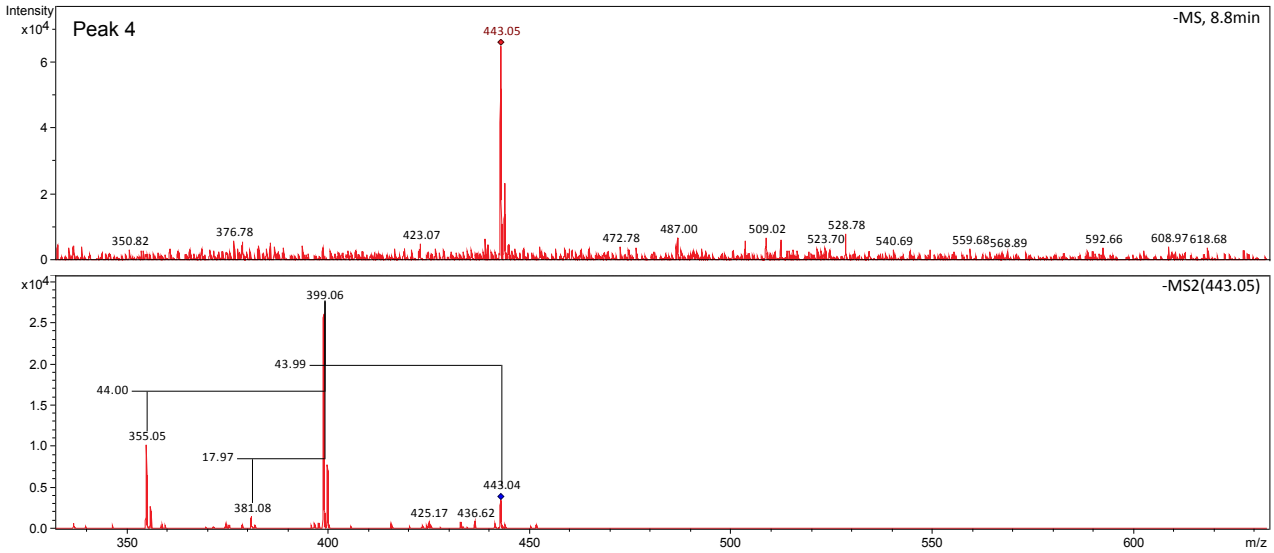
Intensity
Peak 4
-MS, 8.8min
443.05
-MS2(443.05)
399.06
43.99
44.00
355.05
17.97
381.08
443.04
425.17
436.62
m/z

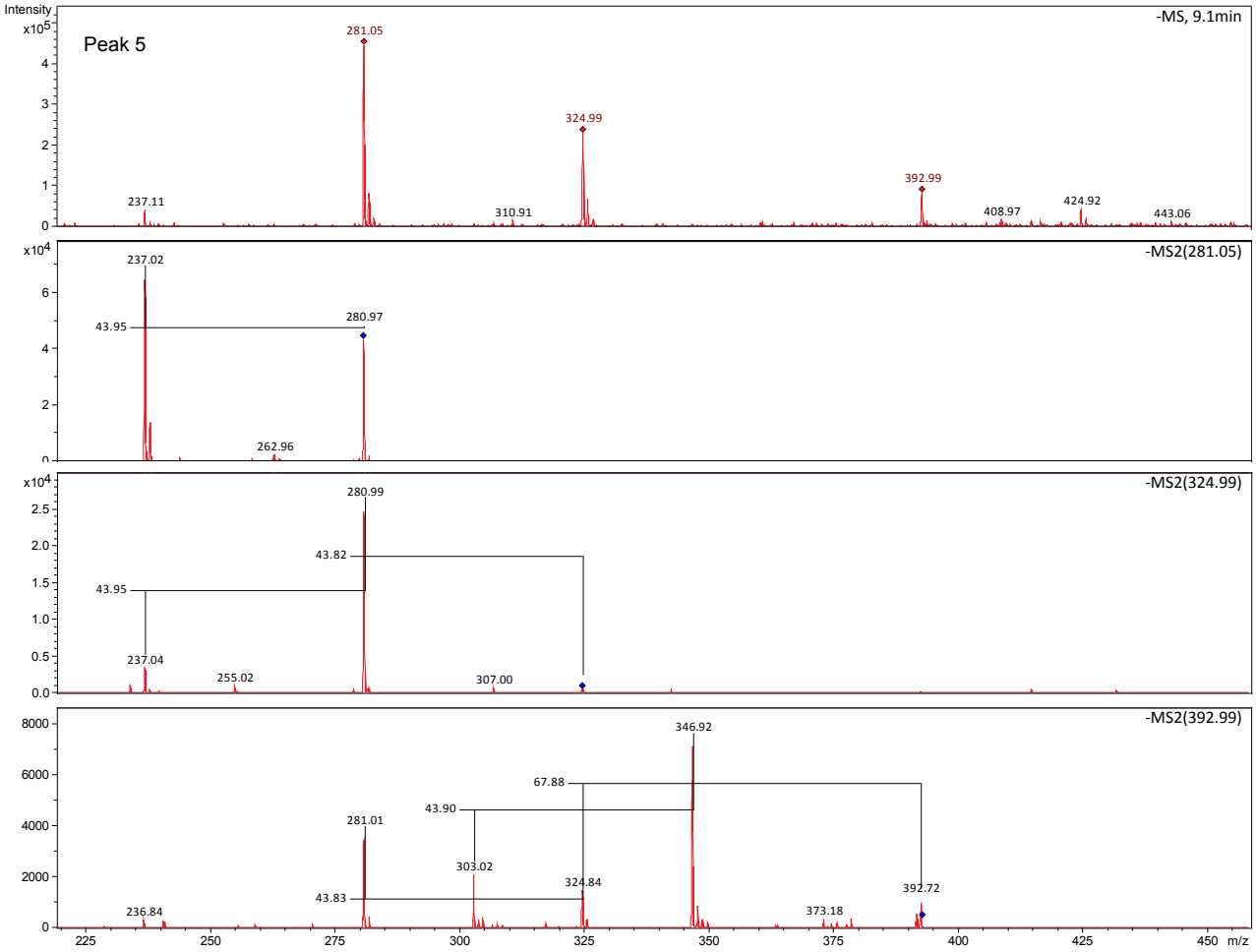
Intensity
Peak 5
-MS, 9.1min
281.05
324.99
392.99
237.11
310.91
408.97
424.92
443.06
-MS2(281.05)
237.02
43.95
280.97
262.96
-MS2(324.99)
280.99
43.82
43.95
237.04
255.02
307.00
-MS2(392.99)
346.92
67.88
43.90
281.01
303.02
324.84
43.83
392.72
236.84
373.18
m/z

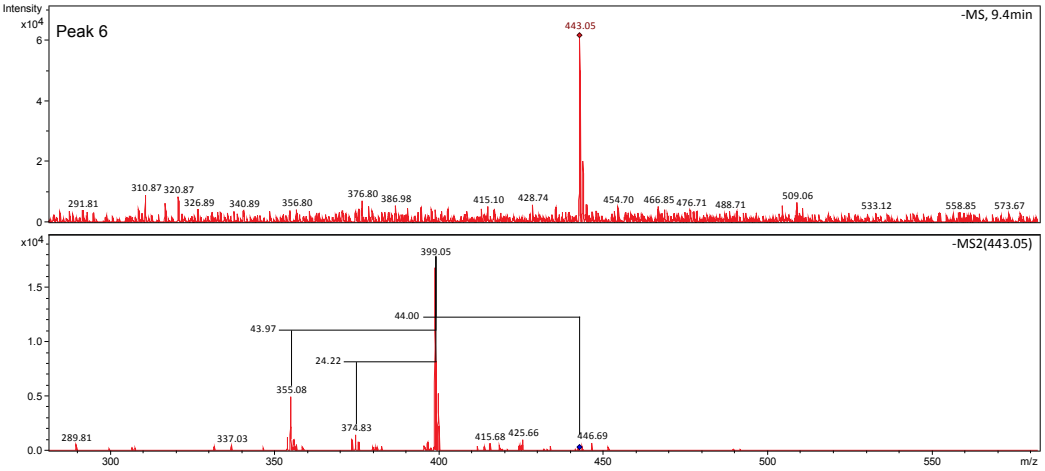
Peak 6
-MS, 9.4min
443.05
-MS2(443.05)
399.05
44.00
43.97
24.22
355.08
374.83
289.81
337.03
415.68
425.66
446.69
m/z

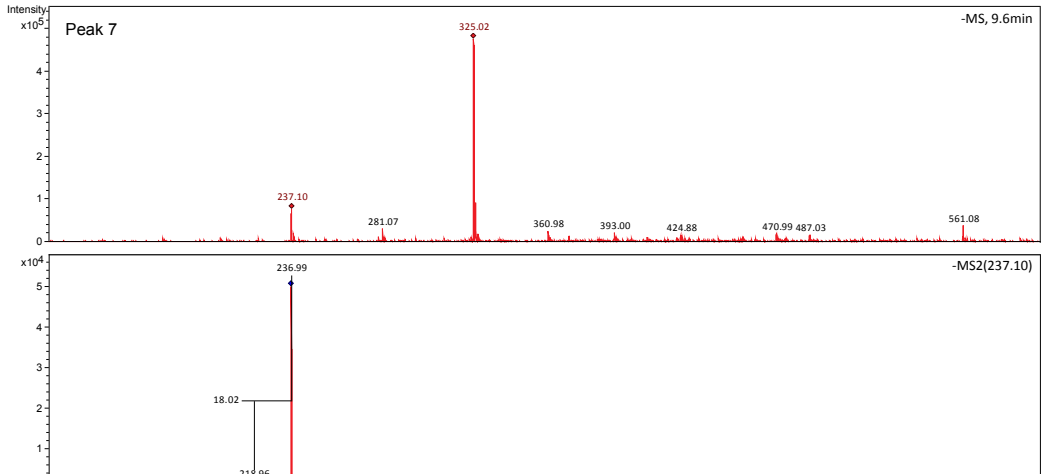
Peak 7
-MS, 9.6min
325.02
237.10
281.07
360.98
393.00
424.88
470.99
487.03
561.08
-MS2(237.10)
236.99
18.02
218.96
-MS2(325.02)
237.02
43.97
34.03
43.77
202.99
280.98
m/z

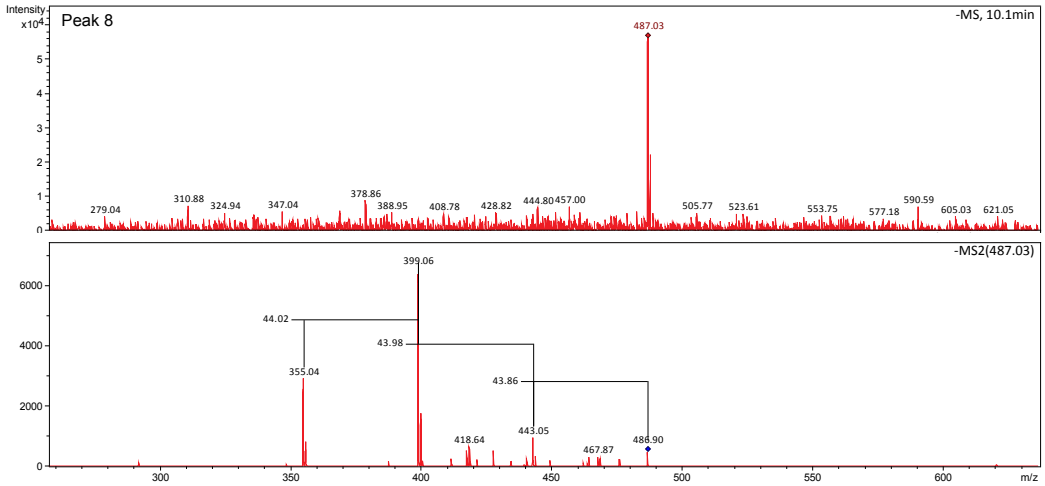
Peak 8
-MS, 10.1min
487.03
279.04
310.88
324.94
347.04
378.86
388.95
408.78
428.82
444.80
457.00
505.77
523.61
553.75
577.18
590.59
605.03
621.05
-MS2(487.03)
399.06
44.02
43.98
355.04
43.86
418.64
443.05
467.87
486.90
m/z

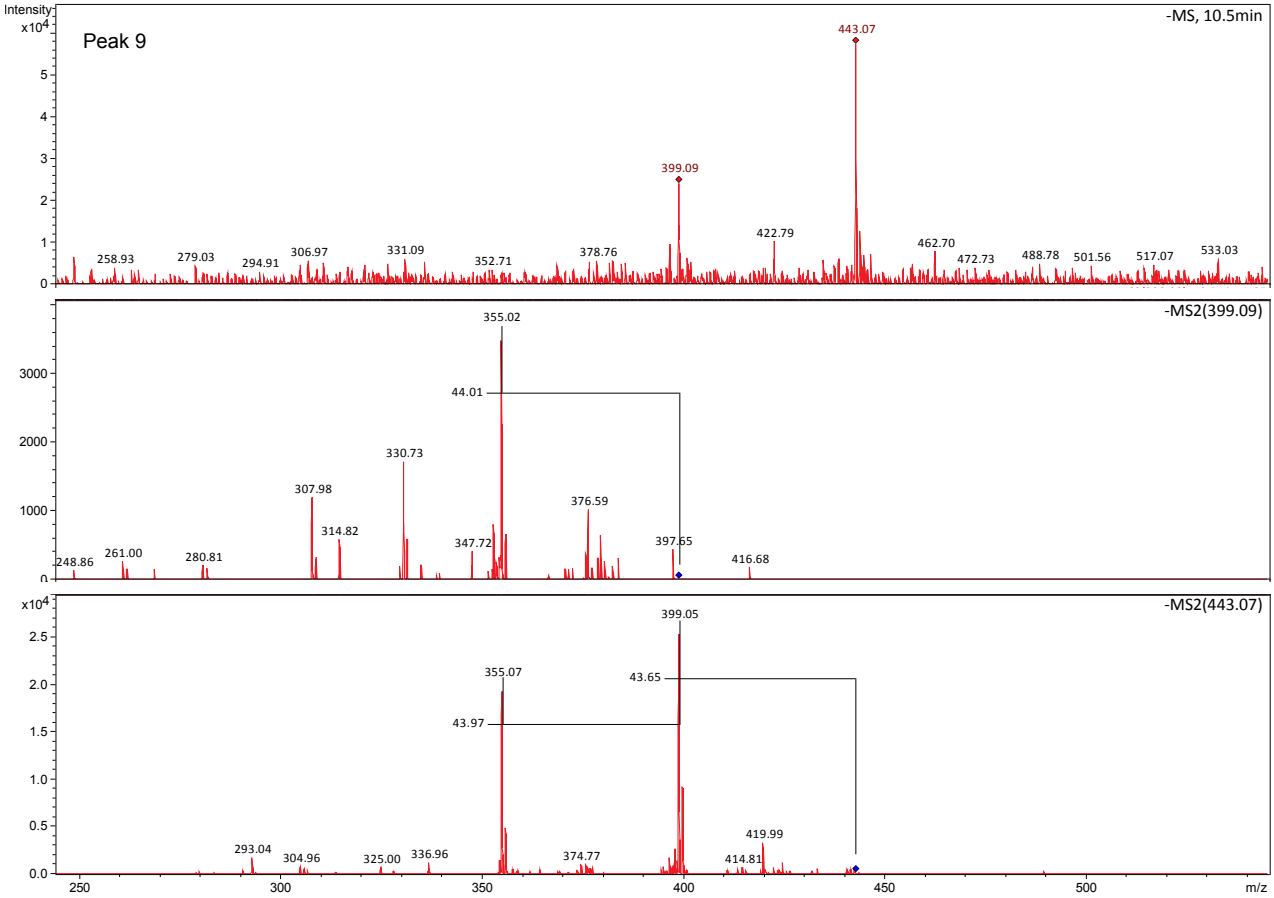
Peak 9
-MS, 10.5min
Intensity
x10^4
443.07
399.09
422.79
462.70
258.93
279.03
294.91
306.97
331.09
352.71
378.76
472.73
488.78
501.56
517.07
533.03
-MS2(399.09)
355.02
44.01
330.73
307.98
376.59
314.82
347.72
397.65
248.86
261.00
280.81
416.68
-MS2(443.07)
399.05
355.07
43.65
43.97
293.04
304.96
325.00
336.96
374.77
414.81
419.99
m/z

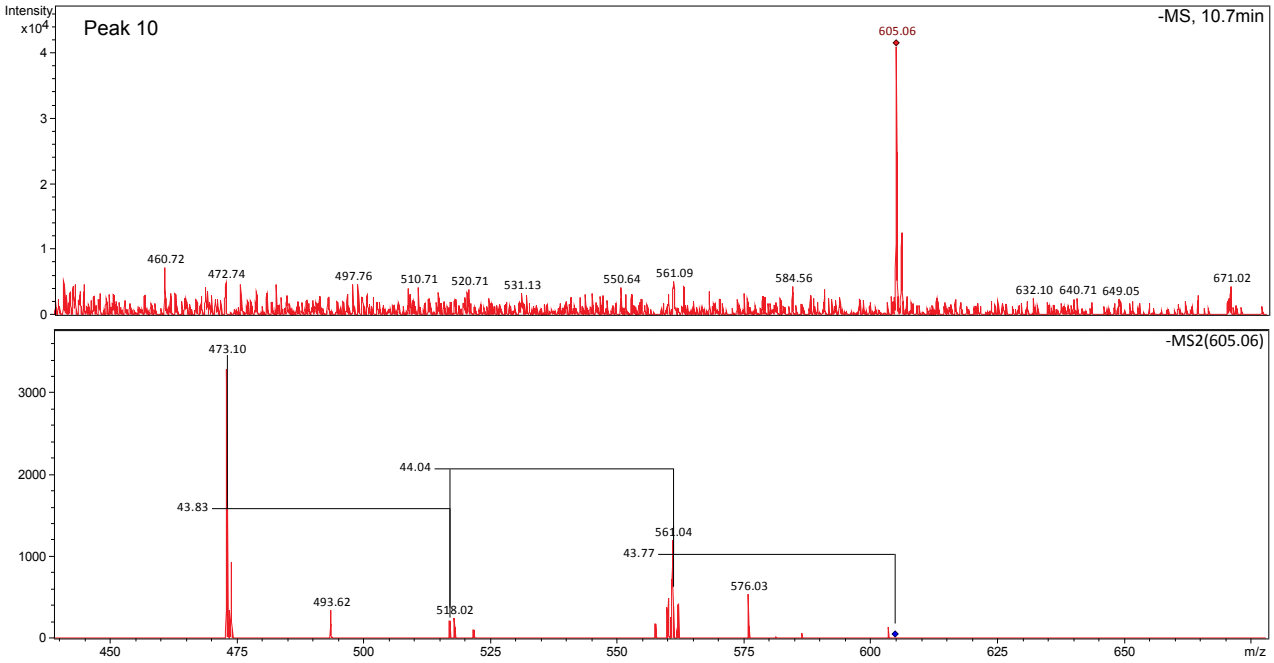
Peak 10
-MS, 10.7min
Intensity
x10^4
605.06
460.72
472.74
497.76
510.71
520.71
531.13
550.64
561.09
584.56
632.10
640.71
649.05
671.02
-MS2(605.06)
473.10
44.04
43.83
561.04
43.77
576.03
493.62
518.02
m/z

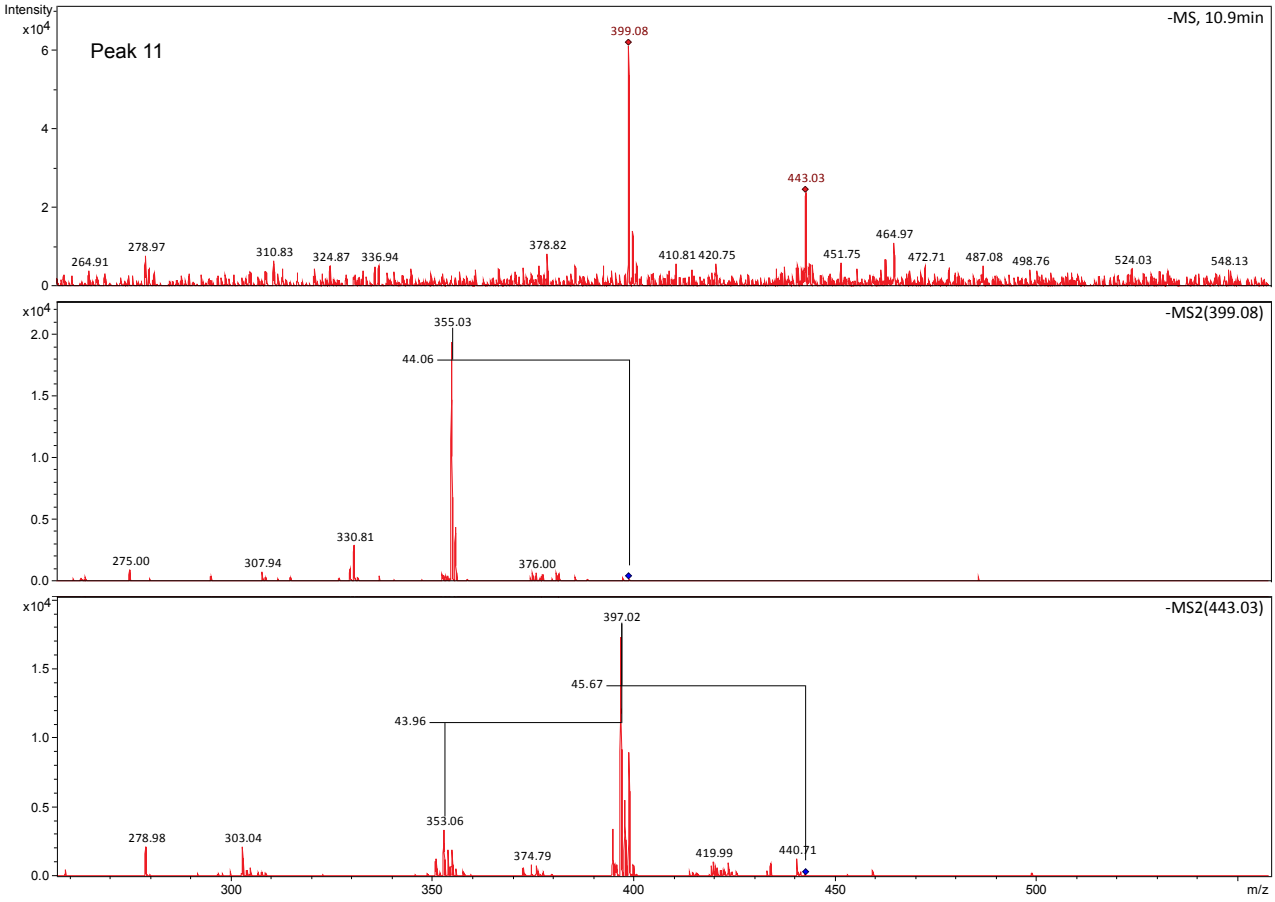

Figure S8. Evolution profile of *p*-coumaric acid oxidation by *Trametes versicolor* laccase. LC chromatograms at different reaction times are shown: 0 minutes (light blue), 10 minutes (yellow), 25 minutes (violet) and 50 minutes (red). MS and MS/MS spectra for each peak are also shown. All ions are observed as $[M-H]^-$. As reaction time is increasing substrate peak (peak 1) is decreasing in intensity, while product peaks are both increasing and decreasing, meaning that the substrate is being consumed and the products formed and then degraded or subjected to further modifications. Major losses during fragmentation are indicated on the MS/MS spectra when relevant. Product peaks are not always characterized by one single mass, but two or more different compounds elute at the same time. Whether it is a result of co-elution of two or more different product or chemical degradation has not be investigated. *p*-coumaric acid (peak 1) is identified with the *m/z* 163.00 and a retention time (RT) of 6.9 min. The product profile is complex compared to the ones from sinapic acid and ferulic acid ones. Three different dimer isomers *m/z* 325.03 are formed already after 10 minutes of reaction at RT 8.3, 9.2 and 9.7 min (peak 2, 5 and 7). Peak 2 also contains the mass of the decarboxylated dimer *m/z* 281.05 (loss of 44) and a sodium formate adduct (+ 68) of the dimer *m/z* 393. After 10 minutes also the trimer *m/z* 487.03 is present RT 10.1 min (peak 8). At longer reaction times (equal or longer than 25 minutes) four isomers of the decarboxylated trimer *m/z* 443.03 are found in peak 4, 6, 9 and 11 as well as the double decarboxylated trimer *m/z* 399.08 in peak 9 and 11. Peak 10 is characterized by *m/z* 605.06 which corresponds to the mass of the decarboxylated tetramer. Peak 2 and 3 contain masses that could not be immediately resolved to a proposed structure. Peak * RT 11.3 min, containing *m/z* 293.13 and *m/z* 361.13, where the latter is a sodium formate adduct of *m/z* 293.13, was also found by Petrucci *et al.*[1] (corresponding MS spectra is shown in Supplementary Figure S10). It is, most likely, an impurity of LC-MS eluent system since it is present also in the blank run. Suggested chemical structure for the major products are shown in Supplementary Figure S14.

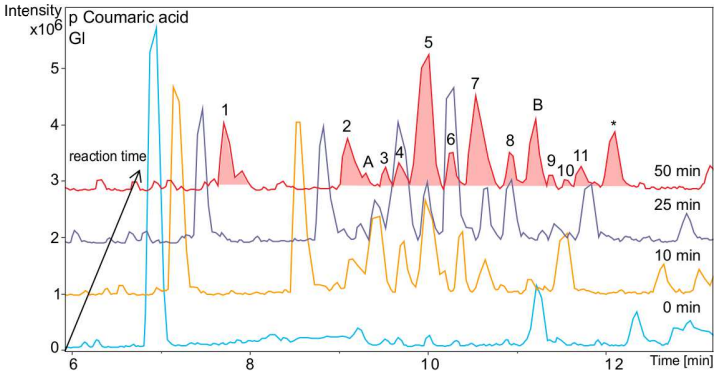
Intensity
x10^6
p Coumaric acid
GI
reaction time
1
2
A
3
4
5
6
7
8
B
9
10
11
*
50 min
25 min
10 min
0 min
Time [min]

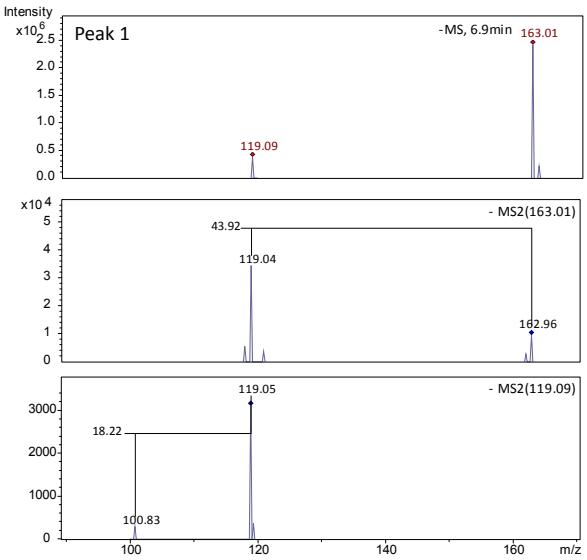
Intensity
x10^6
Peak 1
-MS, 6.9min
163.01
119.09
x10^4
- MS2(163.01)
43.92
119.04
162.96
119.05
- MS2(119.09)
18.22
100.83
m/z

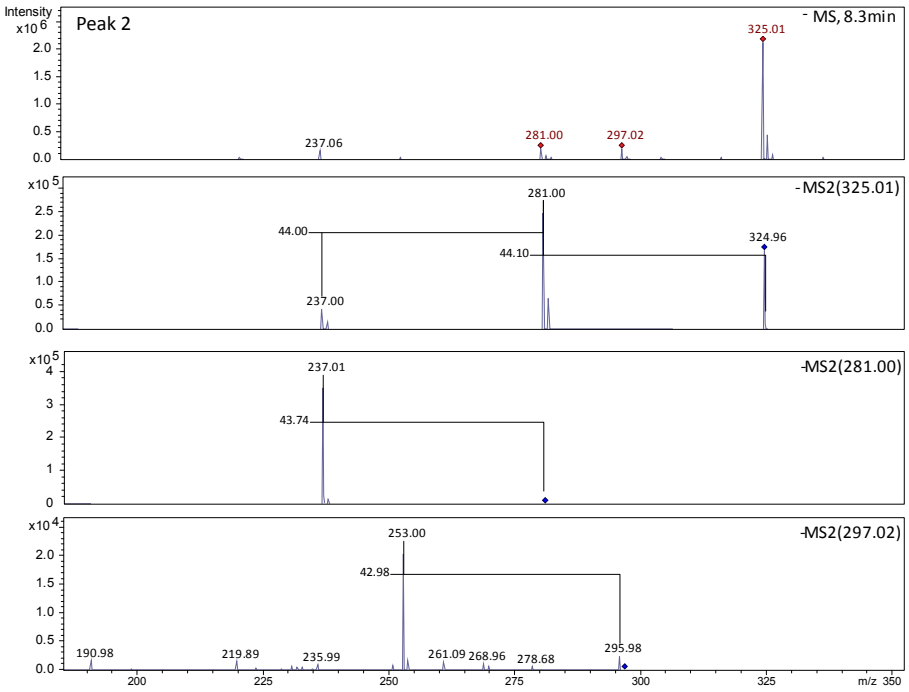
Intensity
x10^6
Peak 2
- MS, 8.3min
325.01
237.06
281.00
297.02
x10^5
-MS2(325.01)
281.00
44.00
44.10
324.96
237.00
-MS2(281.00)
237.01
43.74
x10^4
-MS2(297.02)
253.00
42.98
190.98
219.89
235.99
261.09
268.96
278.68
295.98
m/z

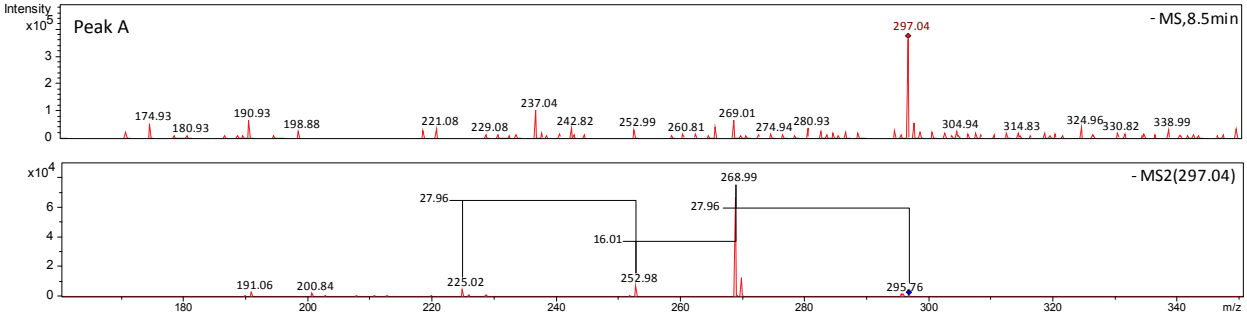
Peak A
- MS,8.5min
297.04
- MS2(297.04)
268.99
27.96
16.01
252.98
225.02
191.06
200.84
295.76
m/z

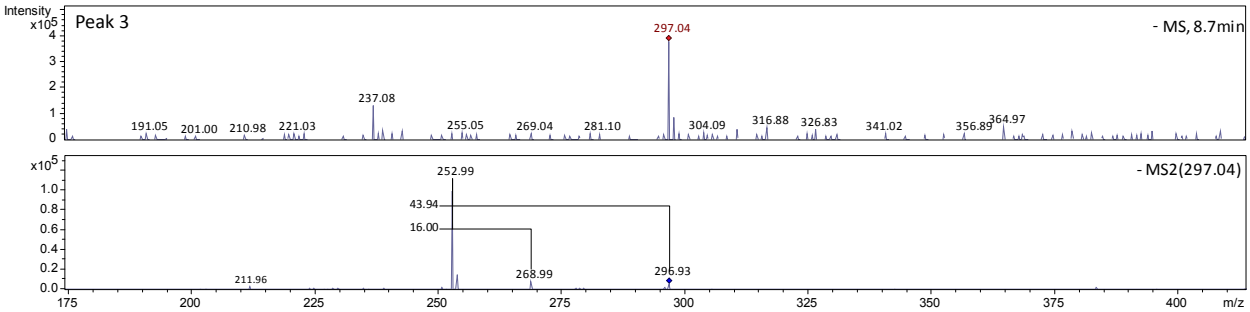
Peak 3
- MS, 8.7min
297.04
237.08
- MS2(297.04)
252.99
43.94
16.00
268.99
296.93
211.96
m/z

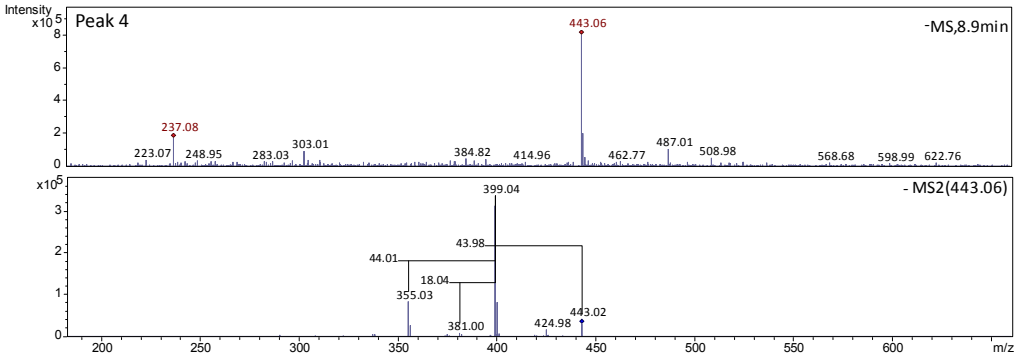
Peak 4
-MS,8.9min
443.06
237.08
- MS2(443.06)
399.04
43.98
44.01
18.04
355.03
381.00
424.98
443.02
m/z

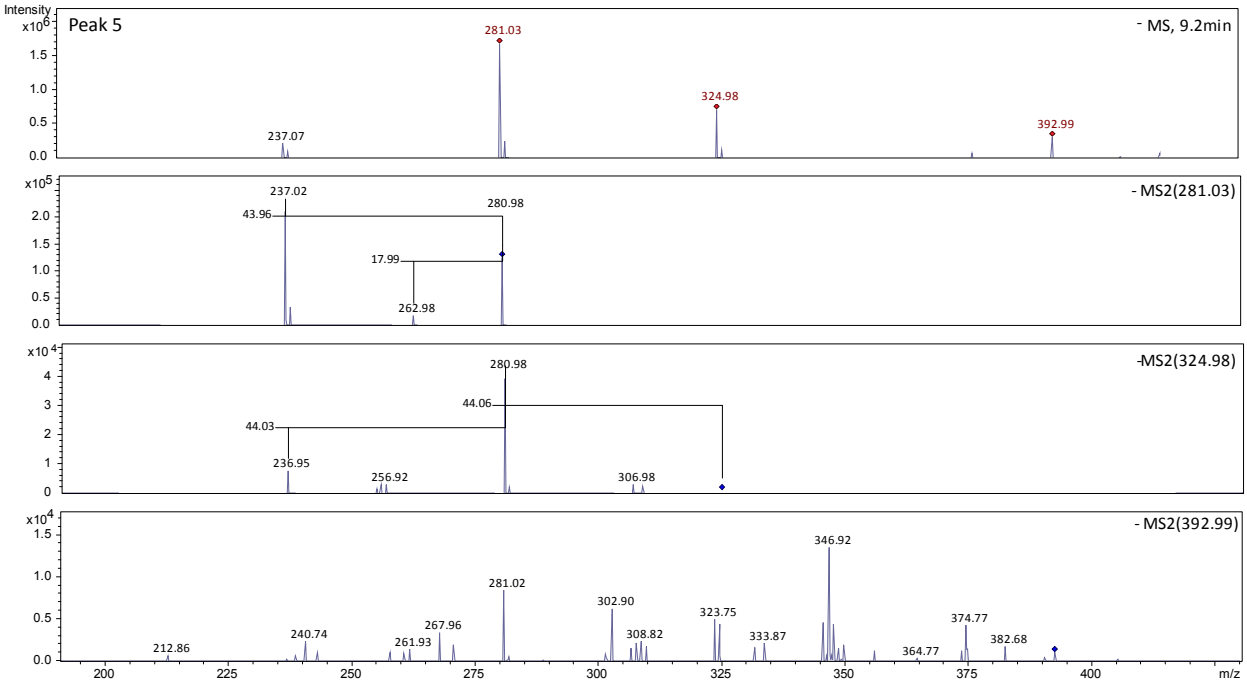
Peak 5
- MS, 9.2min
281.03
324.98
392.99
237.07
- MS2(281.03)
237.02
280.98
43.96
17.99
262.98
-MS2(324.98)
280.98
44.06
44.03
236.95
256.92
306.98
- MS2(392.99)
346.92
281.02
302.90
323.75
374.77
267.96
240.74
261.93
308.82
333.87
382.68
212.86
364.77
m/z

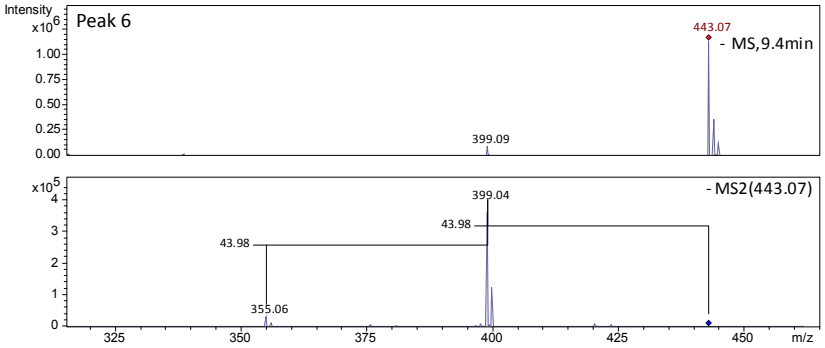
Intensity
Peak 6
443.07
- MS,9.4min
399.09
- MS2(443.07)
399.04
43.98
43.98
355.06
m/z

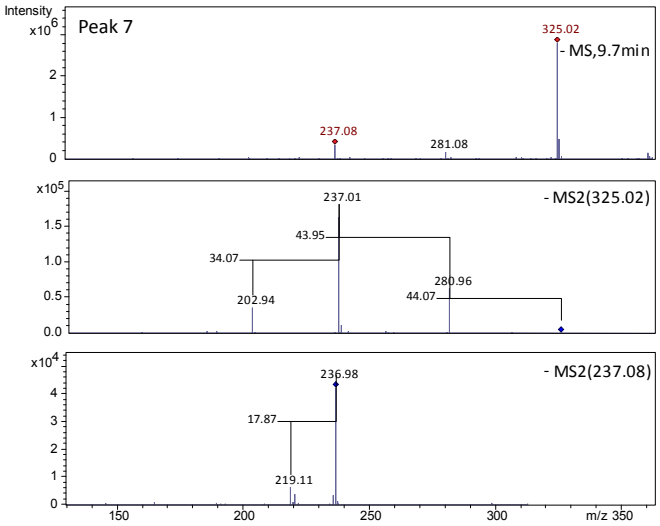
Intensity
Peak 7
325.02
- MS,9.7min
237.08
281.08
237.01
- MS2(325.02)
43.95
34.07
280.96
44.07
202.94
236.98
- MS2(237.08)
17.87
219.11
m/z 350

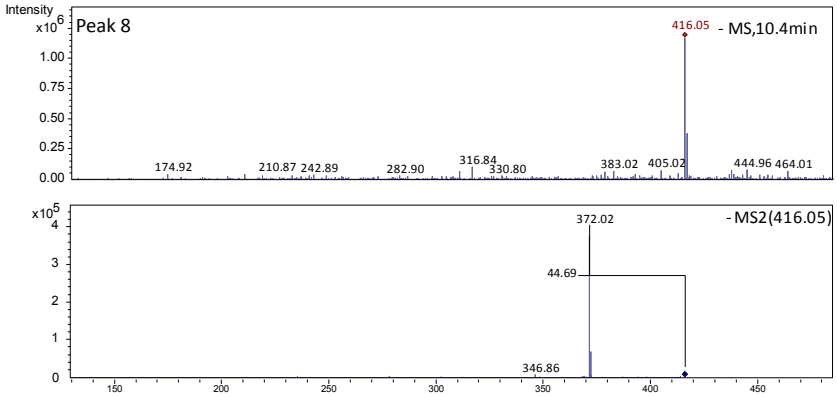
Intensity
Peak 8
416.05
- MS,10.4min
174.92
210.87 242.89
282.90
316.84
330.80
383.02 405.02
444.96 464.01
372.02
- MS2(416.05)
44.69
346.86

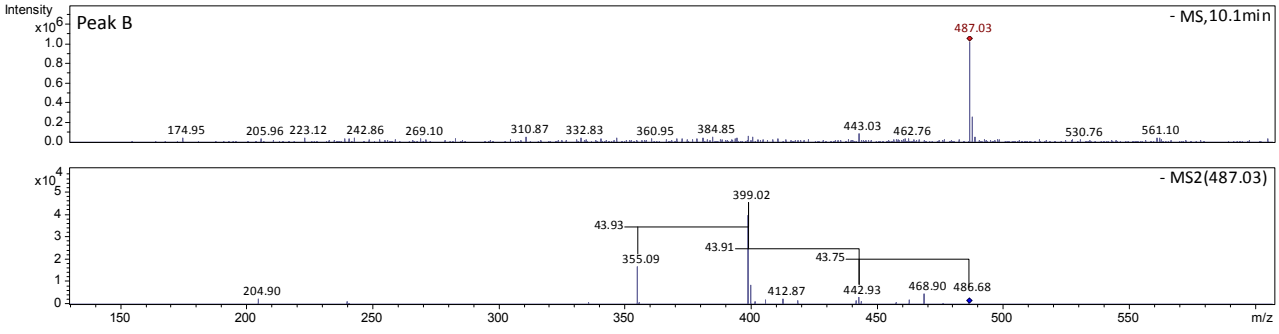
Intensity
Peak B
- MS,10.1min
487.03
174.95
205.96 223.12
242.86
269.10
310.87
332.83
360.95
384.85
443.03
462.76
530.76
561.10
- MS2(487.03)
399.02
43.93
43.91
355.09
43.75
204.90
412.87
442.93
468.90
486.68
m/z

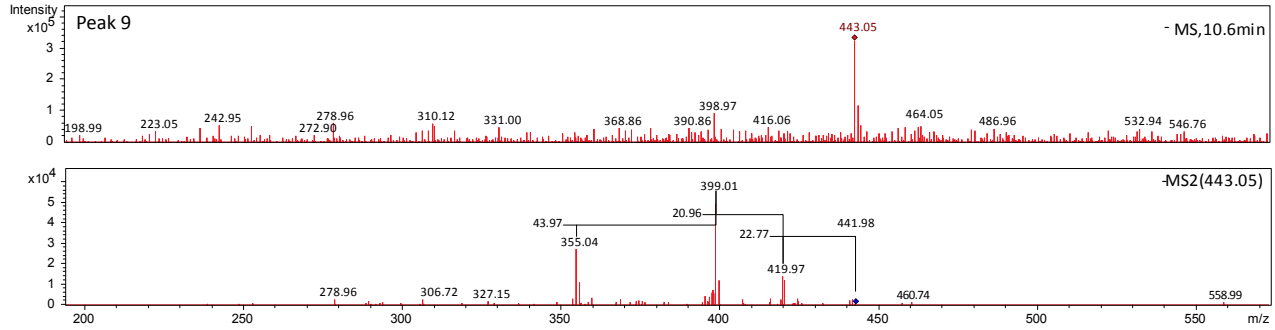
Peak 9
- MS,10.6min
443.05
-MS2(443.05)
399.01
355.04
441.98
419.97

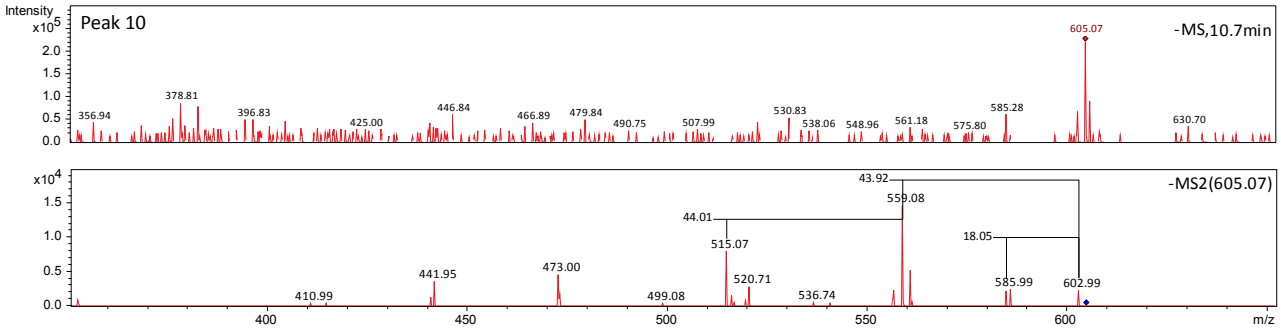
Peak 10
-MS,10.7min
605.07
-MS2(605.07)
559.08
515.07

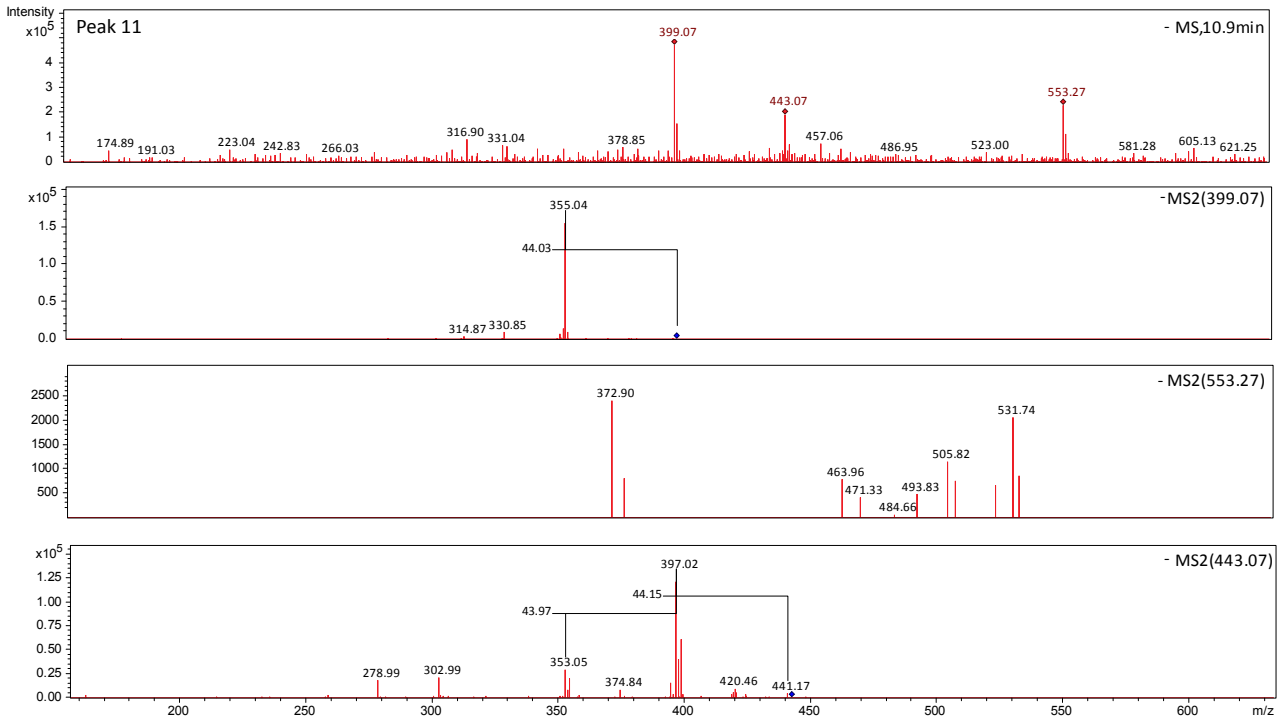
Peak 11
- MS,10.9min
399.07
443.07
553.27
-MS2(399.07)
355.04
- MS2(553.27)
372.90
531.74
- MS2(443.07)
397.02
353.05

Figure S9. Evolution profile of *p*-coumaric acid oxidation by *Ganoderma lucidum* laccase. LC chromatograms at different reaction times are shown: 0 minutes (light blue), 10 minutes (yellow), 25 minutes (violet) and 50 minutes (red). MS and MS/MS spectra for each peak are also shown. All ions are observed as $[M-H]^-$. As reaction time is increasing substrate peak (peak 1) is decreasing in intensity, while product peaks are both increasing and decreasing, meaning that the substrate is being consumed and the products formed and then degraded or subjected to further modifications. Major losses during fragmentation are indicated on the MS/MS spectra when relevant. Product peaks are not always characterized by one single mass, but two or more different compounds elute at the same time. Whether it is a result of co-elution of two or more different product or chemical degradation has not be investigated. *p*-coumaric acid (peak 1) is identified with the *m/z* 163.00 and a retention time (RT) of 6.9 min. The product profile is complex compared to the ones from sinapic acid and ferulic acid ones. Three different dimer isomers *m/z* 325.03 are formed already after 10 minutes of reaction peak 2, 5 and 7 (RT 8.3, 9.2 and 9.7 min). Peaks 2 and 5 contain also the mass of the decarboxylated dimer *m/z* 281.05 (loss of 44) and a sodium formate adduct (+ 68) of the dimer *m/z* 393 (only in peak 5). A double decarboxylated dimer *m/z* 237.08 (peak 7) is also present, it is not present in the oxidation of *p*-coumaric acid by *Trametes versicolor* laccase. After 10 minutes also the trimer *m/z* 487.03 is present RT 10.1 min (peak 8). At longer reaction times (equal or longer than 25 minutes) four isomers of the decarboxylated trimer *m/z* 443.03 are found in peak 4, 6, 9 and 11 as well as the double decarboxylated trimer *m/z* 399.08 in peak 9 and 11. Peak 10 is characterized by *m/z* 605.06 which corresponds to the mass of the decarboxylated tetramer. Peak 2, A, 3, B and 12 contain masses that could not be immediately resolved to a proposed structure. Peak * RT 11.3 min, containing *m/z* 293.13 and *m/z* 361.13, where the latter is a sodium formate adduct of *m/z* 293.13, was also found by Petrucci *et al.*[1] (corresponding MS spectra is shown in Supplementary Figure S11). It is, most likely, an impurity of LC-MS eluent system since it is present also in the blank run. Suggested chemical structure for the major products are shown in Supplementary Figure S14.

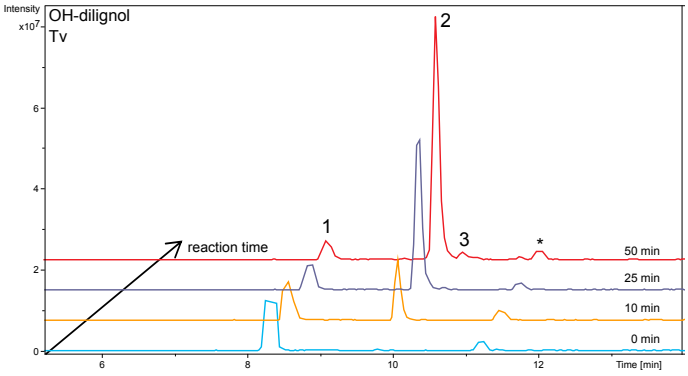
Intensity
x10^7
OH-dilignol
Tv
2
1
3
*
reaction time
50 min
25 min
10 min
0 min
Time [min]

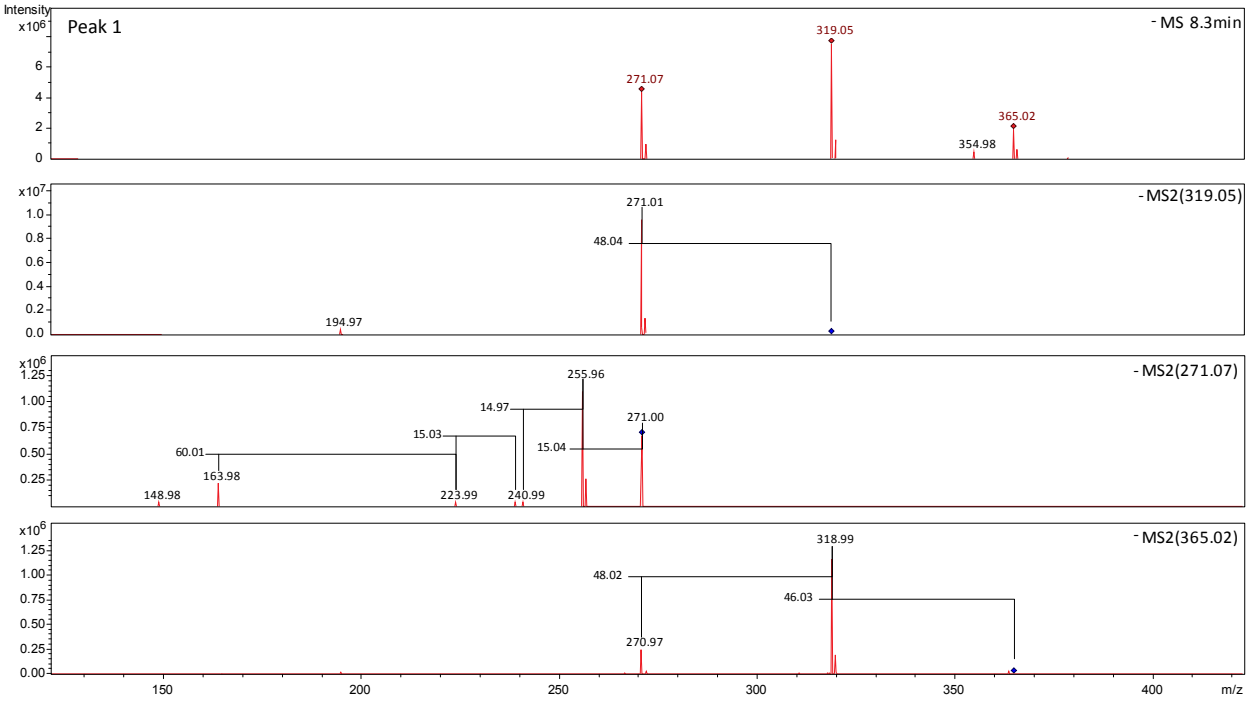
Intensity
Peak 1
MS 8.3min
319.05
271.07
365.02
354.98
MS2(319.05)
271.01
48.04
194.97
MS2(271.07)
255.96
14.97
271.00
15.03
15.04
60.01
163.98
148.98
223.99
240.99
MS2(365.02)
318.99
48.02
46.03
270.97
m/z

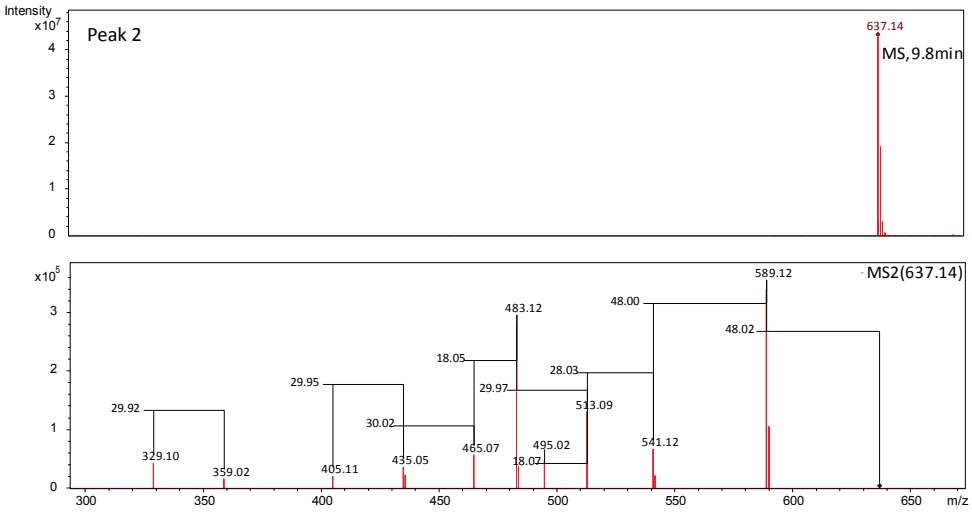
Intensity
Peak 2
637.14
MS, 9.8min
MS2(637.14)
589.12
483.12
48.00
48.02
18.05
28.03
29.95
29.97
513.09
29.92
30.02
541.12
465.07
495.02
329.10
435.05
18.07
359.02
405.11
m/z

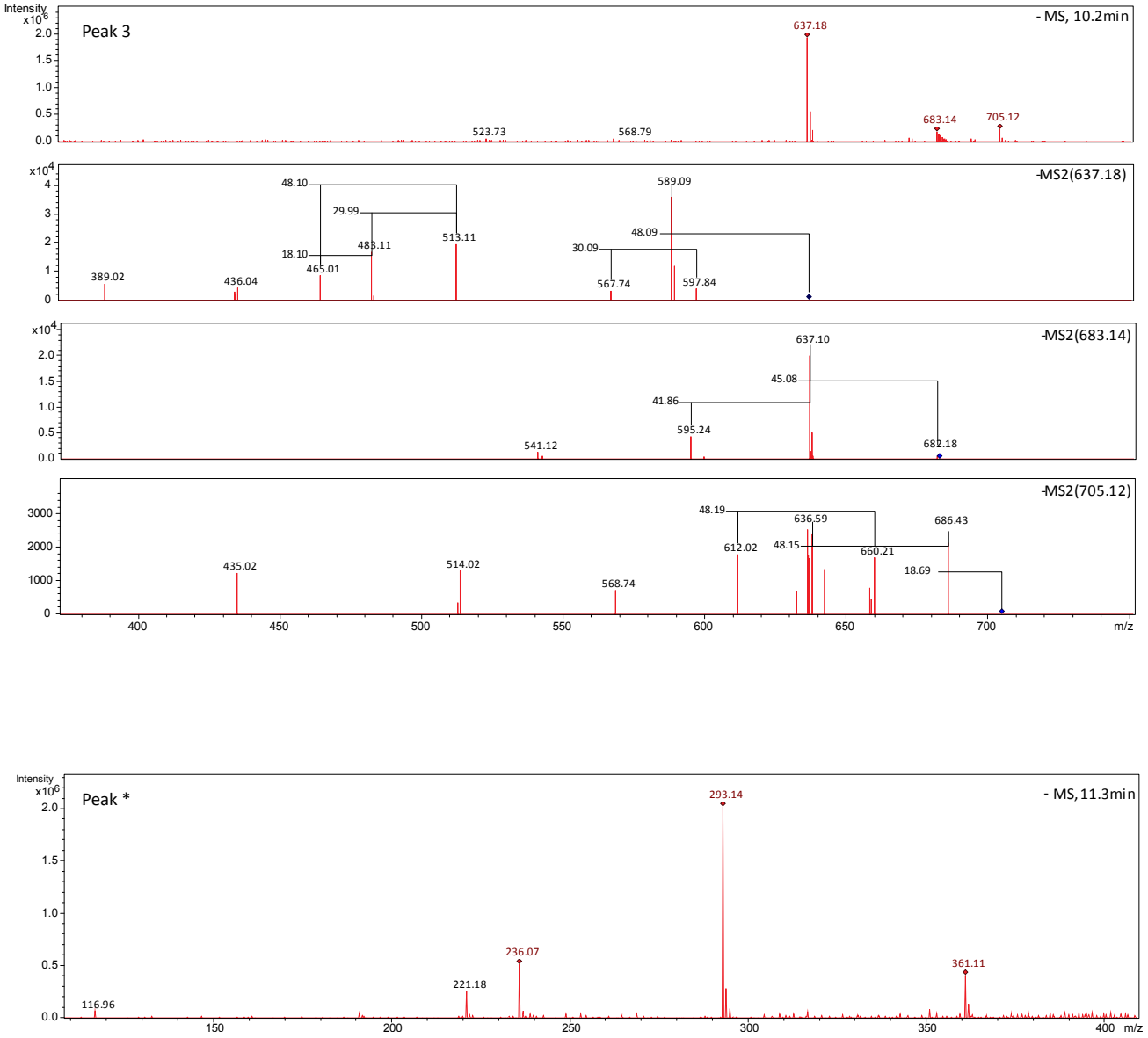

Figure S10. Evolution profile of OH-dilignol oxidation by *Trametes versicolor* laccase. LC chromatograms at different reaction times are shown: 0 minutes (light blue), 10 minutes (yellow), 25 minutes (violet) and 50 minutes (red). MS and MS/MS spectra for each peak are also shown. All ions are observed as $[M-H]^-$. As reaction time is increasing substrate peak (peak 1) is decreasing in intensity, while product peaks are increasing and decreasing, meaning that the substrate is being consumed and the products formed. Major losses during fragmentation are indicated on the MS/MS spectra when relevant. Product peaks are not always characterized by one single mass, but two or more different compound elute at the same time. Whether it is a result of co-elution of two or more different product or chemical degradation has not be investigated. OH-dilignol (peak 1) is identified with the *m/z* 319.05 and a retention time (RT) of 8.3 min. The product profile is simple, only two isomers of the OH-dilignol dimer *m/z* 637.14 are formed (peak 2 and 3) already after 10 minutes of reaction. A formate adduct (+ 46) of the dimer *m/z* 683.14 and a sodium formate adduct (+ 68) of the dimer *m/z* 705.12 are both present in peak 3. Peak * RT 11.3 min, containing *m/z* 293.13 and *m/z* 361.13, where the latter is a sodium formate adduct of *m/z* 293.13, was also found by Petrucci *et al.*[1]. It is, most likely, an impurity of LC-MS eluent system since it is present also in the blank run. Suggested chemical structure for the major products are shown in Supplementary Figure S15.

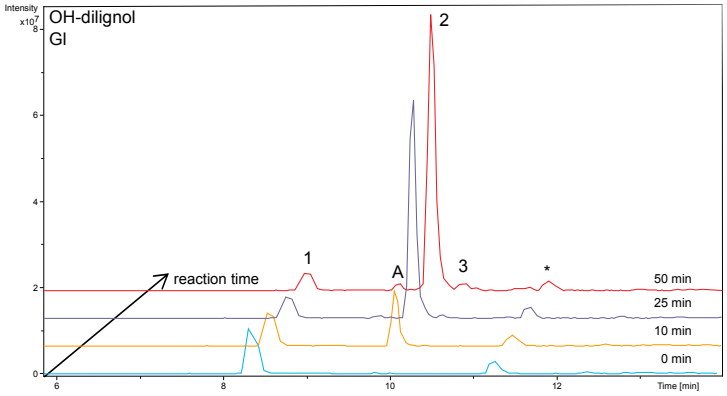
Intensity
x10^7
OH-dilignol
Gl
2
1
A
3
*
reaction time
50 min
25 min
10 min
0 min
Time [min]

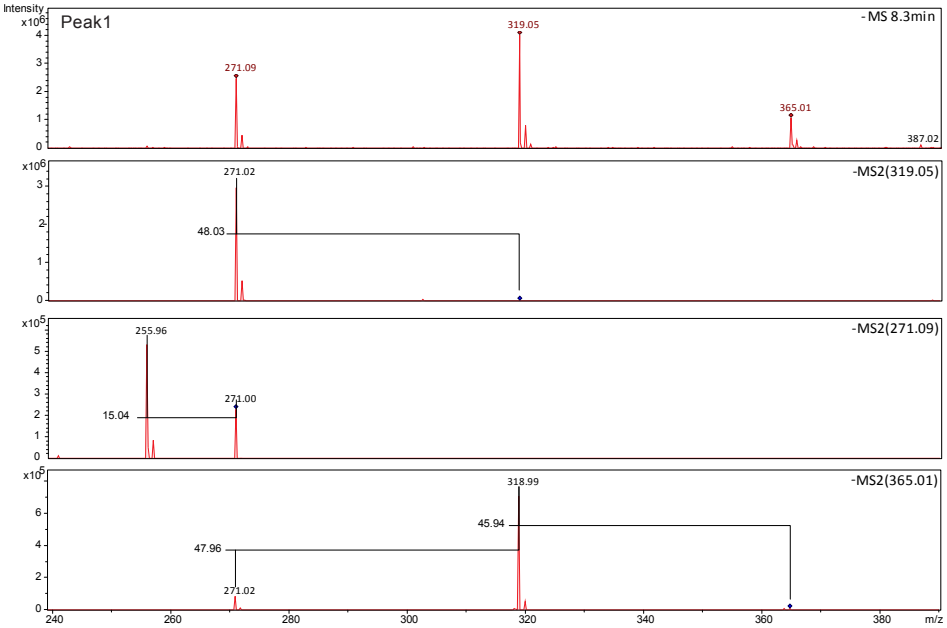
Intensity
Peak1
-MS 8.3min
319.05
271.09
365.01
387.02
-MS2(319.05)
271.02
48.03
-MS2(271.09)
255.96
271.00
15.04
-MS2(365.01)
318.99
45.94
47.96
271.02
m/z

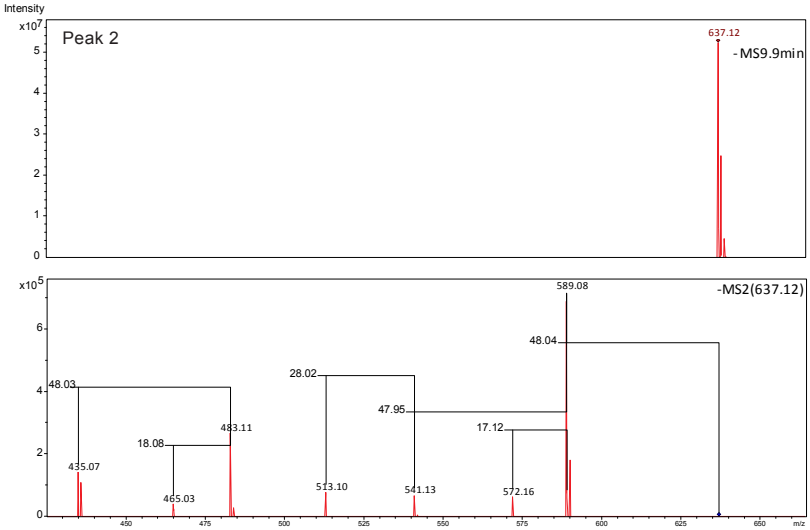
Intensity
Peak 2
637.12
-MS9.9min
-MS2(637.12)
589.08
48.04
28.02
48.03
47.95
17.12
483.11
18.08
435.07
465.03
513.10
541.13
572.16
m/z

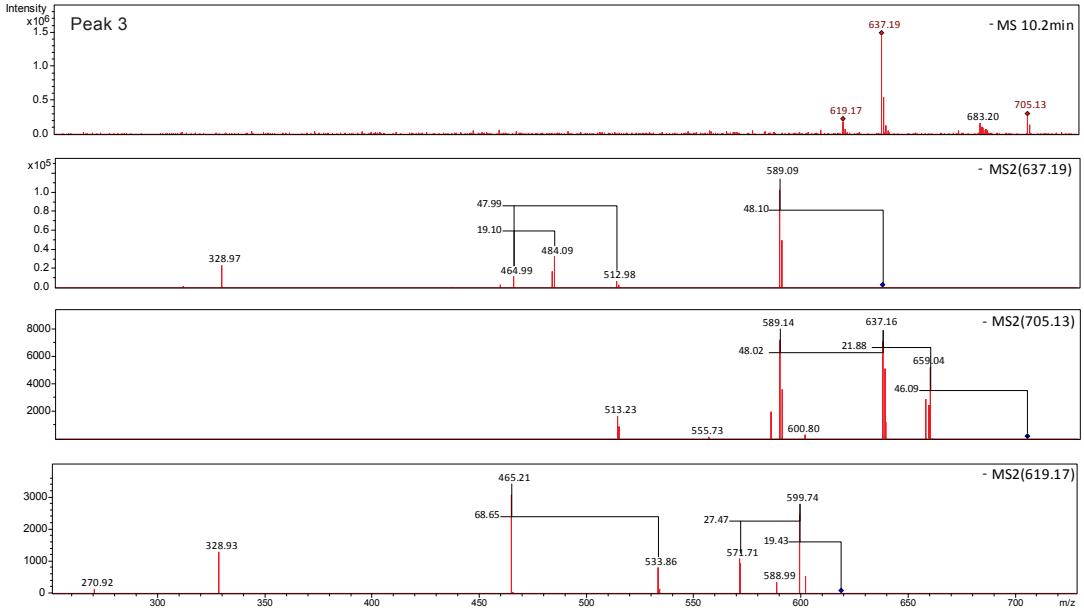
Intensity
Peak 3
- MS 10.2min
637.19
619.17
683.20
705.13
- MS2(637.19)
589.09
47.99
48.10
19.10
484.09
328.97
464.99
512.98
- MS2(705.13)
589.14
637.16
48.02
21.88
659.04
46.09
513.23
555.73
600.80
- MS2(619.17)
465.21
68.65
599.74
27.47
19.43
328.93
571.71
533.86
588.99
270.92
m/z

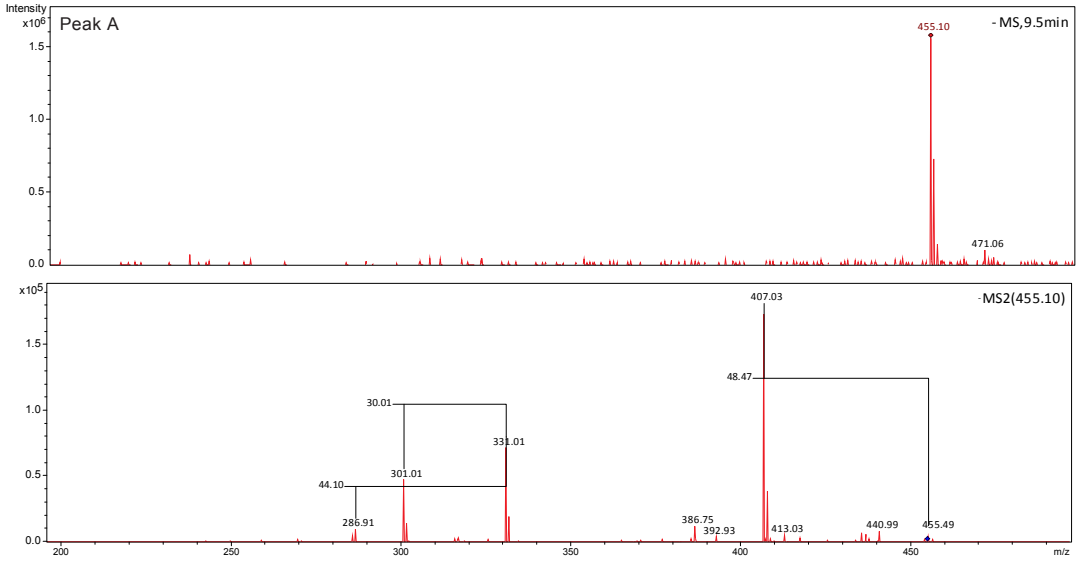
Intensity
Peak A
- MS,9.5min
455.10
471.06
- MS2(455.10)
407.03
48.47
30.01
331.01
301.01
44.10
286.91
386.75
392.93
413.03
440.99
455.49
m/z


Intensity
Peak *
- MS 11.3min
293.14
361.12
609.29
m/z

Figure S11. Evolution profile of OH-dilignol oxidation by *Trametes versicolor* laccase. LC chromatograms at different reaction times are shown: 0 minutes (light blue), 10 minutes (yellow), 25 minutes (violet) and 50 minutes (red). MS and MS/MS spectra for each peak are also shown. All ions are observed as $[M-H]^-$. As reaction time is increasing substrate peak (peak 1) is decreasing in intensity, while product peaks are increasing and decreasing, meaning that the substrate is being consumed and the products formed. Major losses during fragmentation are indicated on the MS/MS spectra when relevant. Product peaks are not always characterized by one single mass, but two or more different compound elute at the same time. Whether it is a result of co-elution of two or more different product or chemical degradation has not be investigated. OH-dilignol (peak 1) is identified with the *m/z* 319.05 and a retention time (RT) of 8.3 min. The product profile is simple, only two isomers of the OH-dilignol dimer *m/z* 637.14 are formed (peak 2 and 3) already after 10 minutes of reaction. A sodium formate adduct (+ 68) of the dimer *m/z* 705.12 is present in peak 3. After 50 minutes a compound with *m/z* 455.10 (peak A) appears, showing a mass of 136 higher than OH dilignol (*m/z* 319.05) indicating a double sodium formate adduct of the substrate. Peak * RT 11.3 min, containing *m/z* 293.13 and *m/z* 361.13, where the latter is a sodium formate adduct of *m/z* 293.13, was also found by Petrucci *et al.*[1]. It is, most likely, an impurity of LC-MS eluent system since it is present also in the blank run. Suggested chemical structure for the major products are shown in Supplementary Figure S15.

	possible products from laccase oxidation of sinapic acid
401	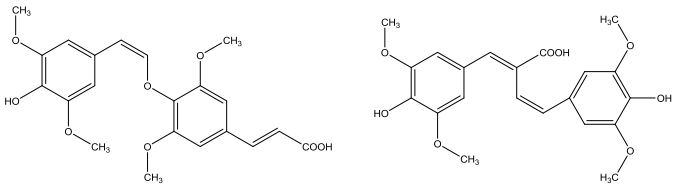
446	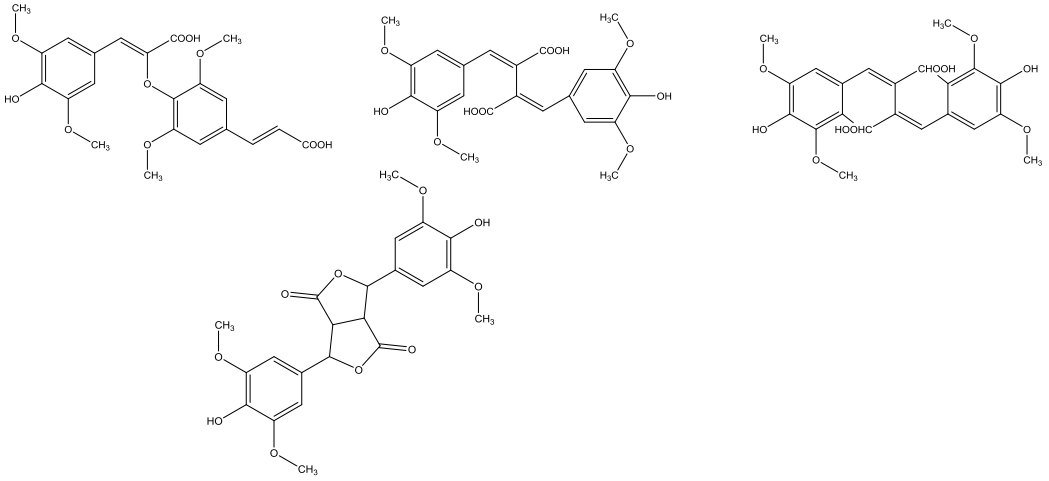

Figure S12. Suggested product structures after laccase oxidation of sinapic acid[2]. Sinapic acid dimer MW 446 g/mol and decarboxylated dimer MW 402 g/mol are the oxidation products fitting the masses found in the reaction evolution profile: Supplementary Figure S2 and S4 peak 3 and 4 and peak 2 and 3, respectively. It has to be noted that these are suggested structures on the basis on what is already known from previous studies[2,3].

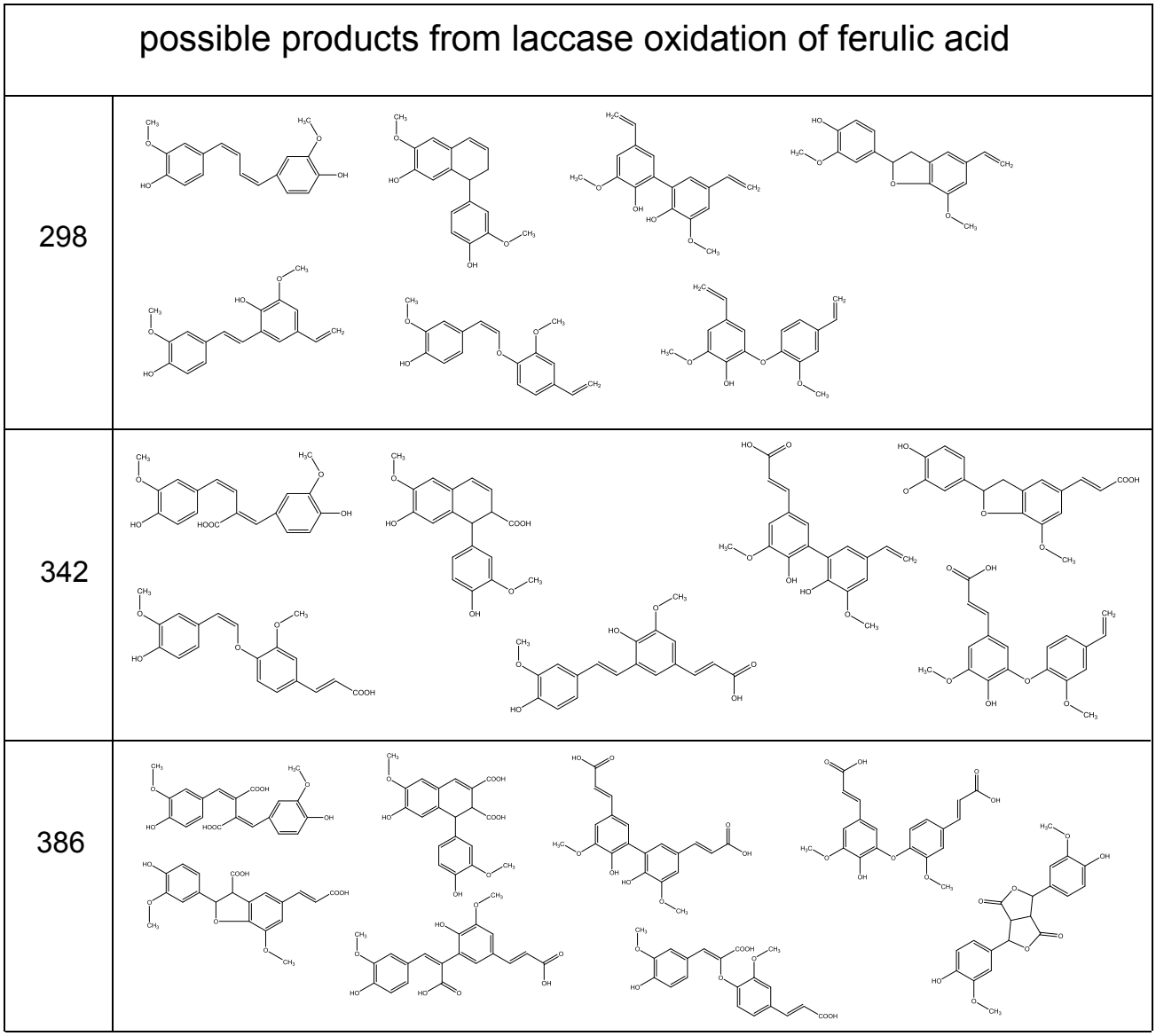

Figure S13. Suggested product structures after laccase oxidation of ferulic acid. Ferulic acid dimer MW 386 g/mol, decarboxylated dimer MW 342 g/mol and doubble decarboxylated dimer MW 298 g/mol are the oxidation products fitting the masses found in the reaction evolution profile: Supplementary Figure S6 and S7 peak 3, 4 and 6 and peak 2, 3 and 4 and peak 4 and 6, respectively. It has to be noted that these are suggested structures on the basis on what is already known from previous studies[3–5].

possible products from laccase oxidation of p-coumaric acid	
282	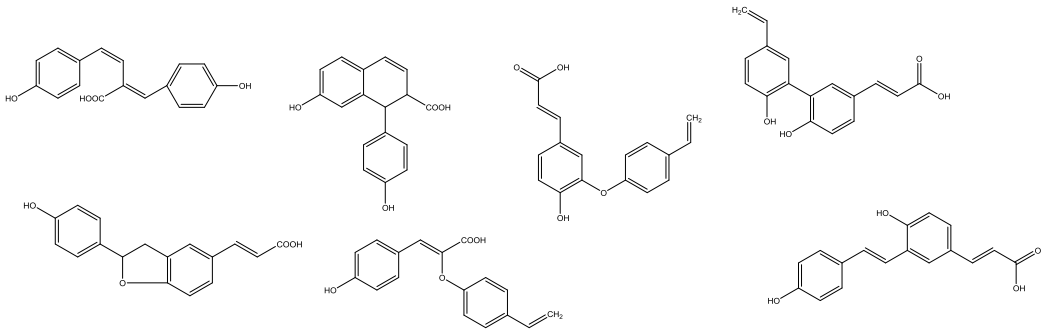
326	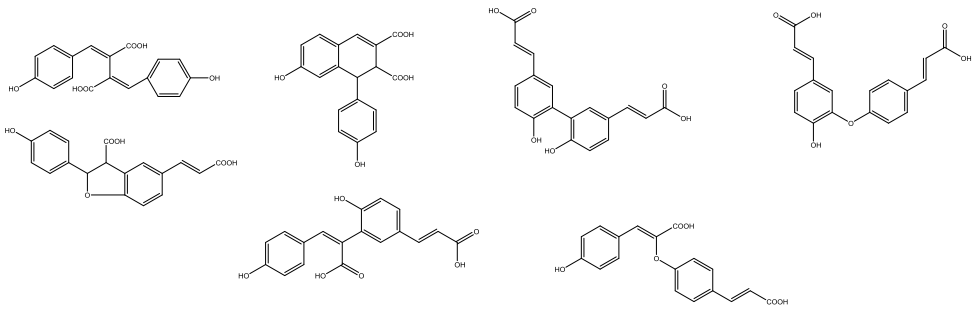
400	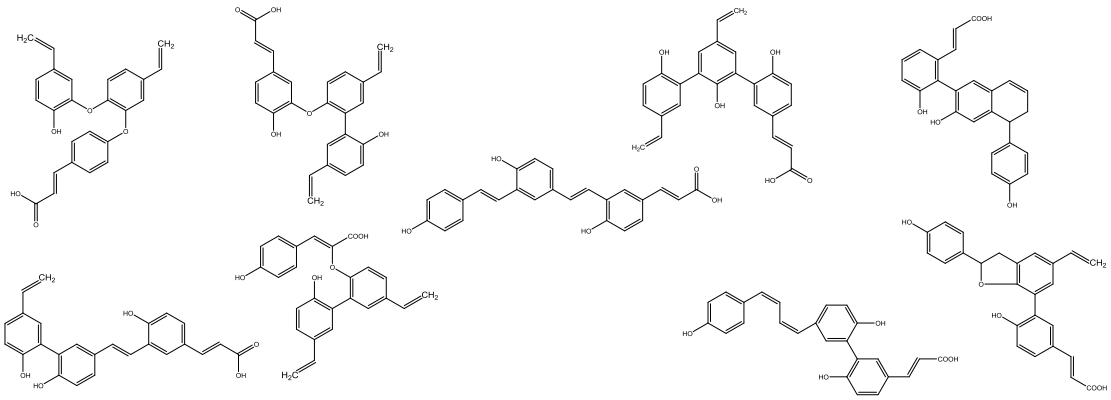
444	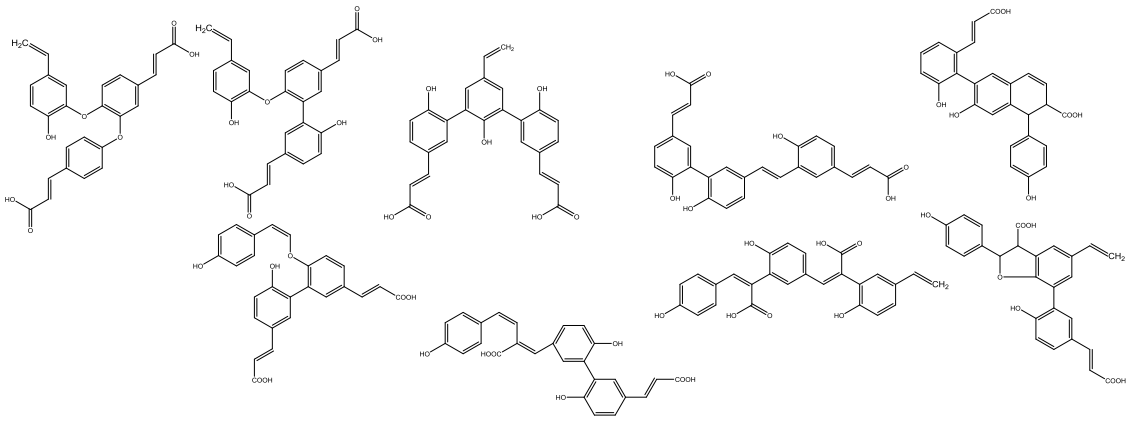

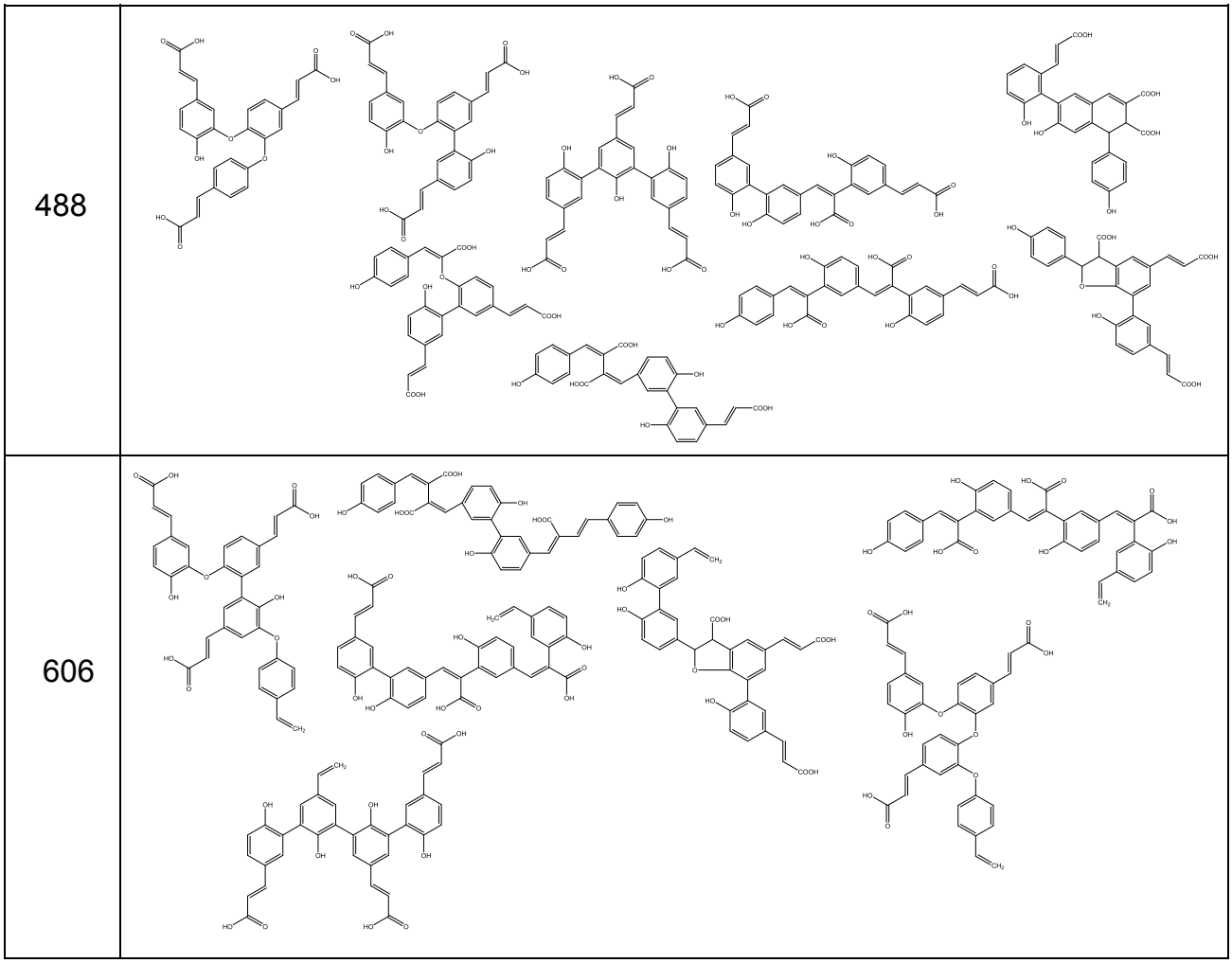

Figure S14. Suggested products structures after laccase oxidation of *p*-coumaric acid. *p*-coumaric acid dimer MW 326 g/mol, decarboxylated dimer MW 282 g/mol, *p*-coumaric acid trimer MW 488 g/mol , decarboxylated trimer MW 444 g/mol, doubble decarboxylated trimer MW 400 g/mol and decarboxylated tetramer 606 g/mol are the oxidation products fitting the masses found in the reaction evolution profile: Supplementary Figure S8 and S9. It has to be noted that these are suggested structures on the basis on what is already known from previous study[3].

possible products from laccase oxidation of OH-dilignol	
638	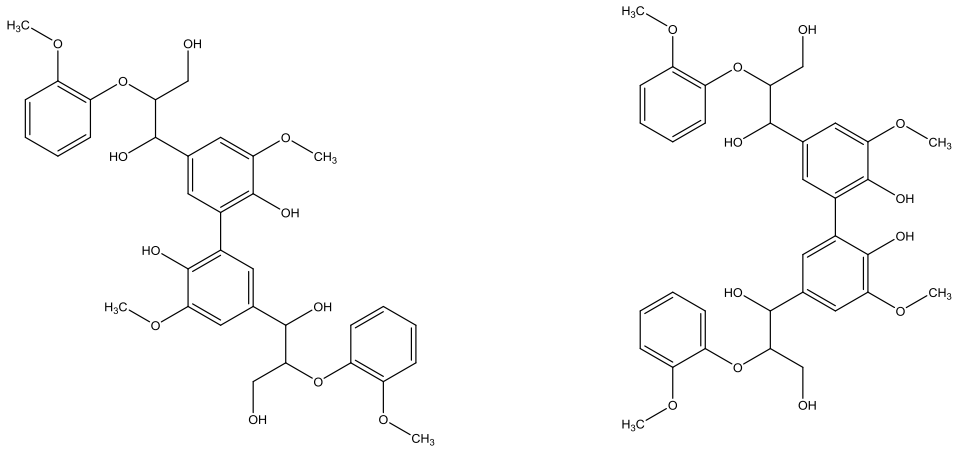

Figure S15. Suggested product structures after laccase oxidation of OH-dilignol. OH-dilignol dimer MW 638 g/mol is the oxidation product fitting the masses found in the reaction evolution profile: Supplementary Figure S10 and S11. Due to the poor conjugated structure, radical propagation outside the aromatic phenolic ring is not possible allowing only formation of a dimer in the para position.

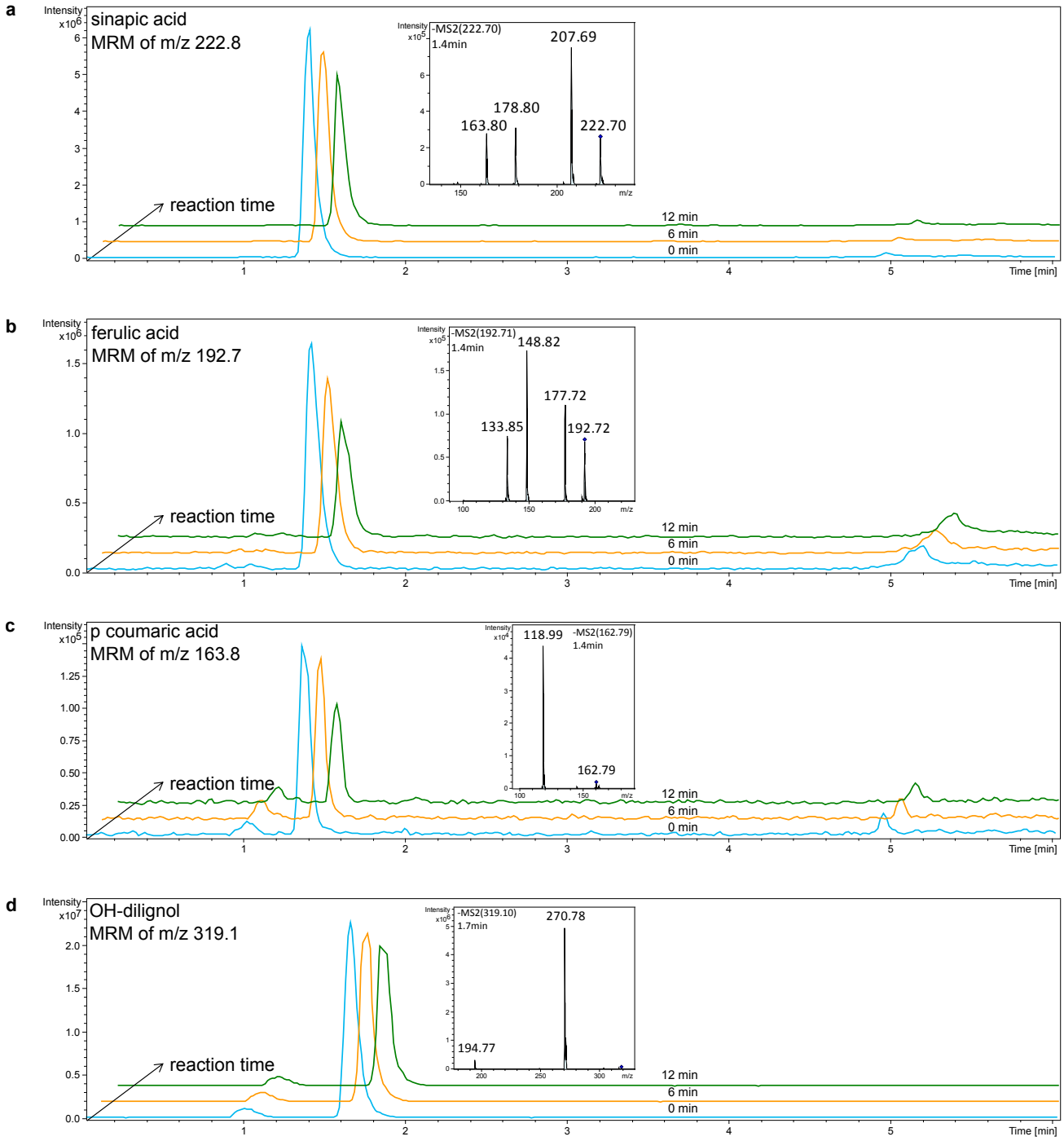

Figure S16. Laccase oxidation evolution profiles for hydroxycinnamic acid and OH-dilignol compound using Multiple Reaction Monitoring (MRM) analysis for substrate quantification: oxidation of sinapic acid (a); oxidation of ferulic acid (b); oxidation of *p*-coumaric acid (c) and oxidation of OH-dilignol (d). Chromatograms show the MRM profile of the oxidation of the different substrates at different reaction time: 0 minutes (light blue), 6 minutes (yellow) and 12 minutes (green). Please note that the intensity scale may differ between chromatograms and is adjusted to give optimal display of figures. Insets show MS/MS of the peak, all the masses found in the MS/MS in addition to the parent mass were used in the quantification methods. All ions are observed as $[M-H]^{-1}$.

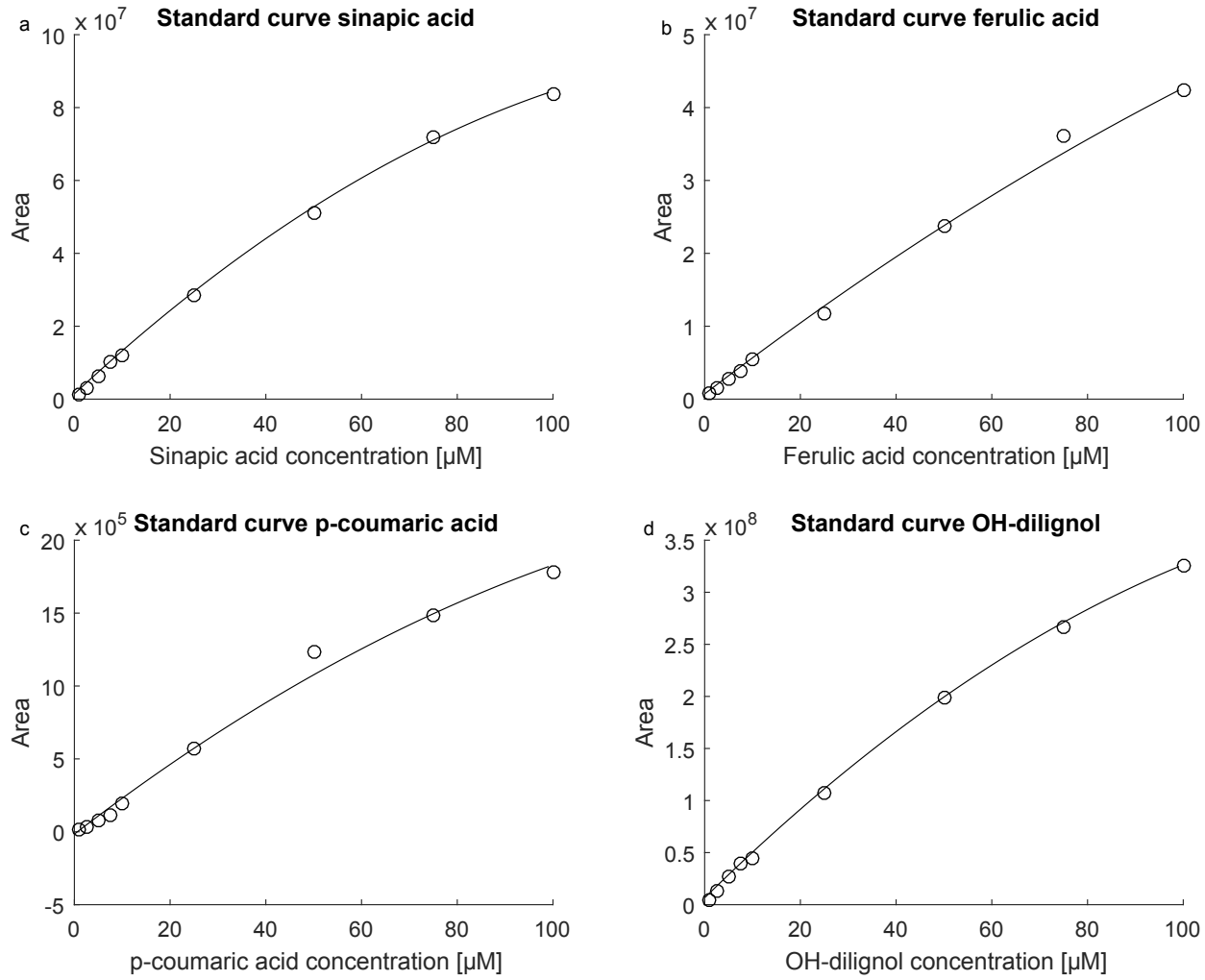

Figure S17. Standard curves for quantification of kinetic: sinapic acid (a), ferulic acid (b), *p*-coumaric acid (c) and OH-dilignol (d). The area is the target area determined as sum of the the different masses reported in Supplementary Figure S16. Nine different level of standards were used: 1, 2.5, 5, 7.5, 10, 25, 50, 75 and 100 μM. Data are fitted with a quadratic curve. Y-axis is optimized in order to have a optimal view of the curves.

References

1. A spectroelectrochemical and chemical study on oxidation of hydroxycinnamic acids in aprotic medium. *Electrochimica Acta* **52**, 2461–2470 (2007).
2. Lacki, K. & Duvnjak, Z. Transformation of 3,5-dimethoxy,4-hydroxy cinnamic acid by polyphenol oxidase from the fungusTrametes versicolor: Product elucidation studies. *Biotechnol. Bioeng.* **57**, 694–703 (1998).
3. Vismeh, R. *et al.* Profiling of diferulates (plant cell wall cross-linkers) using ultrahigh-performance liquid chromatography-tandem mass spectrometry. *The Analyst* **138**, 6683 (2013).
4. Ralph, J. *et al.* Lignins: Natural polymers from oxidative coupling of 4-hydroxyphenyl- propanoids. *Phytochem. Rev.* **3**, 29–60 (2004).
5. Carunchio, F., Crescenzi, C., Girelli, A. M., Messina, A. & Tarola, A. M. Oxidation of ferulic acid by laccase: identification of the products and inhibitory effects of some dipeptides. *Talanta* **55**, 189–200 (2001).

Paper 2

Laccase activity measurment by FTIR spectral fingerprinting

Enzyme and Microbial Technology 122 (2019) 64–73

Contents lists available at ScienceDirect

Enzyme and Microbial Technology

journal homepage: www.elsevier.com/locate/enzmictec

Laccase activity measurement by FTIR spectral fingerprinting

Valentina Perna[a], Andreas Baum[b,*], Heidi A. Ernst[c], Jane W. Agger[a], Anne S. Meyer[a,*]

[a] Protein Chemistry and Enzyme Technology, Department of Biotechnology and Biomedicine, Technical University of Denmark, Kgs. Lyngby, 2800, Denmark
[b] Section for Statistics and Data Analysis, Department of Applied Mathematics and Computer Science, Technical University of Denmark, Kgs. Lyngby, 2800, Denmark
[c] Department of Chemistry, University of Copenhagen, 2100, Copenhagen Ø, Denmark

ARTICLE INFO

Keywords:
Laccase
Enzyme activity assay
Spectral evolution profiles
FTIR
PARAFAC
High-throughput

ABSTRACT

Laccases (EC 1.10.3.2) are enzymes known for their ability to catalyze the oxidation of phenolic compounds using molecular oxygen as the final electron acceptor. Laccase activity is commonly determined by monitoring spectrophotometric changes (absorbance) of the product or substrate during the enzymatic reaction. Fourier Transform Infrared Spectroscopy (FTIR) is a fast and versatile technique where spectral evolution profiling, i.e. assessment of the spectral changes of both substrate and products during enzymatic conversion in real time, can be used to assess enzymatic activity when combined with multivariate data analysis. We employed FTIR to monitor enzymatic oxidation of monolignols (sinapyl, coniferyl and *p*-coumaryl alcohol), sinapic acid, and sinapic aldehyde by four different laccases: three fungal laccases from *Trametes versicolor*, *Trametes villosa* and *Ganoderma lucidum*, respectively, and one bacterial laccase from *Meiothermus ruber*. By coupling the FTIR measurements with Parallel Factor Analysis (PARAFAC) we established a quantitative assay for assessing laccase activity. By combining PARAFAC modelling with Principal Component Analysis we show the usefulness of this technology as a multivariate tool able to compare and distinguish different laccase reaction patterns. We also demonstrate how the FTIR approach can be used to create a reference system for laccase activity comparison based on a relatively low number of measurements. Such a reference system has potential to function as a high-throughput method for comparing reaction pattern similarities and differences between laccases and hereby identify new and interesting enzyme candidates in large sampling pools.

1. Introduction

Laccases (benzenediol: oxygen oxidoreductases; EC 1.10.3.2) belong to the blue multi-copper oxidoreductase enzymes. Laccases are produced mainly by fungi, plants and bacteria [1] and they are well known for catalyzing oxidation of phenolic compounds similar to lignin subunits by using molecular oxygen as final electron acceptor [2]. Enzyme characterization and assessment of laccase activity towards specific substrates are of great importance in enzyme discovery, laccase engineering, and bioprocess development.

However, laccases are notoriously difficult to characterize because they are capable of oxidizing a variety of compounds and because the resulting products are a result of combined enzymatic radical formation and chemical coupling between these radicals. Various techniques have been pursued for characterizing laccase activity [3,4] and the most standardized methods involve monitoring changes in absorbance upon laccase treatment of different substrates such as syringaldazine (4-hydroxy-3,5-dimethoxy-benzaldehyde azine), ABTS (2,2′-azino-bis(3-ethylbenzothiazoline-6-sulphonic acid)), 2,6-dimethoxyphenol and sinapic acid [3,5]. These methods are only accounting for substrate depletion or product formation and can therefore not describe the enzymatic reaction in all its complexity, i.e. monitoring substrate depletion and product formation at the same time.

Vibrational spectroscopy, such as infrared spectroscopy, is known to be a versatile and rapid technique to capture a snapshot of the overall chemical structures in a measured sample. The idea of employing FTIR spectroscopy for assessing laccase activity has been reported previously in relation to analysis of laccase catalyzed fungal pigment decolorization [6] and measurement of lacasse catalyzed decolorization of toxic dyes in industrial textile wastewater (e.g. oxidation of reactive Blue 4 [7] or remazol blue RB19 [8]. These assessments were done by either visually interpreting changes in the FTIR spectra before and after laccase treatment [6,7] or by estimating relative intensity changes in single wavenumbers before and after laccase treatment [8]. However,

Abbreviations: FTIR, Fourier transform infrared spectroscopy; PARAFAC, parallel factor analysis; PCA, principal component analysis; PC, principal components; Tv, laccase from *Trametes versicolor*; Tvil, laccase from *Trametes villosa*; Gl, laccase from *Ganoderma lucidum*; Mr, laccase from *Meiothermus ruber*; SGA, syringaldazine

* Corresponding author.
E-mail addresses: andba@dtu.dk (A. Baum), asme@dtu.dk (A.S. Meyer).

https://doi.org/10.1016/j.enzmictec.2018.12.009
Received 23 October 2018; Received in revised form 16 December 2018; Accepted 17 December 2018
Available online 18 December 2018
0141-0229/

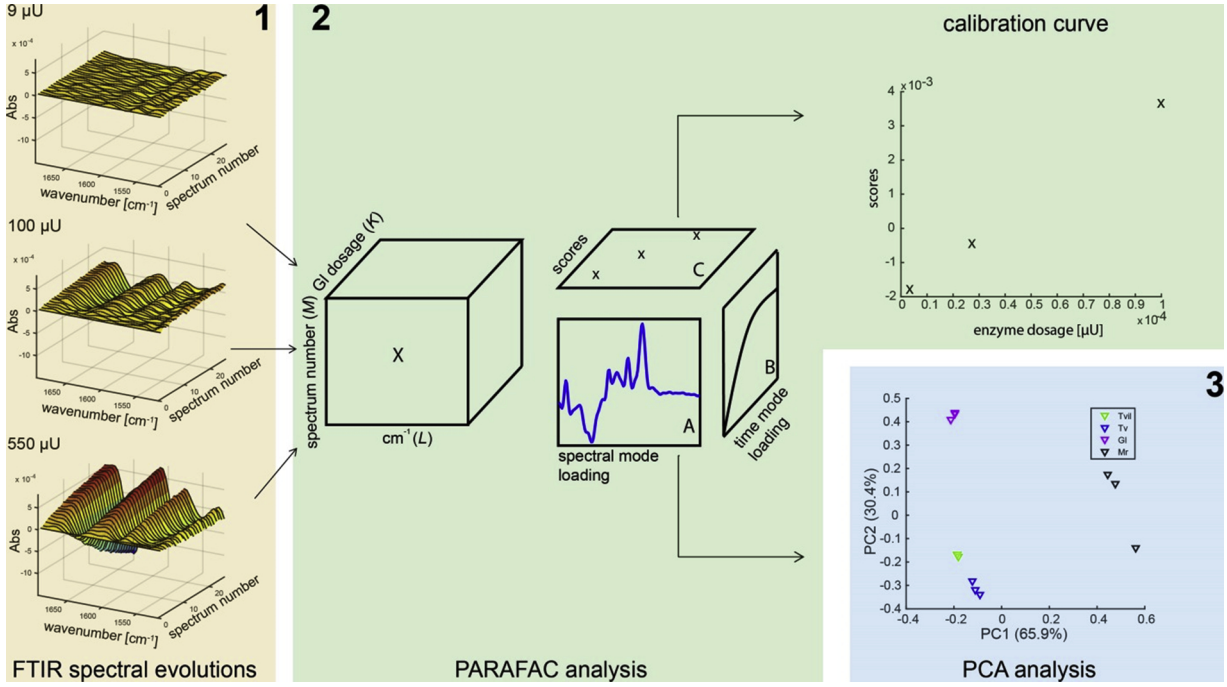

Fig. 1. Schematic representation of chemometric analysis performed in the work. A three step approach is shown: 1. Evolution profiles for three different Gl laccase dosages obtained by FTIR (orange background), 2. PARAFAC decomposition (green background) and 3. PCA analysis (blue background). Evolution profiles are stacked in order to form the tensor X. PARAFAC decomposition of tensor X into loadings and score matrices is illustrated in this example by using one component. The two loading matrices are A; spectral mode loading, B; time mode loadings and matrix C represents scores. PARAFAC scores (matrix C) are plotted vs the enzyme dosage to obtain calibration curves. PARAFAC spectral mode loadings (matrix A) from several PARAFAC models (each replicate analysis) are combined using PCA to perform spectral pattern recognition and hence enzyme similarity clustering (For interpretation of the references to colour in this figure legend, the reader is referred to the web version of this article).

since all organic molecules have intra- and intermolecular bonds that absorb in the mid-infrared frequency, each spectrum obtained by FTIR spectroscopy reflects the particular chemical (structural) composition of the compounds in the sample being analyzed. The absorption pattern of the chemical bonds having an electric dipole moment that changes during vibration will in turn produce a unique spectral fingerprint signature of the molecules present in the sample [9]. Hence, enzyme assays based on FTIR can take advantage of the premise that substrate (s) and product(s) have such distinguishable spectral fingerprints in the mid infrared region. When monitoring the time-course of an enzymatic reaction in real time online, spectral changes from substrate to product will occur during the reaction, resulting in the so called spectral evolution profiles [10–12]. These evolution profiles can be understood as being unique spectral landscapes, representing the chemical nature of a measured enzymatic reaction, i.e. a type of fingerprint of a given chemical reaction. The method has been used to measure, distinguish and quantify the activity of several different enzymes [10,12–14], including another oxidative enzyme such as glucose oxidase [10]. In all of these examples Parallel Factor Analysis (PARAFAC) and/or multiway Partial Least Squares regression (N-PLS) was used for data modelling and quantification. In the present work we hypothesized that FTIR was also a suitable multivariate technique for assessing laccase activity and that multivariate analysis might be a useful tool for clustering laccase activities based on their specific evolution profiles on phenolic substrates, i.e. their FTIR fingerprints. Hence, the objective of the present work was to asses if laccases from different origins had the same or differentiating reaction patterns and hence FTIR fingerprints on a set of naturally occurring phenols including lignin mono-phenols.

The qualitative and quantitative assessment was carried out for four different laccases, i.e. three white-rot fungal laccases from *Trametes versicolor* (Tv), *Trametes villosa* (Tvil), and *Ganoderma lucidum* (Gl), respectively, and one bacterial laccase from *Meiothermus ruber* (Mr). The Tv and Tvil laccases are high redox potential laccases (790 mV [15]), whilst the Gl laccase is a recently discovered laccase that works particularly well in relation to enhancing cellulase catalyzed degradation of lignocellulose [16]. The Mr laccase is a bacterial, thermostable low redox potential laccase that has been identified, recombinantly expressed, and biochemically characterized by our group [17].

2. Materials and methods

2.1. Materials

p-Coumaryl alcohol was purchased from Wuhan ChemFaces Biochemical Co., Ltd. (Wuhan, China). Sinapic acid, sinapic aldehyde, sinapyl alcohol, coniferyl alcohol and all the other chemicals used in the work were purchased from Sigma-Aldrich (Steinheim, Germany).

Laccase from *Trametes versicolor* (Tv) was purchased from Sigma-Aldrich (Steinheim, Germany), *Trametes villosa* (Tvil) laccase was a gift from Novozymes A/S, Bagsværd, Denmark, *Ganoderma lucidum* (Gl) laccase was produced in house using *Pichia pastoris* as heterogeneous expression system and *Meiothermus ruber* (Mr) laccase was produced in house using *Escherichia coli* as expression system. Both recombinant expression procedures are described below.

2.2. Recombinant expression

The construct containing the gene encoding for Gl laccase was equal to the one produced in our previous work [16] except for the deletion of a purification his-tag. Production of recombinant laccase in *P. pastoris* was performed in controlled fermentations at 5 L scale according to Silva et al. [18]. In order to improve the enzyme's stability the methanol fed-batch phase was done at 20 °C. The total time for the fermentation process was 112 h. The laccase-containing fermentation broth was recovered by centrifugation at 5300 x g, at 5 °C for 1 h, subjected to sterile filtration, and concentrated by ultrafiltration using a cross-flow

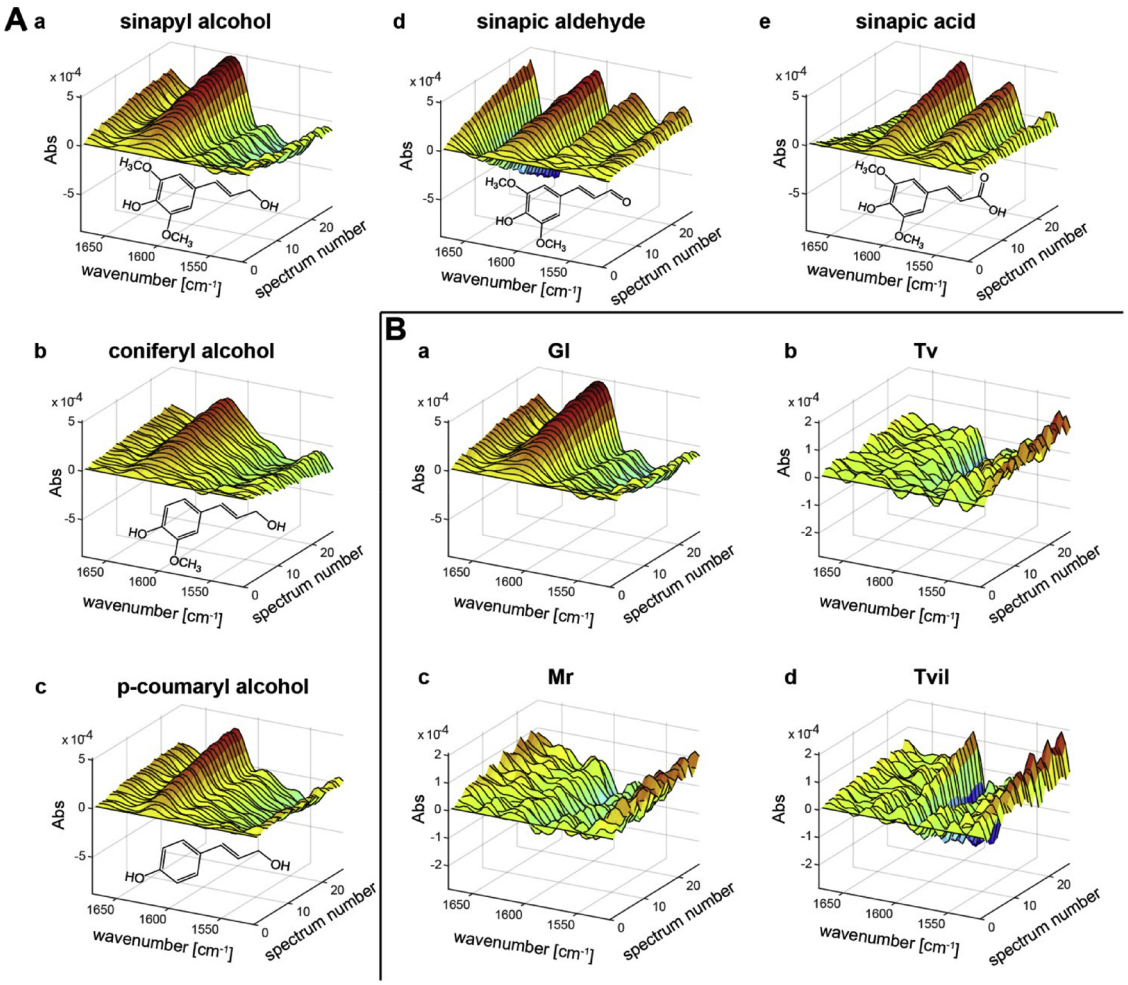

Fig. 2. Examples of FTIR evolution profiles of laccase oxidation of different substrates. Panel A shows the evolution profiles of oxidation of 9 mM of *p*-coumaryl alcohol (a), coniferyl alcohol (b), sinapyl alcohol (c), sinapic aldehyde (d) and sinapic acid (e) using 275 μU of *Ganoderma lucidum* (Gl) laccase. Panel B shows the Evolution Profiles of sinapyl alcohol oxidation of the four laccases *Ganoderma lucidum* (Gl) (a), *Trametes versicolor* (Tv) (b), *Meiothermus ruber* (Mr) (c) and *Trametes villosa* (Tvil) (d) and indicates clear differences in evolution spectra between enzymes. Please note that the intensity scale varies between plots in panel B.

bioreactor system with a 10 kDa cutoff membrane (Millipore, Sartorius, Denmark) as described previously [18]. Enzyme aliquots were stored at −80 °C with addition of 20% (w/v) glycerol.

The construct containing the gene encoding Mr laccase was produced according to Kalyani et al. [17]. The enzyme was expressed in the pGro7/BL21 (DE3) *E. coli* strain and produced in Luria-Bertani (LB) media containing ampicillin (100 μg mL^{-1}), chloramphenicol (34 μg mL^{-1}) and arabinose (0.7 mg mL^{-1}) and incubated at 30 °C with shaking (180 rpm). The cells were induced when they had reached an OD_{600} of 0.5-0.6 with 0.25 mM isopropyl-b-D-thiogalactoside (IPTG), supplemented with 0.2 mM $CuSO_4$. Incubation of the cells was performed at 25 °C in semi-microaerobic conditions (by turning off the shaker 4 h after induction) [17]. After 20 h of induction the cells were harvested by centrifugation (8000 x g, 15 min at 4 °C) and the pellet was suspended in 20 mM potassium phosphate buffer, pH 7.6, and sonicated on ice. Disrupted cells were removed by centrifugation (10,000 x g, 30 min, and 4 °C). The thermostable Mr laccase was partially purified using a heat fractionations step where the supernatant was incubated for 30 min at 65 °C, and the denatured contaminating proteins subsequently removed by centrifugation (10,000 x g, 15 min, 4 °C) [17]. The Gl laccase was used directly after concentration of the fermentation supernatant while Mr laccase was used directly after the heat fractionation step without further purification.

2.3. Laccase activity assay

Activity of laccase was assessed by monitoring the oxidation of syringaldazine (SGA) at 530 nm ($\varepsilon = 6.5 \times 10^4$ M^{-1} cm^{-1}). The assay reaction mixture contained 25 μM syringaldazine, 10% ethanol, 25 mM sodium acetate pH 5.0 and a proper amount of enzyme. Syringaldazine oxidation was monitored at 25 °C for 20 min. Enzyme activity was expressed in units: One International Unit (U) was defined as the amount of enzyme able to catalyze 1 μmol of substrate (syringaldazine) in one minute under the assay reaction conditions and this value is used to define the amount of active enzyme present in a specific enzyme preparation.

SGA activity was used in this work as a measure of enzyme dose to overcome the differences in enzyme purity. Therefore Tv, Tvil, Gl and Mr laccases were dosed according to SGA activity in the FTIR reactions by diluting them in 12.5 mM sodium acetate buffer in D_2O pH 5.

2.4. FTIR measurement

IR spectra were scanned in the range from 1000-2000 cm^{-1} using a FTIR instrument MilkoScan™ FT2 (FOSS ANALYTICAL, Hillerød, Denmark). Acquisition was carried out according to the method described in [19] with an optical resolution of 14 cm^{-1}. The sample was

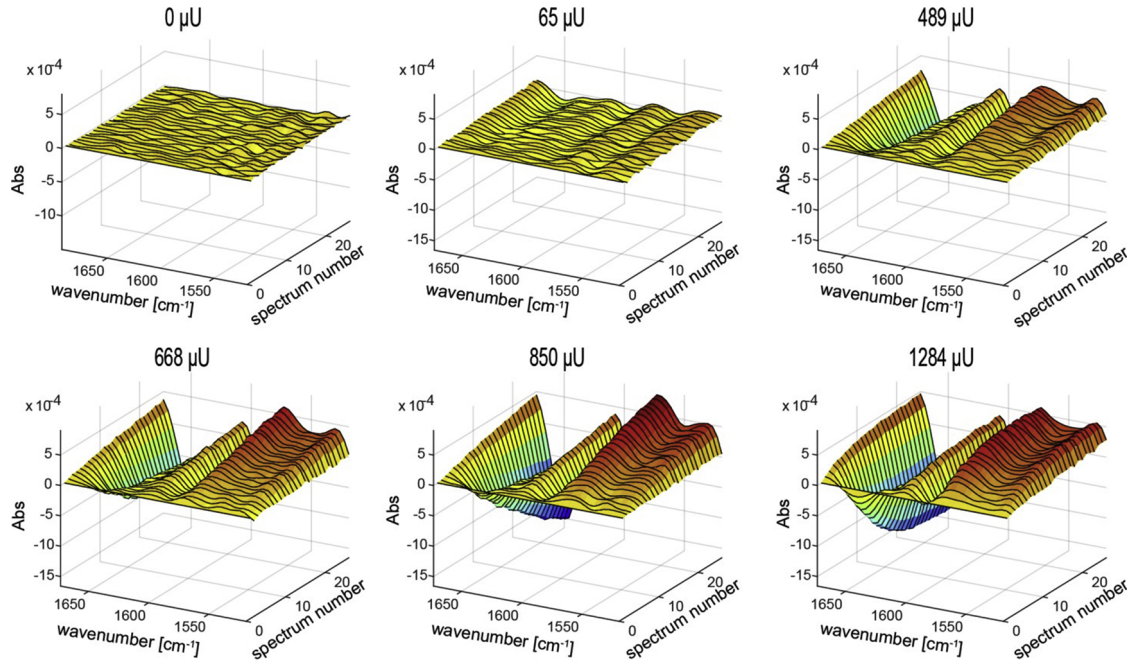

Fig. 3. Spectral evolution profiles for the *Trametes villosa* (Tvil) laccase oxidation of sinapic aldehyde using different enzyme dosages. Tvil dosages are expressed as syringaldazine units. The spectra illustrate how the intensities of wavenumbers affected by the enzyme reaction are changing according to changes enzyme dosages.

manually injected directly into the cuvette using a syringe. The cuvette was temperature controlled (42 °C) and had a path length of 50 µm. Each reaction mixture (1 mL) contained a fixed amount of substrate (9 mM) in 12.5 mM sodium acetate buffer pH 5 in deuterium oxide. The enzymes were deliberately of different degrees of purity and specific activity. Hence, depending on the enzyme either different dosage-ranges were measured: 65, 498, 668, 850 and 1284 µU for Tvil, 17, 33, 69, 136, 306 and 603 µU for Tv, 2.7, 9, 27, 100, 275 and 550 µU for Gl and 0.24, 0.47, 0.95, 1.36 and 2.7 µU for Mr (where needed the enzymes were diluted in 12.5 mM sodium acetate buffer, pH 5 in deuterium oxide). Deuterium oxide was used as solvent for both buffer and enzymes in order to remove obstructive water bands in the examined wavenumber range [14]. After adding the laccase each reaction mixture was injected directly into the cuvette and 50 spectra were acquired consecutively for a total of 15 min.

Three different control measurements were performed, consisting of (1) the evolution profile of the substrate without the enzyme, replacing the enzyme with 12.5 mM sodium acetate buffer, pH 5; (2) the evolution profile of the enzyme with the buffer instead of the substrate, and (3) the evolution profile of inactivated enzyme (incubated at 99° for 4 h prior to reaction) added to the substrates. These controls were necessary to ensure that the observed spectral evolution was due to enzymatic reaction and not due to other temporal effects, induced by e.g. protein denaturation or Fenton chemistry. Measurements of both reactions and controls were performed in triplicates.

2.5. Data handling and analysis

The acquired spectral data were exported using Foss Integrator (version 1.5.3, Foss Analytical, Hillerød, Denmark). All subsequent data analysis was carried out using MATLAB (The Mathworks Inc., MA, USA), the N-Way toolbox (Rasmus Bro & Claus Andersson, Copenhagen University, Denmark) and the Statistics and Machine learning toolbox (The Mathworks Inc., MA, USA). The analysis can be segmented into three sequential steps.

2.5.1. Evolution profiles

FTIR was used for the measurement of evolution profiles for all four laccases on all five substrates individually. In each case, several evolution profiles were measured over time using different laccase dosages leading to changes of the spectral evolution as a result of enzyme dosage. Hence, these dosage measurements were further used to establish quantitative assays for the laccase reactions. All evolution profiles were shown as difference spectra, where the entire spectral background, e.g., signals due to buffer, substrate and protein were subtracted so that only spectral changes were visualized.

2.5.2. PARAFAC analysis

Parallel Factor Analysis (PARAFAC) was employed to establish the calibration curves for all laccase reactions. PARAFAC is able to find common profiles and/or patterns present in all samples and performs a fitting where all those common profiles are taken into account simultaneously. PARAFAC is an unsupervised tensor decomposition method which aims at finding loadings and scores to represent data in a suitable subspace. Tensors are to be understood as a generalization of matrices to higher orders. A two-way tensor can be represented as a matrix, while a three-way tensor can be understood as a “data cube” (Fig. 1, tensor X). The individual axes of the tensor are called modes. PARAFAC decomposition is an iterative process which will yield a unique solution containing a certain number of components. The iteration is related to optimization of the right number of components [20] and in addition to good linearity (R^2), a core consistency diagnostics known as the CORCONDIA number is applied. The CORCONDIA number describes the maximum number of components necessary for the PARAFAC model to fully describe the dataset and should be as close to 100% as possible, yet not lower than 90% [21].

As exemplified in Baum et al. [10,12] a single evolution profile can be represented as a matrix with dimensions L x M, where L represents the number of measured wavenumbers and M the number of spectra. Because each enzyme dosage experiment was measured using similar consecutive time steps the individual matrices from each experiment

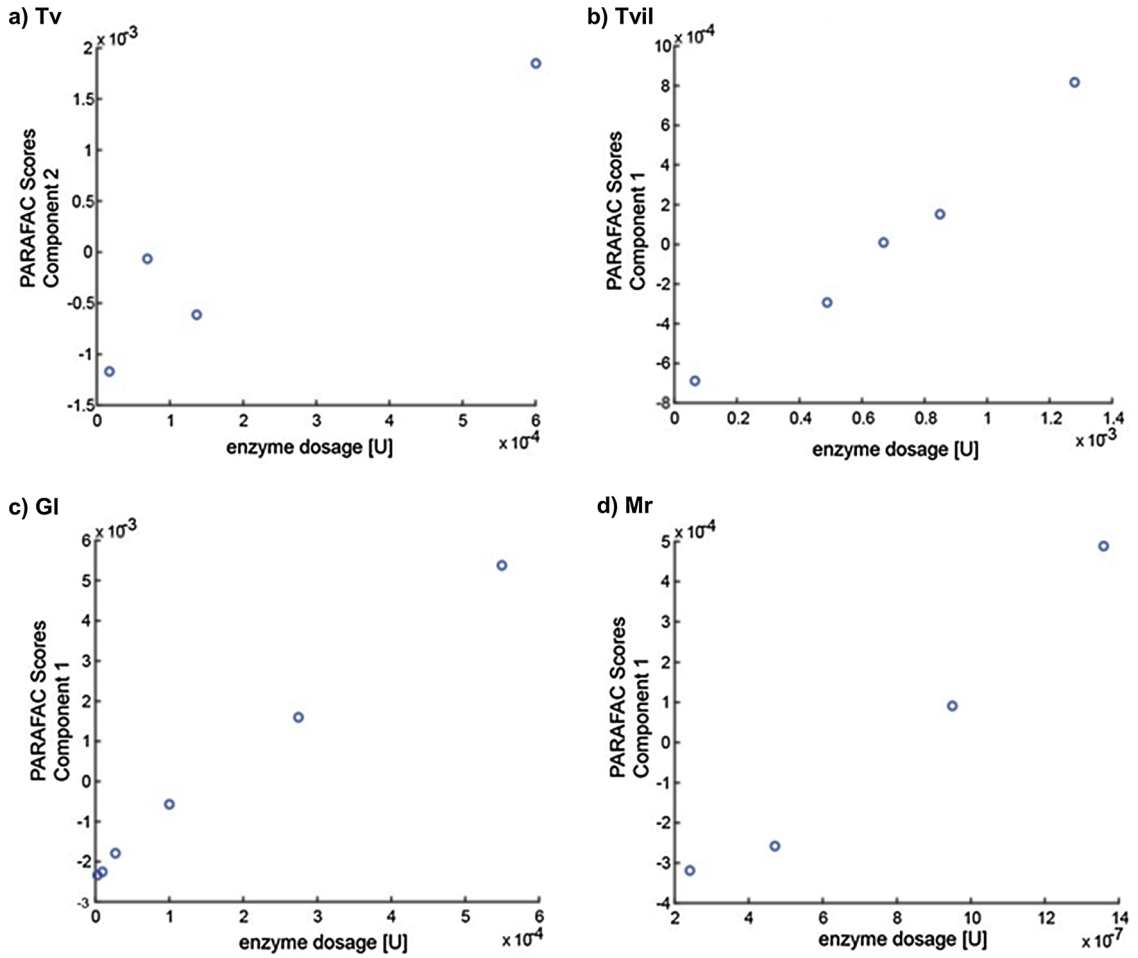

Fig. 4. Enzyme activity calibrations: Calibration data of PARAFAC scores versus enzyme dosage obtained for the different laccases on coniferyl alcohol: a) *Trametes versicolor* (Tv) laccase, b) *Trametes villosa* (Tvil) laccase, c) *Ganoderma lucidum* (Gl) laccase, d) *Meiothermus ruber* (Mr) laccase. Because of sign ambiguity in the component analysis, the slope may be positive or negative in the PARAFAC analysis. The sign of the calibration slope is not related to substrate or product character [10]. (The data on coniferyl alcohol were chosen to illustrate the calibration data. Graphs depicting PARAFAC scores versus enzyme dosage for the other substrates are shown in the Supplementary material Figures S23 - S26).

Table 1
R^2 values (means and standard deviations) of PARAFAC calibration curves. PARAFAC modelling was repeated three times for each reaction corresponding to three replicate measurements.

	Tvil	Tv	Gl	Mr
p-coumaryl alcohol	0.98 ± 0.019	0.93 ± 0.019	0.95 ± 0.026	0.98 ± 0.017
Coniferyl alcohol	0.99 ± 0.011	0.95 ± 0.046	0.99 ± 0.002	0.93 ± 0.066
Sinapyl alcohol	0.96 ± 0.052	0.95 ± 0.011	0.96 ± 0.026	0.83 ± 0.052
Sinapic aldehyde	0.95 ± 0.025	0.98 ± 0.002	0.95 ± 0.041	0.93 ± 0.010
Sinapic acid	0.96 ± 0.047	0.94 ± 0.012	0.95 ± 0.076	0.90 ± 0.096

can be stacked to form a three-way tensor of dimension *K* x *L* x *M* (Fig. 1, tensor X), where K is representing the number of enzyme dosages measured (equal to the number of evolution profiles). In order to remove unwanted offsets all evolution profiles were mean centered across all three modes prior to analysis.

For each enzyme-substrate couple three individual tensors were obtained (one for each replicate) and they were the starting point for PARAFAC analysis. The scores from each PARAFAC model were plotted against the known enzyme dosage to establish enzyme activity calibrations. As PARAFAC is an unsupervised decomposition - meaning that it has no knowledge of the used enzyme dosages - both, the linearity of the calibration curves and the CORCONDIA values were used to find the right number of components and to validate the models.

Fig. 1 schematically illustrates the PARAFAC decomposition of the tensor X into two loading matrices A and B and one score matrix C. Matrix A contains the fingerprints of the enzymatic system (spectral mode loadings, independent of enzyme dosage), matrix B contains the loadings describing the spectral number as a function of enzyme dosage and is hence time dependent (time mode loadings) and matrix C contains projections of the spectral changes in A in relation to enzyme dosage in B and represents the scores of PARAFAC. When the scores are plotted versus the enzyme dosage individual calibration curves are obtained (Fig. 1) and the linearity of the calibration curves is used to assess the fitting of the PARAFAC model. If there is a high degree of correlation it is possible to conclude that the spectral mode loadings (Fig. 1 matrix A) are representing the true enzymatic/oxidation pattern [10]. The calibration curve may also be used as a quantitative measure for enzymatic activity for a given laccase reaction [10].

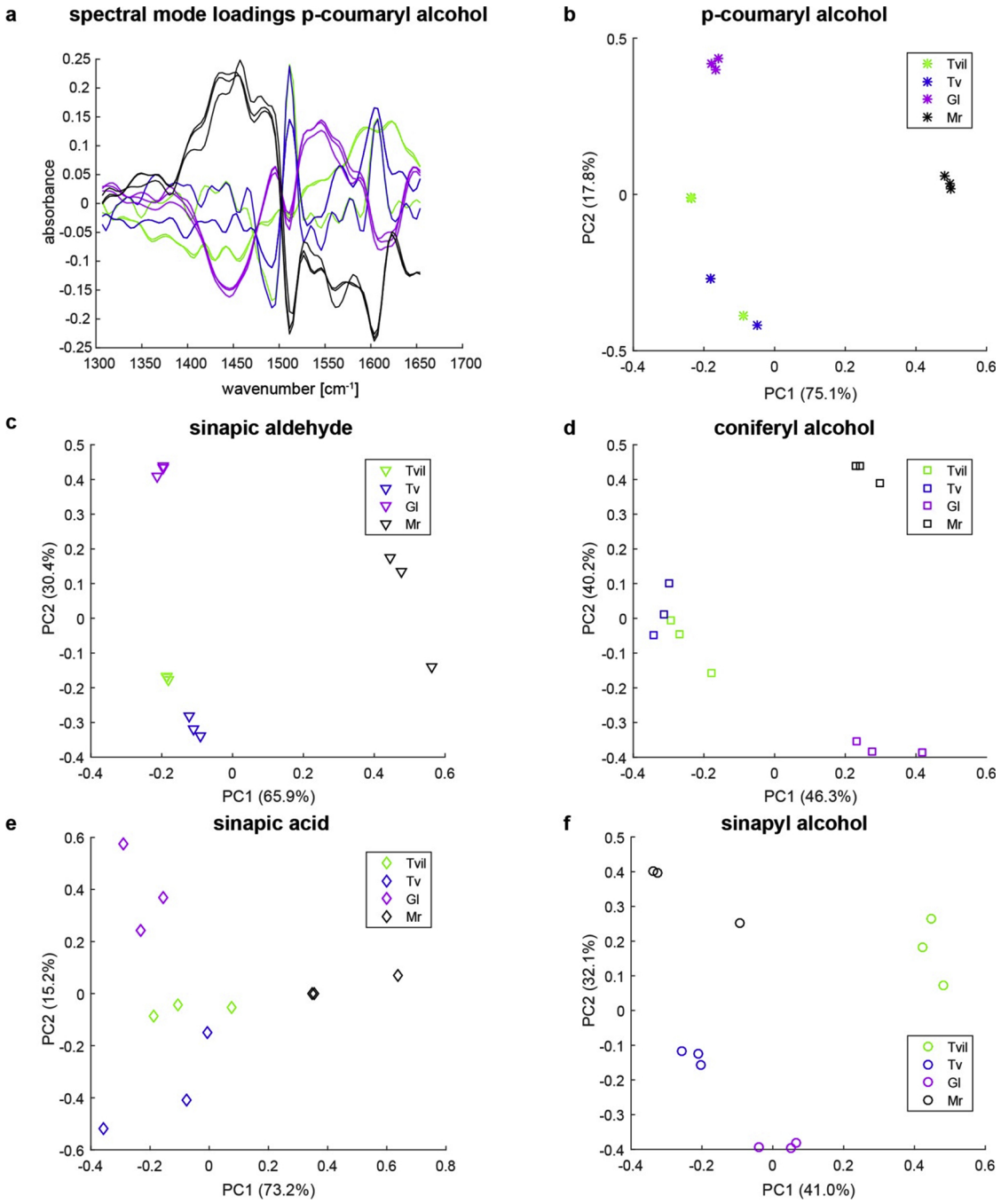

Fig. 5. Spectral mode loadings and PCA analysis of the PARAFAC loadings. Spectral mode loadings from PARAFAC analysis of *p*-coumaryl alcohol (a) are shown for each of the four laccases. For each substrate *p*-coumaryl alcohol (b), coniferyl alcohol (d), sinapyl alcohol (f), sinapic aldehyde (c) and sinapic acid (e) Principal Component 2 (PC2) was plotted vs Principal Component 1 (PC1) in order to show relatedness between enzymes. In each plot the percentage of variance explanation of the two PCs are reported in brackets. In all plots the Tvil laccase is shown in green, the Tv laccase is shown in blue, the Gl laccase is shown in magenta and the Mr laccase is shown in black (For interpretation of the references to colour in this figure legend, the reader is referred to the web version of this article).

2.5.3. PCA analysis

Principal Component Analysis (PCA) is a statistical analysis which simplifies multidimensional datasets into fewer dimensional representations emphasizing differences in the dataset [22]. Such projections are called Principal Components (PC). Usually a small number of PCs is necessary to explain the major variance in a dataset. Ideally, PCA strives towards minimizing the number of components necessary to describe the most differences in the dataset, hereby minimizing the complexity.

Spectral mode loadings from the PARAFAC modelling (Fig. 1 matrix B) were concatenated to form a matrix of dimension $P \times Q$, where P is the number of enzyme-substrate spectral profiles obtained from the PARAFAC models and Q is the number of wavenumbers. PCA analysis was performed on this matrix to represent the spectral patterns of the individual laccases in a two dimensional subspace (Fig. 1, PCA analysis). Two types of interpretations were performed with the PCA results, (1) differences and similarities between laccase reaction patterns, the closer the scores in the PCA plot were laying together, the higher the similarities; and (2) identification of the specific wavenumber ranges reflecting the differences in laccase oxidation.

Data pre-processing prior to PCA analysis was performed in order to remove spectral artifacts where the spectrum mean was subtracted from

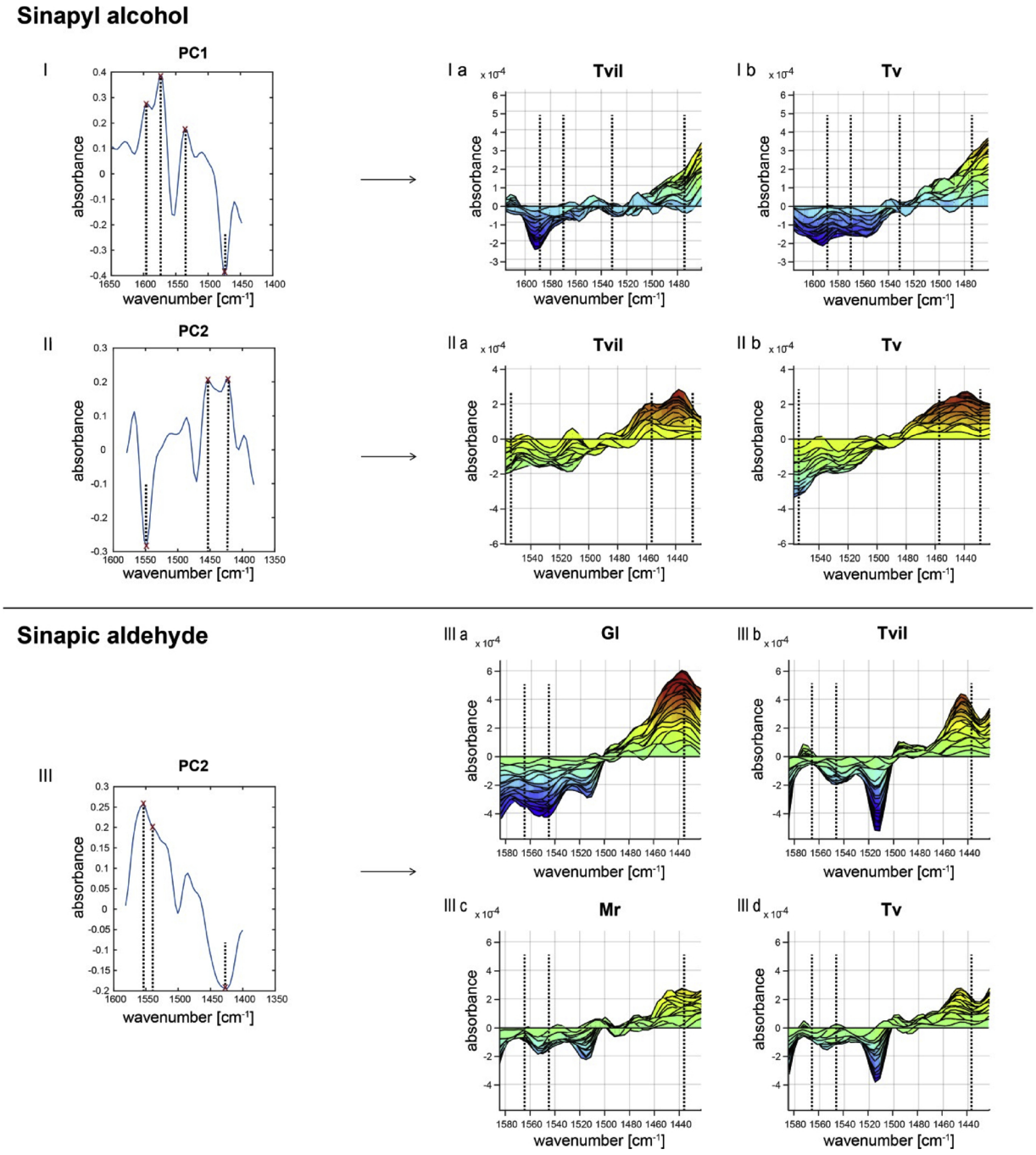

Fig. 6. Comparison of laccases using spectral mode loading projected on the PCs. Differences in reaction pattern of oxidation of sinapyl alcohol (I and II) and sinapic aldehyde (III) are shown. Spectral mode loadings from PARAFAC analysis projected along PC1 (I) and PC2 (II) for sinapyl alcohol and along PC2 for sinapic aldehyde (III) are shown and the wavenumber expressing high variance are highlighted with dashed lines. Zoomed evolution profiles for the different laccases are also shown: sinapyl alcohol spectral evolutions profiles for Tvil (Ia) and Tv (Ib) along PC1 are zoomed in the range 1460-1620 cm^{-1}, while sinapyl alcohol spectral evolutions profiles for Tvil (IIa) and Tv (IIb) along PC2 are zoomed in the range 1420-1560 cm^{-1}. Sinapic aldehyde spectral evolution profiles for Gl (IIIa), Tvil (IIIb) along PC2 are zoomed in the range 1420-1580 cm^{-1}. Wavenumber expressing high variance are marked in the evolution profiles by dashed lines.

each spectral mode loading and the entire data set was hereafter mean-centered.

3. Results and discussion

3.1. Evolution profiles and calibration curves

Four enzymes derived from four different microorganisms were studied. Three of the laccases originate from white rot fungi, i.e. *Trametes versicolor* (Tv), *Trametes villosa* (Tvil) and *Ganoderma lucidum* (Gl), the fourth laccase was of bacterial origin, *Meiothermus ruber* (Mr). Different enzymes were chosen to assess whether FTIR was capable of detecting differences in reaction mechanisms and/or product formation patterns between enzymes of different origin. If such discrimination is possible this would lead to the possible use of FTIR measurements in combination with multiway data analysis for assessing differences and similarities in reaction fingerprints of laccases in a broader sense.

Spectral evolution profiles were obtained for each laccase on the five different substrates (Fig. 2 panel A and Supplementary Figure S1-S3). Each spectrum is characterized by changes evolving over time

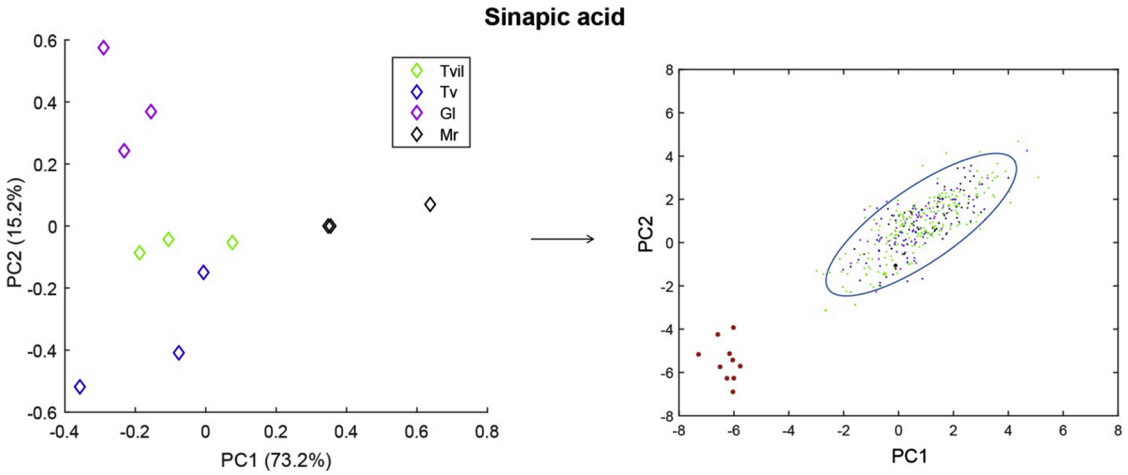

Fig. 7. Principle for data analysis in high throughput types of data comparison. The method enables assessment of differences in clones if they show a different behavior compared to the reference system. The plot on the right hand side is a simulation illustrating a prediction (it does not show genuine experimental data).

where specific wavenumbers are either decreasing or increasing in absorption intensity and hereby creating specific reaction patterns for every single substrate and laccase reaction (Fig. 2). All spectral changes are most likely related to bending and stretching of the unsaturated C—C bonds either aromatic or aliphatic [23]. Since the enzymes used were of different degree of purity, initial preprocessing of the spectra [10] was done to ensure that any signals related to differences in purity among the enzyme preparations were subtracted and hence not interfering with the data interpretation.

By studying the evolution profiles of Gl laccase oxidation of monolignols (Fig. 2 panel A a, b and c) it is possible to recognize differences in the profiles and this indicates that FTIR can indeed register differences in the enzyme catalyzed oxidation of various substrates. From the evolution profiles of the Gl laccase oxidation of sinapic aldehyde and sinapic acid (Fig. 2 panel A d and e) it appears that the enzyme reaction results in more complex profiles compared to those of the alcohols because more wavenumbers are affected by the reaction. Differences in the reaction pattern between the four different enzymes are exemplified by the oxidation of sinapyl alcohol in Fig. 2 panel B. The remaining evolution profiles for the other enzymes are shown in Supplementary Figure S1-S3.

Evolution profiles at different enzyme dosages exemplified for the case of Tvil laccase oxidation of sinapic aldehyde are shown in Fig. 3. It is clear that increased enzyme dosage leads to more intense spectral evolutions. Similar behavior is observed for the other substrates and enzyme reactions (Supplementary Figure S4 – S22). The data obtained in this study reflect laccase reactions on substrate concentrations of 9 mM, which was found to be an appropriate compromise between sensitivity of the technique and short run times (15 min). At substrate concentrations of 1 mM no apparent spectral changes were observed during the analysis time indicating the limit of detection of the technology. However, some of the sensitivity limitation observed in FTIR may be overcome by adjusting other process parameters like reaction time and enzyme loading.

PARAFAC analysis for each enzymatic system resulted in individual models for each replicate of enzyme/substrate reaction and resulted in enzyme activity calibration curves for each reaction replicate. Each calibration curve is a quantitative assay in itself because the PARAFAC scores are linearly dependent on the enzyme dosage (Fig. 4 and Supplementary Figures S23 - S26). This means that the PARAFAC decomposition of the FTIR measurements can be used to quantitatively assess laccase activity. The values of the PARAFAC scores are a summarized quantification of both substrate depletion and product formation peaks. Hence, the activity measured is not only accounting for the enzyme activity on one single wavenumber, i.e. product formation or substrate depletion, but it is considering the overall reaction in its complexity giving rise to a more specialized activity assay.

The CORCONDIA value, number of components for PARAFAC decomposition and R^2 for each calibration curve showed that the PARAFAC modelling of the FTIR data was valid (Supplementary Table S1). The differences in number of decomposing components could be a result of the exchange of H^+ proton with deuterium from D_2O. Analysis in the mid infrared region is greatly affected by H–O bonds and therefore D_2O was used to remove water bands [14]. Proton exchange could superimpose the actual reaction pattern and Baum et al. [11] showed how increasing the number of components in the PARAFAC analysis could resolve the superimposition of two different effects such as enzyme reaction and proton exchange and quantify each of them. In this case two components separated the two distinct patterns and the R^2 value (Table 1) showed high correlation between PARAFAC scores and enzyme dosage. Only in the case of Mr laccase oxidation of sinapyl alcohol a poor value of $R^2 = 0.83$ was found even though the CORCONDIA value was 100%. This lower correlation coefficient could be a result of lower signal to noise ratio compared to the other reactions.

3.2. Laccase mapping using PCA analysis

The PARAFAC models result in spectral mode loadings (Fig. 1 matrix A) that represent each laccase reaction on a given substrate. All spectral mode loadings (exemplified in Fig. 5 panel a and Supplementary Figure S27) are ideally representing the true enzymatic oxidation pattern of each laccase on each of the five substrates.

The laccase oxidation pattern of the phenolic compounds can be further investigated to determine if a specific chemical fingerprint is dependent on the enzyme's origin. Since the spectral mode loadings are dosage independent they can be used to compare the four laccases. Single PCA analyses for all five substrates and the five PCA scatter plots (Fig. 5 b–f) revealed the relatedness of the chemical fingerprints. In all cases, at least 70% variance in the data was explained by PC1 and PC2.

The overall conclusions from the PCA plots are that Gl and Mr laccases have reaction patterns which are always different from one another and which are also always different from the reaction patterns of the other two laccases (Tv and Tvil) on all the substrates (Fig. 5 b–f). Tv and Tvil laccases show a high degree of similarity for the reaction fingerprints on all substrates except sinapyl alcohol where the oxidation patterns reveal that the two enzymes are quite different from one to another (Fig. 5 panel c and Fig. 2 panel B). The PCA analysis can be used to measure the differences between the reaction patterns, but it is also capable of giving information about the specific wavenumber range in which these differences appear by interpreting the loadings

along each PC. A clear example of this is the identification of the major spectral differences between the two *Trametes* originating enzymes on the oxidation of sinapyl alcohol (Fig. 6). The ranges of wavenumbers in which the maximum differences between the two enzymes Tv and Tvil occur is where the loadings (Fig. 6 panel I and II) show the largest magnitudes; in the case of sinapyl alcohol PC1 1446-1615 cm^{-1} (Fig. 6 panel I). Zooming the spectral evolution profiles for the individual enzyme in that particular range of wavenumbers (Fig. 6 panel Ia and Ib) allows for the identification of the major differentiating reaction peaks. On PC1 for sinapyl alcohol examples of wavenumbers that differentiate the most are 1473, 1534, 1573 and 1592 cm^{-1}. Likewise for PC2 the major differences are found in 1426, 1453 and 1550 cm^{-1} (Fig. 6 panel IIa and IIb). Sinapic aldehyde represents an example where the three fungal laccase are very similar along PC1 (Fig. 5 panel c) and where the bacterial laccase, Mr behaves differently from the others. At the same time differences between fungal laccase are explained by PC2 where the two *Trametes* originating enzymes are closely related while the *Ganoderma* laccase is significantly different (Fig. 6 panel III). Examples of wavenumber differences are evident at 1434, 1546 and 1565 cm^{-1}. The method does not allow for the direct coupling between wavenumber and specific chemical interpretations but it could be used as a pattern recognition method for instance in protein engineering screening.

Laccases are driving the oxidation of phenolic compounds by reducing molecular oxygen to water. The reaction is producing free radicals which are then reacting further via non-enzymatic couplings. The redox potential of the laccases affects the active site and electron transfer inside the enzymes. This, in turn, influences the activity towards phenolic substrates [24–26]. The three fungal laccase are characterized by having higher redox potentials than bacterial laccases, including the bacterial Mr laccase tested here, and the structures of fungal and bacterial laccases also differ [15,27]. Although neither the redox potential or the structure of the Mr laccase are known these presumed differences among the fungal and bacterial enzyme might partly explain why the Mr laccase always behave differently than the fungal laccases. The differences found in the reaction pattern of the fungal laccases might be due to differences in the enzymatic structures leading to differences in reaction kinetics and in the speed by which the electrons are abstracted from the substrate and transported inside the enzyme. Such differences might in turn result in different evolution profiles between enzymes, because the rate of oxidation may affect the rate and type of product formation.

PCA analysis of laccase oxidation of sinapic acid (Fig. 5 panel e) does not show large differences between the reaction patterns of the different laccases, i.e. reaction evolutions are the same for the different laccases despite their origin. Previous studies [4] have shown that Gl and Tv laccase oxidation of sinapic acid resulted in a much simplified product profile compared to product profiles from oxidation of ferulic and *p*-coumaric acid. The simpler product profile of sinapic acid is most likely a result of limited number of coupling reactions caused by sterical hindrance because of extensive methoxylation on the aromatic ring. Therefore, sinapic acid is a suitable, reliable, generic substrate for assaying laccase activity on FTIR.

An enzyme activity assay is a fundamental requirement for studying enzyme action, specificity, kinetics, and a prerequisite for identifying the activity of a specific enzyme. The FTIR PARAFAC assay methodology reported here uniquely allows a direct spectral fingerprint comparison of different reaction patterns of different laccases on phenolic substrates. Hence, the perspectives for FTIR-based measurements in combination with PARAFAC modelling is that it is possible to set up a reference system on various lignin related substrates for comparison of unknown laccases, as visualized in Fig. 7. The dataset in Fig. 7 is a fictive set which only serves the purpose of illustrating the potential of applying this type of screening method on a large set of data. In contrast to traditional methods used for laccase activity determination, the PARAFAC model used here thus has the ability to assist in studying laccase oxidation in all its complexity taking into account both substrate depletion and product formation at the same time and hereby obtaining a unique picture of laccase driven reactions. This offers the advantage of identifying unknown odd-behaving laccases without prior knowledge to reaction mechanisms in one type of analysis hence offering a unique tool for fast screening of large numbers of samples e.g. engineered clones or various origins as illustrated in Fig. 7. Once the FTIR based screening has identified laccase candidates that behave differently these can be further analysed using conventional methods such as NMR and HPLC-MS to clarify the chemical origin of these differences.

4. Conclusions

Laccase oxidation of monolignols, sinapic acid and sinapic aldehyde was monitored using FTIR and this resulted in reaction specific spectral evolution profiles which accounted for both substrate depletion and product formation simultaneously. Since the obtained spectral landscapes were specific for each laccase/substrate combination they could be used to distinguish the 12 different laccase/substrate reaction patterns in a multivariate sense. The fingerprinting technique was combined with PARAFAC analysis establishing a quantitative assay for each laccase/substrate reaction, which, in turn, helped to validate the modelling approach. A valid linear calibration curve verified that it was possible to interpret the spectral evolution as a fingerprinting technique. Furthermore, the spectral mode loadings obtained from the PARAFAC models formed the basis for establishing laccase clustering maps useful for comparison of reaction patterns. We used the data to generate a reference system consisting of cluster maps for all five substrates using PCA analysis. These cluster maps identified similarities and differences in a straight forward manner of the four laccases on each individual substrate and showed that it was possible to distinguish the four different laccases by their microbial origin. Moreover, projection of the principal components revealed specific wavenumbers at which the various enzyme reactions result in differentiated spectral evolutions. By deliberately including both highly purified, high activity laccases (such as the Tvil) and unpurified, low activity preparations, the work verified that the FTIR methodology is useful across a broad range of specific activities. FTIR thus represents a method with high potential for establishing a rapid and versatile enzyme assessment method when comparing large populations of laccases for instance during protein engineering.

Acknowledgements

This study was supported by The Danish Council for Independent Research (Project ref. DFF-4184-00355) and by the PhD Program at The Technical University of Denmark. We wish to thank FOSS ANALYTICAL, Denmark for providing us access to use the FTIR instrument MilkoScan™ FT2. We also appreciate the gift of the *Trametes villosa* laccase from Novozymes A/S, Bagsværd, Denmark.

Appendix A. Supplementary data

Supplementary data associated with this article can be found, in the online version, at https://doi.org/10.1016/j.enzmictec.2018.12.009.

References

[1] A.P. Virk, P. Sharma, N. Capalash, Use of laccase in pulp and paper industry, Biotechnol. Prog. 28 (2012) 21–32, https://doi.org/10.1002/btpr.727.
[2] L. Munk, A.K. Sitarz, D.C. Kalyani, J.D. Mikkelsen, A.S. Meyer, Can laccases catalyze bond cleavage in lignin? Biotechnol. Adv. 33 (2015) 13–24, https://doi.org/10.1016/j.biotechadv.2014.12.008.
[3] I. Pardo, X. Chanagá, A.I. Vicente, M. Alcalde, S. Camarero, New colorimetric screening assays for the directed evolution of fungal laccases to improve the conversion of plant biomass, BMC Biotechnol. 13 (2013) 90, https://doi.org/10.1186/1472-6750-13-90.
[4] V. Perna, J.W. Agger, J. Holck, A.S. Meyer, Multiple reaction monitoring for

quantitative laccase kinetics by LC-MS, Sci. Rep. 8 (2018), https://doi.org/10.1038/s41598-018-26523-0.
[5] I. Pardo, G. Santiago, P. Gentili, F. Lucas, E. Monza, F.J. Medrano, C. Galli, A.T. Martínez, V. Guallar, S. Camarero, Re-designing the substrate binding pocket of laccase for enhanced oxidation of sinapic acid, Catal. Sci. Technol. 6 (2016) 3900–3910, https://doi.org/10.1039/C5CY01725D.
[6] R.A.A. El Monssef, E.A. Hassan, E.M. Ramadan, Production of laccase enzyme for their potential application to decolorize fungal pigments on aging paper and parchment, Annals Agric. Sci. 61 (2016) 145–154, https://doi.org/10.1016/j.aoas.2015.11.007.
[7] S. Afreen, T.N. Shamsi, M.A. Baig, N. Ahmad, S. Fatima, M.I. Qureshi, M.I. Hassan, T. Fatma, A novel multicopper oxidase (laccase) from cyanobacteria: Purification, characterization with potential in the decolorization of anthraquinonic dye, PLoS One 12 (2017) e0175144, , https://doi.org/10.1371/journal pone.0175144.
[8] J. Juárez-Hernández, M.E. Zavala-Soto, M. Bibbins-Martínez, R. Delgado-Macuil, G. Díaz-Godinez, M. Rojas-López, FTIR spectroscopy applied in remazol blue dye oxidation by laccases, AIP Conf. Proc. 992 (2008) 1253–1261 doi: 0.1063/1.2926829.
[9] F.L. Martin, Shining a new light into molecular workings, Nat. Methods 8 (2011) 385–387, https://doi.org/10.1038/nmeth.1594.
[10] A. Baum, A.S. Meyer, J.L. Garcia, M. Egebo, P.W. Hansen, J.D. Mikkelsen, Enzyme activity measurement via spectral evolution profiling and PARAFAC, Anal. Chim. Acta 778 (2013) 1–8, https://doi.org/10.1016/j.aca.2013.03.029.
[11] A. Baum, P.W. Hansen, A.S. Meyer, J.D. Mikkelsen, Simultaneous measurement of two enzyme activities using infrared spectroscopy: a comparative evaluation of PARAFAC, TUCKER and N-PLS modeling, Anal. Chim. Acta 790 (2013) 14–23, https://doi.org/10.1016/J.ACA.2013.06.039.
[12] A. Baum, P.W. Hansen, L. Nørgaard, J. Sørensen, J.D. Mikkelsen, Rapid quantification of casein in skim milk using Fourier transform infrared spectroscopy, enzymatic perturbation, and multiway partial least squares regression: Monitoring chymosin at work, J. Dairy Sci. 99 (2016) 6071–6079, https://doi.org/10.3168/jds.2016-10947.
[13] R. Pacheco, A. Karmali, M.L.M. Serralheiro, P.I. Haris, Application of Fourier transform infrared spectroscopy for monitoring hydrolysis and synthesis reactions catalyzed by a recombinant amidase, Anal. Biochem. 346 (2005) 49–58, https://doi.org/10.1016/J.AB.2005.07.027.
[14] K. Karmali, A. Karmali, A. Teixeira, M.J.M. Curto, Assay for glucose oxidase from *Aspergillus niger* and *Penicillium amagasakiense* by Fourier transform infrared spectroscopy, Anal. Biochem. 333 (2004) 320–327, https://doi.org/10.1016/J.AB.2004.06.025.
[15] M. Alcalde, Laccases: Biological Functions, Molecular Structure and Industrial Applications, Ind. Enzym., Springer Netherlands, Dordrecht, 2007, pp. 461–476, https://doi.org/10.1007/1-4020-5377-0_26.
[16] A.K. Sitarz, J.D. Mikkelsen, P. Højrup, A.S. Meyer, Identification of a laccase from *Ganoderma lucidum* CBS-229.93 having potential for enhancing cellulase catalyzed lignocellulose degradation. Enzyme Microb. Technol. 53, 378-385. DOI:https://doi.org/10.1016/j.enzmictec.2013.08.003.
[17] D.C. Kalyani, L. Munk, J.D. Mikkelsen, A.S. Meyer, Molecular and biochemical characterization of a new thermostable bacterial laccase from *Meiothermus ruber* DSM 1279, RSC Adv. 6 (2016) 3910–3918, https://doi.org/10.1039/C5RA24374B.
[18] I.R. Silva, D.M. Larsen, A.S. Meyer, J.D. Mikkelsen, Identification, expression, and characterization of a novel bacterial RGI Lyase enzyme for the production of biofunctional fibers, Enzyme Microb. Technol. 49 (2011) 160–166, https://doi.org/10.1016/J.ENZMICTEC.2011.04.015.
[19] S.K. Andersen, P.W. Hansen, H.V. Andersen, S.K. Andersen, P.W. Hansen, H.V. Andersen, Vibrational spectroscopy in the analysis of dairy products and wine, in: P.R. Griffiths (Ed.), Handb. Vib. Spectrosc. John Wiley & Sons, Ltd, Chichester, UK, 2006, , https://doi.org/10.1002/0470027320.s6602.
[20] R.A. Harshman, M.E. Lundy, PARAFAC: parallel factor analysis, Comput. Stat. Data Anal. 18 (1994) 39–72, https://doi.org/10.1016/0167-9473(94)90132-5.
[21] R. Bro, H.A.L. Kiers, A new efficient method for determining the number of components in PARAFAC models, J. Chemom. 17 (2003) 274–286, https://doi.org/10.1002/cem.801.
[22] N. Altman, M. Krzywinski, Points of significance: clustering, Nat. Methods 14 (2017) 545–546, https://doi.org/10.1038/nmeth.4299.
[23] N. Glagovich, IR Absorptions for Representative Functional Groups, Cent. Connect. State Univ, 2007, http://www.chemistry.ccsu.edu/glagovich/teaching/3.http://www.chemistry.ccsu.edu/glagovich/teaching/316/ir/table.html.
[24] F. Xu, Effects of redox potential and hydroxide inhibition on the pH activity profile of fungal laccases, J. Biol. Chem. 272 (1997) 924–928, https://doi.org/10.1074/JBC.272.2.924.
[25] M.A. Tadesse, A. D'Annibale, C. Galli, P. Gentili, F. Sergi, An assessment of the relative contributions of redox and steric issues to laccase specificity towards putative substrates, Org. Biomol. Chem. 6 (2008) 868, https://doi.org/10.1039/b716002j.
[26] I. Pardo, S. Camarero, Laccase engineering by rational and evolutionary design, Cell. Mol. Life Sci. 72 (2015) 897–910, https://doi.org/10.1007/s00018-014-1824-8.
[27] A.K. Sitarz, J.D. Mikkelsen, A.S. Meyer, Structure, functionality and tuning up of laccases for lignocellulose and other industrial applications, Crit. Rev. Biotechnol. 36 (2016) 70–86, https://doi.org/10.3109/07388551.2014.949617.

Supplementary information

Laccase activity measurement by FTIR spectral fingerprinting

Valentina Perna[a], Andreas Baum[b], Heidi A. Ernst[c], Jane W. Agger[a], Anne S. Meyer[a]

[a] Protein Chemistry and Enzyme Technology, Department of Biotechnology and Biomedicine, Technical University of Denmark, Kgs. Lyngby 2800, Denmark

[b] Section for Statistics and Data Analysis, Department of Applied Mathematics and Computer Science, Technical University of Denmark, Kgs. Lyngby 2800, Denmark

[c] Department of Chemistry, University of Copenhagen, 2100 Copenhagen Ø, Denmark

e-mails addresses:

valper@dtu.dk

andba@dtu.dk

hae@chem.ku.dk

jaag@dtu.dk

asme@dtu.dk

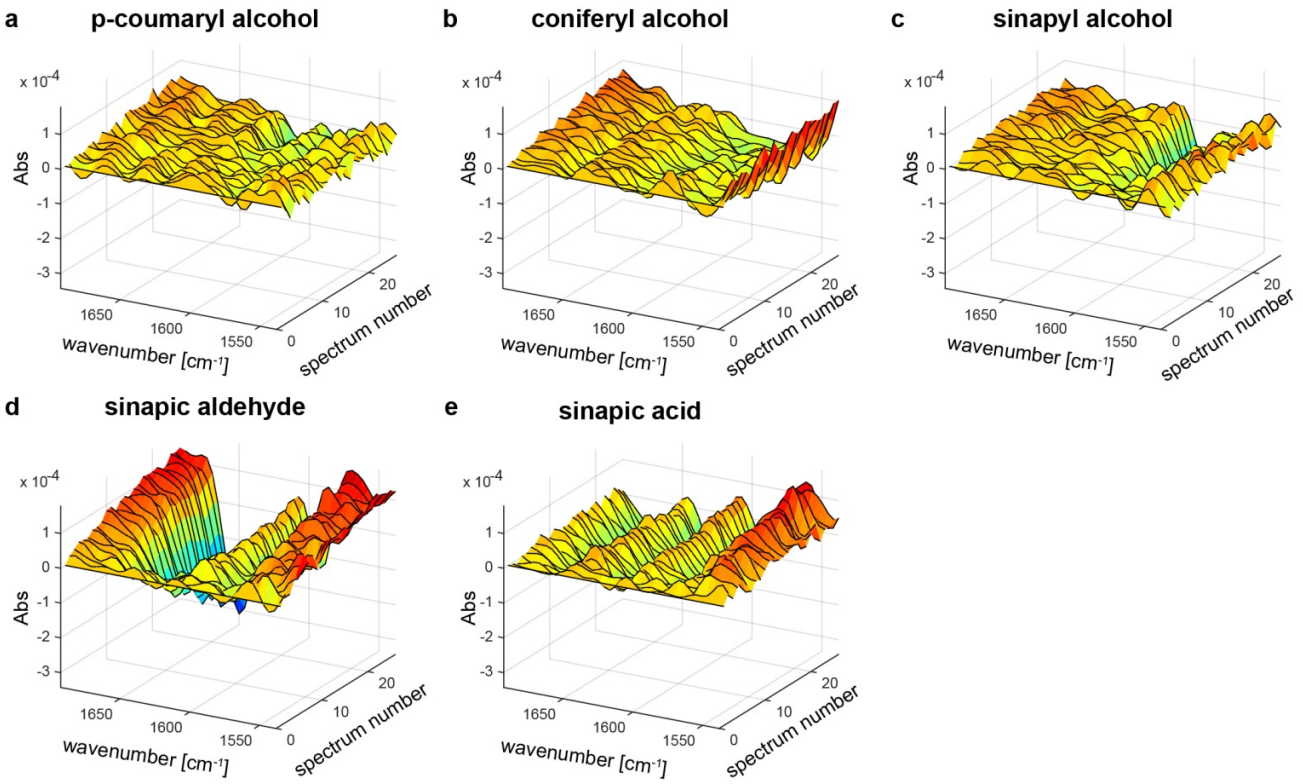

Figure S1. Evolution profiles for laccase oxidation of different substrates. Evolution Profiles are showing the oxidation of 9 mM of *p*-coumaryl alcohol (a), coniferyl alcohol (b), sinapyl alcohol (c), sinapic aldehyde (d) and sinapic acid (e) using 603 µU of *Trametes versicolor* (Tv) laccase.

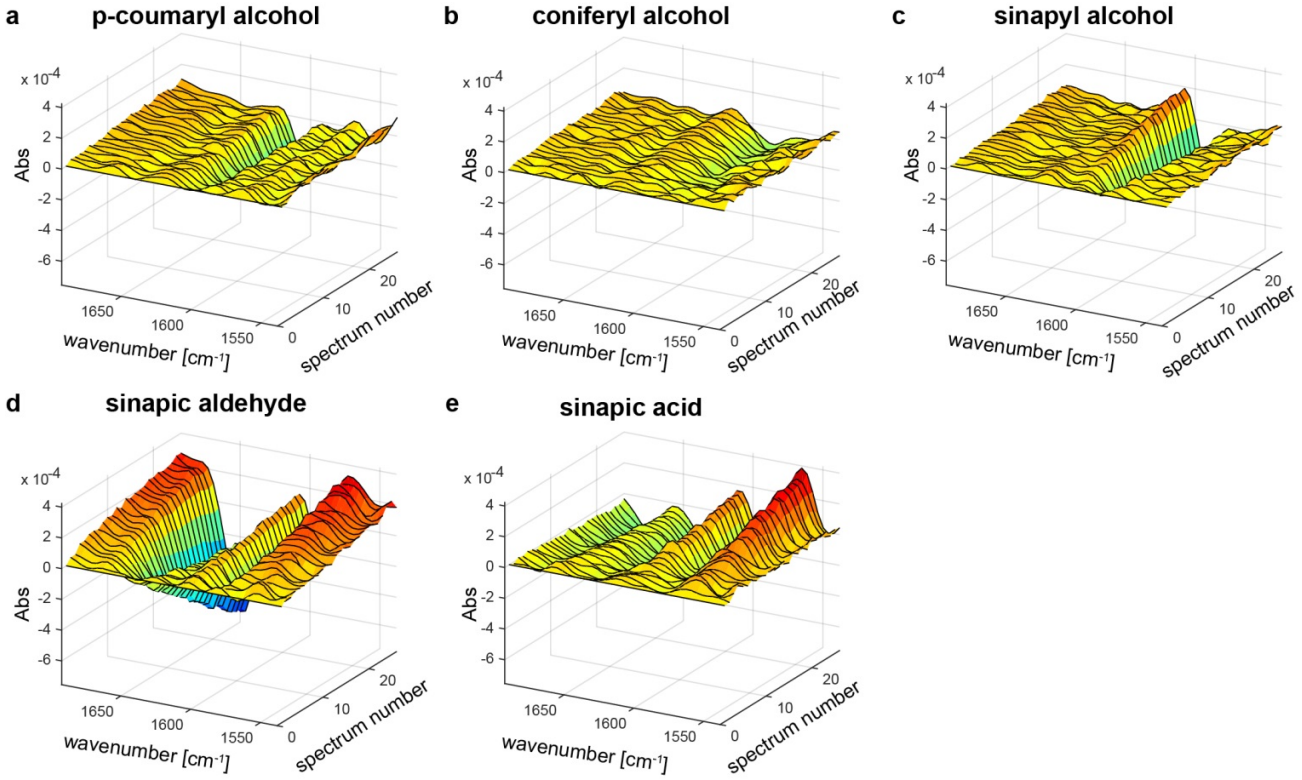

Figure S2. Evolution profiles for laccase oxidation of different substrates. Evolution Profiles are showing the oxidation of 9 mM of *p*-coumaryl alcohol (a), coniferyl alcohol (b), sinapyl alcohol (c), sinapic aldehyde (d) and sinapic acid (e) using 850 µU of *Trametes villosa* (Tvil) laccase.

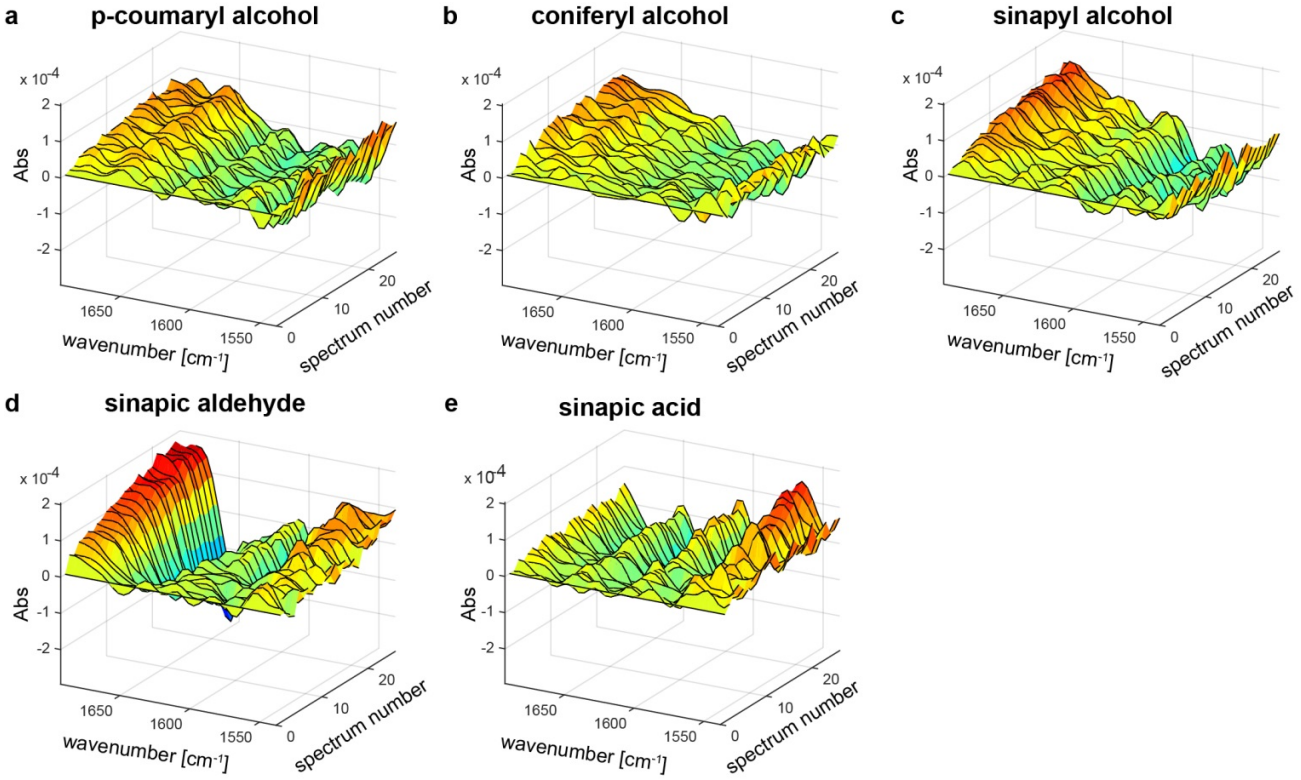

Figure S3. Evolution profiles for laccase oxidation of different substrates. Evolution Profiles are showing the oxidation of 9 mM of *p*-coumaryl alcohol (a), coniferyl alcohol (b), sinapyl alcohol (c), sinapic aldehyde (d) and sinapic acid (e) using 2.7 µU of *Meiothermus ruber* (Mr) laccase.

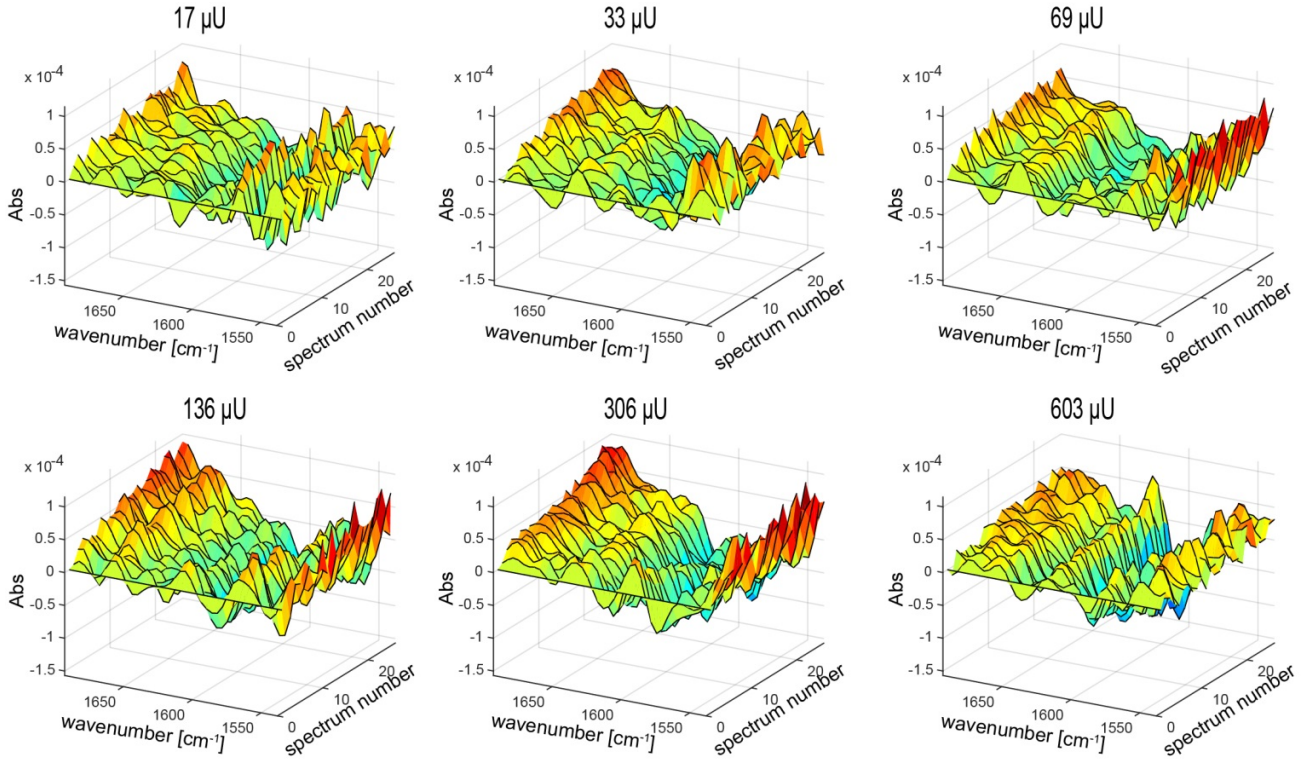

Figure S4. Spectral Evolution Profiles for the *Trametes versicolor* (Tv) laccase oxidation of *p*-coumaryl alcohol using different enzyme dosages. Tv dosages are expressed as syringaldazine units.

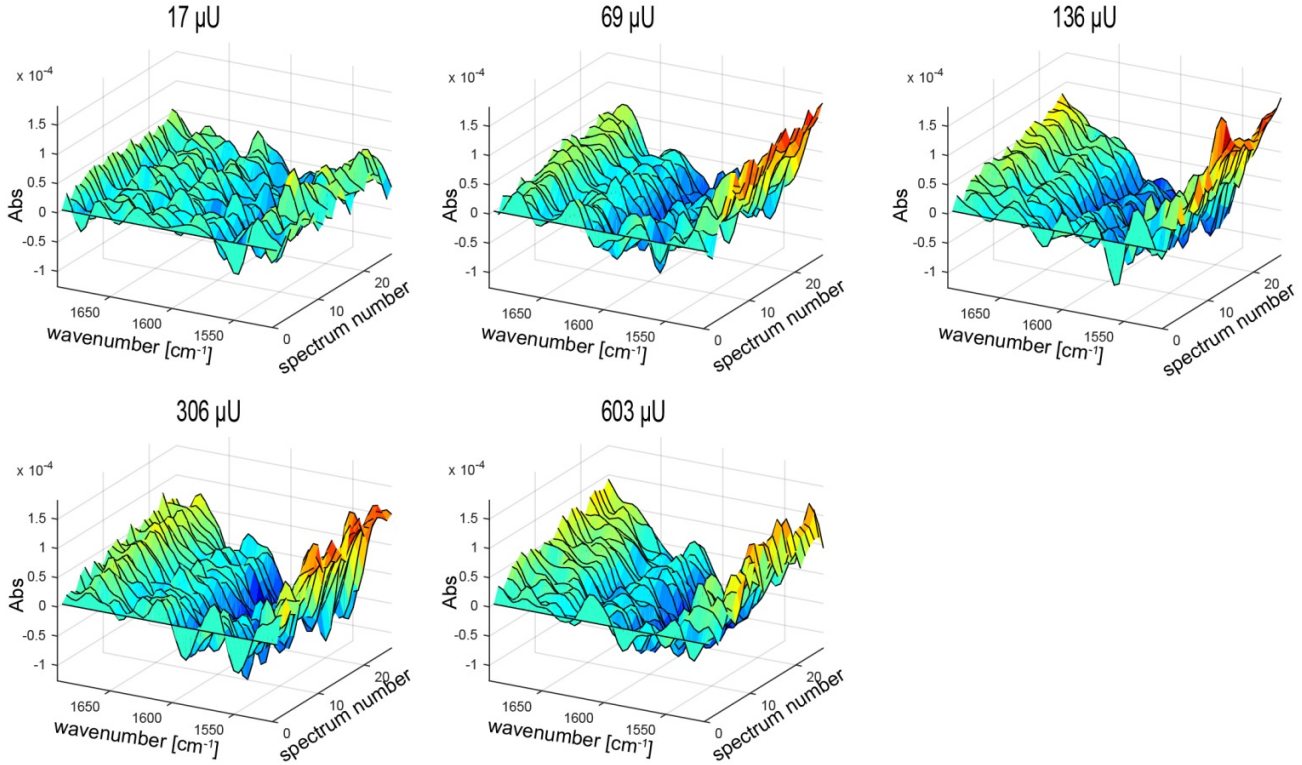

Figure S5. Spectral Evolution Profiles for the *Trametes versicolor* (Tv) laccase oxidation of coniferyl alcohol using different enzyme dosages. Tv dosages are expressed as syringaldazine units.

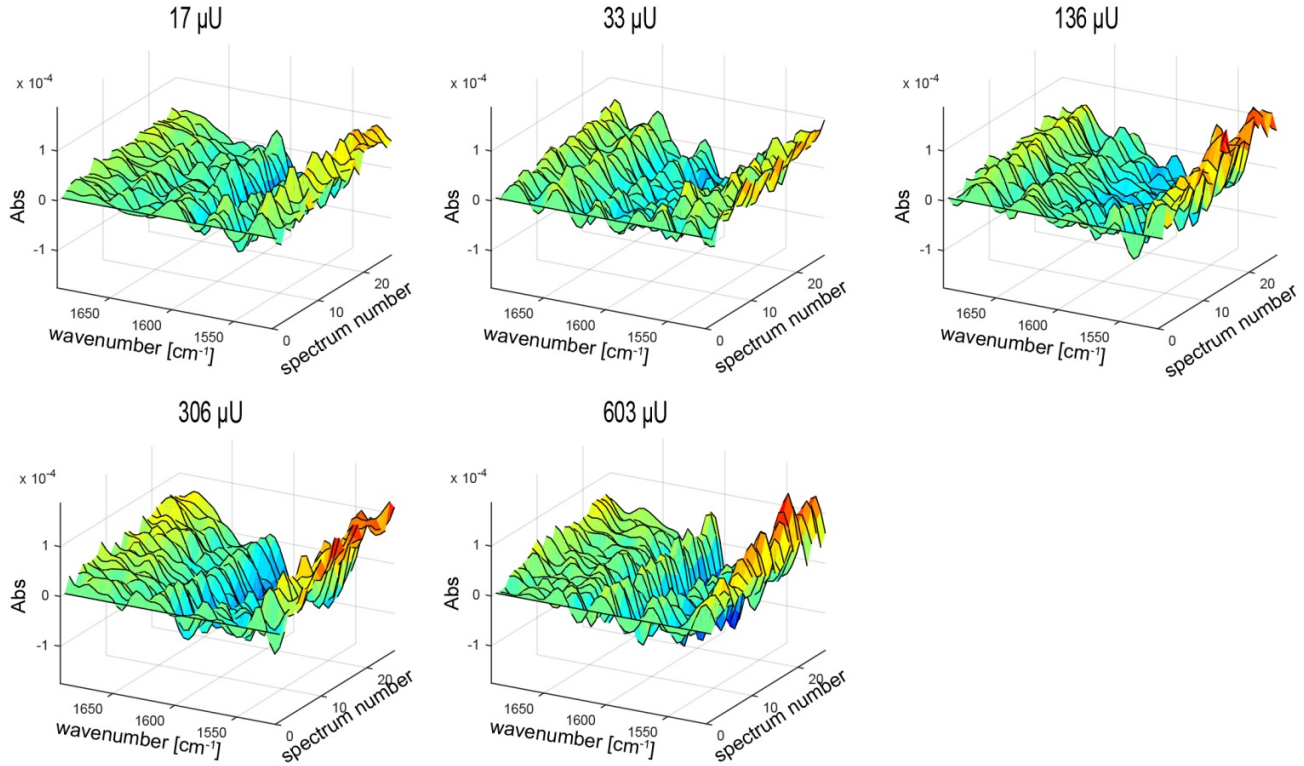

Figure S6. Spectral Evolution Profiles for the *Trametes versicolor* (Tv) laccase oxidation of sinapyl alcohol using different enzyme dosages. Tv dosages are expressed as syringaldazine units.

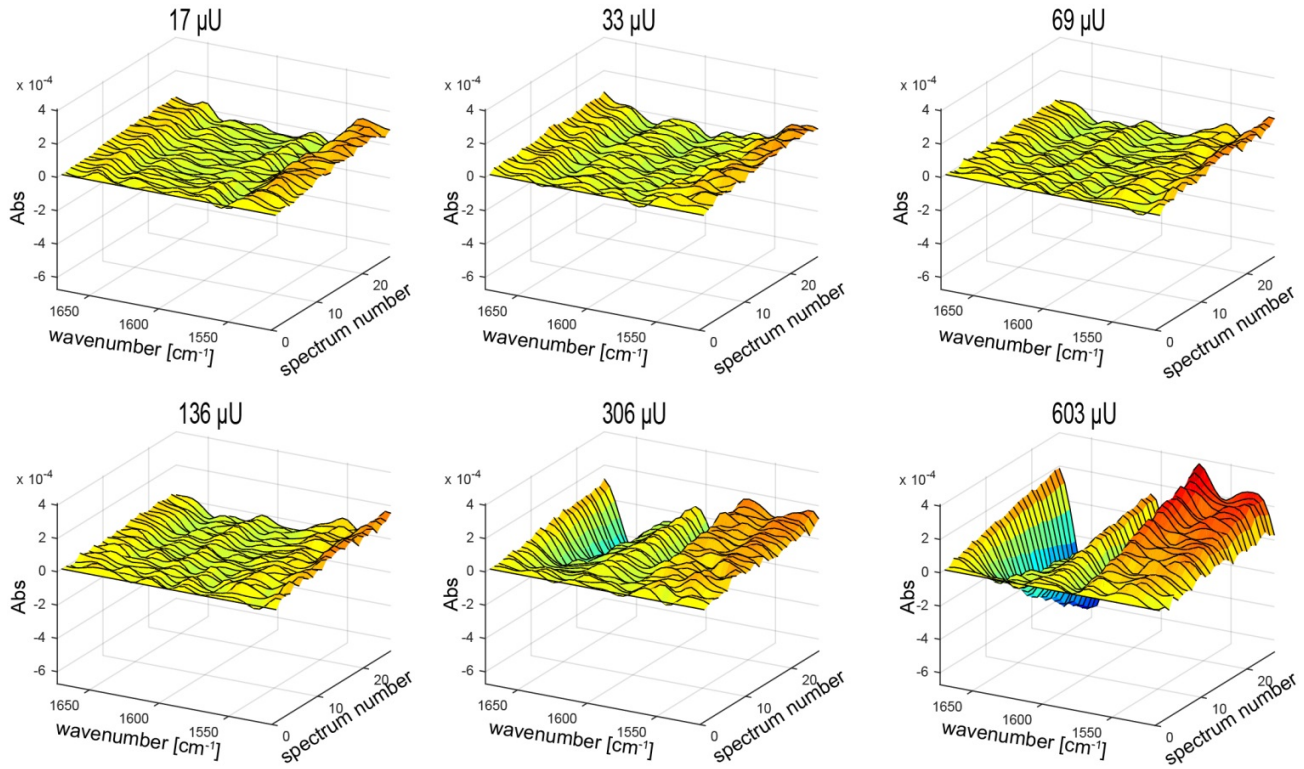

Figure S7. Spectral Evolution Profiles for the *Trametes versicolor* (Tv) laccase oxidation of sinapic aldehyde using different enzyme dosages. Tv dosages are expressed as syringaldazine units.

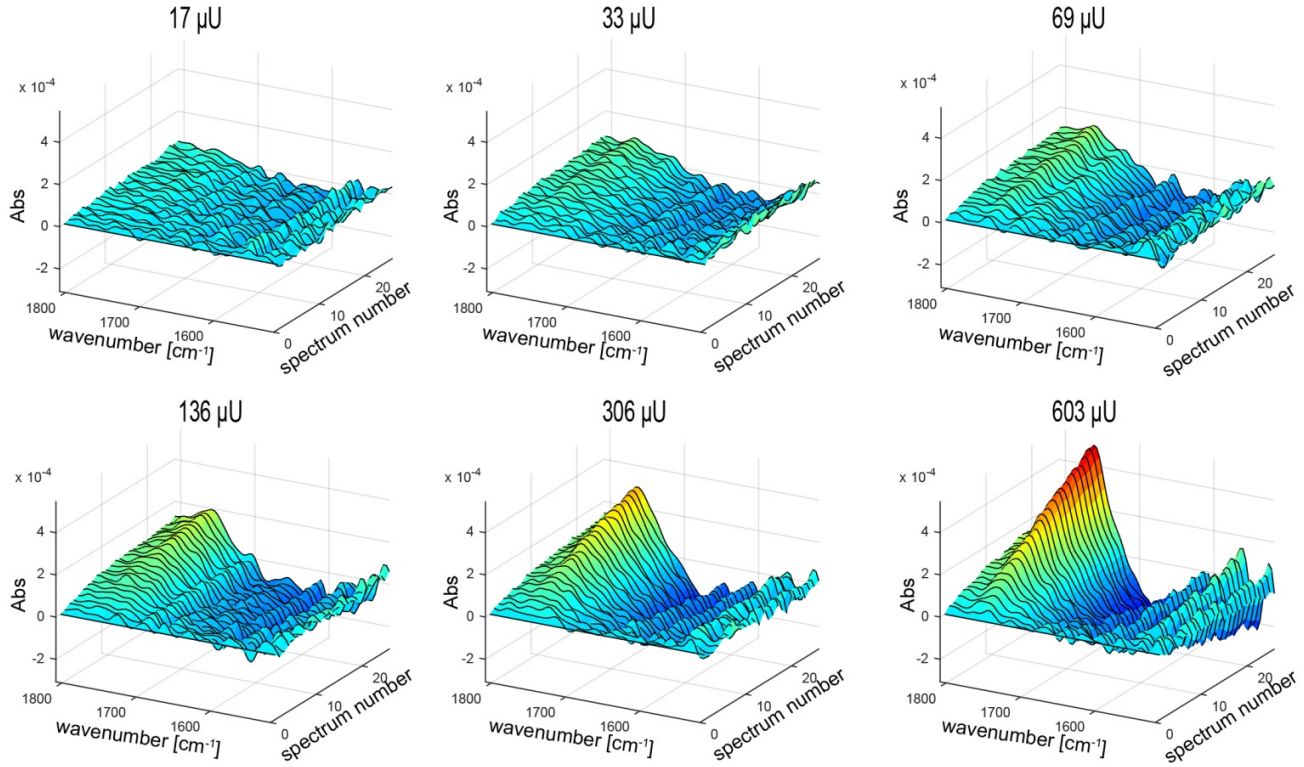

Figure S8. Spectral Evolution Profiles for the *Trametes versicolor* (Tv) laccase oxidation of sinapic acid using different enzyme dosages. Tv dosages are expressed as syringaldazine units.

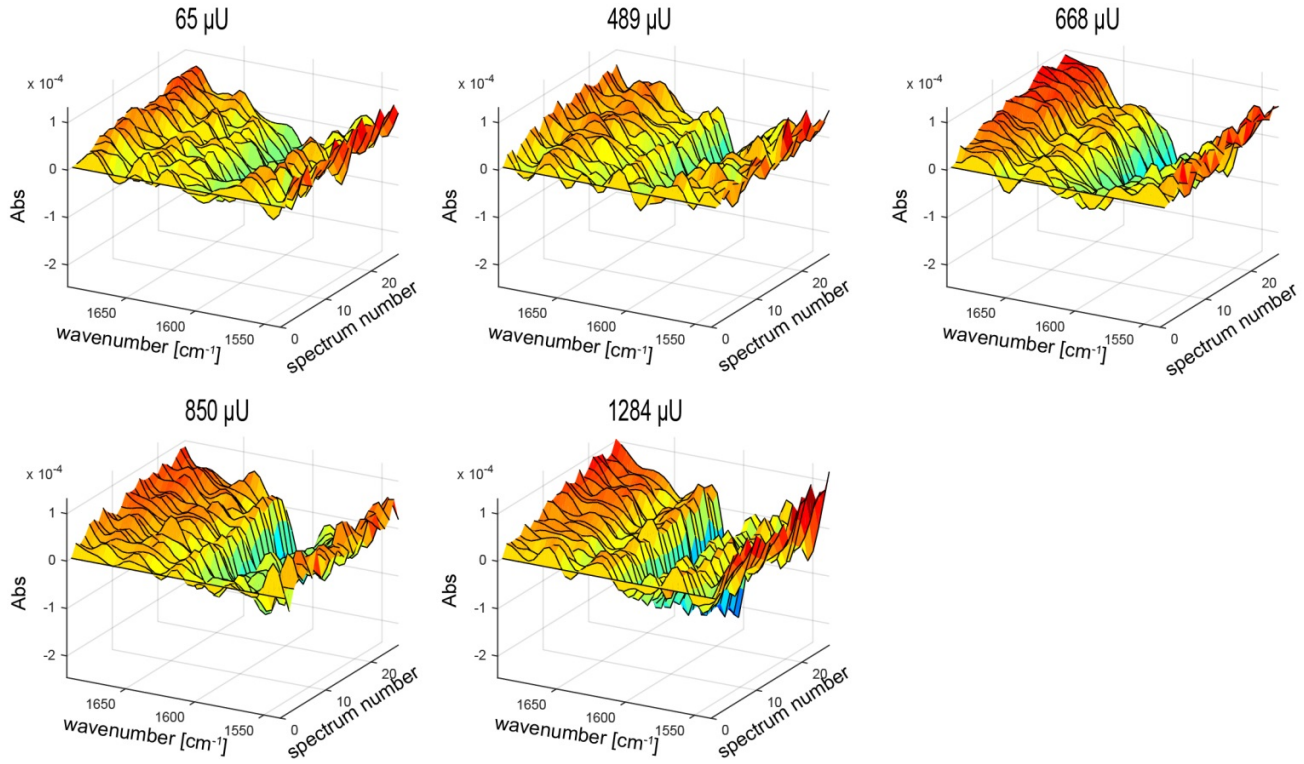

Figure S9. Spectral Evolution Profiles for the *Trametes villosa (*Tvil) laccase oxidation of *p*-coumaryl alcohol using different enzyme dosages. Tvil dosages are expressed as syringaldazine units.

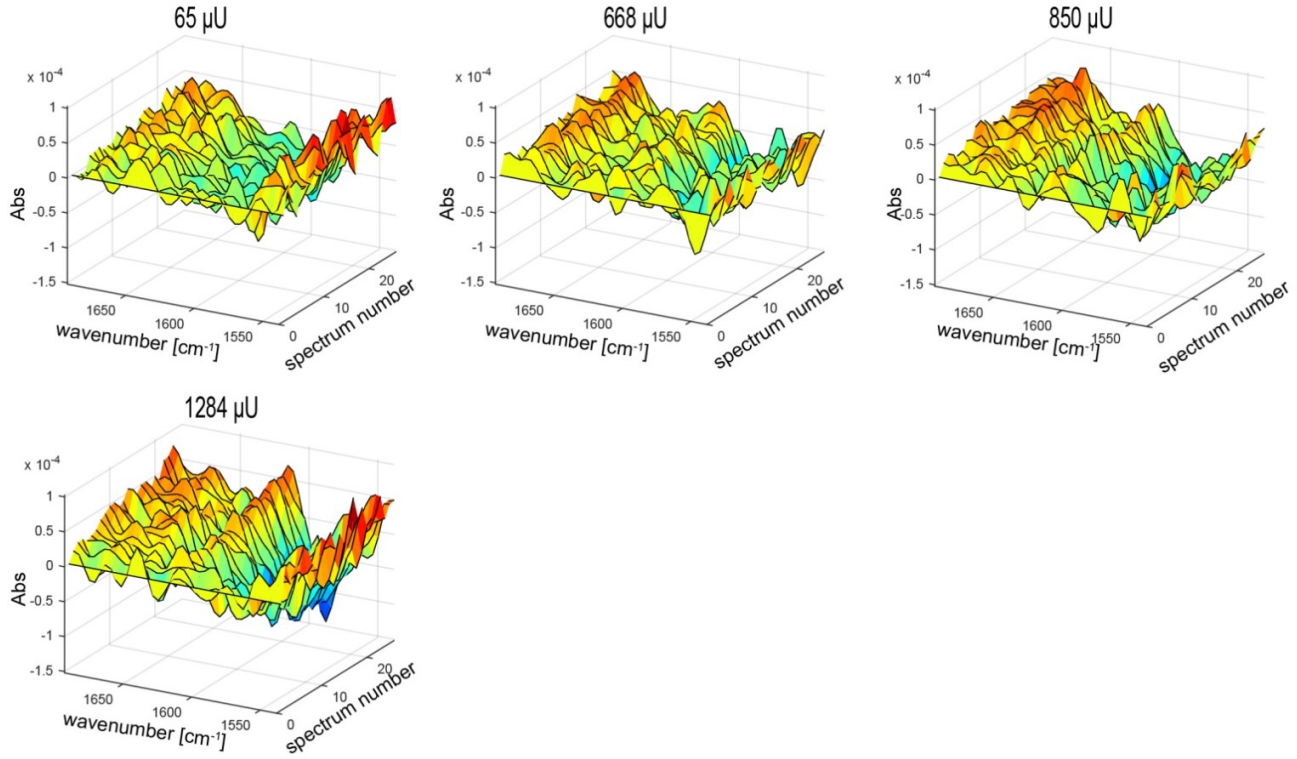

Figure S10. Spectral Evolution Profiles for the *Trametes villosa (*Tvil) laccase oxidation of coniferyl alcohol using different enzyme dosages. Tvil dosages are expressed as syringaldazine units.

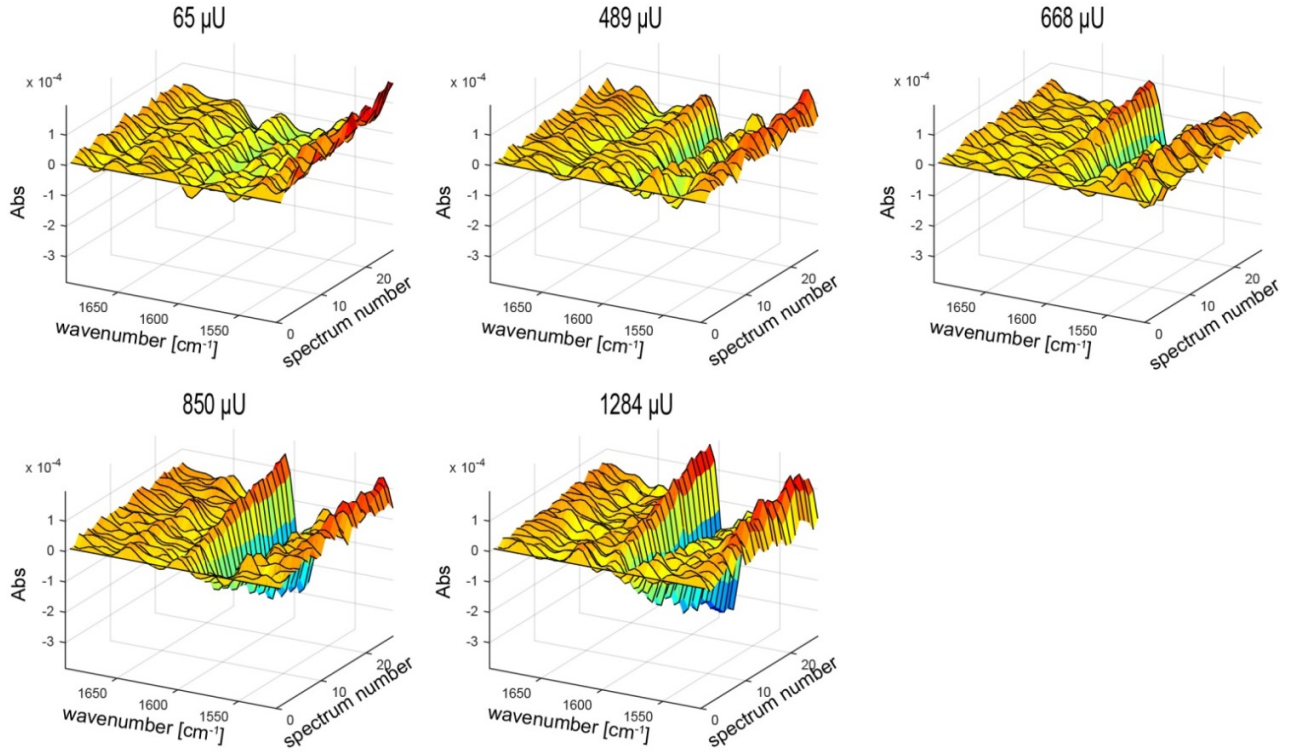

Figure S11. Spectral Evolution Profiles for the *Trametes villosa* (Tvil) laccase oxidation of sinapyl alcohol using different enzyme dosages. Tvil dosages are expressed as syringaldazine units.

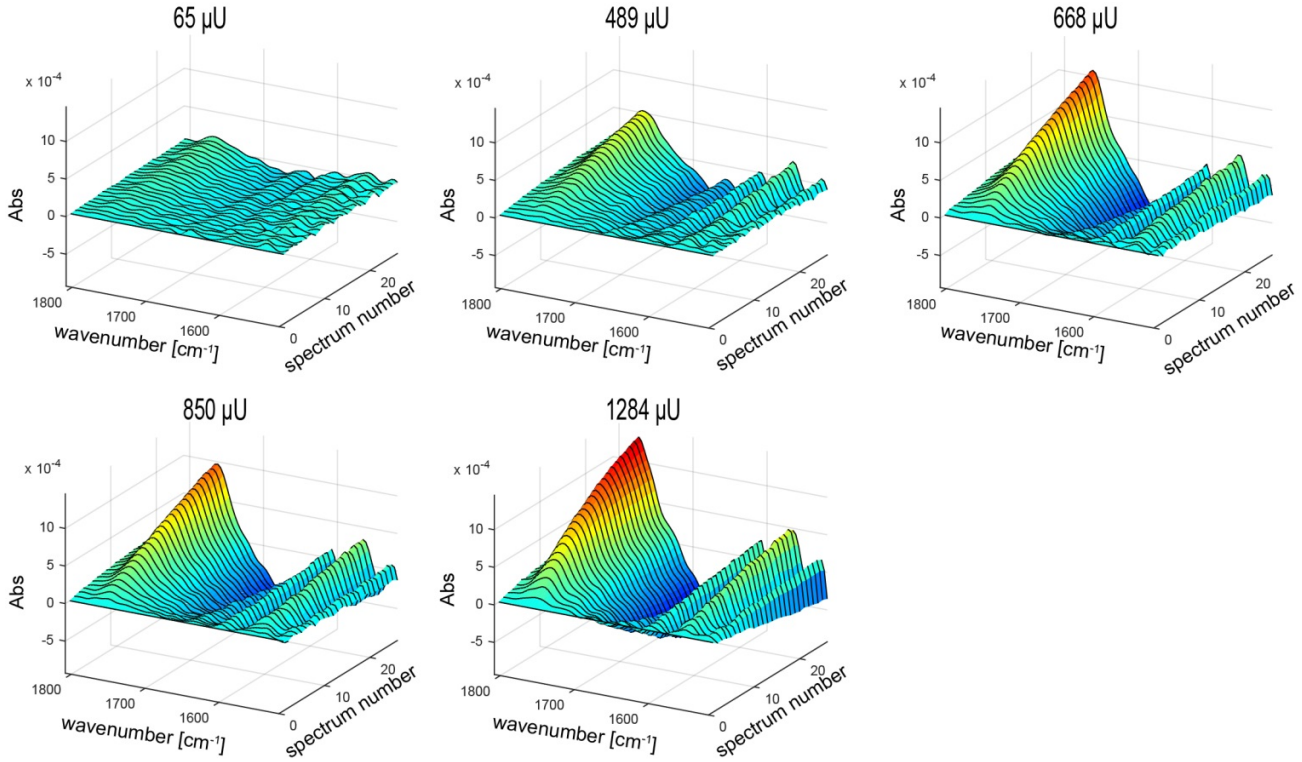

Figure S12. Spectral Evolution Profiles for the *Trametes villosa* (Tvil) laccase oxidation of sinapic acid using different enzyme dosages. Tvil dosages are expressed as syringaldazine units.

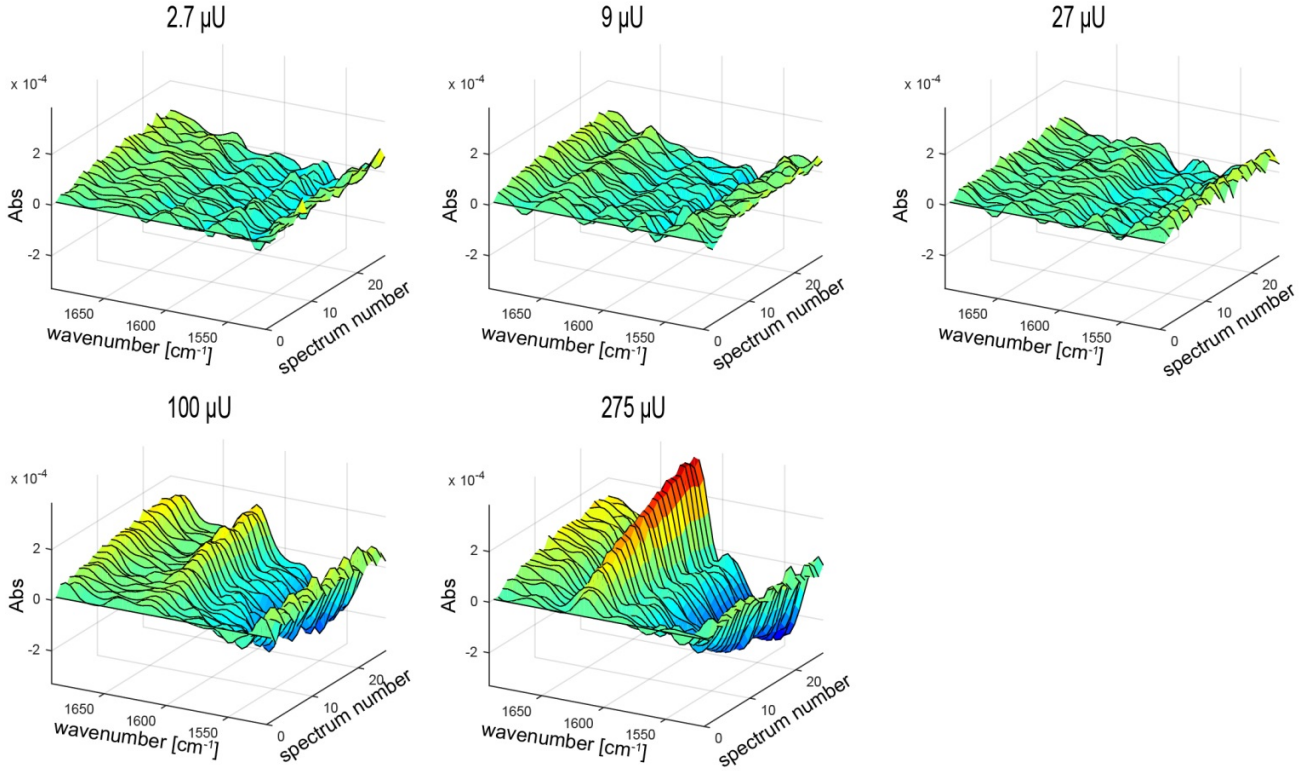

Figure S13. Spectral Evolution Profiles for the *Ganoderma lucidum* (Gl) laccase oxidation of *p*-coumaryl alcohol using different enzyme dosages. Gl dosages are expressed as syringaldazine units.

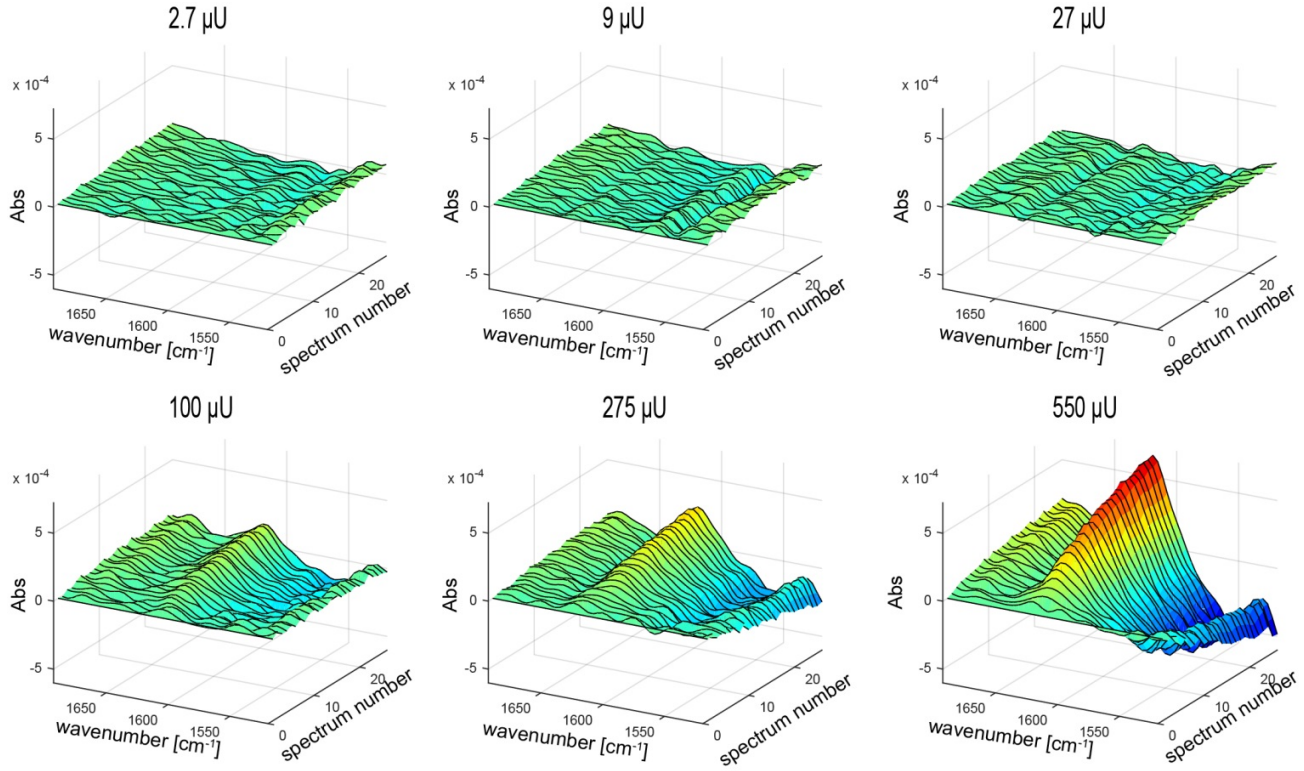

Figure S14. Spectral Evolution Profiles for the *Ganoderma lucidum* (Gl) laccase oxidation of coniferyl alcohol using different enzyme dosages. Gl dosages are expressed as syringaldazine units.

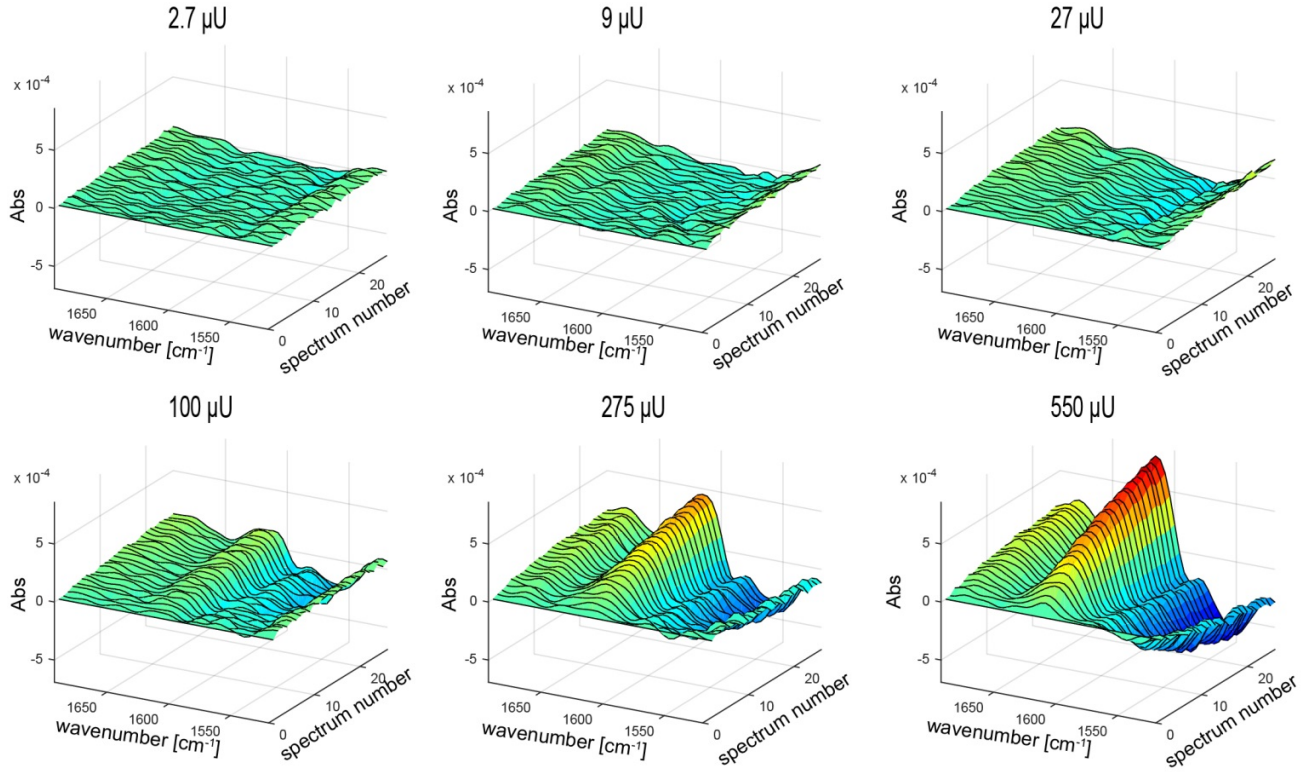

Figure S15. Spectral Evolution Profiles for the *Ganoderma lucidum* (Gl) laccase oxidation of sinapyl alcohol using different enzyme dosages. Gl dosages are expressed as syringaldazine units.

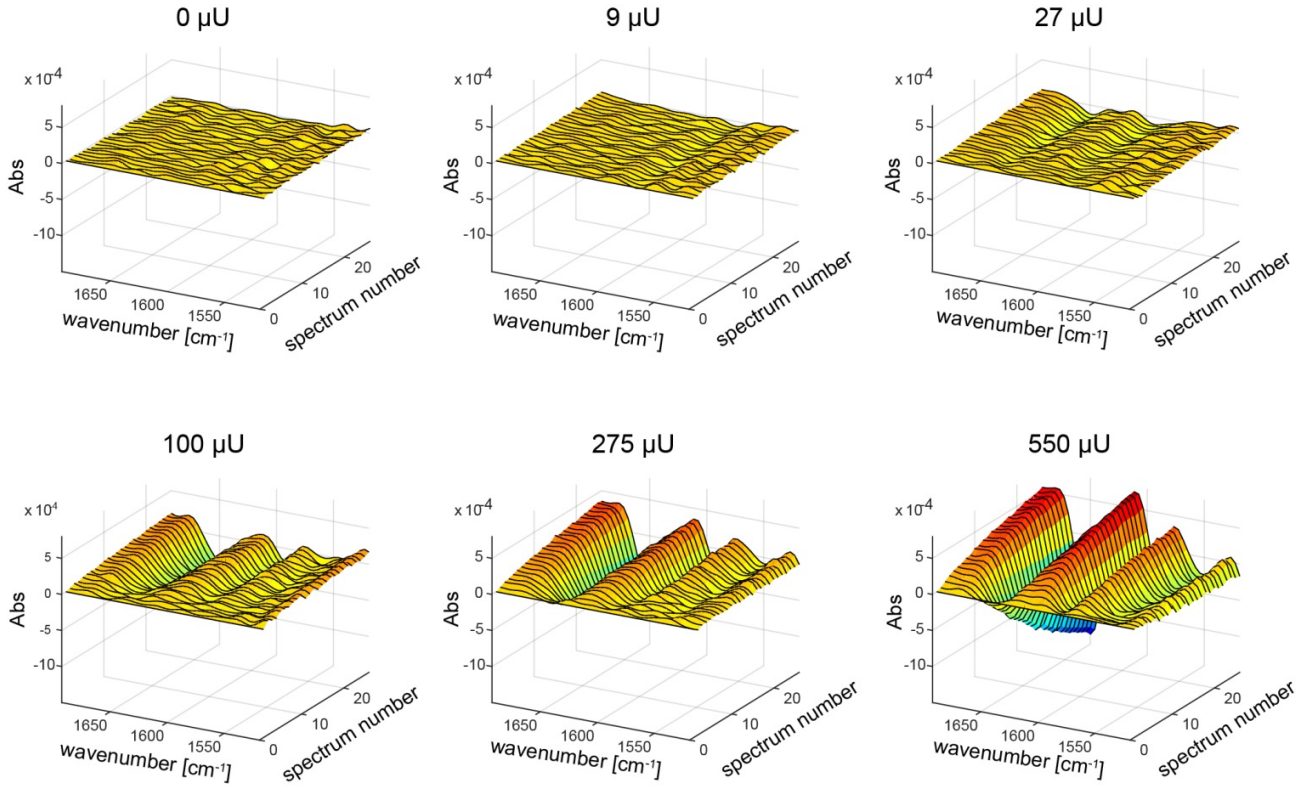

Figure S16. Spectral Evolution Profiles for the *Ganoderma lucidum* (Gl) laccase oxidation of sinapic aldehyde using different enzyme dosages. Gl dosages are expressed as syringaldazine units.

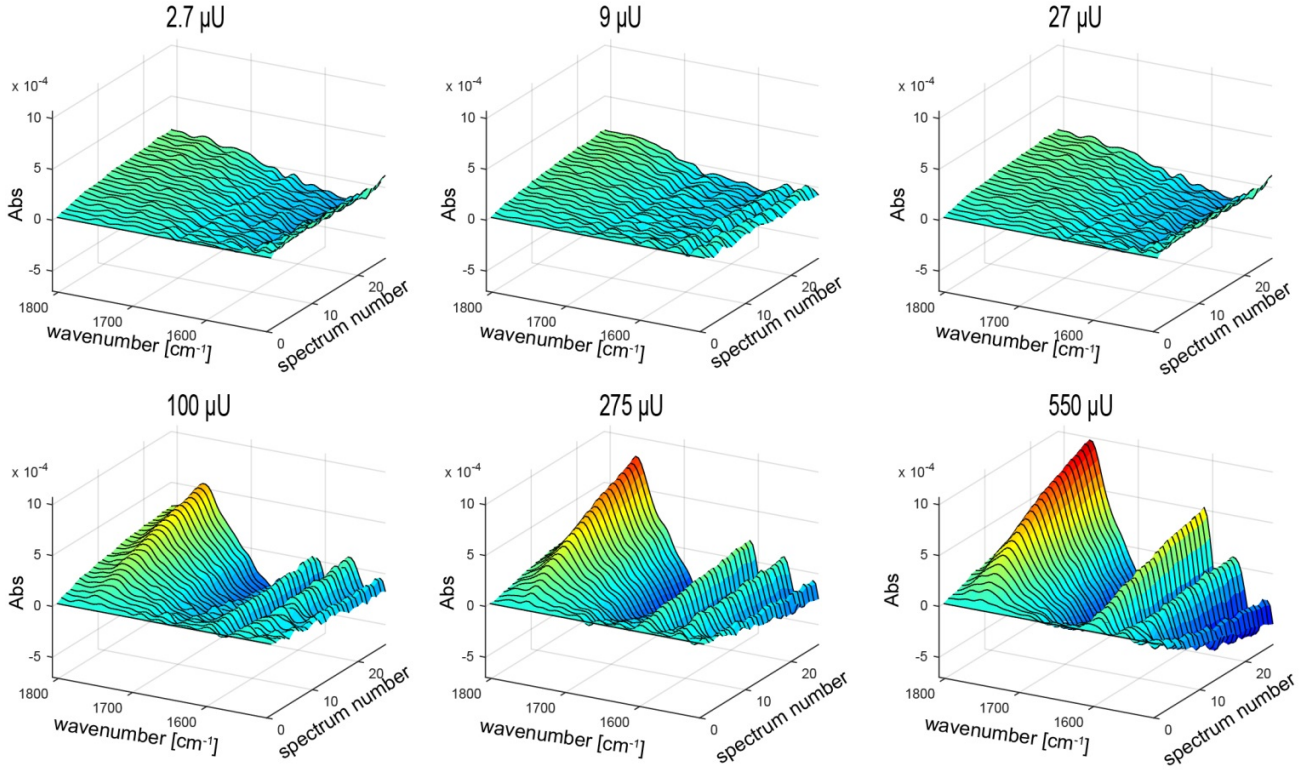

Figure S17. Spectral Evolution Profiles for the *Ganoderma lucidum* (Gl) laccase oxidation of sinapic acid using different enzyme dosages. Gl dosages are expressed as syringaldazine units.

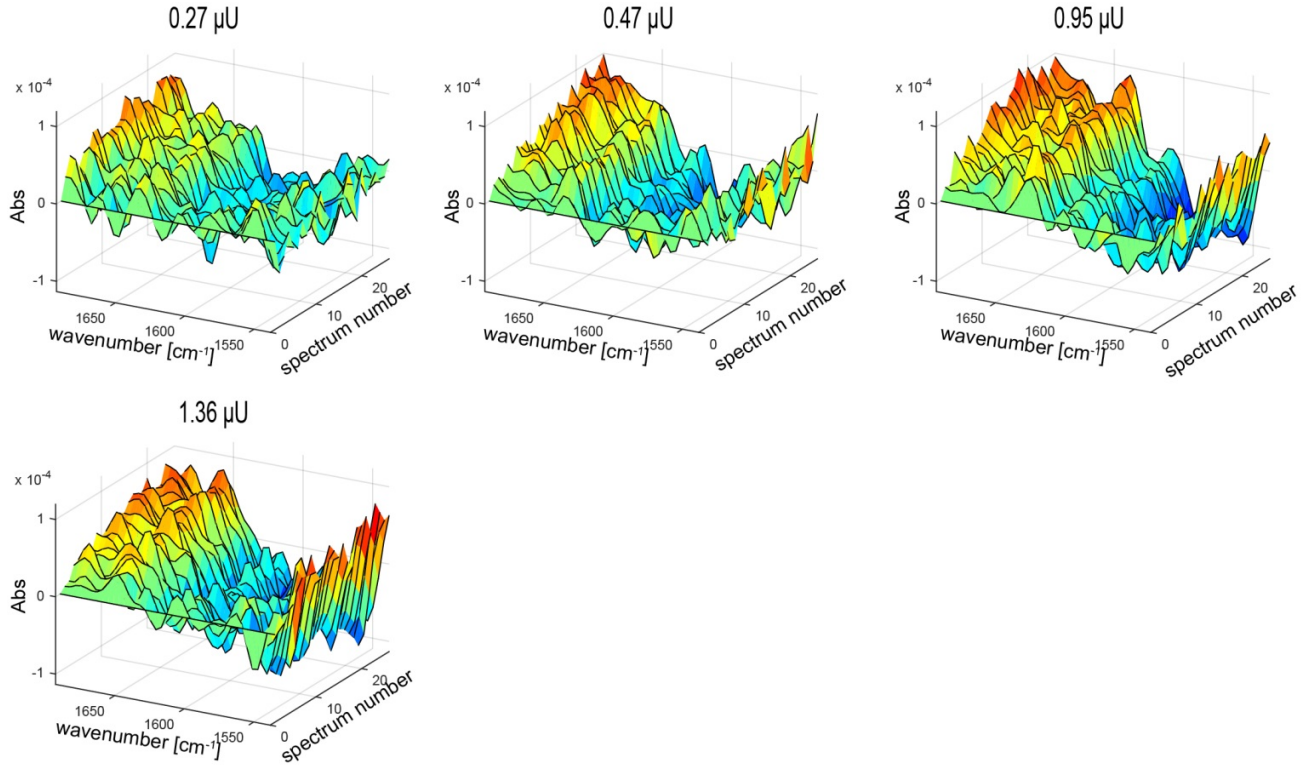

Figure S18. Spectral Evolution Profiles for the *Meiothermus ruber* (Mr) laccase oxidation of *p*-coumaryl alcohol using different enzyme dosages. Mr dosages are expressed as syringaldazine units.

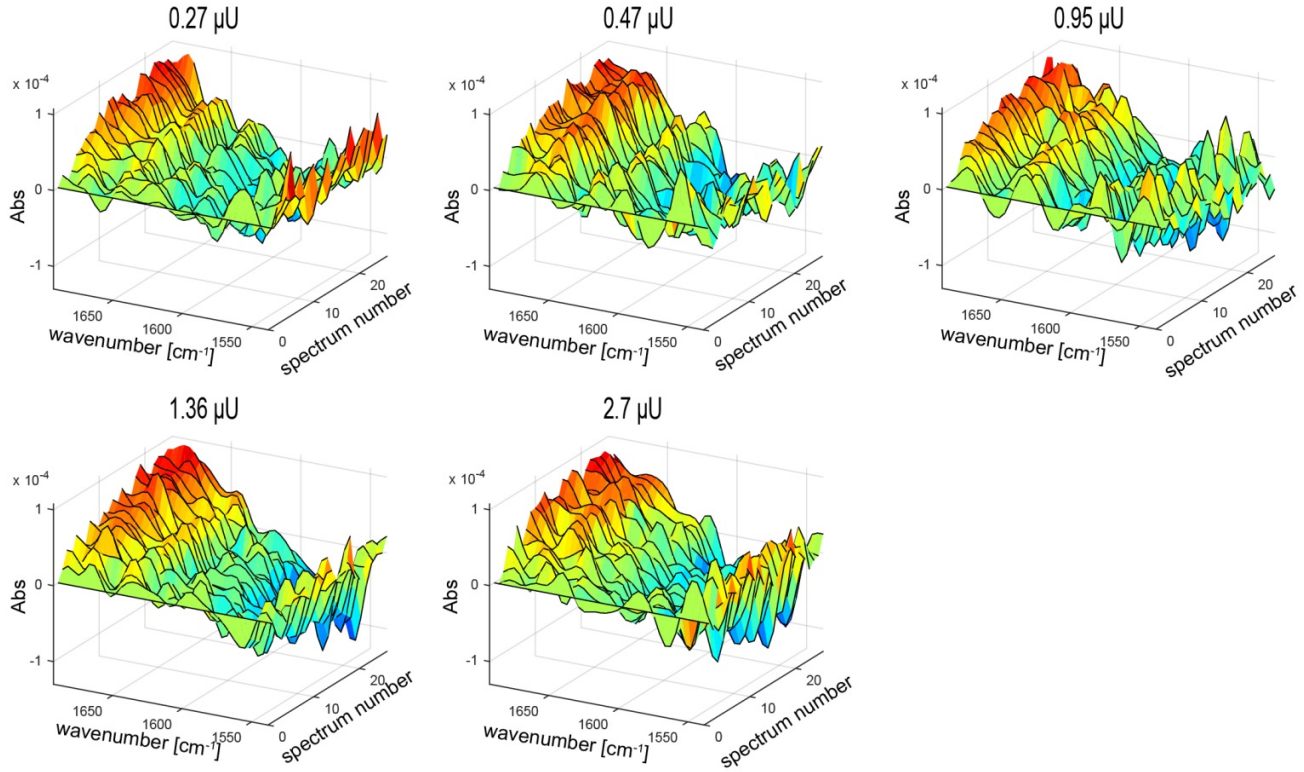

Figure S19. Spectral Evolution Profiles for the *Meiothermus ruber* (Mr) laccase oxidation of coniferyl alcohol using different enzyme dosages. Mr dosages are expressed as syringaldazine units.

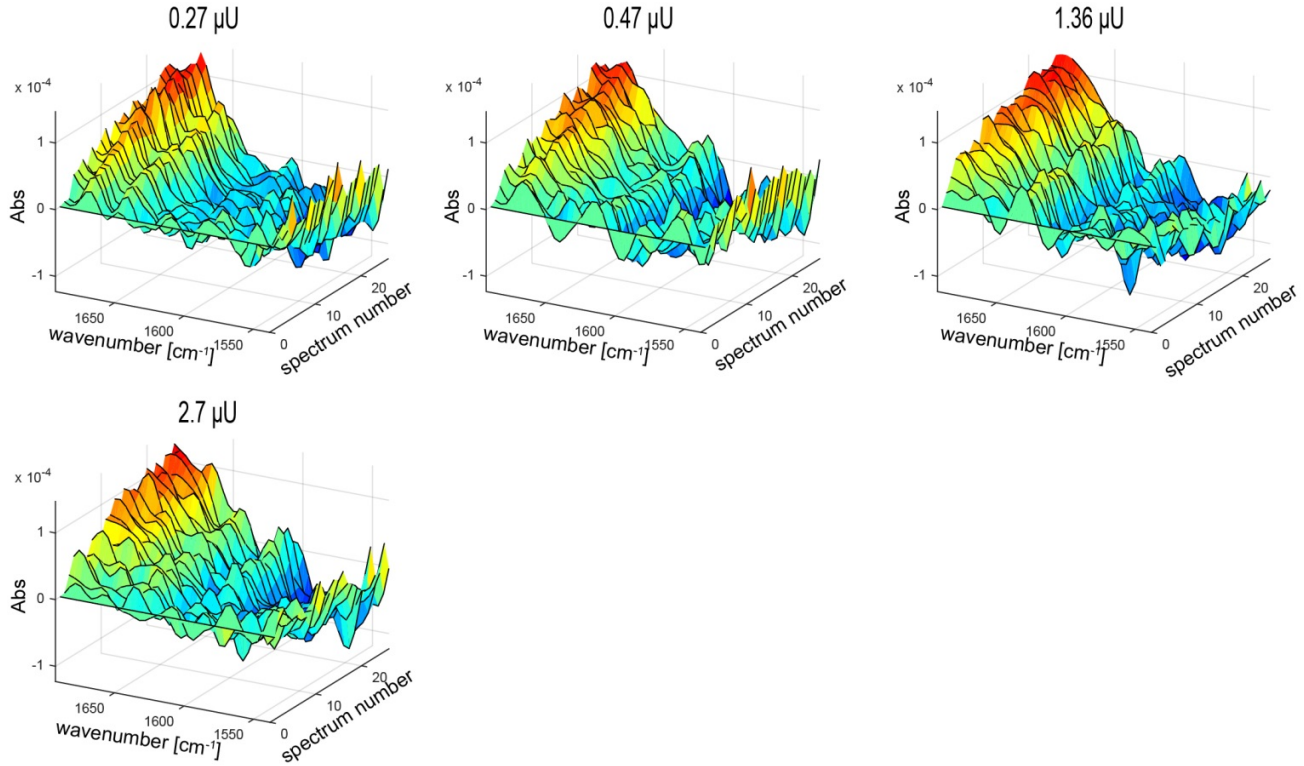

Figure S20. Spectral Evolution Profiles for the *Meiothermus ruber* (Mr) laccase oxidation of sinapyl alcohol using different enzyme dosages. Mr dosages are expressed as syringaldazine units.

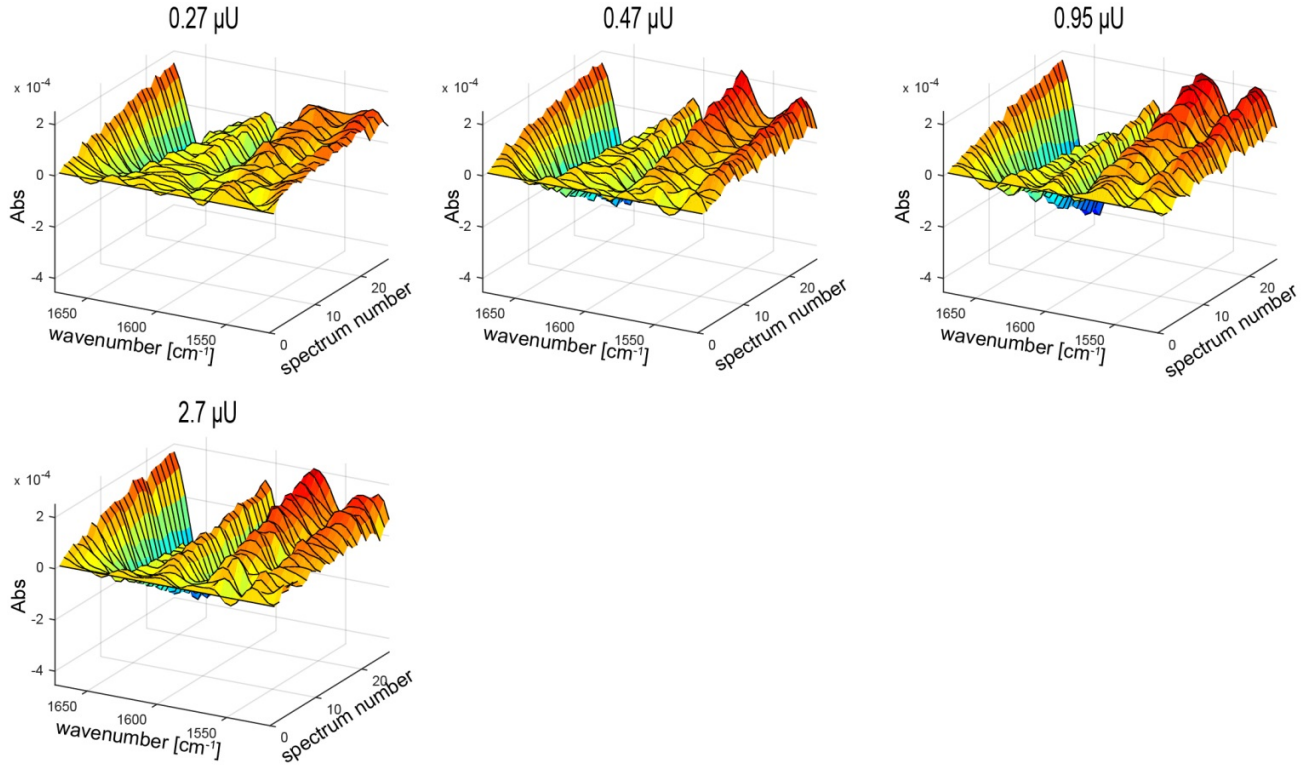

Figure S21. Spectral Evolution Profiles for the *Meiothermus ruber* (Mr) laccase oxidation of sinapic aldehyde using different enzyme dosages. Mr dosages are expressed as syringaldazine units.

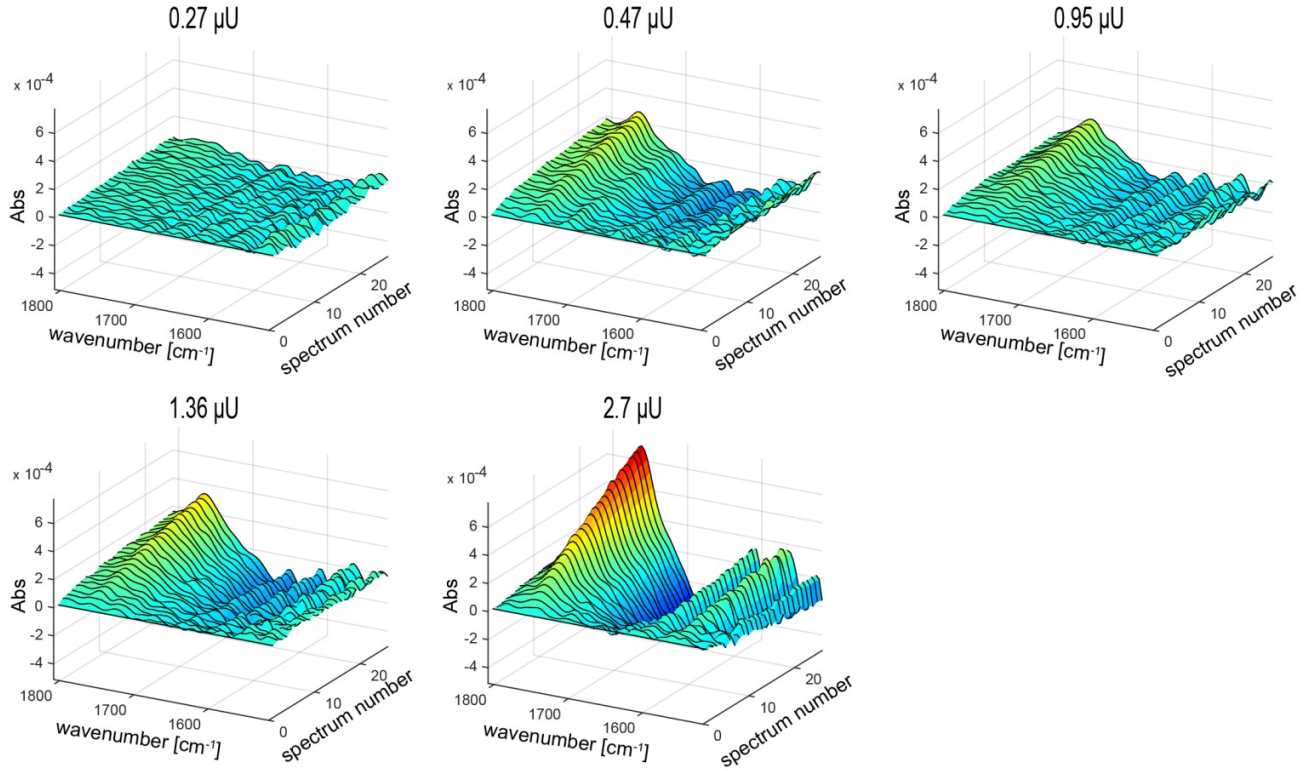

Figure S22. Spectral Evolution Profiles for the *Meiothermus ruber* (Mr) laccase oxidation of sinapic acid using different enzyme dosages. Mr dosages are expressed as syringaldazine units.

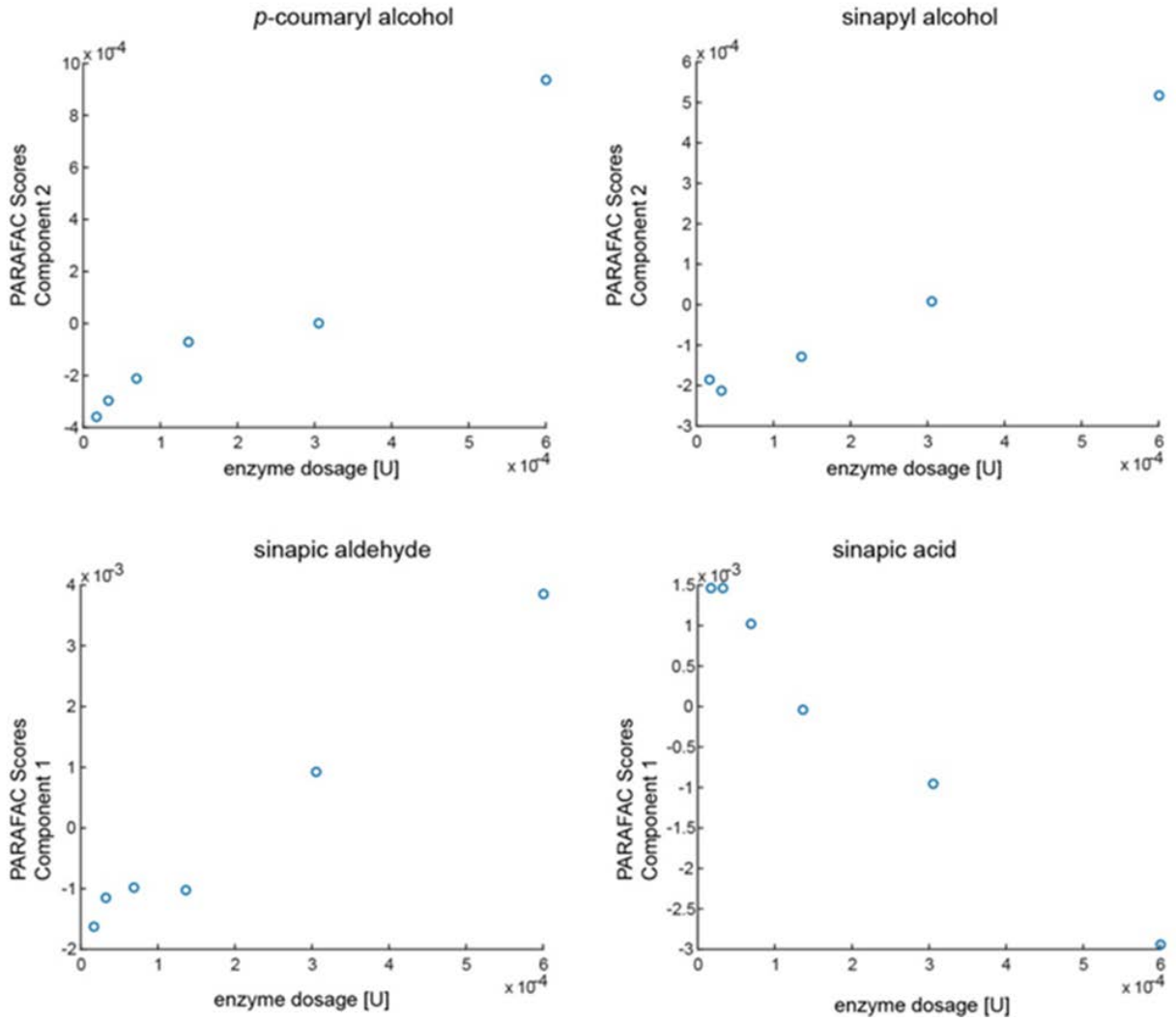

Figure S23. Calibration curves obtained for *Trametes versicolor* (Tv) laccase. PARAFAC scores on *p*-coumaryl alcohol, sinapyl alcohol, sinapic aldehyde and sinapic acid, respectively, plotted vs Tv dosage. The sign of the calibration slope of each individual calibration is not related to substrate or product character as it can result as positive or negative when repeating the PARAFAC analysis [1]. This is due to sign ambiguity in Component analysis [2].

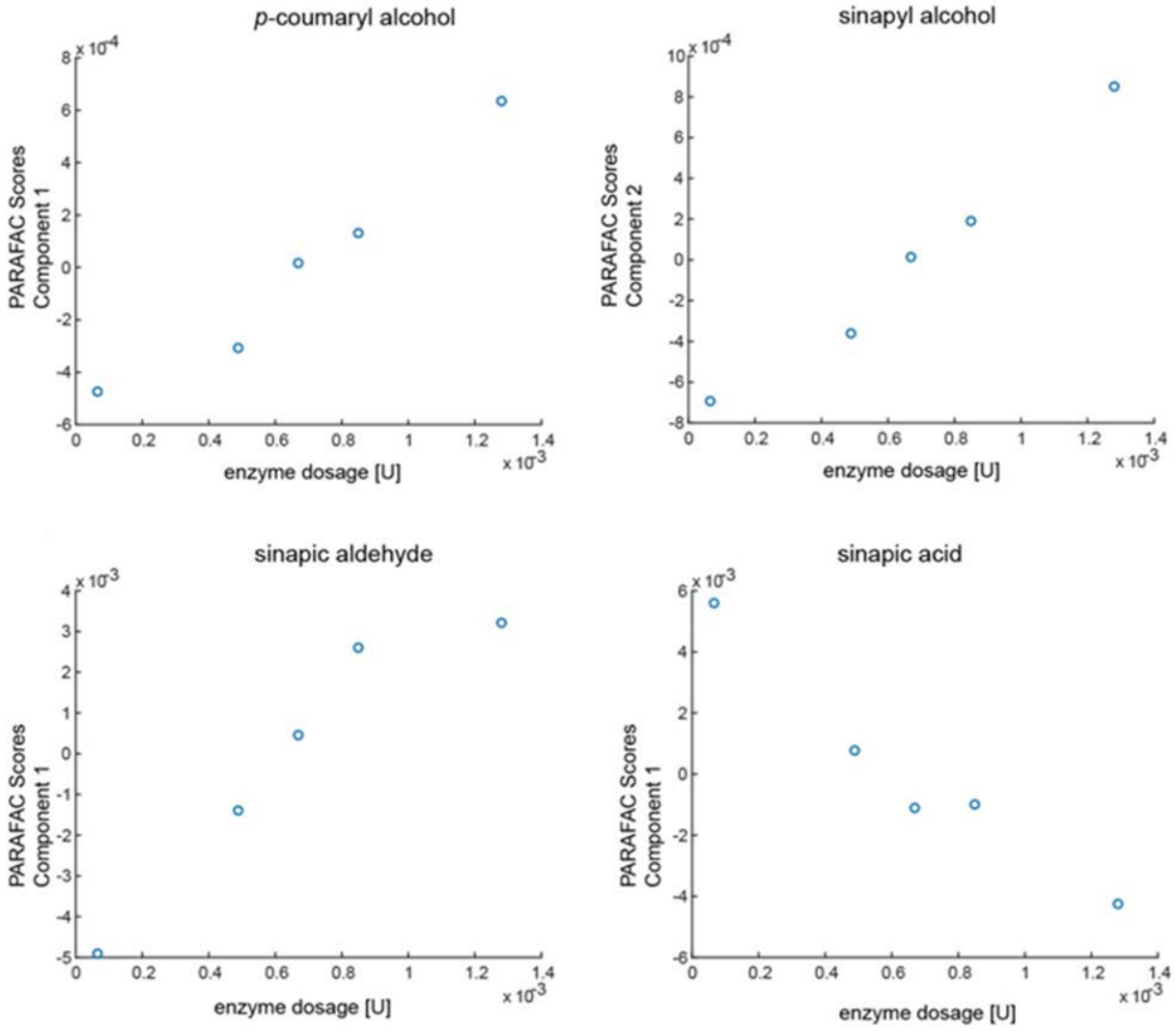

Figure S24. Calibration curves obtained for *Trametes villosa* (Tvil) laccase. PARAFAC scores on *p*-coumaryl alcohol, sinapyl alcohol, sinapic aldehyde and sinapic acid, respectively, plotted vs Tvil dosage. The sign of the calibration slope of each individual calibration is not related to substrate or product character as it can result as positive or negative when repeating the PARAFAC analysis [1]. This is due to sign ambiguity in Component analysis [2].

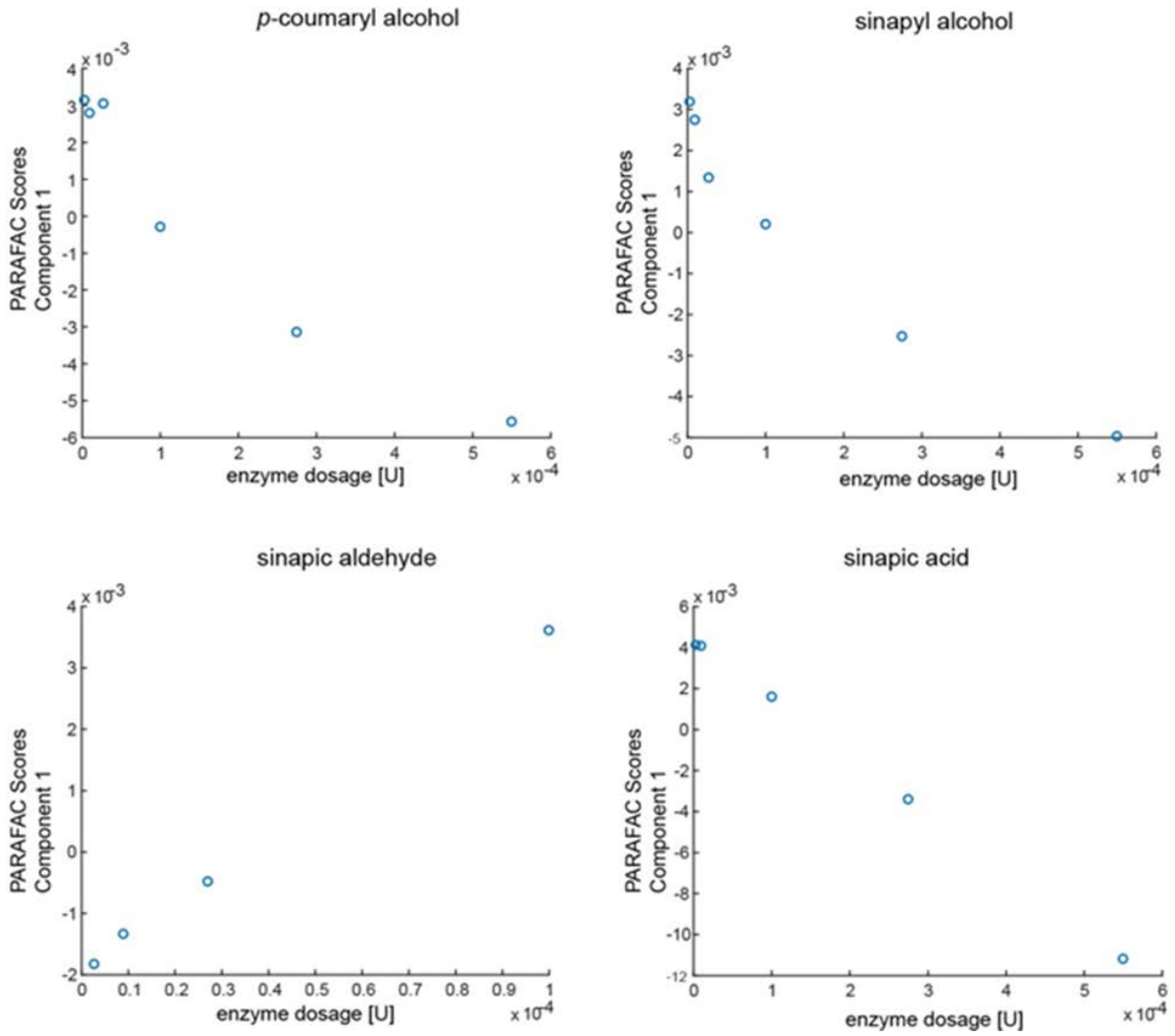

Figure S25. Calibration curves obtained for *Ganoderma lucidum* (Gl) laccase. PARAFAC scores on *p*-coumaryl alcohol, sinapyl alcohol, sinapic aldehyde and sinapic acid, respectively, plotted vs Gl dosage. The sign of the calibration slope of each individual calibration is not related to substrate or product character as it can result as positive or negative when repeating the PARAFAC analysis [1]. This is due to sign ambiguity in Component analysis [2].

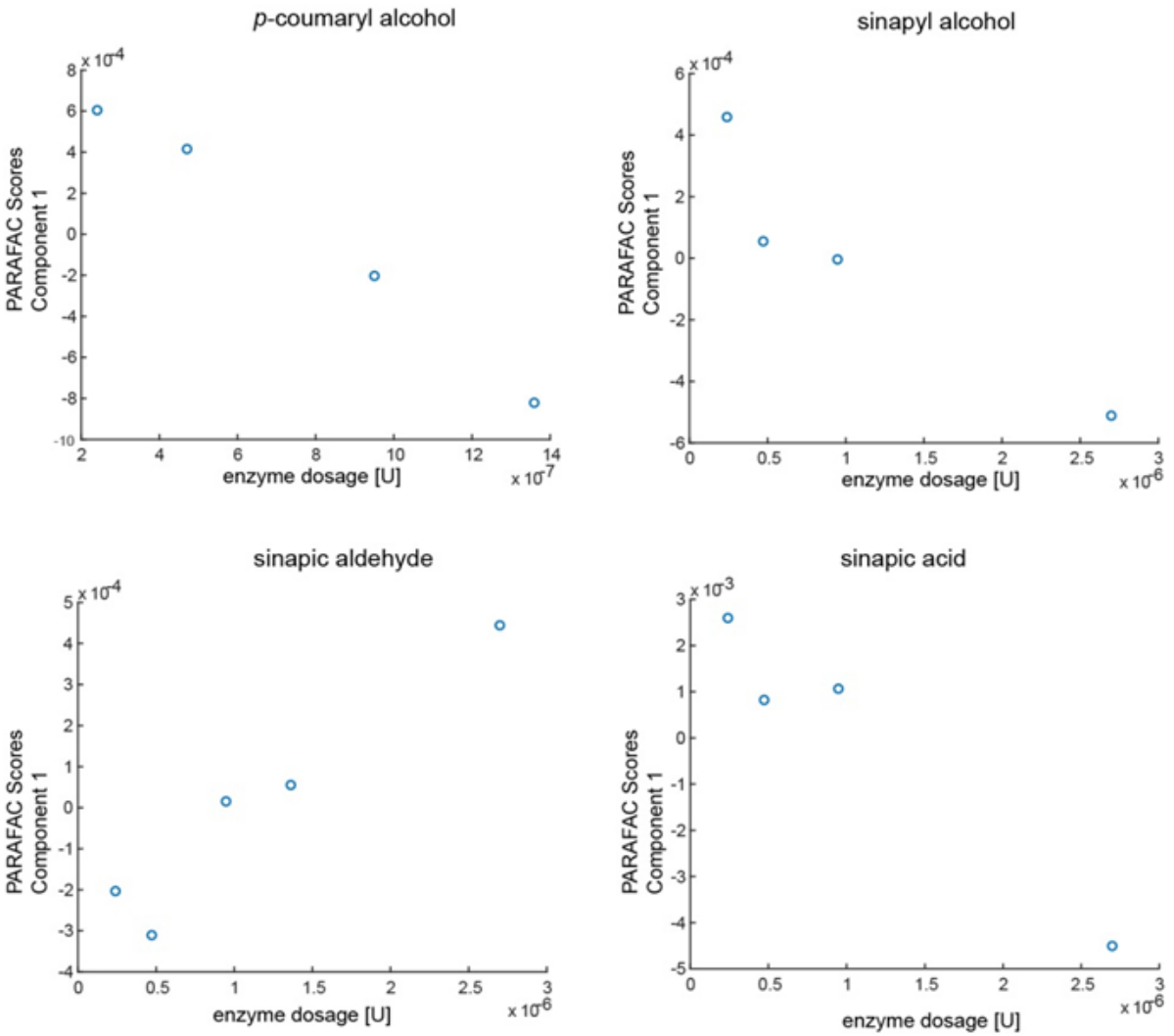

Figure S26. Calibration curves obtained for the *Meiothermus ruber* (Mr) laccase. PARAFAC scores on *p*-coumaryl alcohol, sinapyl alcohol, sinapic aldehyde and sinapic acid, respectively, plotted vs Mr dosage. The sign of the calibration slope of each individual calibration is not related to substrate or product character as it can result as positive or negative when repeating the PARAFAC analysis [1]. This is due to sign ambiguity in Component analysis [2].

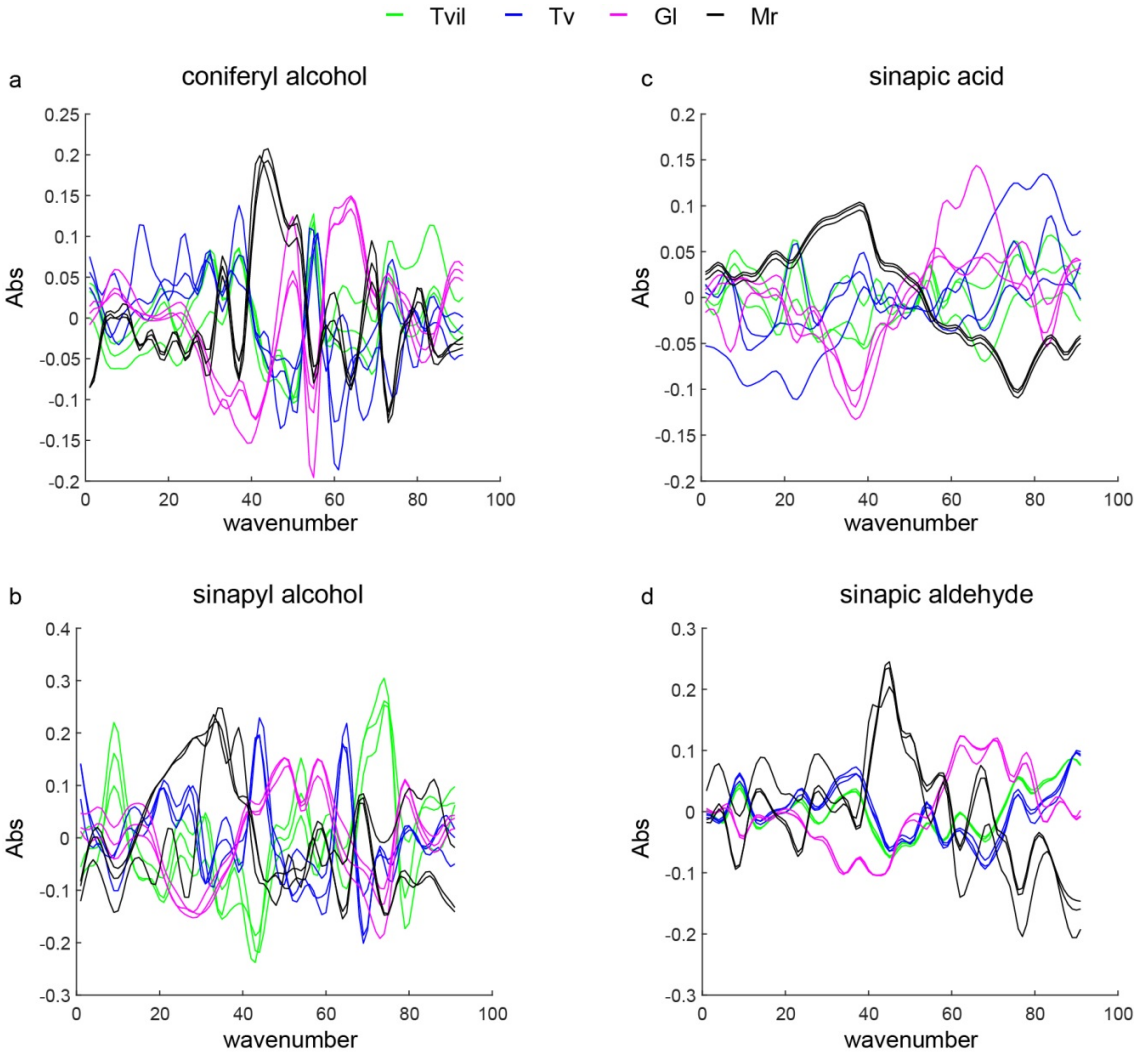

Figure S27. PARAFAC spectral mode loadings of all substrates and laccases. Reaction patterns of coniferyl alcohol (a), sinapyl alcohol (c), sinapic aldehyde (b) and sinapic acid (d) are shown. In all cases the spectral mode loadings for Tvil laccase are shown in green, for Tv laccase are shown in blue, for Gl laccase are shown in magenta and for Mr laccase are shown in black.

Table S1. PARAFAC analysis parameters. Number of components used for PARAFAC decomposition and CORCONDIA number are shown for each laccase/substrate couple. Individual PARAFAC models were obtained for each replicate and standard deviations where present are shown. Valid PARAFAC models are obtained for CORCONDIA values larger than 90 [3].

		Tvil	**Tv**	**Gl**	**Mr**
***p*-coumaryl alcohol**	n° of components	1	2	1	2
	Corcondia value	100	100	99.999 ± 0.0002	99.999 ± 0.001
coniferyl alcohol	n° of components	1	1	2	2
	Corcondia value	100	99.9813 ± 0.032	100	100
sinapyl alcohol	n° of components	2	2	1	1
	Corcondia value	100	92.7624 ± 4.18	100	100
sinapic aldehyde	n° of components	1	1	1	2
	Corcondia value	100	100	100	100
sinapic acid	n° of components	1	1	1	1
	Corcondia value	100	100	100	100

References

[1] A. Baum, A.S. Meyer, J.L. Garcia, M. Egebo, P.W. Hansen, J.D. Mikkelsen, Enzyme activity measurement via spectral evolution profiling and PARAFAC, Anal. Chim. Acta. 778 (2013) 1–8. doi: 10.1016/j.aca.2013.03.029

[2] R. Bro, E. Acar, T.G. Kolda, Resolving the sign ambiguity in the singular value decomposition, J. Chemom. 22 (2008) 135–140. doi:10.1002/cem.1122.

[3] R. Bro, H.A.L. Kiers, A new efficient method for determining the number of components in PARAFAC models, J. Chemom. 17 (2003) 274–286. doi:10.1002/cem.801.

Paper 3

Laccase induced lignin radical formation kinetics evaluated by Electron Paramagnetic Resonance spectroscopy

Laccase induced lignin radical formation kinetics evaluated by Electron Paramagnetic Resonance spectroscopy

Valentina Perna[†], Jane W. Agger[†], Mogens L. Andersen[‡], Jesper Holck[†], Anne S. Meyer[†*]

[†] Section for Protein Chemistry and Enzyme Technology, Department of Biotechnology and Biomedicine, Technical University of Denmark, Kgs. Lyngby 2800, Denmark

[‡] University of Copenhagen, Faculty of Science, Department of Food Science, Rolighedsvej 30, Frederiksberg C 1958, Denmark

[*]Corresponding author, address as above, e-mail: asme@dtu.dk

Abstract

Laccases (EC 1.10.3.2) catalyze oxidation of phenoxyl groups in lignin during reduction of O_2 and the first product is a lignin radical. The determination of laccase kinetics on lignin requires cautious interpretation due to the radical reactions involved. In this study the radicals produced during laccase catalyzed oxidation of organosolv lignin were measured by Electron Paramagnetic Resonance (EPR) spectroscopy and used to assess the enzyme kinetics of three different fungal laccases on the lignin. The laccases originated from *Trametes versicolor*, *Ganoderma lucidum* and *Myceliophthora thermophila*, respectively. The enzymes had different affinities for the organosolv lignin substrate and the kinetic parameters of the three laccases differed. The *T. versicolor* enzyme was the fastest relative to the activity of the three enzymes on the assay substrate syringaldazine, but the *G. lucidum* and the *T. versicolor* laccases had similar apparent catalytic efficiencies on the lignin substrate. The enzyme kinetic parameters must be denoted as apparent because the measured levels of radicals formed is the net sum of laccase driven formation of radicals and spontaneous radical decay reactions occurring simultaneously. Spontaneous quenching of radicals after laccase inactivation was quantitifed by EPR spectroscopy and the initial radical decay rates were confirmed to be laccase independent. The findings expand our understanding of laccase attack on lignin in nature and are of significance in relation to use of laccase in lignocellulose and lignin biorefining.

Keywords: Laccase, lignin, Michaelis-Menten kinetic, EPR, radical

Abbreviations:

EPR, Electron Paramagnetic Resonance; Tv, laccase from *Trametes versicolor*; Mt, laccase from *Myceliophthora thermophila*; Gl, laccase from *Ganoderma lucidum*; SGA, syringaldazine.

Introduction

Lignin is a water-insoluble biopolymer composed of aromatic units i.e. *p*-hydroxyphenyl (H), guaiacyl (G), and syringyl (S).[1] Lignin is present in secondary plant cell walls and typically constitutes 20-30% of lignocellulosic biomass. In nature, certain fungi and bacteria degrade lignin using different enzymatic strategies, and notably peroxidases and laccases are believed to play vital roles in natural enzyme catalyzed oxidation of lignin.[2] Laccases (benzenediol:oxygen oxido-reductase, EC 1.10.3.2) catalyze the oxidation of hydroxyl groups of phenols, including phenolic subunits in lignin, and use molecular oxygen as final electron acceptor.[2] During a laccase catalyzed cycle a total of four moles of phenolic compounds are oxidized during reduction of one mole of O_2 to two moles of H_2O.[3–6] The first product from laccase oxidation is a phenoxy radical, or in fact various resonance-stabilized phenoxy radicals, that usually undergo further chemical reactions, including radical coupling reactions, leading to polymerization.[2,7]

Electron paramagnetic resonance (EPR) spectroscopy is used to study species with unpaired electrons which can move between their two spin states if an external magnetic field is applied.[8–10] Each radical gives a specific EPR spectrum. The simplest spectrum obtainable consists of only one line, while the spin interaction with the nearby nuclear spins gives rise to hyperfine splittings and thereby EPR spectra with more than one line.[8,9] In EPR an intrinsic correlation exists between the unpaired electrons and the magnetic field known as the g-value. The g-value can be interpreted similar to the chemical shift values in NMR and is thus a unique identifier for a given paramagnetic species.[9]

Lignin has been studied by EPR spectroscopy[11–13] and its EPR spectrum is characterized by a sum of stable semiquinone radicals stabilized in the polyphenolic lignin matrix all having nearly identical g-values.[14,15] Hence, the EPR spectrum of lignin appears as a single hyperfine line spectrum (Figure 1 panel a)).[11,13,15,16] It has been observed that the radicals generated in lignin during laccase catalyzed oxidation are stable long enough to be detected by EPR spectroscopy[5,17,18] and recent work in our laboratory[17,18] has shown that EPR spectroscopy can be used to measure laccase activity on lignin.

The objective of the present work was to extend the applicability of the EPR laccase assay technique on lignin[17,18] to quantitatively resolve laccase kinetics on lignin and thereby determine kinetic parameters. We hypothesized that the kinetic parameters on lignin would differ among different laccases and moreover that the kinetic parameters would differ from those obtained on simple hydroxycinnamic acids in a previous study[19] and that the order of relative rates (or efficiencies) on lignin of different laccases might differ from those on soluble substrates. A second objective was to assess the radical disappearance rate in order to determine the significance of any spontaneous radical-radical coupling reactions and clarify how such reactions may affect the observed radical concentrations during laccase oxidation.

Radical formation due to laccase oxidation of organosolv lignin was studied and the kinetics of three different fungal laccases were examined: two white rot basidiomycetes laccases from *Trametes versicolor* (Tv) and from *Ganoderma lucidum* (Gl),[20] respectively, and one laccase from the soft rot ascomycete *Myceliophthora thermophila* (Mt). The redox potential of the Gl enzyme has not been reported, but the Tv enzyme is known to have a high redox potential (~0.7 V vs NHE)[21,22] whilst the Mt is a low-medium redox potential enzyme (~0.5 V vs NHE).[23,24]

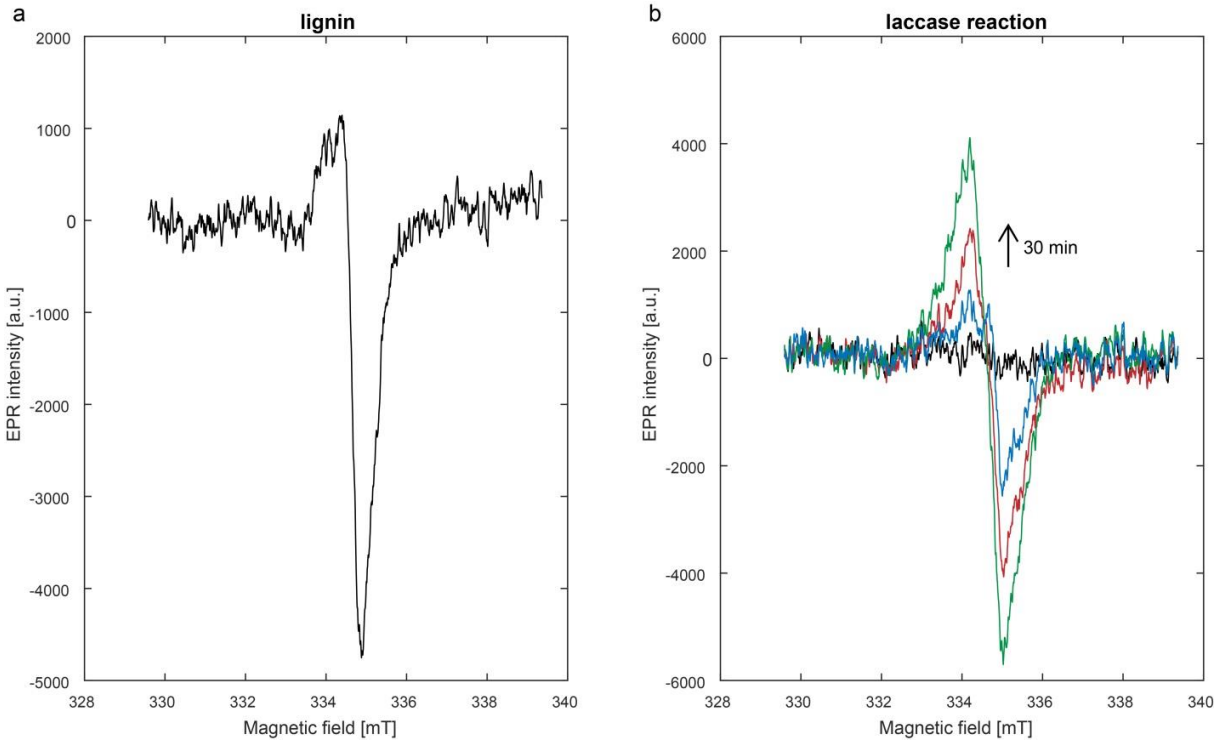

Figure 1. Examples of EPR spectra for 10% w/v organosolv lignin (a) and laccase reaction with 10% w/v organosolv lignin (b). The EPR signals for the laccase reaction in (b) were corrected from the reference state background, i.e. the reference state background (a) was subtracted from the each reaction signal.

Materials and methods

Materials

Organosolv lignin (CAS No. 8068-03-9), presumably from hardwood, was purchased from Sigma-Aldrich (Steinheim, Germany) (SOL) (biomass source not disclosed by the supplier). The lignin had a volume-based particle size of D[4,3] = 6.4 µm, and was composed of 94 wt% of Klason lignin. The phenol content was determined by P-NMR analysis[25,26] to 3.44 mmol/g, obtained by the sum of 0.16 mmol/g of *p*-hydroxyl-OH, 0.97 0.16 mmol/g of guaiacyl-OH and 2.31 mmol/g 5-substituted-OH. The latter is the overall sum of syringyl-OH and condensed-OH resulting in an approximate S/G of 2.37. 2,2,6,6-tetramethylpiperidin-1-yloxy (TEMPO),

syringaldazine, and the laccase from *Trametes versicolor* (Tv) were also obtained from Sigma-Aldrich (Steinheim, Germany). The *Myceliophthora thermophila* (Mt) laccase was a gift from Novozymes A/S (Bagsværd, Denmark), and the *Ganoderma lucidum* (Gl) laccase was produced in house using *Pichia pastoris* as host for heterologous expression.

The construct containing the gene encoding for the Gl laccase[20] was codon optimized for *P. pastoris* and transformed into a protease free *P. pastoris* strain (SMD1168H) and production of the of recombinant laccase in *P. pastoris* was accomplished at a 5 L production scale as described previously.[27] However, in order to improve the enzyme's stability the methanol Fed-Batch phase was accomplished at 20°C. The total time for the fermentation process was 160 h. The laccase-containing fermentation broth was recovered by centrifugation at 5300 x g at 5°C for 1 h, then subjected to sterile filtration, and concentrated by ultrafiltration using a cross-flow bioreactor system with a 10 kDa cutoff membrane (Millipore, Sartorius, Denmark), as described by Silva *et al.*[27]

Laccase activity assay

Laccase activity was assessed by monitoring the oxidation of syringaldazine (SGA) at 530 nm $\varepsilon = 6.5 \times 10^4\ M^{-1}\ cm^{-1}$. The assay reaction mixture contained 25 µM syringaldazine, 10% ethanol, 25 mM sodium acetate pH 5.0 and a proper amount of enzyme. Enzyme catalyzed SGA oxidation was monitored at 25°C for 20 minutes. Enzyme activity was expressed in units: One International Unit (U) was defined as the amount of enzyme able to catalyze 1 µmol of substrate (SGA) in one minute under the assay conditions and this value was used to define the amount of active enzyme present in a specific enzyme preparation.

All three enzymes, i.e. the Tv, Mt and Gl laccases, were dosed according to their SGA activity in the reactions on lignin after dilution in MilliQ water.

Enzyme kinetics

The lignin was suspended in water and adjusted to pH 5.0 using NaOH prior to reaction. Enzyme kinetics were determined using different lignin concentrations ranging from 0.25% to 15% weight/volume (w/v), corresponding to a phenolic content ranging from 0.009 to 0.516 M, respectively. Each reaction (1.5 mL) was initiated by the addition of laccase; the dosing of the enzymes based on their syringaldazine activity were: 1.38, 0.3 and 6.48 mU for Gl, Tv and Mt laccase, respectively. The reactions were performed in a thermomixer at 25°C and 900 rpm. At different reaction times, depending on the substrate concentration, 50 µL of the reaction suspension were drawn into a 50 µL capillary tube (BRAND® disposable BLAUBRAND® micropipettes, intraMark) securing the complete absence of air bubbles during the EPR spectroscopy measurements, explained below.

The radicals formed during laccase oxidation of the lignin suspension were measured directly by EPR spectroscopy according to Munk *et al.*[18] EPR detection was performed with a MiniScope MS200 (Magnettech, Berlin, Germany) at 20°C with modulation amplitude 0.2 mT, sweep width 10 mT and sweep time of 30 s. Each EPR measurement was accomplished with particular care ensuring that the time between the sampling and the measurement was minimal and always the same in order to avoid sedimentation in the capillary tube (observed approximately after 2 minutes). All reactions and measurements were done in triplicates. A double integration of the resonance signal after background subtraction (i.e. subtraction of the resonance signal line of the reference treatment) (Figure 1 panel b) was used to calculate the number of spins. A linear standard curve of the stable nitroxyl radical TEMPO (Sigma-Aldrich, Steinheim, Germany), concentrations ranging from 0.5–100 µM, was used to convert the number of spins to a radical concentration. TEMPO is a suitable quantitative standard for lignin because oxidized lignin moieties and TEMPO share the same overall g-value as the stable lignin phenoxy radical signals are within the magnetic field of the middle peak of the TEMPO radical. A schematic representation of the EPR technique and data analysis is shown in Figure S1.

Kinetic parameters V_{max} and K_m were obtained using Hanes' linearization of the Michaelis-Menten curve for the different enzymes assessed. Apparent specific activity was determined by normalizing V_{max} over the enzyme dosage used. The normalization was performed using 6.48 mU for Mt, 1.38 mU for Gl, and 0.3 mU for Tv. Apparent catalytic efficiency was determined by dividing the apparent specific activity by K_m.

Radical disappearance

The radical disappearance was studied after inactivation of the enzyme with NaN_3 at different reaction times. 2 mL reaction of 10% w/v lignin (0.344 M phenolic concentration) was initiated by laccase addition dosing the enzyme based on syringaldazine activity: 1.38, 1.5 and 6.48 mU for Gl, Tv and Mt laccase, respectively, and performed in a thermomixer at 25°C and 750 rpm. At different reaction times: 30, 60, 120 and 150 minutes for Gl and 10, 30, 60 and 100 for Tv and Mt, the laccases were inactivated by addition of 0.86 mM of NaN_3. This concentration of NaN_3 was found to be the lowest dose of NaN_3 that completely inactivated the enzyme during the SGA assay. The spontaneous radical disappearance was monitored by EPR spectroscopy. Two control experiments were performed to ensure that the added NaN_3 was only inactivating the enzyme and not producing any effect on the radicals. (1) Different amounts of NaN_3 ranging from 0.86 to 77.85 mM were added to 20 µM of the stable nitroxyl radical TEMPO to asses at which NaN_3 concentration a decrease in the TEMPO radical signal was observed. This occurred only after addition of 77.85 mM (w/v) NaN_3, which was 90.52 times more concentrated compared to the amounts used to inactivate the laccase. (2) Different amounts of NaN_3 ranging from 0.86 to 7.78 mM were added after 30 minutes to the Gl laccase reaction with 5% w/v organosolv lignin to study any effect of the NaN_3 on the radical disappearance.

The initial radical disappearance rate was determined by linear fitting of three first points obtained for the radical concentration at each inactivation point, i.e. the radical concentration before enzyme inactivation and two points after inactivation (3.5 minutes in total).

Substrate and enzyme addition during an ongoing laccase reaction on lignin

Extra substrate addition was studied by adding 250 µL of 15% w/v lignin suspension to an ongoing reaction after 30 minutes. The substrate addition was studied on the reaction (1.5 mL) of 2.5% w/v lignin suspension (0.086 M phenolic concentration) with 1.38 mU of Gl laccase and on the reaction of 5% w/v lignin suspension (0.172 M phenolic concentration) with 1.5 and 6.48 mU of Tv and Mt, respectively. A control reaction with no extra substrate addition was performed where an equal amount of MilliQ water (250 µL) was added in order to determine the dilution.

Extra enzyme addition was studied using a similar set up as explained above. After 30 or 40 minutes reaction time extra enzyme was added in the same amount as the one used to start the reaction, i.e. 1.38, 1.5 and 6.48 mU for Gl, Tv and Mt laccase, respectively. As for the case of substrate addition the enzyme addition reactions (1.5 mL) were performed with 2.5% w/v lignin suspension (0.086 M phenolic concentration) for Gl and 5% w/v lignin suspension (0.172 M phenolic concentration) for Tv and Mt laccases. A control reaction with no extra enzyme addition was performed where an equal amount of MilliQ water was added in order to determine the dilution.

Statistical analysis

One-way ANOVA for determination of statistical significance for the kinetic data using Tukey's test with a pooled standard deviation and confidence intervals determination for radical disappearance rate were made in RStudio (RStudio Inc., Boston, USA). Statistical significance was established at $p \leq 0.05$.

Results and discussion

Laccase kinetics on lignin

Michaelis-Menten kinetics curves were obtained for three laccases *Ganoderma lucidum* (Gl), *Trametes versicolor* (Tv) and *Myceliophthora thermophila* (Mt) (Figure 2 panel a)) oxidizing organosolv lignin. The reactions were run on lignin suspensions and the lignin was insoluble during the reactions with laccase. The enzyme reactions were followed by measuring the radical formation with Electron Paramagnetic Resonance (EPR) spectroscopy. The phenolic concentration in lignin as determined by P-NMR[25,26] and the lignin percentage used in the reactions were converted into a resulting phenolic concentration and used as substrate concentration in the calculations of kinetic parameters (Table 1). Direct comparison of V_{max} (Table 1) for the different enzymes could not be performed due to the different enzyme dosages used to measure the kinetics

(because the enzymes were of different purity and had different activities on syringaldazine). The mechanism of the laccase catalyzed oxidation of the (phenolic) substrate during the four electron reduction of O_2 to H_2O is well described.[3,4] The transient kinetics of the reaction steps have been modeled to describe the reaction of the reduced form of the enzyme (E) with O_2 and the reactions of the oxidized enzyme with electron donating substrate (S).[28,29] In these transient kinetics modeling the laccase-catalyzed reaction is considered to consist of two successive irreversible reactions, reaction 1 and 2, respectively, that each has an overall rate constant specified as k_1 and k_2, respectively. The model thus includes conversion of the laccase enzyme to its oxidized state (E*) by O_2 and the reaction back to its reduced state (E) during the 4-electron formation of radicals ($S^{\bullet}$) during the reaction with the electron donating substrate (S) as follows:[28]

$$\text{Reaction 1: } E + O_2 \xrightarrow{k_1} E^* \qquad \text{R2: } E^* + 4\,S \xrightarrow{k_2} E + 4\,S^{\bullet} + H_2O$$

Considering the catalytic mechanism[3,4] it is relevant to consider the unique oxidative activation of the enzyme and then one overall reaction for describing the four sequential single electron reduction steps, with this second 4-step part of the reaction having a common rate constant (k_2). The currently available models[28,30] rely on soluble phenols as electron donating substrates, but they still do not capture the details of the real sequential mechanism, that involves the delicate formation of two different, partially oxidized enzyme intermediates and a secondary path that implicates the release of one molecule of H_2O during addition of two protons.[3,4] However, although very recent data imply that soluble (mono)phenolic substrates exhibit different binding modes to achieve an optimal position to reach the T1 copper site of fungal laccases,[31] at present there are no indications in the literature that laccases bind particularly tightly to insoluble lignin phenols or have binding domains or processive reaction modes that require specific kinetic considerations. In the present study the kinetics were indeed successfully modelled using pseudo first order Michaelis-Menten modeling (Figure 2). As discussed later, the quantitative kinetics and modeling revealed that only a small fraction of the total lignin phenols appear to be available for the enzyme catalysis explaining why the enzyme-catalysed reaction obeyed pseudo first order Michaelis-Menten kinetics with the phenolic concentration in lignin being the limiting substrate.

The reaction rates of Gl laccase reactions reached a plateau at lower phenol substrate concentrations than the Tv and Mt laccases (Figure 2 panel a)). It was investigated whether the presence of other components than the active laccase in the Gl preparation could affect the laccase reaction rate negatively. This was done by adding heat inactivated Gl laccase to both the Tv and Mt catalyzed reactions. These control experiments showed no influence on either the Tv or the Mt reaction rate compared to experiments without the addition of inactive Gl preparation (Figure 3).

Apparent specific activity (Table 1), corresponding to k_{cat}, is a measure of the rate at which the radicals are formed in lignin per enzyme dosage. This rate was highest for Tv laccase. Apparent catalytic efficiency represents the enzyme specificity constant, i.e. k_{cat}/K_m, and measures how efficiently the enzyme is converting substrate at low substrate concentrations. Tv and Gl laccase displayed the same apparent catalytic efficiency (Table 1) as a result of differences in K_m values. Even though Gl laccase showed a lower apparent specific activity its K_m is ca. five times lower than the one for Tv laccase and therefore Gl laccase has a much higher affinity to this type of lignin compared to Tv laccase. Mt laccase showed the lowest value of apparent catalytic efficiency caused by low apparent specific activity and high K_m compared to Gl laccase. A comparison of K_m values (expressed as mM) obtained for the three enzymes on organosolv lignin to K_m values determined previously in our group[19] on simple hydroxycinnamic acids, showed that the Gl and Tv laccases display K_m values three orders of magnitude lower on simple substrates compared to on the lignin used here (Mt was not included in the study of simple phenols). Considering the markedly lower enzyme dosage applied in our previous work [19] on the simple substrates this results in an apparent catalytic efficiency that is in the order of eight magnitudes higher on small soluble hydroxycinnamates compared to on the insoluble organosolv lignin.

Table 1. K_m, V_{max}, apparent specific activity and apparent catalytic efficiency for organosolv lignin[1].

		Mt	Gl	Tv
V_{max} [µM/min]		0.62 ± 0.01	0.36 ± 0.03	0.30 ± 0.04
K_m	[mM]	30.1 ± 0.7^{b}	15.3 ± 3.7^{c}	73.0 ± 5.9^{a}
	[g lignin/L]	8.7 ± 0.2^{b}	4.4 ± 1.1^{c}	21.2 ± 7.0^{a}
Apparent specific activity [µM/U·s]		1.59 ± 0.02^{c}	4.52 ± 0.14^{b}	16.8 ± 2.2^{a}
Apparent catalytic efficiency [1/U·s]		$0.53 \cdot 10^{-4} \pm 0.02 \cdot 10^{-4\ b}$	$3.03 \cdot 10^{-4} \pm 0.65 \cdot 10^{-4\ a}$	$2.42 \cdot 10^{-4} \pm 0.56 \cdot 10^{-4\ a}$

[1] K_m value is shown in mM of phenols and as g of lignin/L. Apparent specific activity is defined as the amount of substrate that is converted by the enzyme in one second; the apparent catalytic efficiency is the number of oxidation cycles that the enzyme is capable of in one second. Apparent specific activity and apparent catalytic efficiency are expressed based on syringaldazine activity units. Standard deviations are shown and significant difference ($p \leq 0.05$) of K_m and V_{max} are shown as superscripted letters (a-c).

Radical formation and disappearance

The time course for radical formation showed that after a certain time period depending on the lignin concentration a plateau in radical concentration was reached and hereafter the concentration of radicals started to decrease (Figure 2 panel b-d). The amount of lignin also determined the maximum level of radicals and the higher the lignin concentration the longer the time before the maximum was reached (Figure 2 panel b and c). This maximum level of radicals of could be converted into estimated concentrations of phenol oxidation achieved on the lignin by assuming that the laccases only catalyze the oxidation of phenol moieties. Such conversion corresponds to a maximum extent of 0.010% oxidation of the phenols by e.g. the Gl laccase after 60 min (Figure 2 panel b). The low levels of phenol oxidation suggest that the majority of phenol moieties in organosolv lignin are inaccessible to laccase oxidation possibly by steric hindrance/shielding or solid liquid interaction limitations.

This quantitative assessment furthermore explains why it is possible to model the bi-substrate laccase kinetics by simple pseudo-first order Michaelis-Menten kinetics of $E+S \rightleftarrows ES \rightarrow E+P$ for the kinetics parameter estimations with the lignin phenols as limiting substrate (S). The lignin phenols being available for reaction are the limiting substrate since the initial O_2 substrate concentration is ~260 µM in the reactions at 25 °C, which is 5-6 times higher than the maximum concentration of phenol radicals achieved, and, especially considering the stoichiometry of 4:1 of electron-donating phenols to O_2.

The laccase dosage in the reaction moreover affects the time it takes for the radical plateau to be reached (Figure 2 panel d). By increasing the dosage of Tv by a factor 5 it was possible to shorten the time to reach the plateau by 140 minutes (closed red left-pointed triangle in Figure 2 panel d).

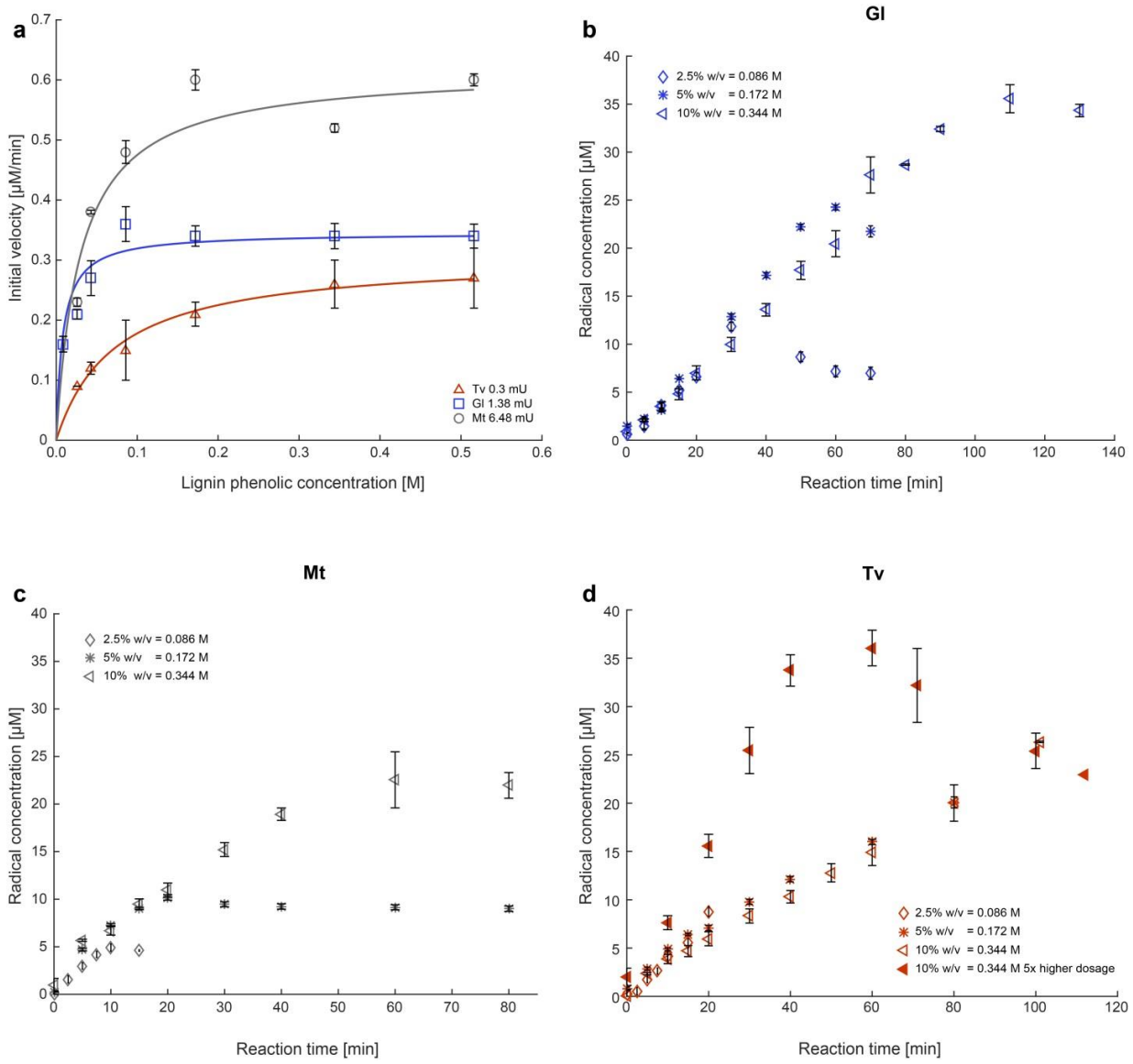

Figure 2. Michaelis-Menten curves for the Tv, Gl and Mt laccases (a) and radical formation at different lignin phenol concentrations for Gl (b), Mt (c) and Tv (d). Panel a; Tv (red triangle), Gl (blue square) and Mt (grey circle) kinetic curves are shown. Phenol concentration determined based on phenol content in lignin. Panel b-d; radical formation vs. extended reaction times at different lignin concentrations: 2.5% w/v, diamond; 5% w/v, star and 10% w/v, left-pointing triangle, are shown. Gl laccase (b) dosed 1.38 mU, Mt laccase (c) dosed 6.48 mU and Tv laccase (d) dosed 0.3 mU and Tv laccase dosed five times higher on 10% w/v lignin (1.5 mU). Standard deviations are also shown.

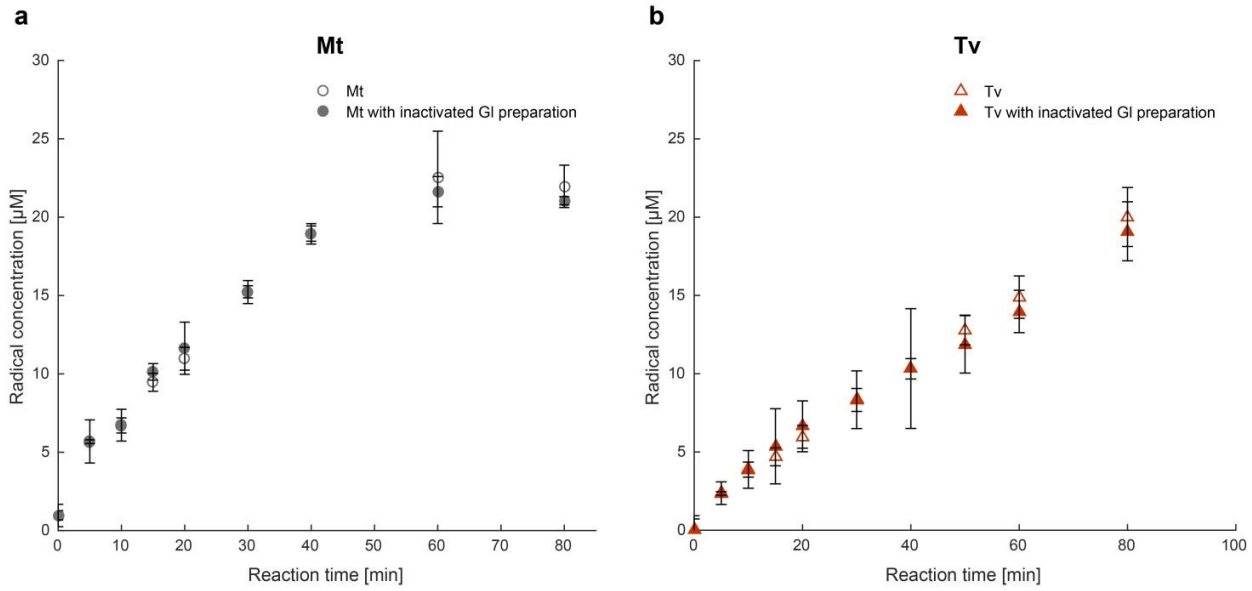

Figure 3. Comparison of radical formation kinetics of normal laccase catalyzed reactions for the Mt and Tv laccases, respectively, on 5 % w/v lignin, and the radical formation rates for each of those reactions in the presence of heat inactivated GI laccase preparation: (a) Radical concentrations of Mt laccase catalysis on lignin (grey open circle) and of Mt laccase catalysis on lignin with the heat inactivated GI preparation added (grey closed circle), and (b) radical concentrations of Tv laccase catalysis on lignin (red open triangle) and of Tv laccase with heat inactivated GI preparation added (red closed triangle). Standard deviations are shown as vertical bars on each point.

In order to investigate why the plateau was reached, additional enzyme or additional substrate was added to the ongoing laccase catalyzed reaction when the plateau was reached to study if either an enzyme inhibition/inactivation or substrate depletion event was taking place (Figure 4 and Supplementary Figure S2 and S3). As exemplified in the case of Tv laccase (Figure 4), addition of 57.5 mM fresh lignin-phenol substrate results in additional radical formation (Figure 4 panel a) while additional enzyme (Figure 4 panel b) did not promote the formation of new radicals after the plateau was reached (30 minutes), showing that substrate depletion is occurring and that the enzyme is apparently not inactivated to any detectable extent. After addition of 57.5 mM fresh substrate the radical rate formation of 1 µM/min obtained in the reaction from 30 to 40 minutes was equal to the rate obtained from 0 to 10 minutes. This result corroborates that the laccase remains active, and is in accord with the laccase working at V_{max}, which is consistent with the addition of extra lignin phenol substrate (57.5 mM) giving a total lignin substrate concentration of 6.67% w/v (ignoring the minor loss resulting from the reaction during the first 30 mins) and this radical formation rate of 1 µM/min agrees with the enzyme dosage being five times higher than the dosage used in the kinetic assay (Figure 2a).

Knowing that the radicals are unstable species, they seek to form stable products and thereby disappear.[32] Quenching of radicals is also expected to occur during laccase oxidation and the spontaneous chemical quenching of radicals was studied in order to access the extent of this reaction (Figure 5). Laccase oxidation was halted at distinct reaction time points by adding NaN_3 and the disappearance of radicals was followed (Figure 5 panel a, b and c). Control experiments verified that NaN_3 was not promoting the quenching of radicals certifying that NaN_3 only inactivated the enzyme (Figure 5 panel d). Immediately after enzyme inactivation the amount of radicals was measured and monitored until the decrease levelled out (Figure 5 panel a, b and c). The radical disappearance can be divided in two parts: the first part showing a fast initial disappearance interpreted as a first order reaction, where the rate can be described by a constant, and a second part where the radical disappearance rate is slowing down (Figure 5 panel a, b and c). This behaviour may be due to differences in reactivity of the radical species and to differences in the type of radical reactions taking place (Figure 5 panel f). The initial fast disappearance could be due to spontaneous quenching of two radical species leading to formation of non-radical species (Figure 5 panel f 1).

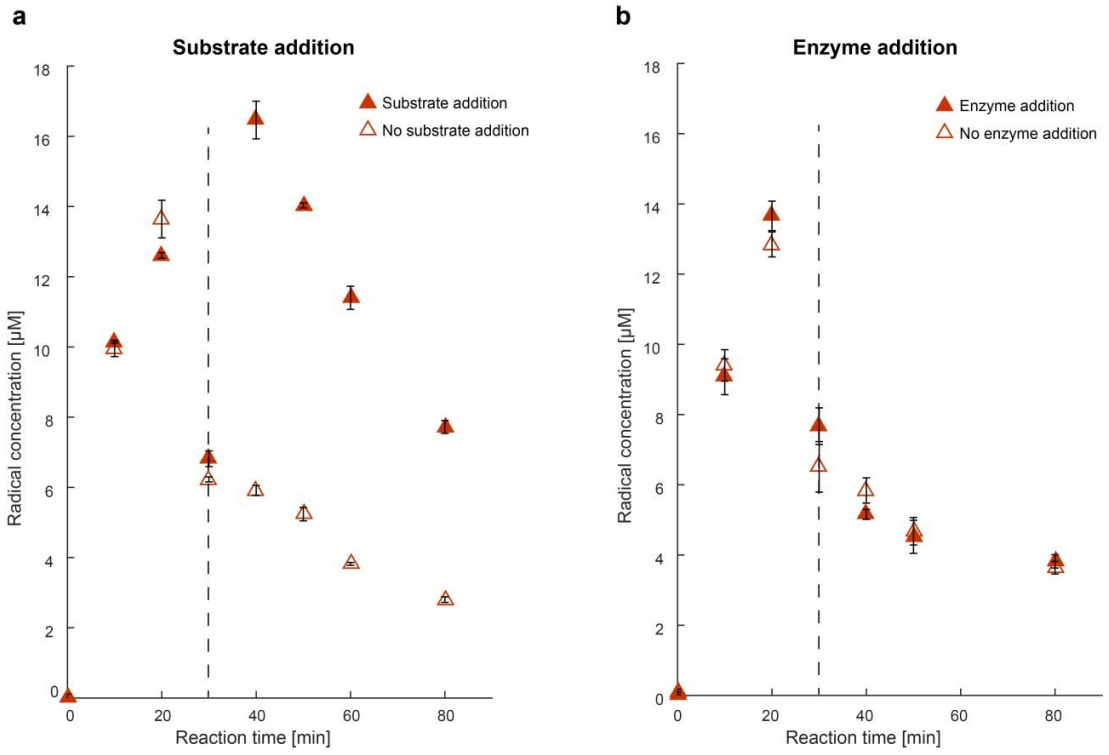

Figure 4. Extra substrate addition (a) and extra enzyme addition (b) on the reaction of 5% w/v lignin with Tv. For the additional substrate (a) 250 µL of 15% w/v lignin (red closed triangle) and 250 µL of water (red open triangle) were added after 30 min to the on-going reaction. For the additional enzyme (b) 60 µL of Tv (red closed triangle) and 60 µL of water (red open triangle) were added after 30 min to the on-going reaction. Data are shown ± standard deviation. Dashed vertical lines highlight the time point at which extra substrate or enzyme was added.

The second slower part could instead be due to secondary reactions of the radicals such as radical spreading and electron transfer reactions (Figure 5 panel f 2), both of which give rise to species with lower energy, i.e. with higher thermodynamic stability, thereby being less reactive leading to a slower disappearance rate.[33] A graphical plot of the rate of initial disappearance during the first 3.5 minutes for each radical disappearance measurement against the starting concentration of radicals yields a rate constant plot (Figure 5 panel e) and in each case displays a clear rate dependency of the radical concentration. When the rate constants were fitted using linear correlation and plotted with their 95% confidence intervals (Figure 5 panel e) the 95% confidence intervals for each enzyme reaction overlapped, signifying that the initial decay rates for each enzyme are not statistically different. Thus, as expected, the radical decay is non enzymatic as the rates are independent of the enzyme reaction and is purely a chemical reaction with a reaction rate depending on the radical concentration.

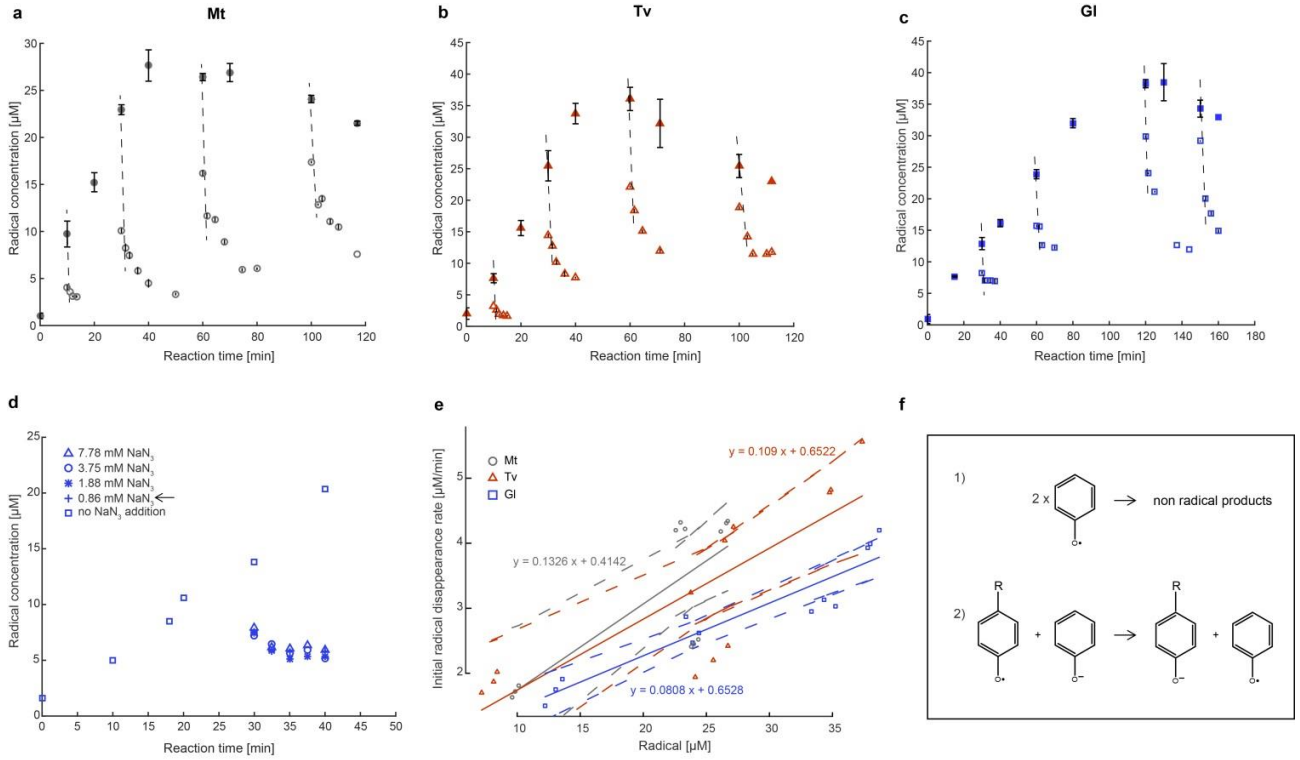

Figure 5. Radical disappearance (a, b, c), effect of NaN_3 concentration on the radical disappearance (d), radical disappearance rate (e), and possible radical reaction happening during disappearance (f). (a) The reaction of Mt laccase with 10% w/v lignin was followed over time and the enzyme was inactivated at different time point (10, 30, 60 and 100 min) with NaN_3 (grey open circle). (b) The reaction of Tv laccase with 10% w/v lignin was followed over time and the enzyme was inactivated at different time point (10, 30, 60 and 100 min) with NaN_3 (red open triangles). (c) The reaction of Gl laccase with 10% w/v lignin was followed over time and the enzyme was inactivated at different time point (30, 60, 120 and 150 min) with NaN_3 (blue open squares). In all (a), (b) and (c) the black dashed lines indicate the initial radical disappearance rates and the close marker are showing

the reaction without enzyme inactivation. (d) Radical decay for the reaction of Gl with 5% w/v organosolv lignin. Different concentrations of NaN_3 were used to stop the enzymatic reaction after 30 minutes and study in the NaN_3 concentration was affecting the radicals: 7.78 mM, blue triangle; 3.75 mM, blue circle 1.88 mM, blue star and 0.86 mM, blue plus. The Gl laccase reaction with no addition of NaN_3 is also shown (open blue square). The different NaN_3 concentration caused the same radical decay. The arrow is indicating the concentration of 0.86 mM NaN_3 used in the study to stop the enzymatic reactions in panel a. In order to improve (a), (b), (c) and (d) plot resolutions x and y axis do not show the same range. (e) Radical disappearance rate vs the radical concentration before enzyme inactivation for the three laccase: Gl, blue square; Mt, grey circle and Tv, red triangle. 95% confidence intervals (Gl, blue dotted line; Mt, grey dotted line and Tv, red dotted line) and linear correlations between disappearance rate and radical concentration (Gl, blue line; Mt, grey line and Tv, red line) show that the decay rates are essentially the same and following on average the equation $y = 0.1075 x + 0.5731$. (f) Two possible reaction pathways taken by the radical during quenching (1) and electron transfer reaction (2).

The detected radical levels are the result of two reactions: formation by enzyme oxidation of the phenolic groups and spontaneous radical quenching, both reactions taking place at the same time. During the first part of the reaction the enzymatic reaction is fast enough to generate a net positive formation of radicals. However, at the point at which the plateau is reached, the substrate starts to be less available and the enzymatic reaction slows down, and the radical disappearance takes over, producing a net decrease in the total radical levels is observed. The theoretical amount of radicals that the enzyme is able to produce is thus higher than the measured levels. The kinetic values presented in this work therefore must be considered as apparent because the rate calculations are based on the net steady state radical levels of the two competing reactions.

Laccase action on lignin has long been presumed to be dependent on mediators, or at least be vastly improved by mediators. Mediators are defined as low molecular weight compounds that are reactive in their oxidized as well as in their reduced form (depending on the mechanism of oxidation, the oxidation of mediators may produce radical intermediates). Mediators are believed to be able to enhance laccase catalyzed lignin modification either by acting as electron transfer reagents between the enzyme and the lignin phenol substrate or by expanding the oxidation capability of the enzyme.[34,35] The present work affirmed that fungal laccases can attack lignin directly without mediators. EPR measurements on laccase-mediator system (LMS) reactions on lignin has already shown that the presence of mediators does not enhance laccase catalyzed activation of lignin.[17] Hence, the use of EPR to monitor laccase-catalysis on lignin has not only enhanced our understanding of how laccase directly activates lignin, but also in a separate study changed the understanding of how LMS systems affect laccase-action on lignin. The EPR measurements captured the initial laccase-catalyzed reaction on lignin, confirming the presumed initial activation of lignin described in the literature[2]. The further fate of the lignin structure, and any possible further reactions and/or changes in the properties of the lignin induced by the initial laccase-catalyzed radical formation cannot be affirmed by EPR in the current set-up, but is part of our ongoing research.

Conclusions

EPR is a unique methodology able to assess radical formation and hence directly assessing lignin oxidation by laccase without prior extensive disruptive sample handling (like solubilisation or pyrolysis) and thus represents a unique method to detect the actual first product of such enzyme catalyzed reaction, namely radicals. In this work, we used EPR spectroscopy to determine laccase kinetics on organosolv lignin. Three laccases were tested and showed different behaviour towards organosolv lignin; Tv laccase showed the highest apparent specific activity while Gl showed the lowest K_m value, and the Gl laccase exhibited an apparent catalytic efficiency on lignin similar to the Tv laccase. In accord with the mechanism of action of laccases, the rate of the initial radical formation measured by EPR was interpreted as the direct laccase action on the lignin and the rates were used as a base to calculate the kinetic parameters. The kinetic parameters obtained for organosolv lignin were compared to the ones determined on monomeric hydroxycinnamates in a previous study[19] and showed that the laccases had significantly lower affinity towards lignin than towards the soluble hydroxycinnamic acids and consequently much lower turnover rates were recorded for the enzyme action on lignin. By following the radical formation over time for more extended reaction times for each enzymatic reaction, a plateau in radical concentration was reached in all the catalyzed reactions and this was found to be due to substrate depletion. Also the spontaneous radical disappearance was monitored and assessed and initial radical decay rates after laccase inactivation at different reaction time were determined. Comparing the initial radical decay rates for the different laccases no statistical difference between enzyme reactions were evident meaning that the radical decay is enzyme independent and due to chemical quenching of radicals via non-enzyme catalyzed radical-radical reactions. When a laccase catalyzed oxidation of lignin is monitored by EPR spectroscopy the radical concentration measured is a net value of the sum of two reactions happening at the same time: the spontaneous radical quenching and laccase catalyzed oxidation of lignin and thus the kinetic values obtained should be considered apparent. The findings obtained by direct measurement by EPR of radical formation (and decay) for laccase-catalysis on lignin thus enhance our understanding of how laccase attacks lignin and may furthermore be of significance for development of enzyme assisted lignin and lignocellulose refining processes.

Conflicts of interest

The authors declare no competing financial interest.

Acknowledgements

This study was supported by the Danish Council for Independent Research (Project ref. DFF-4184-00355) and by the PhD Program at the Technical University of Denmark. We thank University of Hamburg, Germany for the P-NMR data on organosolv lignin and Novozymes (Bagsværd, Denmark) for donating the *Myceliophthora thermophila* laccase.

Supporting information

Schematic representation of the EPR technique and data analysis, substrate and enzyme addition for Mt and Gl laccase and radical disappearance for Gl and Tv laccase.

File name Supporting_information.pdf

References

(1) Belgacem, M. N.; Gandini, A.; Boston, A. *Monomers, Polymers and Composites from Renewable Resources*; 2008.

(2) Munk, L.; Sitarz, A. K.; Kalyani, D. C.; Mikkelsen, J. D.; Meyer, A. S. Can Laccases Catalyze Bond Cleavage in Lignin? *Biotechnol. Adv.* **2015**, *33* (1), 13–24. https://doi.org/10.1016/j.biotechadv.2014.12.008.

(3) Sitarz, A. K.; Mikkelsen, J. D.; Meyer, A. S. Structure, Functionality and Tuning up of Laccases for Lignocellulose and Other Industrial Applications. *Crit. Rev. Biotechnol.* **2016**, *36* (1), 70–86. https://doi.org/10.3109/07388551.2014.949617.

(4) Jones, S. M.; Solomon, E. I. Electron Transfer and Reaction Mechanism of Laccases. *Cell. Mol. Life Sci.* **2015**, *72* (5), 869–883. https://doi.org/10.1007/s00018-014-1826-6.

(5) Mai, C.; Schormann, W.; Hüttermann, A.; Kappl, R.; Hüttermann, J. The Influence of Laccase on the Chemo-Enzymatic Synthesis of Lignin Graft-Copolymers. *Enzyme Microb. Technol.* **2002**, *30* (1), 66–72. https://doi.org/10.1016/S0141-0229(01)00457-4.

(6) Virk, A. P.; Sharma, P.; Capalash, N. Use of Laccase in Pulp and Paper Industry. *Biotechnol. Prog.* **2012**, *28* (1), 21–32. https://doi.org/10.1002/btpr.727.

(7) Hilgers, R.; Vincken, J.-P.; Gruppen, H.; Kabel, M. A. Laccase/Mediator Systems: Their Reactivity toward Phenolic Lignin Structures. **2018**. https://doi.org/10.1021/acssuschemeng.7b03451.

(8) Khulbe, K. C.; Ismail, A. F.; Matsuura, T. Electron Paramagnetic Resonance (EPR) Spectroscopy. *Membr. Charact.* **2017**, 47–68. https://doi.org/10.1016/B978-0-444-63776-5.00003-6.

(9) Roessler, M. M.; Salvadori, E. Principles and Applications of EPR Spectroscopy in the Chemical Sciences. *2534 | Chem. Soc. Rev* **2018**, *47*, 2534. https://doi.org/10.1039/c6cs00565a.

(10) Gerson, F.; Huber, W. *Electron Spin Resonance Spectroscopy of Organic Radicals*; Wiley-VCH, 2003.

(11) Steelink, C.; Hansen, R. E. A Solid Phenoxy Radical from Disyringylmethane–a Model for Lignin Radicals. *Tetrahedron Lett.* **1966**, *7* (1), 105–111. https://doi.org/10.1016/S0040-4039(01)99639-X.

(12) REX, R. W. Electron Paramagnetic Resonance Studies of Stable Free Radicals in Lignins and Humic Acids. *Nature* **1960**, *188* (4757), 1185–1186. https://doi.org/10.1038/1881185a0.

(13) Steelink, C. Free Radical Studies of Lignin, Lignin Degradation Products and Soil Humic Acids. *Geochim. Cosmochim. Acta* **1964**, *28* (10–11), 1615–1622. https://doi.org/10.1016/0016-7037(64)90010-9.

(14) Patil, S. V.; Argyropoulos, D. S. Stable Organic Radicals in Lignin: A Review. *ChemSusChem* **2017**, *10* (17), 3284–3303. https://doi.org/10.1002/cssc.201700869.

(15) Bährle, C.; Nick, T. U.; Bennati, M.; Jeschke, G.; Vogel, F. High-Field Electron Paramagnetic Resonance and Density Functional Theory Study of Stable Organic Radicals in Lignin: Influence of the Extraction Process, Botanical Origin, and Protonation Reactions on the Radical **g** Tensor. *J. Phys. Chem. A* **2015**, *119* (24), 6475–6482. https://doi.org/10.1021/acs.jpca.5b02200.

(16) Stephen Y. Lin, C. W. D. Chapter 5.5 Electron Spin Resonance (ESR) Spectroscopy. In *Methods in Lignin Chemistry*; 1992; pp 274–286.

(17) Munk, L.; Andersen, M. L.; Meyer, A. S. Influence of Mediators on Laccase Catalyzed Radical Formation in Lignin. *Enzyme Microb. Technol.* **2018**, *116*, 48–56.

https://doi.org/10.1016/J.ENZMICTEC.2018.05.009.

(18) Munk, L.; Andersen, M. L.; Meyer, A. S. Direct Rate Assessment of Laccase Catalysed Radical Formation in Lignin by Electron Paramagnetic Resonance Spectroscopy. *Enzyme Microb. Technol.* **2017**, *106*, 88–96. https://doi.org/10.1016/J.ENZMICTEC.2017.07.006.

(19) Perna, V.; Agger, J. W.; Holck, J.; Meyer, A. S. Multiple Reaction Monitoring for Quantitative Laccase Kinetics by LC-MS. *Sci. Rep.* **2018**, *8* (1), 8114. https://doi.org/10.1038/s41598-018-26523-0.

(20) Sitarz, A. K.; Mikkelsen, J. D.; Højrup, P.; Meyer, A. S. Identification of a Laccase from Ganoderma Lucidum CBS 229.93 Having Potential for Enhancing Cellulase Catalyzed Lignocellulose Degradation. *Enzyme Microb. Technol.* **2013**, *53* (6–7), 378–385. https://doi.org/10.1016/J.ENZMICTEC.2013.08.003.

(21) Han, M.-J.; Han, M.-J.; Choi, H.-T.; Song, H.-G. Purification and Characterization of Laccase from the White Rot Fungus Trametes Versicolor. *J. Microbiol.* **2005**, *43* (6), 555–560.

(22) Jönsson, L.; Sjöström, K.; Häggström, I.; Nyman, P. O. Characterization of a Laccase Gene from the White-Rot Fungus Trametes Versicolor and Structural Features of Basidiomycete Laccases. *Biochim. Biophys. Acta - Protein Struct. Mol. Enzymol.* **1995**, *1251* (2), 210–215. https://doi.org/10.1016/0167-4838(95)00104-3.

(23) Berka, R. M.; Schneider, P.; Golightly, E. J.; Brown, S. H.; Madden, M.; Brown, K. M.; Halkier, T.; Mondorf, K.; Xu, F. Characterization of the Gene Encoding an Extracellular Laccase of Myceliophthora Thermophila and Analysis of the Recombinant Enzyme Expressed in Aspergillus Oryzae. *Appl. Environ. Microbiol.* **1997**, *63* (8), 3151–3157.

(24) Hollmann, F.; Gumulya, Y.; Tölle, C.; Liese, A.; Thum, O. Evaluation of the Laccase from Myceliophthora Thermophila as Industrial Biocatalyst for Polymerization Reactions. *Macromolecules* **2008**, *41*, 8520–8524. https://doi.org/10.1021/ma801763t.

(25) Podschun, J.; Saake, B.; Lehnen, R. Reactivity Enhancement of Organosolv Lignin by Phenolation for Improved Bio-Based Thermosets. *Eur. Polym. J.* **2015**, *67*, 1–11. https://doi.org/10.1016/j.eurpolymj.2015.03.029.

(26) Granata, A.; Argyropoulos, D. S. 2-Chloro-4,4,5,5-Tetramethyl-1,3,2-Dioxaphospholane, a Reagent for the Accurate Determination of the Uncondensed and Condensed Phenolic Moieties in Lignins. *J. Agric. Food Chem.* **1995**, *43* (6), 1538–1544. https://doi.org/10.1021/jf00054a023.

(27) Silva, I. R.; Larsen, D. M.; Meyer, A. S.; Mikkelsen, J. D. Identification, Expression, and Characterization of a Novel Bacterial RGI Lyase Enzyme for the Production of Bio-Functional Fibers. *Enzyme Microb. Technol.* **2011**, *49* (2), 160–166. https://doi.org/10.1016/J.ENZMICTEC.2011.04.015.

(28) Rangelov, S.; Nicell, J. A. A Model of the Transient Kinetics of Laccase-Catalyzed Oxidation of Phenol at Micromolar Concentrations. *Biochem. Eng. J.* **2015**, *99* (99), 1–15. https://doi.org/10.1016/j.bej.2015.02.034.

(29) Kurniawati, S.; Nicell, J. A. A Comprehensive Kinetic Model of Laccase-Catalyzed Oxidation of Aqueous Phenol. *Biotechnol. Prog.* **2009**, *25* (3), 763–773. https://doi.org/10.1002/btpr.111.

(30) Rangelov, S.; Nicell, J. A. Modelling the Transient Kinetics of Laccase-Catalyzed Oxidation of Four Aqueous Phenolic Substrates at Low Concentrations. *Biochem. Eng. J.* **2018**, *132*, 233–243. https://doi.org/10.1016/J.BEJ.2018.01.016.

(31) Mehra, R.; Muschiol, J.; Meyer, A. S.; Kepp, K. P. A Structural-Chemical Explanation of Fungal Laccase

Activity. *Sci. Rep.* **2018**, *8* (1), 17285. https://doi.org/10.1038/s41598-018-35633-8.

(32) Samanta, A.; Bhattacharyya, K.; Das, P. K.; Kamat, P. V; Weir, D.; Hug, G. L. *Quenching of Excited Doublet States of Organic Radicals by Stable Radicals*; 1989; Vol. 93.

(33) Sawada, H. Chapter 3. Thermodynamics of Radical Polymerization. *J. Macromol. Sci. Part C Polym. Rev.* **1969**, *3* (2), 357–386. https://doi.org/10.1080/15583726908545928.

(34) Rochefort, D.; Leech, D.; Bourbonnais, R. Electron Transfer Mediator Systems for Bleaching of Paper Pulp. *Green Chem.* **2004**, *6* (1), 14. https://doi.org/10.1039/b311898n.

(35) Astolfi, P.; Brandi, P.; Galli, C.; Gentili, P.; Gerini, M. F.; Greci, L.; Lanzalunga, O. New Mediators for the Enzyme Laccase: Mechanistic Features and Selectivity in the Oxidation of Non-Phenolic Substrates. *New J. Chem.* **2005**, *29* (10), 1308. https://doi.org/10.1039/b507657a.

For Table of Contents Only

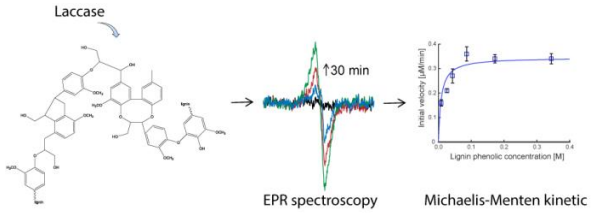

Synopsis

Determination of laccase reaction kinetics on lignin and concurrent radical reactions of significance for biotechnological lignin valorization and natural carbon cycling.

SUPPORTING MATERIAL

Laccase induced lignin radical formation kinetics evaluated by Electron Paramagnetic Resonance spectroscopy

Valentina Perna[a], Jane W. Agger[a], Mogens Larsen Andersen[b], Jesper Holck[a], Anne S. Meyer[a*]

[a] Section for Protein Chemistry and Enzyme Technology, Department of Biotechnology and Biomedicine, Technical University of Denmark, Kgs. Lyngby 2800, Denmark

[b] University of Copenhagen, Faculty of Science, Department of Food Science, Rolighedsvej 30, Frederiksberg C 1958, Denmark

[*]Corresponding author, address as above, e-mail: asme@dtu.dk

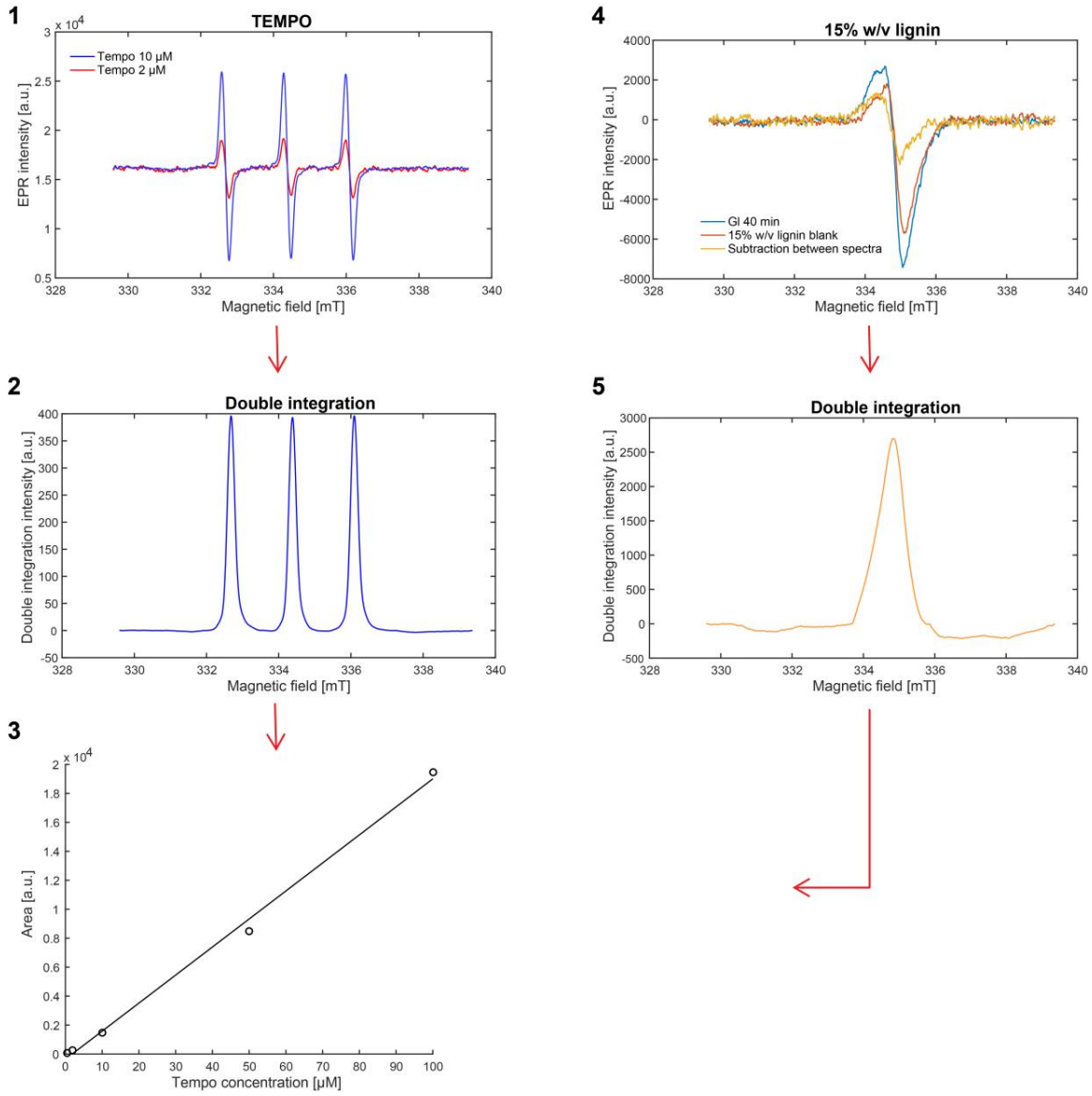

Figure S1. Schematic representation of the EPR technique and data analysis. 1) Typical three line EPR spectra of 10 µM (blue) and 2 µM (red) TEMPO. 2) Double integration of the TEMPO spectra. The double integration was performed directly with the MPlot software (Magnettech, Berlin, Germany) and the area below the three peaks was determined. 3) TEMPO calibration curve. The areas obtained in 2) were plotted vs the TEMPO concentrations. 4) EPR spectra of Gl laccase 15 minutes reaction (blue) with 15% w/v lignin, EPR spectra of the blank 15% w/v lignin (red) and the resulted EPR spectra after subtraction of the blank from the reaction spectra (yellow). The subtraction of blank lignin spectra was performed for all reaction time in order to determine only the amount of radical formed during laccase oxidation of lignin. 5) Double integration of the subtracted spectra in 4). The area below the peak was then converted into a radical concentration by employing the TEMPO calibration curve in 3).

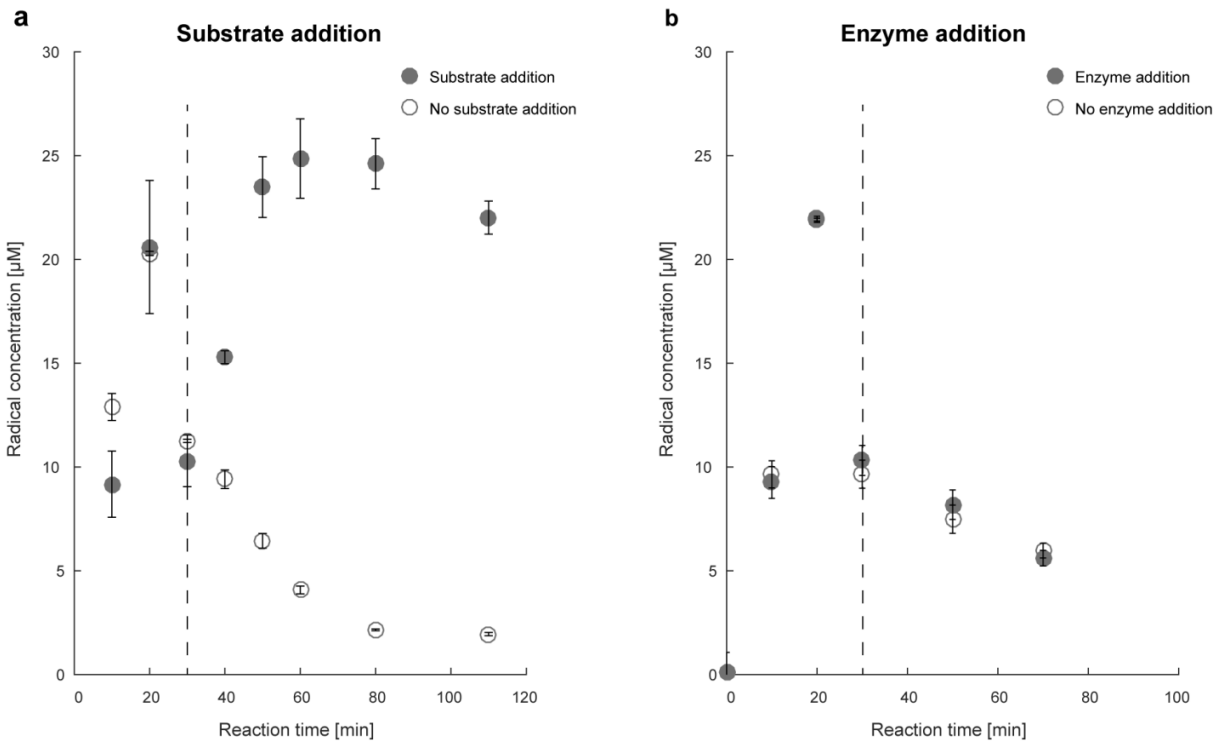

Figure S2. Extra substrate addition (a) and extra enzyme addition (b) on the reaction of 5% w/v lignin content with the Mt laccase. For the additional substrate (a) 250 µL of 15% w/v lignin (grey close circle) and 250 µL of water (grey open circle) were added after 30 min to the on-going reaction. For the additional enzyme (b) 60 µL of Mt (grey close circle) and 60 µL of water (grey open circle) were added after 30 min to the on-going reaction. Standard deviations are shown. Dashed vertical lines are highlighting the time point at which extra substrate or enzyme was added.

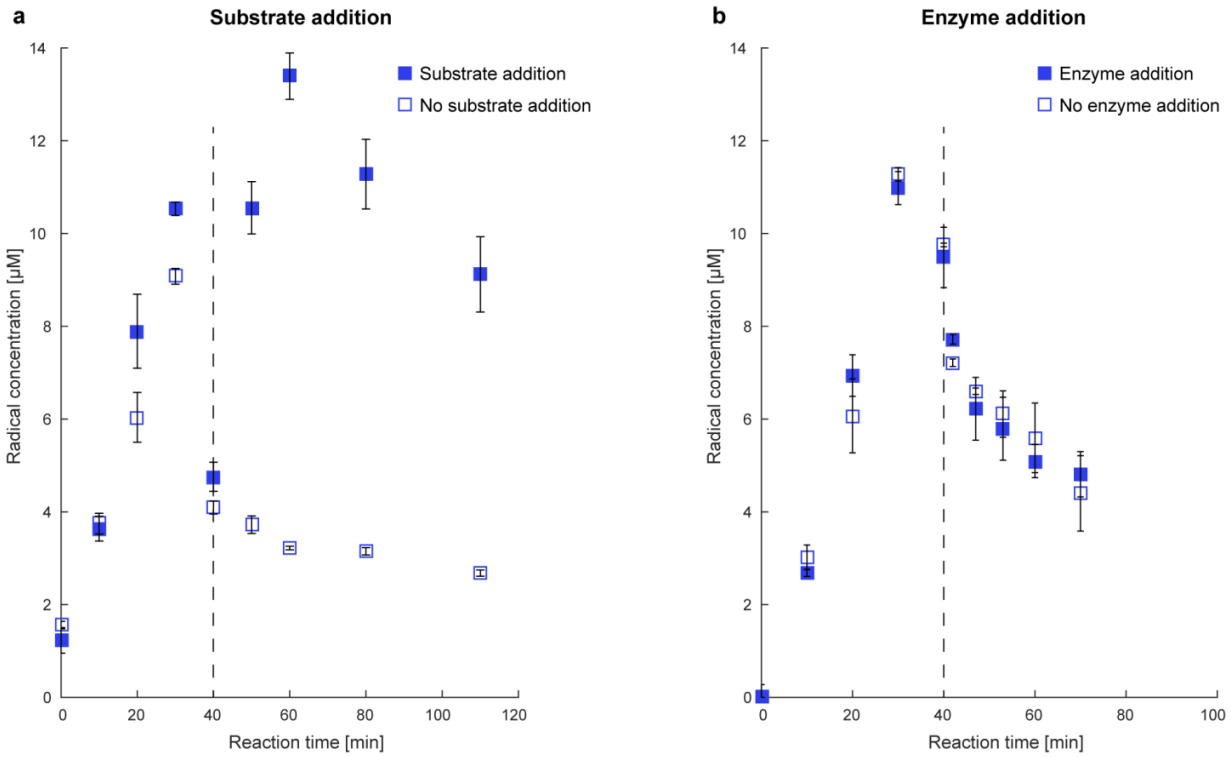

Figure S3. Extra substrate addition (a) and extra enzyme addition (b) on the reaction of 2.5% w/v lignin content with GI. For the additional substrate (a) 250 µL of 15% w/v lignin (blue close square) and 250 µL of water (blue open square) were added after 40 min to the on-going reaction. For the additional enzyme (b) 60 µL of GI (blue close square) and 60 µL of water (blue open square) were added after 40 min to the on-going reaction. Standard deviations are shown. Dashed vertical lines are highlighting the time point at which extra substrate or enzyme was added.

Paper 4

Laccase catalyzed oxidation of lignin induces production of H2O2

ARTICLE

Laccase catalyzed oxidation of lignin induces production of H_2O_2

Valentina Perna[a], Anne S. Meyer[a], Jesper Holck[a], Vincent Eijsink[b] and Jane Wittrup Agger*[a]

Received 00th January 20xx,
Accepted 00th January 20xx

DOI: 10.1039/x0xx00000x

Laccases are blue copper enzymes known for their ability to oxidize phenols. Laccases are abundant enzymes in microorganisms specialised in lignocellulose degradation but their exact role in this process is still not well described. Laccases can oxidize lignin and the first product is a reactive lignin radical in the form a phenoxy radical. The heterogeneous lignin structure can stabilize these radicals for a certain time period but eventually they propagate, likely via several routes that remain largely unknown. We show that laccase oxidation of lignin leads to formation of hydrogen peroxide, likely because lignin radicals react with molecular oxygen. This observation is new and has implications to the understanding of the roles of laccases in lignocellulose degradation. Hydrogen peroxide is a common co-substrate for other enzymes acting on lignin (e.g. peroxidases) and for cellulose degrading enzymes currently known as lytic polysaccharide monooxygenases (LPMOs). Accordingly, we show that the hydrogen peroxide produced after laccase oxidation of lignin can activate LPMOs. In addition, we show that hydrogen peroxide formation is a common phenomenon in laccase reactions, as it occurs in all tested laccase reactions with four different enzymes on both organosolv lignin and birch wood. These results shed new light on the role of laccases during lignocellulose conversion and reveal a possible connection between the conversion of the lignin and the polysaccharides in this co-polymeric material.

Introduction

Lignocellulose and lignin in particular offer numerous possibilities for sustainable production of chemicals and high value products like carbon fibers, elastomers, composite materials and platform chemicals.[1,2] A new movement in sustainable chemistry known as "Lignin-first"[3] seeks to better exploit natural lignin sources through increased understanding of the oxidative degradation routes that lignin may undergo. Lignin has the potential to become a pillar stone in the future biobased economy.[1]

Laccases (EC 1.10.3.2) are versatile enzymes known for their oxidative action on a variety of phenolic compounds.[4] These blue copper enzymes are widely present in both fungal and bacterial microorganisms[5] capable of enzymatic degradation of lignocellulosic plant material, and laccases have been postulated to play an important role in oxidative modification of lignin, although their role in biological lignin turnover remains enigmatic.[6] Laccases oxidize a range of phenols including the monomeric units in lignin. During one complete reaction cycle laccases oxidize four moles of phenolic substrate by abstracting four electrons, which are then shuttled through the enzyme to reduce one mole of O_2 into two moles of H_2O.[5] The first product of laccase oxidation of a phenol is a semiquinone, which is a radical species with high reactivity.[7] Hence, laccase oxidation often leads to polymerization of products as these semiquinones react spontaneously with each other. On lignin, laccases also induce radical formation,[8] but the large heterogeneous polyaromatic structure of lignin leads to resonance stabilization that causes these radical species to exist long enough to be detectable.[9,10] Eventually, lignin radicals propagate but their exact fate is not known.

Possible routes for quenching lignin radicals include polymerization, grafting of small soluble phenols,[7] and even processes that lead to bond breakage. However, bond cleavage is difficult to prove and is yet speculative. Considering the reactivity of lignin radicals, we hypothesized that formation of reactive oxygen species, such as hydrogen peroxide, might also be a possible destination for the unpaired electrons in lignin after laccase oxidation. Hydrogen peroxide is an important oxidizing species in lignocellulose degradation as several other lignocellulose-degrading or -modifying enzymes consume hydrogen peroxide. Such enzymes include various lignin peroxidases[11] and also lytic polysaccharide monooxygenases (LPMOs) that act on cellulose and other polysaccharides in lignocellulose.[12,13] White-rot fungi and other microorganisms possess enzyme systems for hydrogen peroxide generation like aryl alcohol oxidases (AAO, CAZy auxiliary activities family 3, AA3).[14,15] In support of our hypothesis concerning the role of laccases, fungal genomes and transcriptomes show high co-existence of laccases and hydrogen peroxide utilizing enzymes.[16,17]

In this paper we show that laccase-catalyzed oxidation of lignin induces the formation of micro molar concentrations of hydrogen peroxide in reaction supernatants and that the rate of H_2O_2 formation is dependent on type of laccase and enzyme

[a] *Technical University of Denmark, Department of Biotechnology and Biomedicine, Søltofts Plads 221, DK-2800 Kgs. Lyngby*
[b] *Norwegian University of Life Sciences, Faculty of Chemistry, Chr. M. Falsensvei 1, NO-1430 Ås.*
* Corresponding author
Electronic Supplementary Information (ESI) available: [details of any supplementary information available should be included here]. See DOI: 10.1039/x0xx00000x

dosage. We show that this is a general phenomenon, by analysing four different laccases (three fungal and one bacterial) on two different lignin rich substrates, one of which is milled birch wood. In addition, we show that the levels of hydrogen peroxide generated as a result of lignin oxidation are sufficient to fuel the activity of LPMOs. Hence, these results suggest a plausible important role for laccases during enzymatic lignocellulose degradation, namely the controlled formation of hydrogen peroxide.

Experimental

Materials

Organosolv lignin (CAS No. 8068-03-9) with a volume-based particle size of D[4,3] = 6.4 µm and composed of 94 wt% Klason lignin was purchased from Sigma-Aldrich (Milwaukee, WI, USA). Birch wood originating from Norway was subjected to ball milling and the fraction with D < 250 µm was collected. Birch wood and organosolv lignin were suspended in Milli-Q water to a final concentration of 5% w/v and 10% w/v, respectively. After 30 minutes magnetic stirring, the pH was adjusted to 5.0 with NaOH. An AA10 LPMO from *Serratia marcescens* (CBP21 or *Sm*LPMO10A) and an AA9 LPMO from *Neurospora crassa* (*Nc*LPMO9C) were produced and purified as described earlier.[18,19] Laccase from *Trametes versicolor* (Tv) was purchased from Sigma-Aldrich (Steinheim, Germany), *Myceliophthora thermophila* (*Mt*) laccase was a kind gift from Novozymes A/S, Bagsværd, Denmark, *Amycolatopsis sp. 75iv2* (*Slac*) laccase was a kind from Professor Lindsay D. Eltis from the University of British Columbia and *Ganoderma lucidum* (Gl) laccase was produced in house using *Pichia pastoris* as heterogeneous expression system.

The construct containing the gene encoding for Gl laccase was codon optimized for *Pichia* in a *p*PICZalpha vector with yeast α-factor as signal peptide and zeocin as selective marker and transformed in a protease free *Pichia pastoris* strain (SMD1168H).[20] Positive clones were selected on YDP plates containing 100 µg/mL zeocin and fermented in 5 L scale according to Silva *et al.*[21] In short, a 5L Sartorius Biostat Aplus fermenter with basal salt medium was inoculated with an overnight culture of the transformed *Pichia*-strain. The total fermentation time was approx. 160 hours and the fermenter was operated in three modes; glycerol batch, glycerol fed-batch and lastly methanol fed-batch for induction. In order to improve the enzyme's stability the methanol fed-batch phase was carried out at 20°C. Laccase-containing fermentation broth was recovered by centrifugation at 5300 x g, 5°C for 1 h, subjected to sterile filtration and concentrated by ultrafiltration using a cross-flow bioreactor system with a 10 kDa cutoff membrane (Millipore, Sartorius, Denmark), as described by Silva *et al.*[21]

Laccase activity assay

Laccase activity was assessed by monitoring the oxidation of syringaldazine (SGA) at 530 nm ($\varepsilon = 6.5 \times 10^4\ M^{-1}\ cm^{-1}$). The assay reaction mixture contained 25 µM syringaldazine, 10% ethanol, 25 mM sodium acetate pH 5.0 and a proper amount of enzyme. Syringaldazine oxidation was monitored at 25°C for 20 minutes. Enzyme activity was expressed in units: One Unit (U) was defined as the amount of enzyme able to catalyse oxidation of 1 µmol of substrate (syringaldazine) in one minute under the assay reaction conditions. SGA activity was used in this work as a measure of enzyme dose to overcome the differences in enzyme purity between preparations. Therefore Tv, Mt, Gl and Slac laccases were dosed according to SGA activity in the reactions.

Dose response study of H_2O_2 formation after laccase oxidation of lignin

H_2O_2 formation during laccase oxidation of 5% w/v birch wood was followed for 0, 0.5, 1, 3 and 6 h using independent reactions for each time point and reaction volumes of 250 µL, with incubation at 25°C and 1100 rpm. Reactions were started by adding laccase, in different dosages: 0.3, 0.9, 1.8 mU and 3.5 mU for Tv; 6.5, 19.4 and 38.9 mU for Mt; 1.4, 4.1 and 8.3 mU for Gl and 0.03, 0.07 and 0.13 mU for Slac. After incubation, samples were centrifuged at 15000 g for 3 minutes, the supernatant containing the laccase was recovered and the enzyme was heat inactivated by incubation at 100°C for 10 minutes. The H_2O_2 concentration was measured using the Amplex™ Red Hydrogen Peroxide/Peroxidase Assay Kit (ThermoFisher Scientifics) following the manufacturer's instructions.

Qualitative assessment of LPMO activity

Activity of both CBP21 and *Nc*LPMO9C was tested in a standardized setup with ascorbic acid using β-chitin or phosphoric acid swollen cellulose (PASC) as substrate, respectively. The standard setup for CBP21 was 1 µM enzyme incubated with 5 mg/mL β-chitin in 20 mM Tris-HCl buffer pH 8.0 and 2 mM ascorbic acid as reductant. The standard setup for *Nc*LPMO9C was 1 µM enzyme incubated with 5 mg/mL PASC suspended in 20 mM sodium acetate buffer pH 5.0 and 1 mM ascorbic acid. Both standard reactions were incubated 24 hours at 50 °C and 800 rpm. Product formation was confirmed by using MALDI-TOF MS, using an Ultraflex MALDI-TOF/TOF instrument (Bruker Daltonics GmbH, Bremen, Germany) equipped with a nitrogen 337 nm laser beam. Two µL of 10 mg/mL of 2,5-dihydroxybenzoic acid (DHB) in 75% acetonitrile was applied to an MTP 384 ground steel target plate TF (Bruker Daltonics). 1 µL of each sample was mixed with the DHB followed by drying with a stream of air. The analyses of the samples were performed in positive acquisition and the instrument was controlled by the FlexControl 3.3 software package. All spectra were obtained using the linear mode with an acceleration voltage of 20 kV, and pulsed ion extraction of 10 ns. The data were collected from averaging 400 laser shots, with the lowest laser energy necessary to obtain sufficient signal to noise ratios. Peak lists were generated from the MS spectra using Bruker flexAnalysis software (version 3.3). This set up was used to assess whether the used LPMOs were active, and this was indeed the case (Fig S1).

LPMO reactions

5% w/v birch wood or 10% w/v organosolv lignin was incubated for one hour with the highest laccase dose of those listed above, except for the Mt laccase, which was dosed at the second highest dose (19.4 mU). The laccase dosages were set in order for all reactions to reach approximately the same level of hydrogen peroxide after one hour reaction. The samples were treated as mentioned above, i.e. after one hour the samples were centrifuged and the supernatants were heat inactivated. The supernatants were subjected to removal of small phenols by solid phase extraction through a Dionex OnGuard™ IIP column consisting of a polyvinylpyrrolidone polymer with high selectivity for phenols (ThermoFisher Scientifics). The UV absorption profile before and after this extraction step was analysed by LC-MS as described below and by basic absorbance scan readings in the range from 230-400 nm using a TECAN Infinite® 200 instrument (Tecan Trading AG, Switzerland) in 96-well plate format. The H_2O_2 concentrations in the cleaned supernatant were measured and control experiments were performed to assess if the cleaning step was removing any H_2O_2. The conclusion was that the H_2O_2 concentration was not affected by the solid phase extraction.

From each laccase reaction 300 µL of cleaned or uncleaned supernatant were added to 100 µL reaction mixture containing 1 µM CBP21, 5 mg/mL β-chitin in 20 mM Tris-HCl buffer pH 8.0 and 2 µM ascorbic acid or to 100 µL reaction mixture containing 1 µM *Nc*LPMO9C, 5 mg/mL PASC in 20 mM sodium acetate buffer pH 5.0 and 50 µM ascorbic acid. A number of control experiments were performed as described below. The reactions mixtures were incubated at 50 °C and 800 rpm for 24 h. The reaction products were analysed by LC-MS as described below. In addition to the reactions described above, anaerobic LPMO experiments, were conducted where 300 µL of clean reaction supernatant from Tv laccase oxidation of organosolv lignin was added to 100 µL suspension of β-chitin (5 mg/mL) in 20 mM Tris-HCl buffer pH 8.0 and flushed with nitrogen gas for 5 minutes. Then, 1 µM CBP21 and 2 µM ascorbic acid were added (in this order) to start the reaction after which the head space of the reaction tube was flushed with nitrogen gas for one minute before closing. The lid was sealed with parafilm. The same type of anaerobic experiment was performed with standard reaction conditions containing 5 mg/mL β-chitin, 1 µM CBP21 and 2 mM ascorbic acid. All anaerobic reaction mixtures were incubated at 50 °C, 850 rpm for 24 h.

LC-MS analysis of β-chitin oxidation products

Lytic oxidation of β-chitin was assessed using liquid chromatography and mass spectroscopy (LC-MS). Prior to analysis the samples were diluted in 70% acetonitrile. 10 µL was injected onto a TSKgel Amide 80 HILIC column (150 mm × 2 mm; 2 µm, TOSOH, Greisheim, Germany). The chromatography was performed on a Dionex UltiMate 3000 UPLC (Thermo Fischer Scientific, Sunnyvale, CA, USA) at 0.2 mL min^{-1} and 55°C with a two-eluent system consisting of eluent A, 0.1% formic acid in water, and eluent B, acetonitrile. The elution was performed as follows: 0-5 min, isocratic 25% A, 75% B; 5–25 min, linear gradient to 70% A, 30% B; hereafter going directly to 25–30 min isocratic regeneration with 95% A, 5% B followed directly by 30–40 min isocratic equilibration with 25% A, 75% B. The HPLC was connected to an ESI-iontrap (model Amazon SL from Bruker Daltonics, Bremen, Germany) and the electrospray was operated in full scan mode with target mass settings of 1200 *m/z* and a scan range from 70 to 2200 *m/z*. Automatic MS2 events was excecuted for the two highest prevalent precursor ions. 100% amplitude for fragmentation reaction was selected in order to obtain sufficient fragmentation. The spray settings were: capillary voltage of 4.5 kV, end plate offset 0.5 kV, nebulizer pressure at 3.0 bar, dry gas flow at 12.0 L min^{-1}, and dry gas temperature at 280 °C. Chromatograms were smoothed with a Gaussian function using Compass DataAnalysis 4.2 SR2 software (Bruker Daltonics GmbH, Bremen, Germany). Examples of ESI-mass spectra are provided in Fig S2. For the sake of simplicity, product analysis was focused on dominating products in the DP3 – DP6 range. Even numbered products (DP4 & DP6) were dominant, as expected.[18]

LC-MS analysis of PASC oxidation products

Oxidation of PASC was assessed using liquid chromatography and mass spectroscopy (LC-MS). 5 µL supernatant from the reaction mixture was injected onto a Hypercarb column (150 mm × 2.1 mm; 3 µm, Thermo Fischer Scientific, Sunnyvale, CA, USA). The chromatography was performed on the same instrument as described above and operated as inspired by[22], specifically at 0.4 mL min^{-1} at 70°C with a two-eluent system consisting of eluent A, 0.1 µM NaCl in water and eluent B, acetonitrile,. The elution was performed as follows: 0-1 min, isocratic, 100% A; 1–15 min, linear gradient to 50% A, 50% B; hereafter directly to 15–22, isocratic regeneration with 20% A, 80% B, and followed directly by 22–32 min isocratic equilibration at 100% A. The electrospray was operated in positive ultra-scan mode with target mass settings of 600 *m/z*. Other instrument settings and data handling were identical to those described above.

LC-MS analysis of phenolic profiles

The phenolic profiles of the biomass and laccase reaction supernatants were assessed by LC-MS. Supernatants of either untreated 5% w/v birch wood, 10% w/v organosolv lignin or laccase reaction supernatants before and after solid phase extraction were injected onto a Hypersil Gold Phenyl column (150 mm × 2.1 mm; 3 µm, Thermo Fisher Scientific, Waltham, MA, USA). The chromatography was performed on the same system as described above, operated at 0.4 mL min^{-1} and 40 °C, with a three-eluent system: eluent A, 0.1% formic acid in water, eluent B, acetonitrile and eluent C, water. The elution was performed as follows: 0 min, 10% A, 0% B, 90% C; 0–15 min linear gradient to 10% A, 90% B, 0% C; hereafter going directly for 15–20 min to isocratic regeneration at 10% A, 90% B, 0% C followed by 20–25 min, isocratic equilibration with

10% A, 0% B, 90% C. A diode array detector was placed inline prior to the MS detector and data was collected in the spectrum ranging from 190-700 nm. The electrospray was operated in negative full-scan mode with target mass settings of 200 *m/z*. A scan range from 50 to 2200 *m/z* was selected and the spray settings were identical to those described above.

Results and discussion

Hydrogen peroxide formation after laccase oxidation of lignin

Fig. 1a shows that oxidation of birch wood with four different laccases originating from *Trametes versicolor* (Tv), *Ganoderma lucidum* (Gl), *Myceliophthora thermophilia* (Mt) and *Amycolatopsis sp. 75iv2* (Slac) led to production of hydrogen peroxide. The concentrations of H_2O_2 reached 12-20 µM and maximum levels were reached within the first three hours of the reaction. The H_2O_2 formation differed between the four enzymes and these differences are most likely related to different levels of activity of the laccases on this particular substrate. Fig. 1A also shows that the birch wood substrate contains an intrinsic amount of H_2O_2 and that control experiments with heat-inactivated laccases showed no effects on this background level. Variation of the enzyme dosage (Fig. 1b) showed a clear dependence between H_2O_2 formation and enzyme dosage, signifying that the H_2O_2 formation indeed is a result of laccase action. Laccase reactions without substrate did not show any hydrogen peroxide formation (data in Table S1). After a certain reaction period (> 3 hours), the concentration of H_2O_2 started to decrease which may be due to decomposition, for example caused by the presence of trace levels of metals in the biomass.

Fig. 1. H_2O_2 formation during incubation of 5 % (w/v) birch wood with various laccases. Panel a shows the time course of H_2O_2 formation during a 6 hours incubation with four different laccases in a reaction volume of 250 µL. The laccase dosage was: Slac, 0.1 mU; Tv, 3.5 mU; Gl, 8.3 mU; Mt: 19.4 mU. Panel b shows the initial hydrogen peroxide formation rates and how they depend on the laccase dosage. Legends apply to both panel a and b; green triangle, Slac laccase; red triangle, Tv laccase; blue square, Gl laccase; grey circle; Mt laccase; black asteriks, no enzyme added. Open symbols in panel a represent control reactions with heat-inactivated laccases and show no formation of hydrogen peroxide above the inherent background level present in birch wood. Control experiments of laccase reactions with no substrate showed zero levels of hydrogen peroxide and results are shown in Table S1.

The H_2O_2 is most likely formed via a series of events which all start by the generation of semi-stable lignin radicals.[23] After this one possible pathway could be the direct reaction with molecular oxygen (Scheme 1a), similar to the mechanism proposed by Valgimigli *et al*.[24] According to this mechanism, the lignin radical becomes amenable to react with molecular oxygen when the free electron is in the para position. The next step would be intermolecular abstraction of a hydrogen atom, leading to the formation of a hydroperoxyl radical which leaves the lignin molecule and results in an unsaturated bond in the aliphatic chain (Scheme 1a). The hydroperoxyl may abstract yet another hydrogen atom from lignin[25] or it could react with another hydroperoxyl radical to form hydrogen peroxide (Scheme 1b).

Scheme 1. Possible reaction mechanism for hydrogen peroxide formation upon laccase oxidation of lignin. Panel a shows reaction steps where native lignin (1) is oxidized by laccase to form a lignin radical (2). When the unpaired electron is positioned para on the phenol the radical is prone to attack from oxygen (3) and may form an unstable peroxyl intermediate (4). Intermolecular abstraction of a proton produces a hydroperoxyl radical with concomitant formation of an unsaturated C-C bond in the aliphatic chain (5).[24] Panel b shows two possible reaction routes for the hydroperoxyl radical. 1. Reaction with another hydroperoxyl to form hydrogen peroxide and oxygen 2. Abstraction of a proton from lignin by hydroperoxyl, leading to the formation of hydrogen peroxide and a new lignin radical.[25]

LPMO reactions with H_2O_2 from laccase oxidation of lignin

The formation of hydrogen peroxide after laccase oxidation also occurs when a processed organosolv lignin is the substrate (Table 1). It is worth noticing that the levels of hydrogen peroxide formed after laccase oxidation of both birch wood and organosolv are similar (Fig. 2), despite the fact that the reactions with organosolv lignin (10% w/v; 94 % Klason lignin) contained much more lignin than the reactions with birch wood (5% w/v; approx. 20% Klason lignin[26]). The latter indicates that the availability of laccase accessible phenols in native birch wood is much higher than in this particular type of processed lignin.

Table 1. Hydrogen peroxide formation after incubation of organosolv lignin with various laccases. The table shows hydrogen peroxide concentrations after one hour of incubation and the values are the average of triplicate determinations. The lowest row shows the inherent background level of hydrogen peroxide present in the organosolv lignin.

Laccase	H_2O_2 [µM]
Mt	20.8 +/- 4.4
Tv	26.1 +/- 0.6
Gl	19.6 +/- 1.8
Slac	19.0 +/- 0.2
Organosolv lignin	5.2 +/- 0.5

In order to verify that the levels of hydrogen peroxide formed in these laccase reactions are biologically significant we incubated the supernatants of the laccase reactions with a C1-oxidizing, chitin-active LPMO known as CBP21[18] in the presence of an LPMO substrate (β-chitin) and a small (2 µM) amount of ascorbic acid ensuring the initial reduction of the LPMO. After removing the major part of soluble components (possibly phenols) from the supernatants by solid phase extraction (see below for further discussion), the supernatants were indeed capable of driving LPMO-catalyzed oxidation of β-chitin to a similar extent as reactions driven by mM amounts of ascorbic acid (Fig. 2). A control reaction with externally added hydrogen peroxide at a level similar to that achieved in reactions with laccase supernatants (12.5 µM) resulted in comparable CBP21 activity (Fig. 2). Other control experiments (Table S2, Fig. S3 & S4) showed that LPMO activity was inhibited by (H_2O_2-consuming) catalase, did not occur when adding supernatants from reactions without added laccase or

with heat-inactivated laccase, and was dependent on the presence of CBP21. Thus, it is clear that the ability of the supernatant to drive the LPMO reaction depends on the laccase-mediated generation of H_2O_2.

Fig. 2. LC-MS chromatograms showing oxidized products generated upon incubation of β-chitin with CBP21. Panel a shows oxidized products (DP3-DP6) generated in reactions containing either ascorbic acid alone (2 mM or 2 μM), or 2 μM ascorbic acid and H_2O_2 (12.5 μM), or supernatants from 1 hour reactions of organosolv lignin with GI, Tv, Mt or Slac laccase. All reactions containing laccase reaction supernatants also contain 2 μM ascorbic acid (final concentration). The right side column shows the actual measured concentration of H_2O_2 in each reaction supernatant after solid phase extraction. Note that the final concentrations of H_2O_2 at the start of the LPMO reaction equaled 75 % of this value. The inset in panel a shows the effect of reducing the amount of Tv supernatant by 50 %. Panel b shows data for an almost identical set of reactions, the only difference being that the substrate in the laccase reactions was birch wood. The peaks labeled DP3 – DP6 represent C1-oxidized chito-oligosaccharides. Traces are depicted with a slight time offset to increase readability and display extracted ion chromatograms of *m/z*-values corresponding to: DP3ox (grey trace), DP4ox (blue trace), D5ox (green trace) and DP6ox (red trace). See supplementary fig S2 for exact observed *m/z*-values, as well as MS and MS2 spectra. Note the differences in signal intensities (and scaling of the Y-axis) between panels a and b.

H_2O_2-driven catalysis by LPMOs requires an initial reduction of Cu(II) to Cu(I) in the LPMO, after which the enzyme can catalyse multiple reactions as long as hydrogen peroxide and substrate are present.[12,27] Fig. 2 shows that the amounts of LPMO products vary between reactions and this variation is to some extent correlated with varying hydrogen peroxide concentrations in the reaction supernatants. A dose-response experiment with the Tv laccase reaction supernatant showed that reduction of the amount of added supernatant indeed led to reduced generation of LPMO products (Fig. 2a, insert). Comparison of signal intensities in panels a and b of Fig. 2 shows that supernatants from laccase reactions with organosolv lignin generated more LPMO products compared to supernatants from laccase reactions with birch wood, despite similar concentrations of hydrogen peroxide formed. These differences may relate to the extent of non-LPMO related decomposition of hydrogen peroxide happening, for example due to the presence of trace metals or remaining reactive organic compounds.

The laccase oxidation reaction is inherently dependent on the presence of oxygen. LPMOs may also use oxygen as electron acceptor, either directly, or indirectly, via prior formation of H_2O_2 in the reaction mixture.[12,13] Such O_2-driven LPMO action would, however require mM amounts of externally added reductant, i.e. 1000-fold more than what was used here. Control experiments where the LPMO reactions with supernatants from the (aerobic) laccase reactions were made anaerobic showed similar product levels as the reactions depicted in Fig. 2 (Fig S5). This confirms that in the reactions with laccase supernatants, hydrogen peroxide is the main oxidizing agent responsible for fuelling the LPMO reaction.

For the laccase reaction supernatants to be able to drive LPMO reactions they needed to be subjected to hydrophobic solid phase extraction. This process step resulted in a decrease in UV signal in the low UV range (from 230 to 400 nm) indicative of the removal of small aromatic and/or phenolic compounds (Fig 3). Simple profiling by reverse phase LC-UV-MS corroborated the assumption that the immediate laccase reaction supernatants contain aromatic compounds (Fig. S6). Without the initial clean up by solid phase extraction, the CBP21 reactions were vastly inhibited and showed no release of oxidized products in any of the reactions with laccase treated samples. The inhibitory effect was tested by combining uncleaned laccase reaction supernatants with a fixed amount of hydrogen peroxide (12.5 μM) in CBP21 experiments and these showed no oxidation products from β-chitin (control experiment C7, Table S2, Figs. S3 & S4). Further work is needed to unravel the nature of this inhibitory effect, which likely is due to side reactions that consume either the reductant or the hydrogen peroxide.

Fig. 3. UV spectra of laccase reaction supernatants before and after solid phase extraction. Solid lines show UV spectral absorbance of reaction supernatants before solid phase extraction, while dashed lines show UV spectral absorbance of the supernatants after solid phase extraction ("clean"). Panels a and b show supernatants from reactions with organosolv lignin and birch wood, respectively. Color coding is according to legends provided in the panels. Black traces show UV spectral absorbance of lignin substrate supernatants without laccase treatment. More UV profiles obtained by LC-MS analysis of laccase reaction supernatants before and after solid phase extraction are provided in Fig. S6 and corroborates the removal of UV-absorbing compounds by solid phase extraction.

In another control experiment, supernatants from either birch wood or organosolv lignin were treated with laccases to investigate if soluble lignin components could play a role. These laccase-treated supernatants could not drive the LPMO reaction (control experiment C8; Table S2, Figs. S3 & S4). Hence, it does not seem plausible that small phenolic compounds present in the laccase reaction supernatants are contributing to LPMO activity in our reaction set-ups, as it was previously suggested.[28] In light of the present results, one may speculate that the effects observed in this previous study[28] were in fact caused by the presence of hydrogen peroxide in supernatant from laccase reactions. On the other hand, it has been shown that insoluble lignin itself in combination with soluble low molecular lignin can act as an electron transfer system and activate LPMOs.[29] Westereng *et al.*[29] showed that radicals are inherently present in insoluble wheat straw lignin and that the presence of low molecular weight lignin allows for the transfer of electrons to LPMO reactions. Whether or not hydrogen peroxide was present and partly responsible for the effects observed in this previous studies is unknown and was not addressed at the time, because the study was conducted prior to the discovery that hydrogen peroxide is a co-substrate for LPMOs.

Laccases are abundant in microorganisms that degrade lignocellulose and hence it is relevant to investigate if the laccase reaction supernatants can also boost the activity of an

LPMO active on cellulose. *Nc*LPMO9C originating from *Neurospora crassa* oxidizes amorphous cellulose into short C4-oxidized oligosaccharides (Fig. S1).[30] Figure 4 shows that incubation of this LPMO with PASC, ascorbic acid, and supernatants from the laccase reactions indeed led to formation of oxidized products. Optimal concentrations of hydrogen peroxide and reductant needs differ considerably between LPMO enzymes.[12] For the *Nc*LPMO9C reactions a higher level of reductant (50 µM ascorbic acid) compared to CBP21 was necessary. These 50 µM ascorbic acid lead to a small degree of oxidative reaction in itself (Fig. 4). There may be a slightly negative effect of the laccase reaction supernatants on the performance of *Nc*LPMO9C, which can be observed when comparing the reaction with externally added hydrogen peroxide (12.5 µM) to the reactions with laccase supernatants, which did not show higher product yields despite higher H_2O_2 concentrations of approximately 19-26 µM.

Fig. 4. LC-MS chromatograms showing products generated by NcLPMO9C in reactions with PASC. The chromatograms show products generated in reactions containing ascorbic acid alone (1 mM or 50 µM), 50 µM ascorbic acid and H_2O_2 (12.5 µM), or 50 µM ascorbic acid and supernatants from 1 hour reactions of organosolv lignin with the Gl, Tv, Mt or Slac laccases. The right side column shows the actual measured concentration of H_2O_2 in each reaction supernatant after solid phase extraction. Note that the final concentrations of H_2O_2 at the start of the LPMO reaction equaled 75 % of this value. The two main peaks represent C4-oxidized cello-oligosaccharides of DP3 (Glc4gemGlc2) and, to a lesser extent, DP2 (Glc4gemGlc).The traces are depicted with a slight time offset to increase readability and display extracted ion chromatograms of *m/z*-values corresponding to DP3 (grey trace) and DP2 (green trace). Mass spectra below the chromatogram show the major peaks appearing at retention time 10.6 min in full scan mode, corresponding to grey trace (DP3), and show *m/z* 543.12 and 525.12, which correspond to the sodium adducts of the gemdiol and ketone of the trimeric oxidation product, respectively. MS2 fragmentation spectra of *m/z* 543.12 and 525.12 are shown below the full scan spectrum.

Control experiments (Table S3, Fig. S7), which were slightly different from those done for the CBP21 reactions, underpinned features of the laccase-lignin-LPMO interplay. Like for the CBP21 reaction, the laccase reaction supernatants needed to be cleaned by solid phase extraction. The control reactions also substantiated the inhibitory effects that seemed apparent in Fig. 4. Addition of uncleaned supernatants from the laccase reactions reduced product formation in all reactions, including a standard reaction with 1 mM ascorbic acid (control experiments C2-C4, Fig. S7). Also catalase reduced product formation in reactions with supernatants from all the laccase reactions (control experiment C1, Fig. S7). All in all, while the interplay of the laccase-lignin-LPMO system with other compounds in the reactions remains somewhat enigmatic, the results obtained with *Nc*LPMO9C substantiate the notion that the ability of laccases to drive LPMO reaction is due to lignin-mediated generation of H_2O_2.

Hydrogen peroxide is a common denominator in many redox processes in lignocellulose degradation, including both enzymatic and chemical degradation.[13,31] In white-rot fungi, where laccases are most abundant, manganese and lignin peroxidases use hydrogen peroxide as oxidants in the breakdown of lignin, whereas LPMOs use hydrogen peroxide to degrade polysaccharides. It is a known fact that white-rot fungi and other microorganisms that degrade lignocellulose have GMC oxidoreductases (glucose-methanol-choline oxidases) that produce extracellular hydrogen peroxide from various substrates.[32,33] However, the substrates for these oxidases are small compounds like mono-/oligomeric hexoses and small aromatic alcohols, components that become available as the degradation of both polysaccharides and lignin progresses. Hence the contribution of hydrogen peroxide resulting from laccase oxidation reactions may be to initiate the overall degradation process because laccases are capable of attacking intact lignocellulose surfaces, as demonstrated here by the studies with untreated birch wood. Laccases may therefore indeed be tightly connected to lignin depolymerisation, without necessarily being the direct catalytic causal agent itself. Previous studies have shown that laccases are highly expressed during fungal colonization of substrate and during early stages of mycelium growth.[16,34] Of note, the observation that laccases can improve the efficiency of commercial cellulose blends in cellulose degradation[20,35] may be due to production on hydrogen peroxide, which could lead to improved activity of the LPMOs in these blends.[36]

As suggested in the H_2O_2 formation pathways depicted in Scheme 1, laccase oxidation and subsequent release of a hydroperoxyl radical would cause the lignin structure to become less saturated compared to the native lignin, with the formation of a double bond in the aliphatic chain. These pathways do not include a plausible route towards bond cleavage as a result of laccase oxidation. However, the pacification of the lignin radicals by reaction with oxygen implies that a potential polymerization reaction is eliminated. Whether the oxidized, less saturated lignin structure is more prone to bond cleavage compared to the native structure, is not known.

Conclusions

Hydrogen peroxide is formed simultaneously with laccase oxidation of lignin, most likely as a result of reactions involving lignin radicals and molecular oxygen. This seems to be a general phenomenon, as formation of hydrogen peroxide occurred in reactions with all four different laccases enzymes tested in this study and for both tested lignin-containing substrates. Laccase induced formation of hydrogen peroxide has never been reported before and unravels new pathways for interplay between various enzymes and substrate components during enzymatic conversion of lignocellulose. Formation of hydrogen peroxide formation suggests a new possible role for laccases in lignocellulose degradation, namely the fuelling of other hydrogen peroxide-dependent reactions like those catalysed by lignin peroxidases or LPMOs.

Conflicts of interest

There are no conflicts to declare.

Acknowledgements

We thank Prof. Mogens Larsen Andersen, Copenhagen University for his advice on reaction mechanisms and Prof. Lindsay Eltis and staff from The University of British Columbia, Canada for providing the bacterial laccase from *Amycolatopsis sp. 75iv2*. We also thank Novozymes (Bagsværd, Denmark) for donating the *Myceliophthora thermophila* laccase. This study was supported by the Danish Council for Independent Research (Project ref. DFF-4184-00355), by the PhD Program at the Technical University of Denmark and by the Research Council of Norway through grants 262853 & 269408.

References

1 A. J. Ragauskas, G. T. Beckham, M. J. Biddy, R. Chandra, F. Chen, M. F. Davis, B. H. Davison, R. a Dixon, P. Gilna, M. Keller, P. Langan, A. K. Naskar, J. N. Saddler, T. J. Tschaplinski, G. a Tuskan and C. E. Wyman, *Science*, 2014, **344**, 1246843.

2 Z. Sun, B. Fridrich, A. De Santi, S. Elangovan and K. Barta, *Chem. Rev.*, 2018, **118**, 614–678.

3 W. Schutyser, T. Renders, S. Van Den Bosch, S. F. Koelewijn, G. T. Beckham and B. F. Sels, *Chem. Soc. Rev.*, 2018, **47**, 852–908.

4 D. M. Mate and M. Alcalde, *Microb. Biotechnol.*, 2017, **10**, 1457–1467.

5 S. M. Jones and E. I. Solomon, *Cell. Mol. Life Sci.*, 2015, **72**, 869–83.

6 C. Eggert, U. Temp and K.-E. L. Eriksson, *FEBS Lett.*, 1997, **407**, 89–92.

7 L. Munk, A. K. Sitarz, D. C. Kalyani, J. D. Mikkelsen and A. S. Meyer, *Biotechnol. Adv.*, 2015, **33**, 13–24.

8 L. Munk, M. L. Andersen and A. S. Meyer, *Enzyme Microb. Technol.*, 2017, **106**, 88–96.

9 C. Steelink, *J. Am. Chem. Soc.*, 1965, **87**, 2056–2057.

10 R. W. Rex, *Nature*, 1960, **188**, 1185–1186.

11 T. K. Lundell, M. R. Mäkelä and K. Hildén, *J. Basic Microbiol.*, 2010, **50**, 5–20.

12 B. Bissaro, Å. K. Røhr, G. Müller, P. Chylenski, M. Skaugen, Z. Forsberg, S. J. Horn, G. Vaaje-Kolstad and V. G. H. Eijsink, *Nat. Chem. Biol.*, 2017, **13**, 1123–1128.

13 B. Bissaro, A. Várnai, Å. K. Røhr and V. G. H. Eijsink, *Microbiol. Mol. Biol. Rev.*, 2018, **82**, e00029-18.

14 J. Carro, A. Serrano, P. Ferreira and A. T. Martínez, in *Microbial Enzymes in Bioconversions of Biomass*, ed. V. K. Gupta, Springer, International Publishing Switzerland, Biofuel an., 2016, pp. 301–322.

15 A. Levasseur, E. Drula, V. Lombard, P. M. Coutinho and B. Henrissat, *Biotechnol. Biofuels*, 2013, **6**, 41.

16 S. Zhou, J. Zhang, F. Ma, C. Tang, Q. Tang and X. Zhang, *PLoS One*, 2018, **13**, 1–20.

17 H. Suzuki, J. MacDonald, K. Syed, A. Salamov, C. Hori, A. Aerts, B. Henrissat, A. Wiebenga, P. A. VanKuyk, K. Barry, E. Lindquist, K. LaButti, A. Lapidus, S. Lucas, P. Coutinho, Y. Gong, M. Samejima, R. Mahadevan, M. Abou-Zaid, R. P. de Vries, K. Igarashi, J. S. Yadav, I. V Grigoriev and E. R. Master, *BMC Genomics*, 2012, **13**, 444.

18 G. Vaaje-Kolstad, B. Westereng, S. J. Horn, Z. Liu, H. Zhai, M. Sorlie and V. G. H. Eijsink, *Science (80-.).*, 2010, **330**, 219–222.

19 Y. Kojima, A. Várnai, T. Ishida, N. Sunagawa, D. M. Petrovic, K. Igarashi, J. Jellison, B. Goodell, G. Alfredsen, B. Westereng, V. G. H. Eijsink and M. Yoshida, *Appl. Environ. Microbiol.*, 2016, **82**, 6557–6572.

20 A. K. Sitarz, J. D. Mikkelsen, P. Højrup and A. S. Meyer, *Enzyme Microb. Technol.*, 2013, **53**, 378–385.

21 I. R. Silva, D. M. Larsen, A. S. Meyer and J. D. Mikkelsen, *Enzyme Microb. Technol.*, 2011, **49**, 160–6.

22 B. Westereng, M. Ø. Arntzen, F. L. Aachmann, A. Várnai, V. G. Eijsink and J. W. Agger, *J. Chromatogr. A*, 2016, **1445**, 46–54.

23 V. Perna, J. W. Agger, M. L. Andersen, J. Holck and A. S. Meyer, *ACS Sustain. Chem. Eng.* **Submitted**

24 L. Valgimigli, R. Amorati, M. G. Fumo, G. A. DiLabio, G. F. Pedulli, K. U. Ingold and D. A. Pratt, *J. Org. Chem.*, 2008, **73**, 1830–1841.

25 A. N. Kapich, K. A. Jensen and K. E. Hammel, *FEBS Lett.*, 1999, **461**, 115–119.

26 C. Mosbech, J. Holck, A. S. Meyer and J. W. Agger, *Biotechnol. Biofuels*, 2018, **11**, 1–9.

27 S. Kuusk, R. Kont, P. Kuusk, A. Heering, M. Sørlie, B. Bissaro, V. G. H. Eijsink and P. Väljamäe, *J. Biol. Chem.*, 2018, **294**, jbc.RA118.006196.

28 L. Brenelli, F. M. Squina, C. Felby and D. Cannella, *Biotechnol. Biofuels*, 2018, **11**, 10.

29 B. Westereng, D. Cannella, J. Wittrup Agger, H. Jørgensen, M. Larsen Andersen, V. G. H. Eijsink and C. Felby, *Sci. Rep.*, 2015, **5**, 18561.

30 T. Isaksen, B. Westereng, F. L. Aachmann, J. W. Agger, D. Kracher, R. Kittl, R. Ludwig, D. Haltrich, V. G. H. Eijsink and S. J. Horn, *J. Biol. Chem.*, , DOI:10.1074/jbc.M113.530196.

31 S. M. Cragg, G. T. Beckham, N. C. Bruce, T. D. Bugg, D. L. Distel, P. Dupree, A. G. Etxabe, B. S. Goodell, J. Jellison, J. E. McGeehan, S. J. McQueen-Mason, K. Schnorr, P. H. Walton, J. E. Watts and M. Zimmer, *Curr. Opin. Chem. Biol.*, 2015, **29**, 108–119.

32 P. Ferreira, J. Carro, A. Serrano and A. T. Martinez, *Mycologia*, 2015, **107**, 1105–1119.

33 P. Ferreira, A. Hernández-Ortega, B. Herguedas, J. Rencoret, A. Gutiérrez, M. J. Martínez, J. Jiménez-Barbero, M. Medina and A. T. Martínez, *Biochem. J.*, 2010, **425**, 585–93.

34 V. Elisashvili, E. Kachlishvili and M. Penninckx, *Acta Microbiol. Immunol. Hung.*, 2008, **55**, 157–168.

35 R. Singh, J. Hu, M. R. Regner, J. W. Round, J. Ralph, J. N. Saddler and L. D. Eltis, *Sci. Rep.*, 2017, **7**, 1–13.

36 G. Müller, P. Chylenski, B. Bissaro, V. G. H. Eijsink and S. J. Horn, *Biotechnol. Biofuels*, 2018, **11**, 1–17.

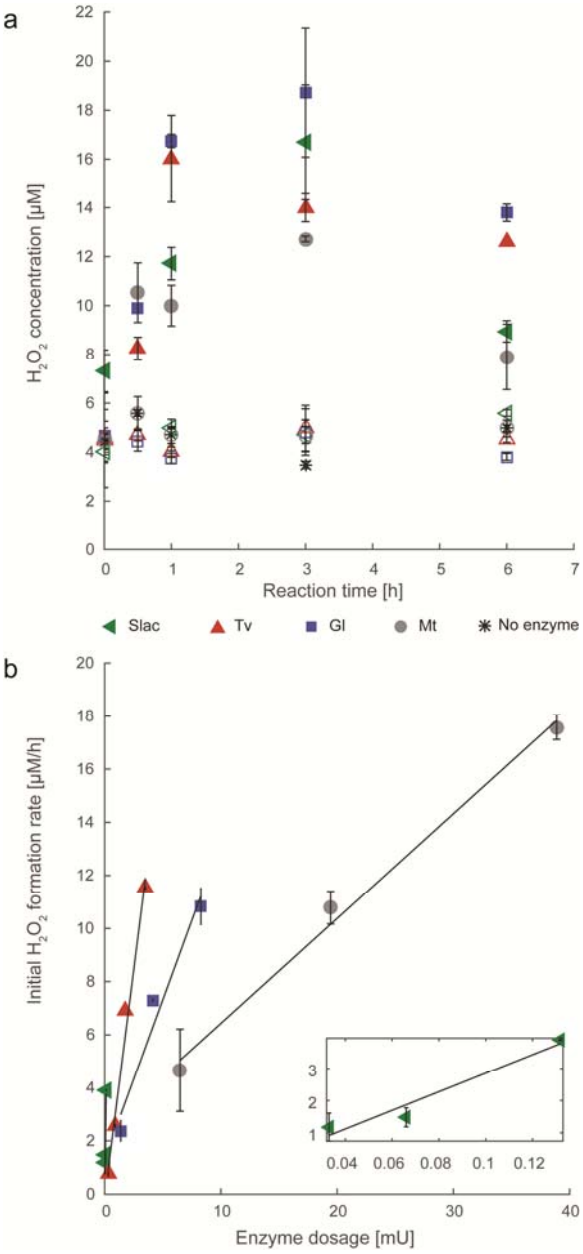

Figure 1

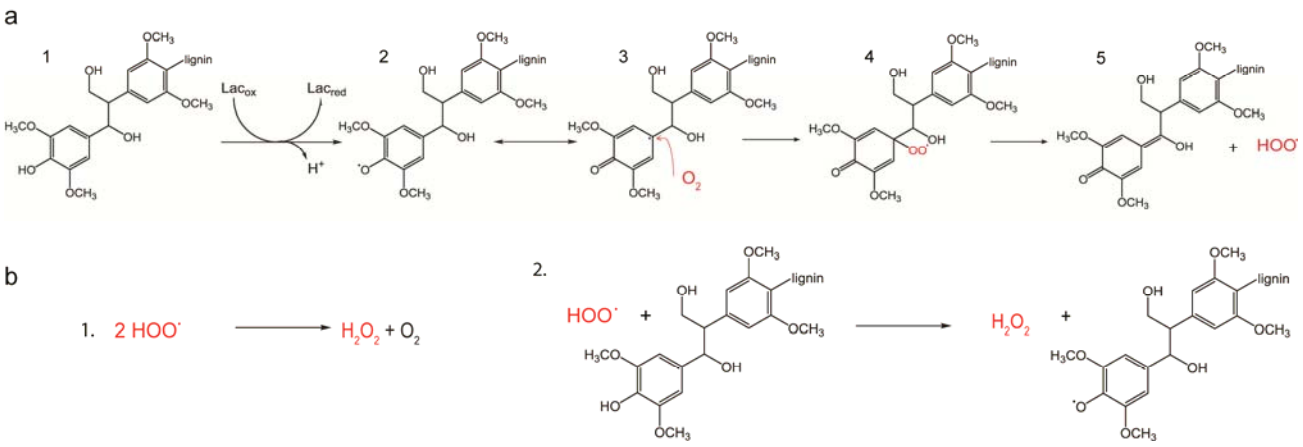
a
1
2
3
4
5
lignin
OCH3
OH
H3CO
HO
Lacox
Lacred
H+
O2
HOO·
b
1. 2 HOO·
H2O2 + O2
2.
HOO·
+
H2O2

Scheme 1

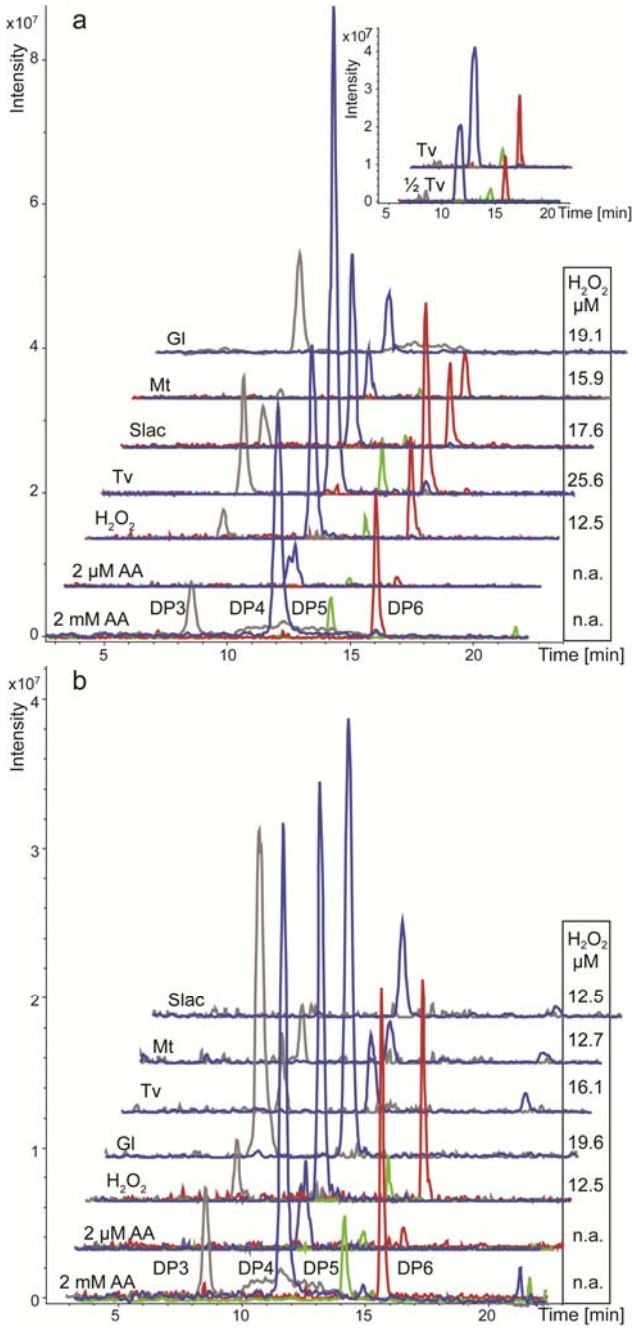

Figure 2

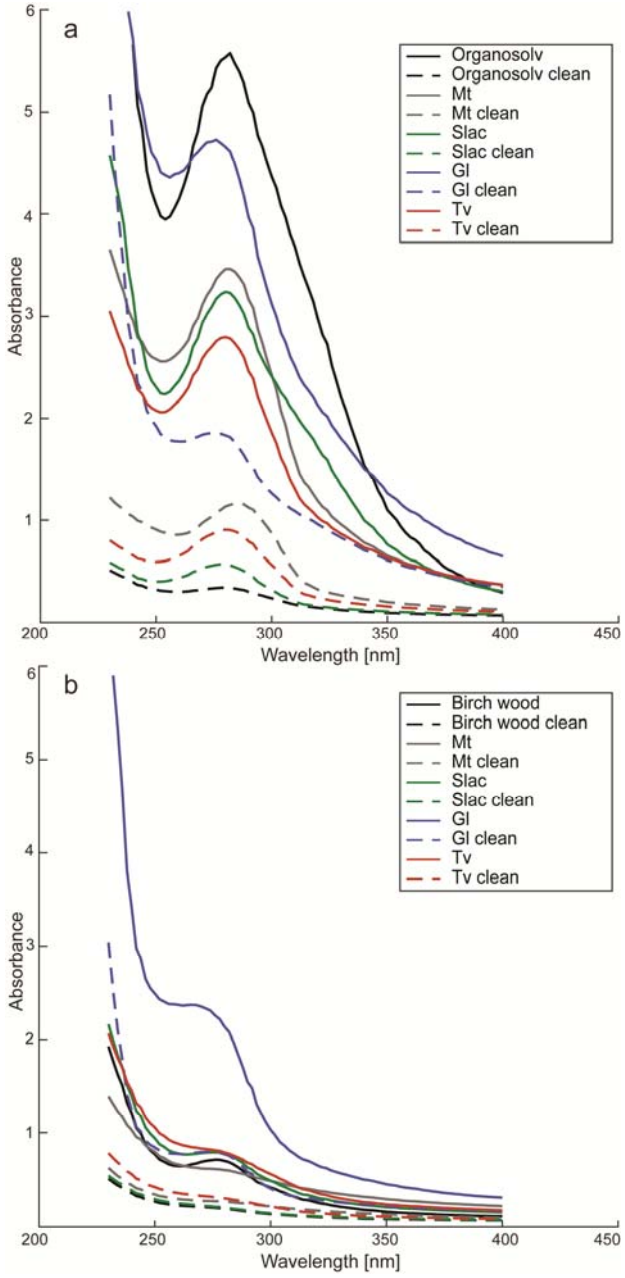
a
Organosolv
Organosolv clean
Mt
Mt clean
Slac
Slac clean
Gl
Gl clean
Tv
Tv clean
Absorbance
Wavelength [nm]
b
Birch wood
Birch wood clean
Mt
Mt clean
Slac
Slac clean
Gl
Gl clean
Tv
Tv clean
Absorbance
Wavelength [nm]

Figure 3

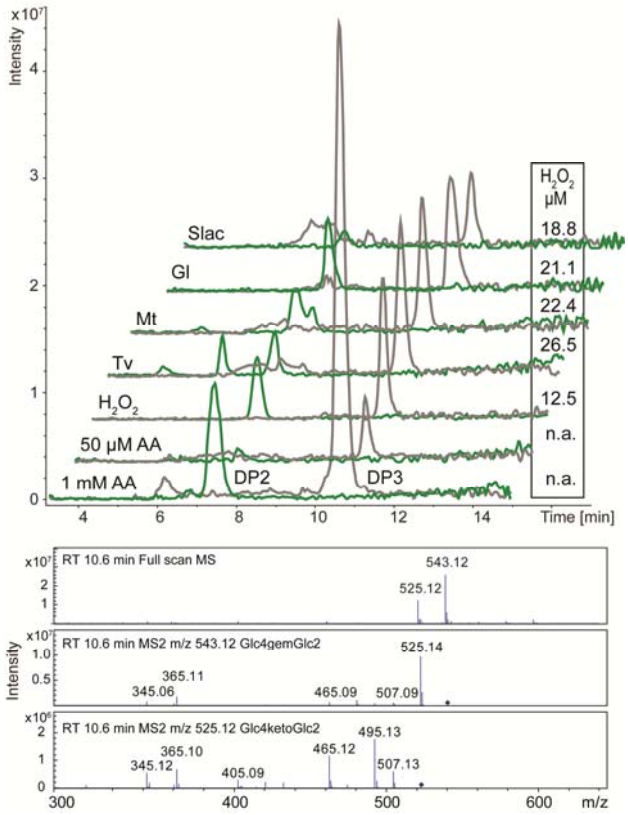

Figure 4

Supplementary information

Laccase catalyzed oxidation of lignin induces production of H_2O_2

Valentina Perna[a], Anne S. Meyer[a], Jesper Holck[a], Vincent Eijsink[b] and Jane Wittrup Agger*[a]

[a]Technical University of Denmark, Department of Biotechnology and Biomedicine, Søltofts Plads 221, DK-2800 Kgs. Lyngby

[b]Norwegian University of Life Sciences, Faculty of Chemistry, Chr. M. Falsensvei 1, NO-1430 Ås.

* Corresponding author

Contents

Supplementary Figure S1: MALDI-ToF analysis of standard reactions of CBP21 and *Nc*LPMO9C

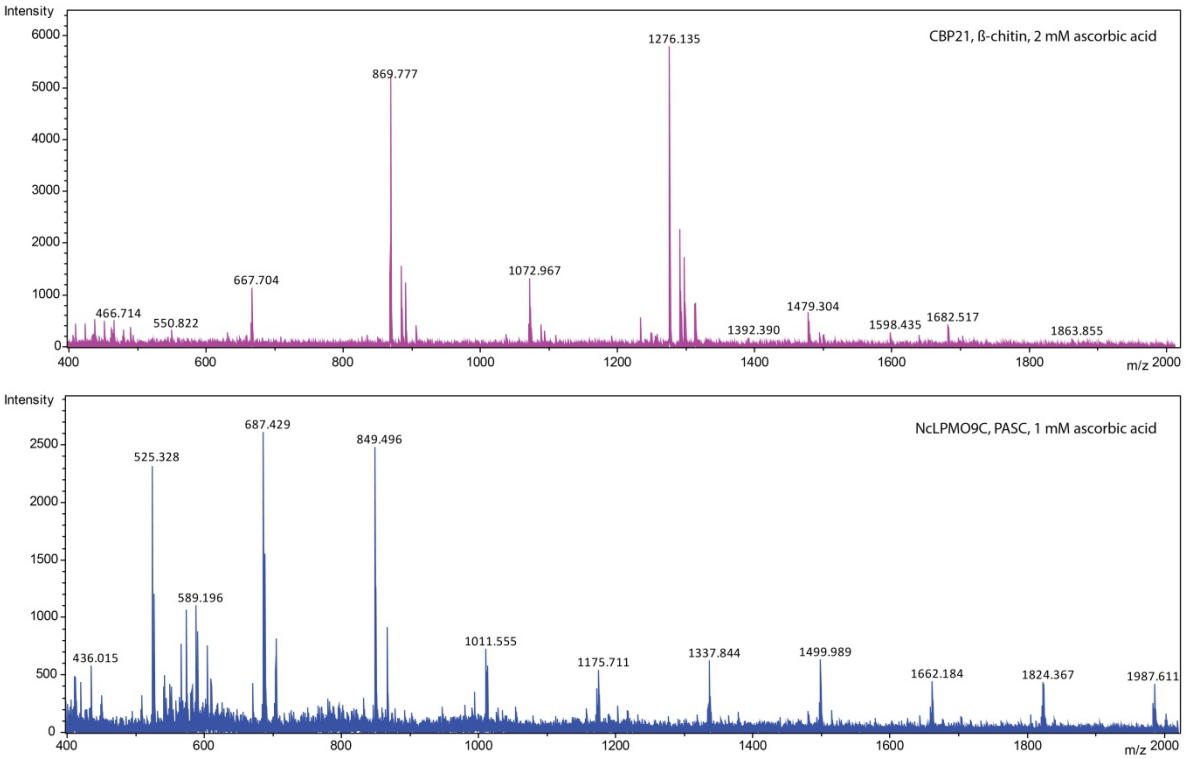

Fig S1: MALDI-ToF analysis of standard reactions with CBP21, β-chitin and 2 mM ascorbic acid (top panel) and *Nc*LPMO9C, PASC and 1 mM ascorbic acid (lower panel). The top panel shows predominately masses corresponding to the sodium adducts of the aldonic form of C1-oxidized chito-oligosaccharides DP4 (*m/z* 869.777) and DP6 (*m/z* 1276.135) and to a lesser extent DP5 (*m/z* 1072.967). The lower panel shows masses corresponding to the sodium adduct of the ketone form of C4-oxidized cello-oligosaccharides ranging from DP3 to DP12 with an overrepresentation of shorter DPs (DP3 *m/z* 525.328, DP4 *m/z* 687.429 and DP5 *m/z* 849.496). The ketone form of C4-oxidized products is commonly dominating in MALDI-ToF analysis, rather than the hydrated gemdiol form, because the analysis occurs without the presence of water.

Supplementary Figure S2: LC-MS spectra and fragmentations of CBP21 reaction products

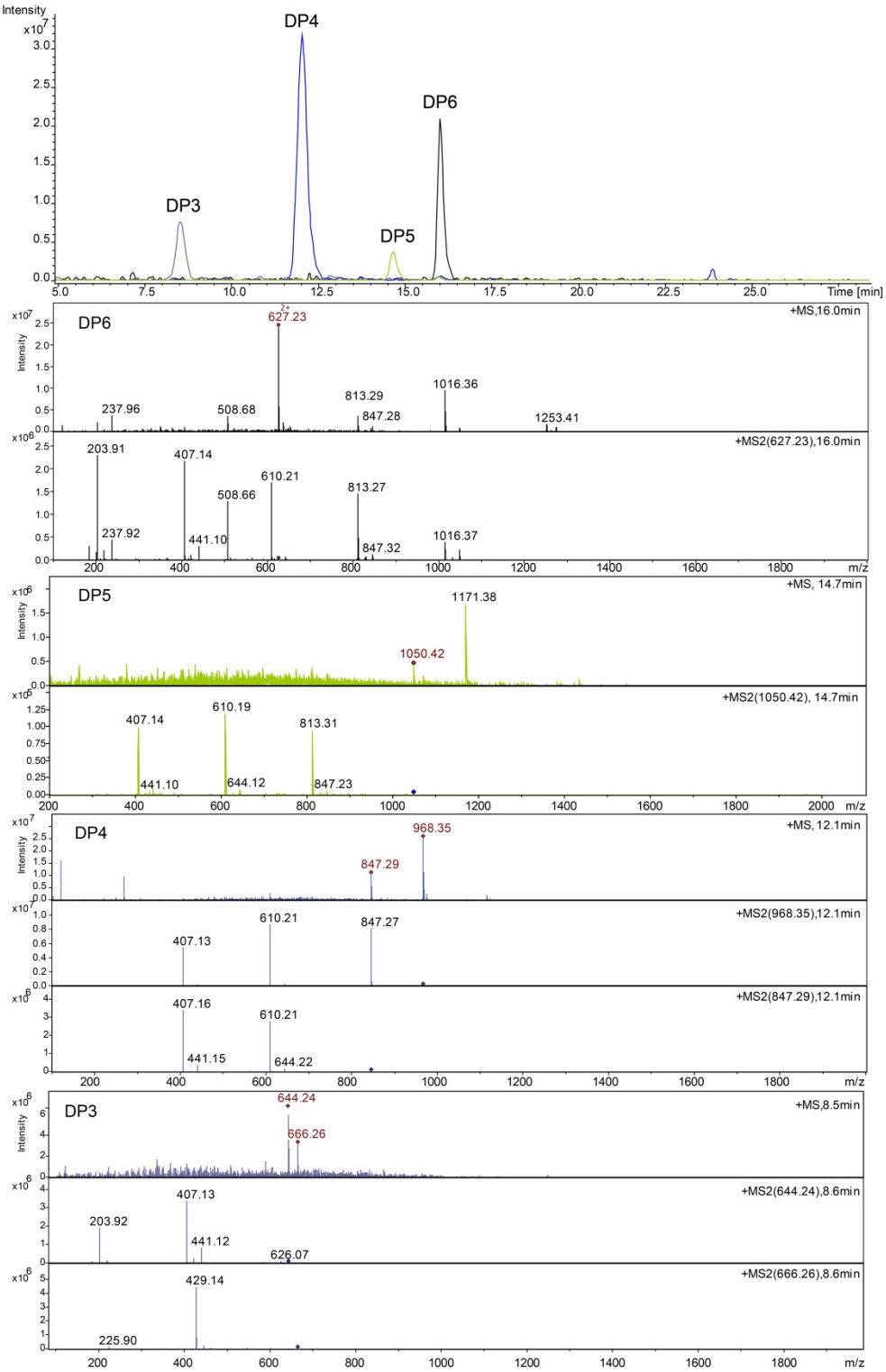

Fig S2: Extracted ion chromatograms of LC-MS analysis of reaction products generated upon incubation of CBP21 with β-chitin in the presence of 2 mM ascorbic acid. Traces are sums of the following observed masses of oxidized chito-oligosaccharides in their hydrated form: DP3; *m/z* 644.24 ($[M+H]^+$) + *m/z* 666.26 ($[M+Na]^+$), DP4; *m/z* 847.29 ($[M+H]^+$) + *m/z* 968.35 ($[M+H]^+$ + Tris), DP5; *m/z* 1050.42 ($[M+H]^+$) + *m/z* 1171.38 ($[M+H]^+$ + Tris), DP6; *m/z* 627.23 ($[M+H]^{2+}$). Below the chromatograms: MS and MS2 spectra of

each product peak. Retention times and relevant *m/z* values are listed in the upper right corner of each spectrum. The fragmentations show characteristic losses for oxidized chito-oligosaccharides, e.g. loss of 237 amu corresponding to the loss of the oxidized monosaccharide unit, and additional losses of 203 amu corresponding to the loss of dehydrated monosaccharide units from the oxidized end. Please note that the DP6 product appears as a double charged adduct hence giving rise to a slightly different fragmentation pattern compared to the other products.

Supplementary Table S1: H_2O_2 concentration during laccase oxidation of birch wood

Incubation time (h)		Laccase				
	Sample content	Tv (3.5 mU)	Gl (8.5 mU)	Mt (19.4 mU)	Slac (0.13 mU)	No enzyme
		H_2O_2 concentration (µM)				
0	Birch wood	4.5 ± 1.9	4.6 ± 1.1	4.5 ± 0.2	7.3 ± 0.9	4.4±0.8
	Birch wood + heat inactivated enzyme	4.6 ± 0.4	4.7 ± 0.1	4.4 ± 0.0	4.0 ± 0.1	n.a.
	No substrate	0.0	0.1	0.1	0.0	n.a.
0.5	Birch wood	8.2 ± 0.5	9.9	10.5 ± 1.2	-	5.6±0.7
	Birch wood + heat inactivated enzyme	4.7 ± 0.2	4.5 ± 0.4	5.6 ± 0.1	-	n.a.
	No substrate	0.0	0.0	0.1	0.1	n.a.
1	Birch wood	16.0 ± 1.8	16.7 ± 0.3	10.0 ± 1.8	11.7 ± 0.7	4.7±0.6
	Birch wood + heat inactivated enzyme	4.0 ± 0.2	3.7 ± 0.2	4.7 ± 0.3	4.7 ± 0.3	n.a.
	No substrate	0.1	0.0	0.0	0.1	n.a.
3	Birch wood	14.0 ± 0.6	18.7 ± 2.6	12.7 ± 0.1	16.7 ± 2.4	3.5±0.2
	Birch wood + heat inactivated enzyme	5.0 ± 0.9	4.8 ± 0.9	4.7 ± 0.6	5.6 ± 0.1	n.a.
	No substrate	0.0	0.0	0.0	0.0	n.a.
6	Birch wood	12.6	13.8 ± 0.4	7.9 ± 1.3	8.9 ± 0.4	5.0±0.3
	Birch wood + heat inactivated enzyme	4.5 ± 0.1	3.8 ± 0.1	5.0 ± 0.2	3.5 ± 0.3	n.a.
	No substrate	0.0	0.1	0.0	0.0	n.a.

Table S1: Table overview of H_2O_2 concentrations measured after time studies of laccase oxidation of lignin as presented in Fig. 1 in the main text. H_2O_2 concentration was measured after laccase oxidation of birch wood with active laccase enzyme (named Birch wood), with birch wood and heat inactivated laccase (named Birch wood + heat inactivated enzyme) and in the absence of birch wood substrate but with active laccase (named No substrate). The results are given as average values of triplicate determinations with standard deviations for reactions including substrate. Experiments only including laccase and no substrate were performed as single determinations. n.a.: not applicable; - : no data

Supplementary Table S2: Overview of control experiment in relation to CBP21 reactions

	Cleaned supernatant			Uncleaned supernatant	Cleaned supernatant	β-chitin	CBP21	AA	Catalase	H_2O_2	Product formation
	with Laccase	without Laccase	with heat inactivated Laccase	No solid phase extraction	without insoluble biomass	5 mg/mL	1 µM	2 µM	39 µg/mL	12.5 µM	
C1	+					+		+			No
C2		+				+	+	+			No
C3	+					+	+	+	+		Reduced for Tv, none for Mt, Gl and Slac
C4			+			+	+	+			No
C5						+	+	+			No
C6				+		+	+	+			No
C7				+		+	+	+		+	No
C8					+	+	+	+			No

All control experiments above are performed for all four laccases tested in this study (Tv, Mt, Gl and Slac) on both birch wood and organosolv lignin. Hence one set of control experiments exist for each laccase on each substrate. (Fig. S3 + S4)

C1: Solid phase extracted laccase reaction supernatant incubated with β-chitin and 2 µM ascorbic acid (AA)

C2: Solid phase extracted reaction supernatant without laccase incubated with CBP21, β-chitin and 2 µM ascorbic acid (AA)

C3: Solid phase extracted laccase reaction supernatant incubated with CBP21, β-chitin, 2 µM ascorbic acid (AA) and catalase

C4: Solid phase extracted laccase reaction supernatant with heat inactivated laccase preparation incubated with CBP21, β-chitin and 2 µM ascorbic acid (AA)

C5: CBP21 incubated with β-chitin and 2 µM ascorbic acid (AA)

C6: Laccase reaction supernatant incubated with CBP21, β-chitin and 2 µM ascorbic acid (AA)

C7: Laccase reaction supernatant incubated with CBP21, β-chitin, 2 µM ascorbic acid (AA) and H_2O_2

C8: Laccase reaction supernatant after treatment of the soluble biomass alone (no insoluble biomass) incubated with CBP21, β-chitin and 2 µM ascorbic acid (AA)

Supplementary Figure S3: Control experiments with CBP21 and laccase reaction supernatants from organosolv lignin

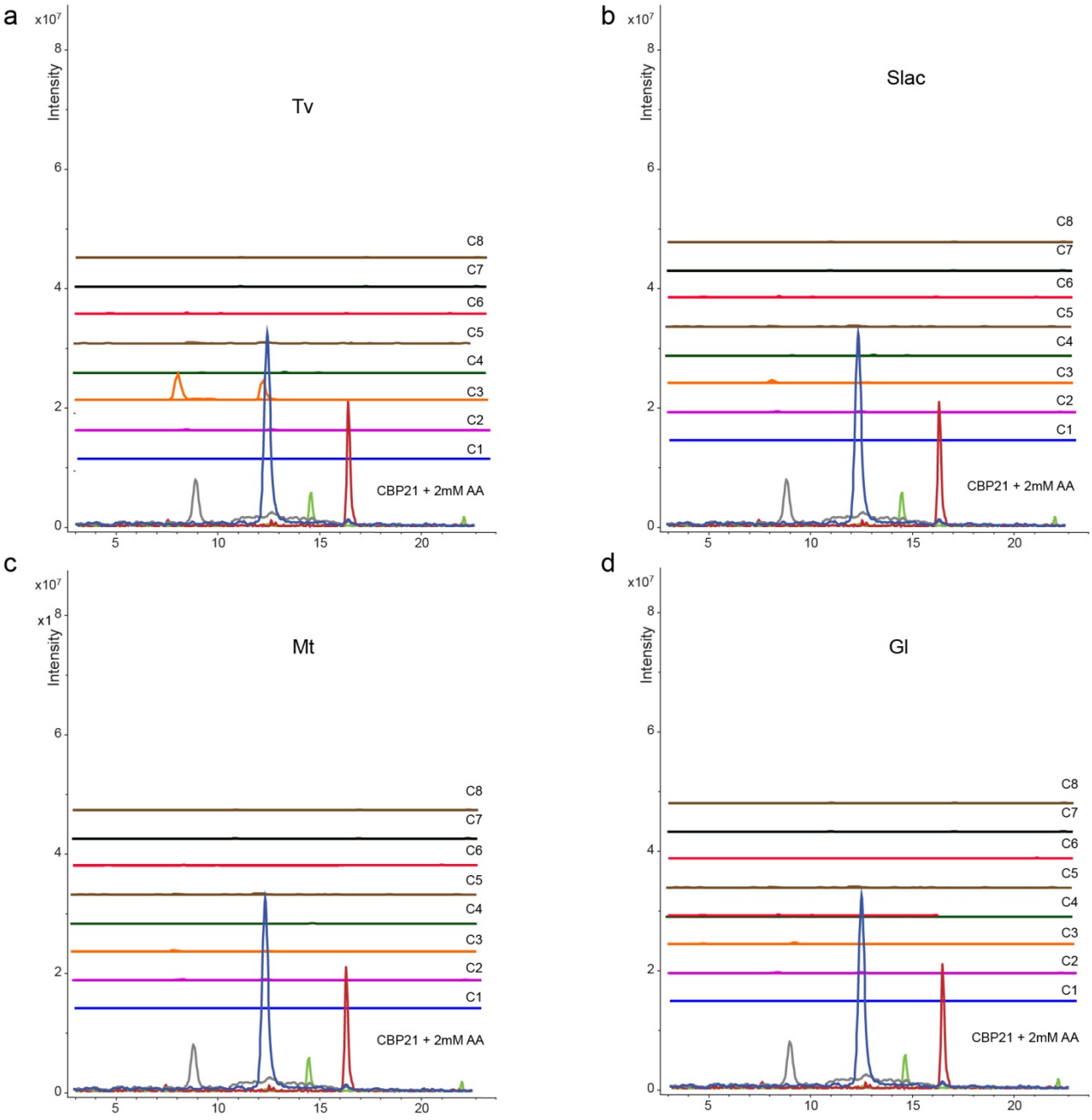

Fig S3: LC-MS chromatograms showing results from control experiments of CBP21 reaction on β-chitin after 24 h incubation with laccase oxidized organosolv lignin supernatant. The naming of control experiment is in accordance with Table S2. The four different panels show control experiments with the four different laccases, namely Panel a: Tv laccase, panel b: Slac laccase, panel c: Mt laccase and panel d: Gl laccase. The four peaks in the chromatogram for the positive control reaction (CBP21 + 2 mM AA) represent DP3ox (grey trace), DP4ox (blue trace), DP5ox (green trace) and DP6ox (red trace). All control reactions (C1-C8) show no product formation by CBP21, except for control experiment C3 incubated with Tv laccase supernatant,

where some products are formed. C3 includes the addition of catalase to the CBP21 reaction and the results indicate that the dosage of catalase may not be high enough to convert all H_2O_2 in that reaction.

Supplementary Figure S4: Control experiments with CBP21 and laccase reaction supernatants from birch wood

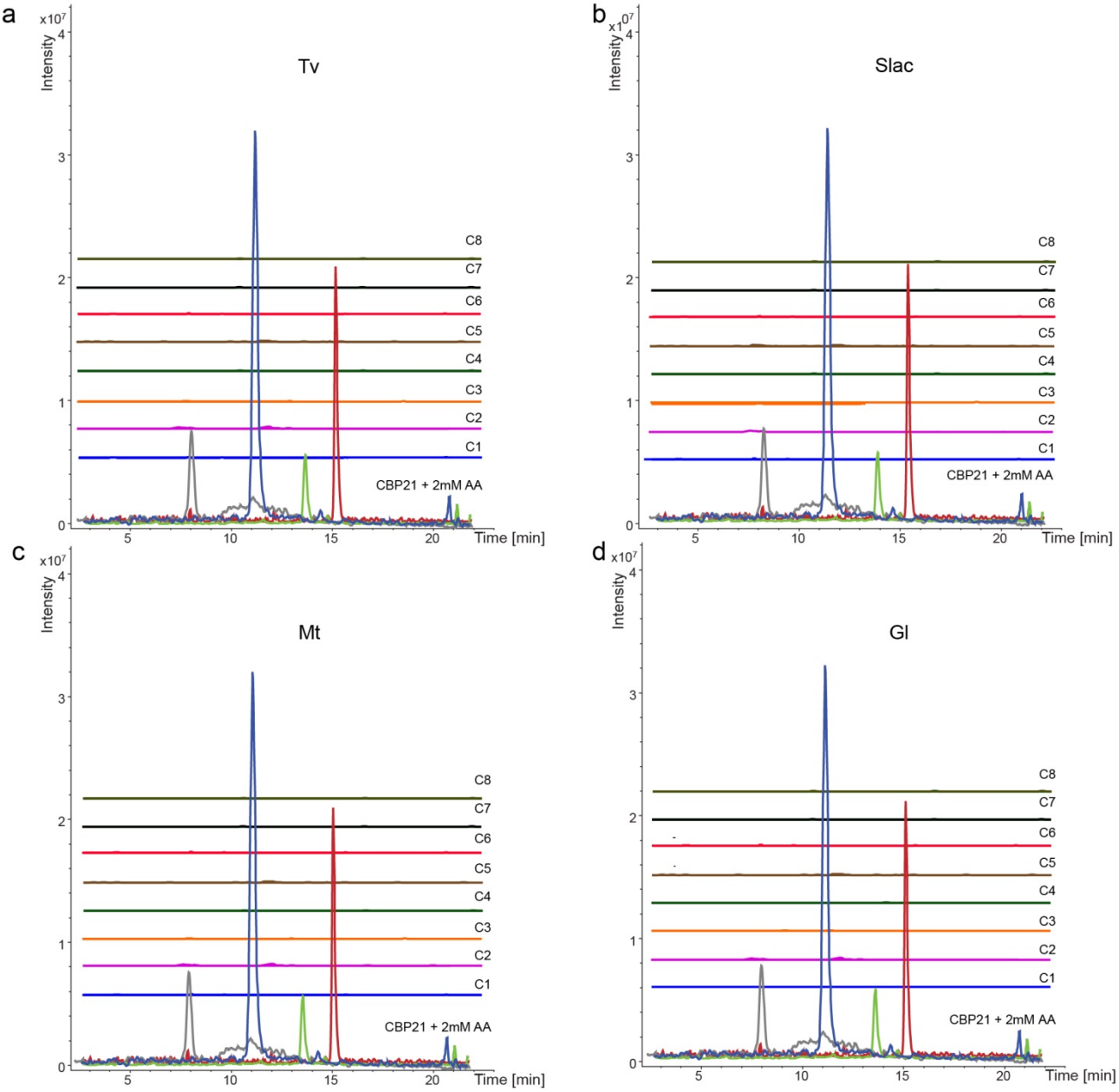

Fig S4: : LC-MS chromatograms showing results from control experiments of CBP21 reaction on β-chitin after 24 h incubation with laccase oxidized birch wood supernatant. The naming of control experiment is in accordance with Table S2. The four different panels show control experiments with the four different laccases, namely Panel a: Tv laccase, panel b: Slac laccase, panel c: Mt laccase and panel d: Gl laccase. The

four peaks in the chromatogram for the positive control reaction (CBP21 + 2 mM AA) represent DP3ox (grey trace), DP4ox (blue trace), DP5ox (green trace) and DP6ox (red trace). All control reactions (C1-C8) show no product formation by CBP21.

Supplementary Figure S5: Anaerobic control experiments with laccase reaction supernatants from *Trametes versicolor* and CBP21

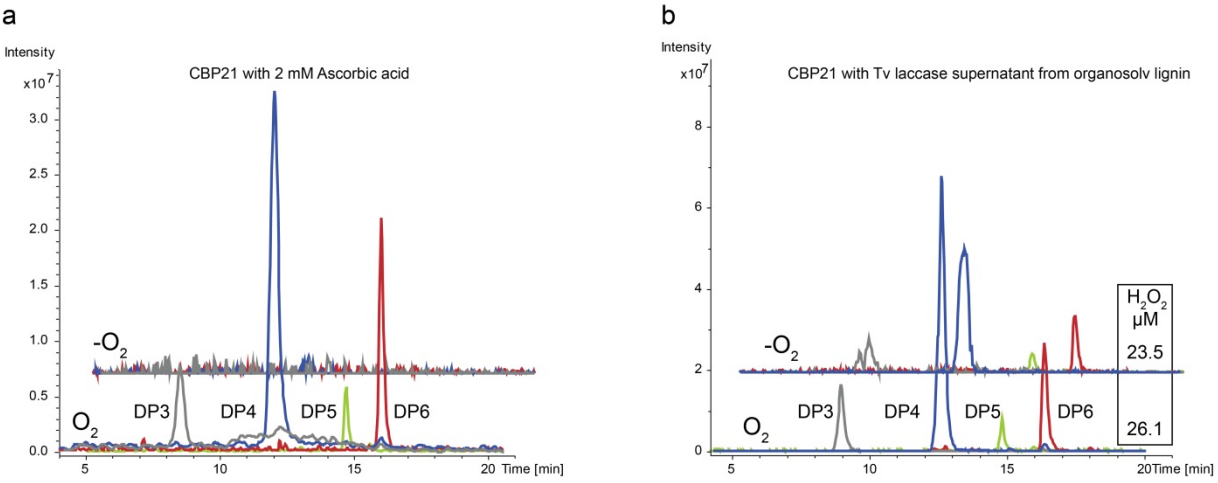

Fig S5: LC-MS chromatograms of CBP21 reactions with and without oxygen. Panel a: CBP21 with 2 mM ascorbic acid with oxygen (lower traces) and without oxygen (upper traces). Panel b: CBP21 with supernatant from a reaction with Tv laccase and organosolv lignin with oxygen (lower traces) and without oxygen (upper traces). Note that the H_2O_2 concentration in the experiment without oxygen is lower compared to the experiment with oxygen, however this difference is within the generally observed standard deviation for the H_2O_2 measurements after laccase oxidation (as reported in Table S1). The results show that action of CBP21 is not occurring in the case where the reaction is running on ascorbic acid alone and no oxygen is present (panel a). On the contrary, similar extent of product formation is observed for CBP21 action in experiments where the Tv laccase supernatants are added both in the presence or absence of oxygen (panel b).

Supplementary Figure S6.1-4: Phenolic profiling by (RP)-LC-MS of laccase reaction supernatants before and after cleaning with solid phase extraction

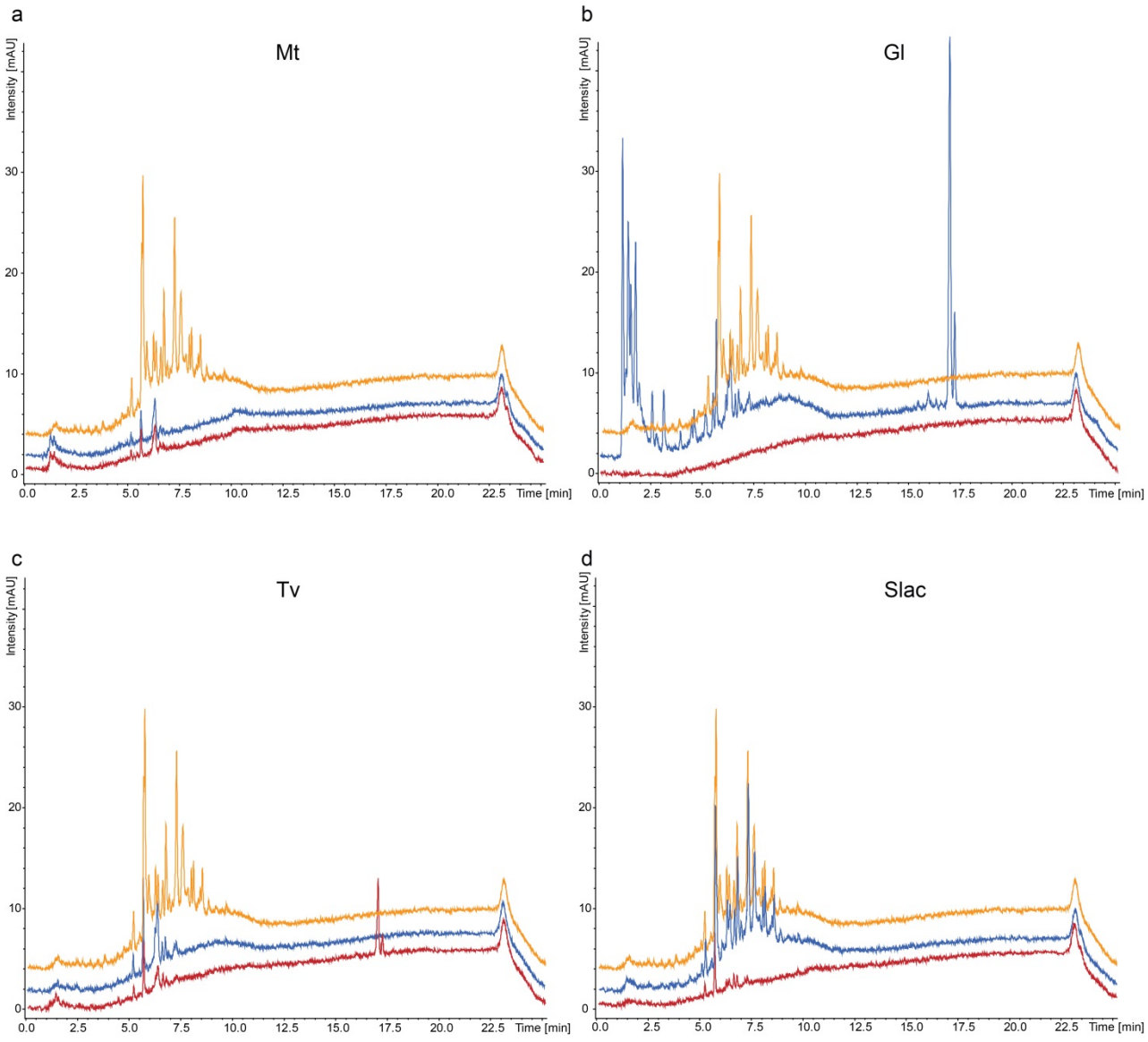

Fig S6.1: LC-UV profiles at 280 nm of supernatants from 1-hour reactions of laccases with birch wood, before and after solid phase extraction. Panel a-d represent laccase treatment of the entire birch wood slurry with Mt, Gl, Tv and Slac laccase, respectively. In all cases, the orange traces show UV profiles of supernatants before laccase treatment, blue traces show UV profiles of supernatants after laccase treatment and red traces show UV profiles of supernatants after laccase treatment and solid phase extraction. In all solid phase extraction procedures, the eluted volume was identical to the loaded volume, and H_2O_2 spiking tests showed no loss of H_2O_2 in the procedure. The differences observed between UV profiles of supernatants before (orange) and after laccase treatment (blue) are most likely a result of laccases acting on soluble phenols, where the products tend to polymerize and possibly precipitate. Hence the signal intensities in the UV profiles after laccase treatment appear in some cases lower and simplified with respect to peak profile compared to the UV profiles before laccase treatment.

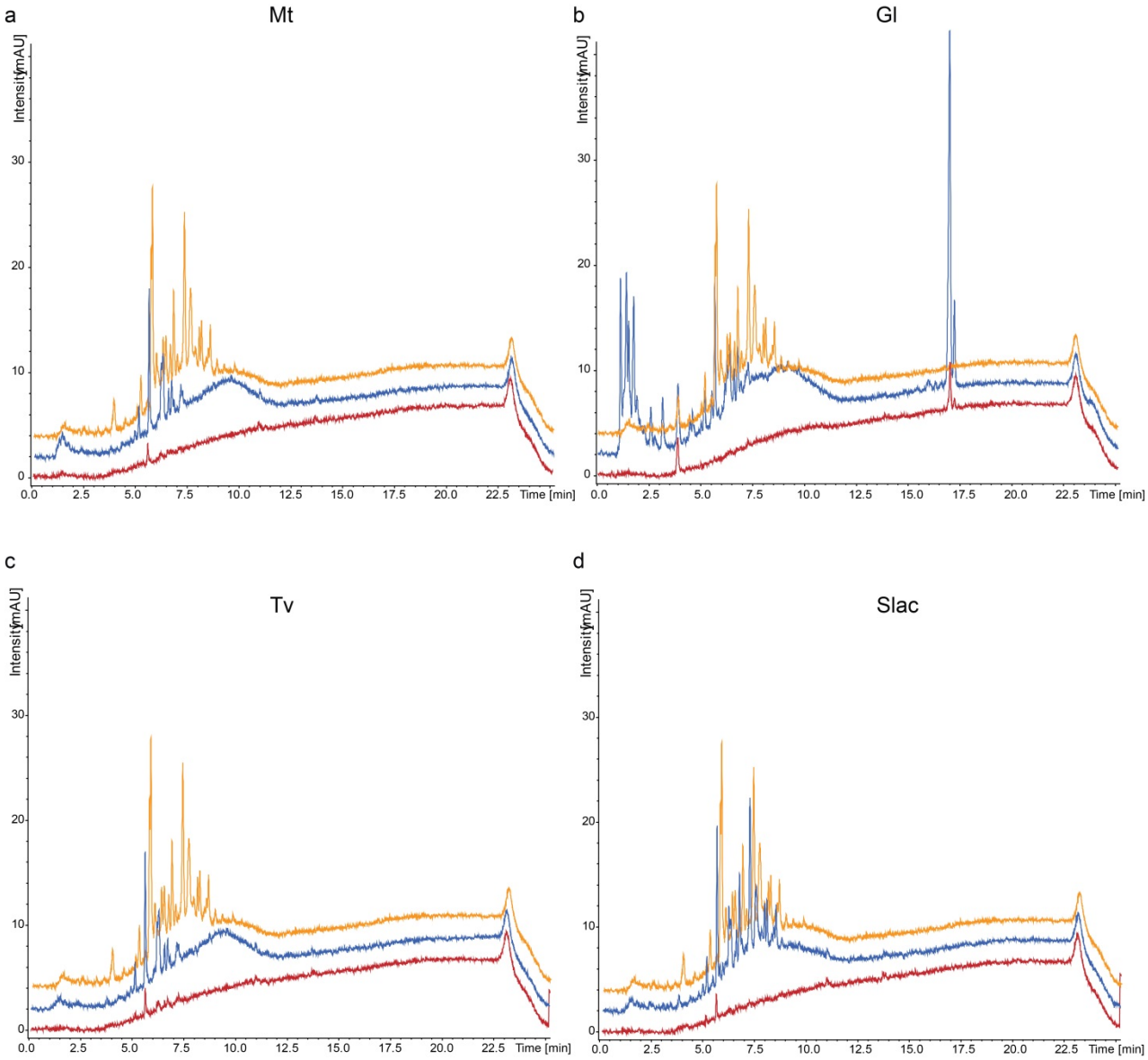

Fig S6.2: LC-UV profiles at 280 nm of supernatants from 1-hour reactions of laccases acting on the soluble parts of birch wood only, before and after solid phase extraction. Panel a-d represent laccase treatment of the birch wood supernatant only with Mt, Gl, Tv and Slac laccase respectively. In all cases, the orange traces show UV profiles of supernatants before laccase treatment, blue traces show UV profiles of supernatants after laccase treatment and red traces show UV profiles of supernatants after laccase treatment and solid phase extraction. In all solid phase extraction procedures, the eluted volume was identical to the loaded volume, and H_2O_2 spiking tests showed no loss of H_2O_2 in the procedure. The differences observed between UV profiles of supernatants before (orange) and after laccase treatment (blue) are most likely a result of laccases acting on soluble phenols, where the products tend to polymerize and possibly precipitate. Hence the signal intensities in the UV profiles after laccase treatment in some cases appear lower and simplified with respect to peak profile compared to the UV profiles before laccase treatment.

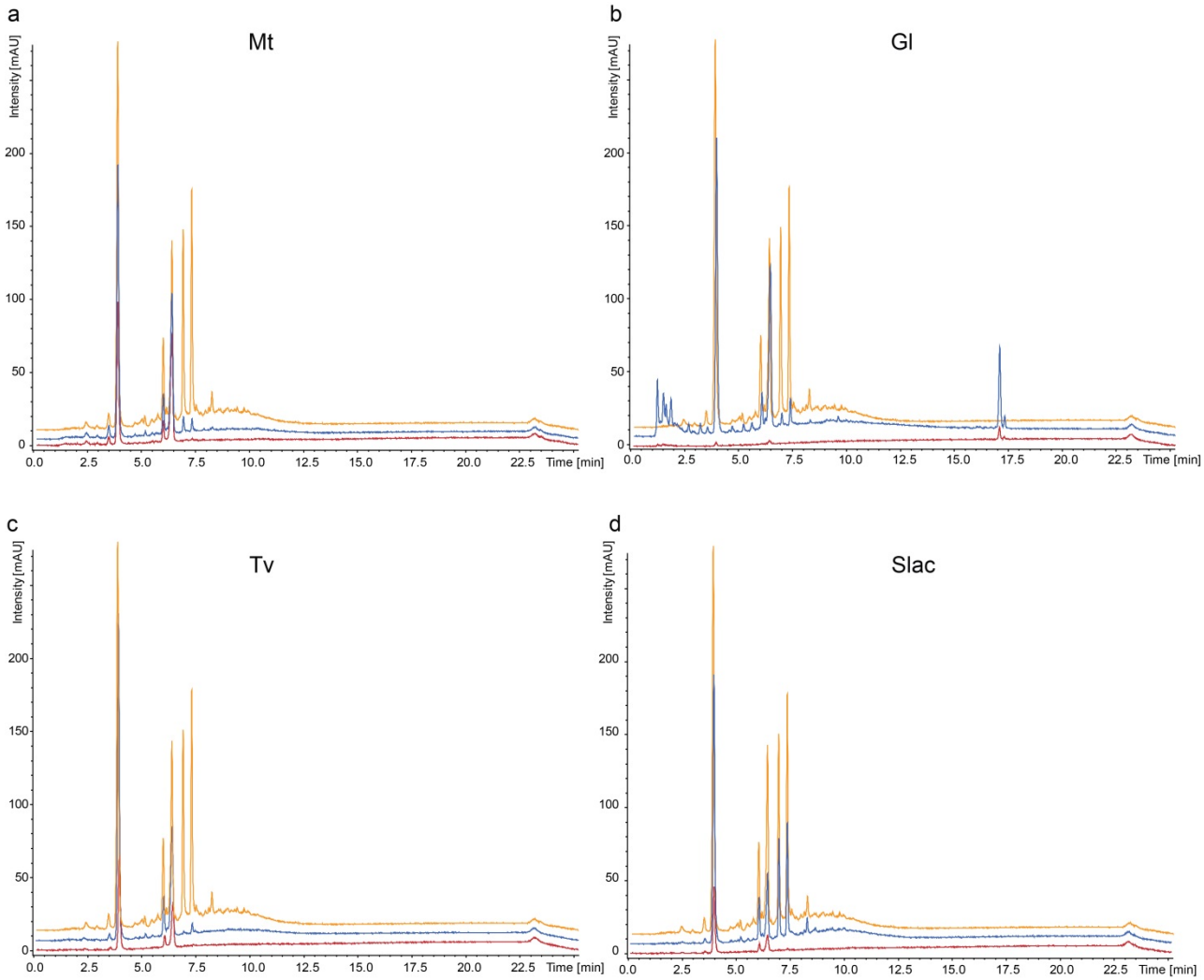

Fig S6.3: LC-UV profiles at 280 nm supernatants from 1-hour reactions of laccases with organosolv lignin, before and after solid phase extraction. Panel a-d represent laccase treatment of the entire organosolv lignin slurry with Mt, Gl, Tv and Slac laccase respectively. In all cases, the orange traces show UV profiles of supernatants before laccase treatment, blue traces show UV profiles of supernatants after laccase treatment and red traces show UV profiles of supernatants after laccase treatment and solid phase extraction. In all solid phase extraction procedures, the eluted volume was identical to the loaded volume, and H_2O_2 spiking tests showed no loss of H_2O_2 in the procedure. The differences observed between UV profiles of supernatants before (orange) and after laccase treatment (blue) are most likely a result of laccases acting on soluble phenols, where the products tend to polymerize and possibly precipitate. Hence the signal intensities in the UV profiles after laccase treatment in some cases appear lower and simplified with respect to peak profile compared to the UV profiles before laccase treatment.

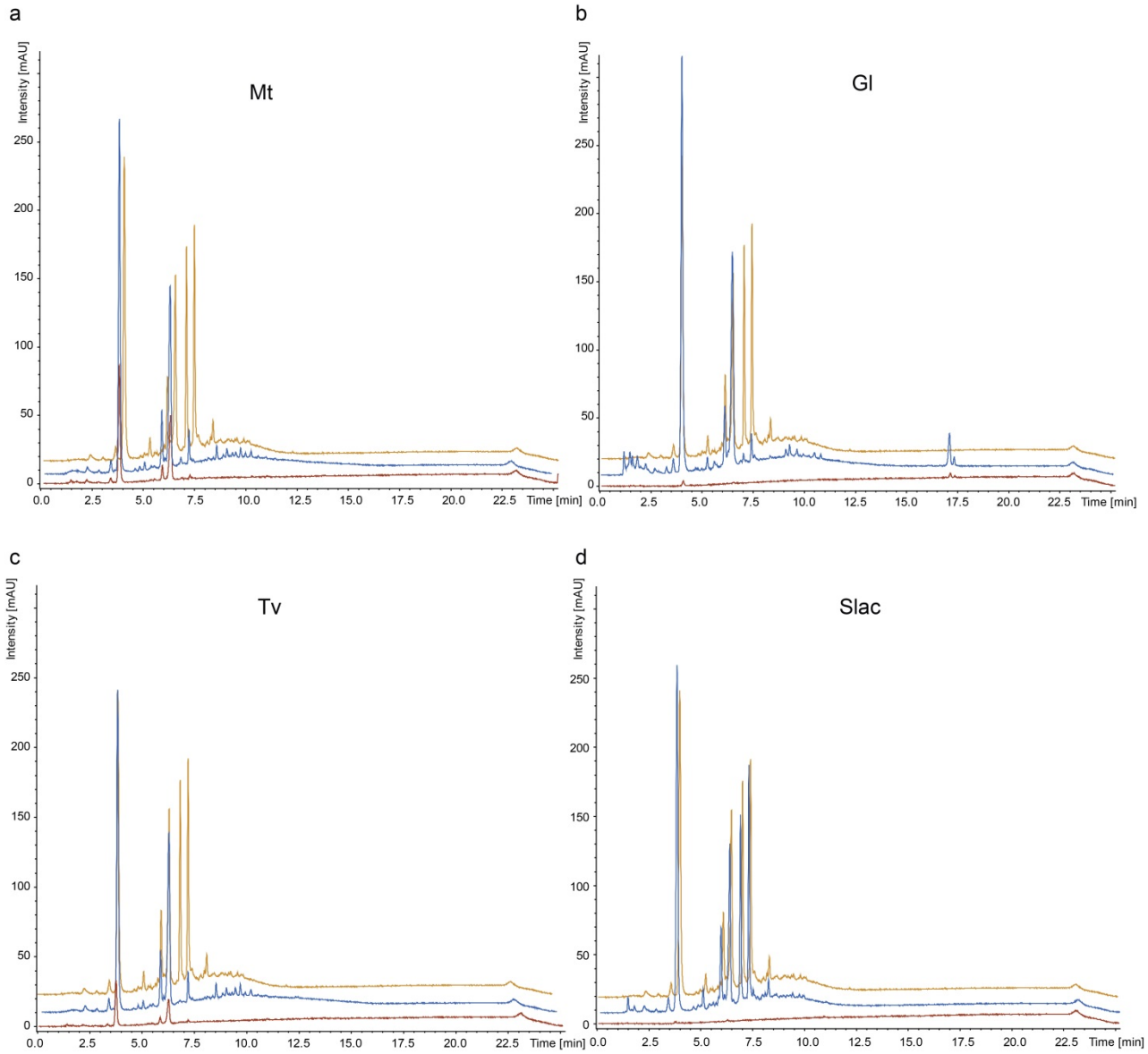

Fig S6.4: LC-UV profiles at 280 nm of supernatants from 1-hour reactions of laccases with organosolv lignin only, before and after solid phase extraction. Panel a-d represent laccase treatment of the supernatant of organosolv lignin only with Mt, Gl, Tv and Slac laccase respectively. In all cases, the orange traces show UV profiles of supernatants before laccase treatment, blue traces show UV profiles of supernatants after laccase treatment and red traces show UV profiles of supernatants after laccase treatment and solid phase extraction. In all solid phase extraction procedures, the eluted volume was identical to the loaded volume, and H_2O_2 spiking tests showed no loss of H_2O_2 in the procedure The differences observed between UV profiles of supernatants before (orange) and after laccase treatment (blue) are most likely a result of laccases acting on soluble phenols, where the products tend to polymerize and possibly precipitate. Hence the signal intensities in the UV profiles after laccase treatment in some cases appear lower and simplified with respect to peak profile compared to the UV profiles before laccase treatment.

Supplementary Table S3: Overview of control experiment in relation to *Nc*LPMO9C reactions

	Cleaned supernatant	Uncleaned supernatant	PASC	*Nc*LPMO9C	AA		Catalase	H_2O_2	Product formation
	with Laccase	with Laccase	5 mg/mL	1 µM	1 mM	50 µM	39 µg/mL	12.5 µM	
C1	+		+	+		+	+		Reduced for Tv, none for Mt, Gl and Slac
C2		+	+	+		+			Reduced
C3		+	+	+		+		+	Reduced
C4		+	+	+	+				Reduced

All control experiments above are performed for all four laccases tested in this study (Tv, Mt, Gl and Slac) on organosolv lignin. Results are presented in Fig. S7.

C1: Solid phase extracted laccase reaction supernatant incubated with *Nc*LPMO9C, PASC, 50 µM ascorbic acid (AA) and catalase

C2: Laccase reaction supernatant (uncleaned) incubated with *Nc*LPMO9C, PASC and 50 µM ascorbic acid (AA)

C3: Laccase reaction supernatant (uncleaned) incubated with *Nc*LPMO9C, PASC, 50 µM ascorbic acid (AA) and 12.5 µM H_2O_2

C4: Laccase reaction supernatant (uncleaned) incubated with *Nc*LPMO9C, PASC, 1 mM ascorbic acid (AA)

Supplementary Figure S7: Control experiments with *Nc*LPMO9C and laccase reaction supernatants from organosolv lignin

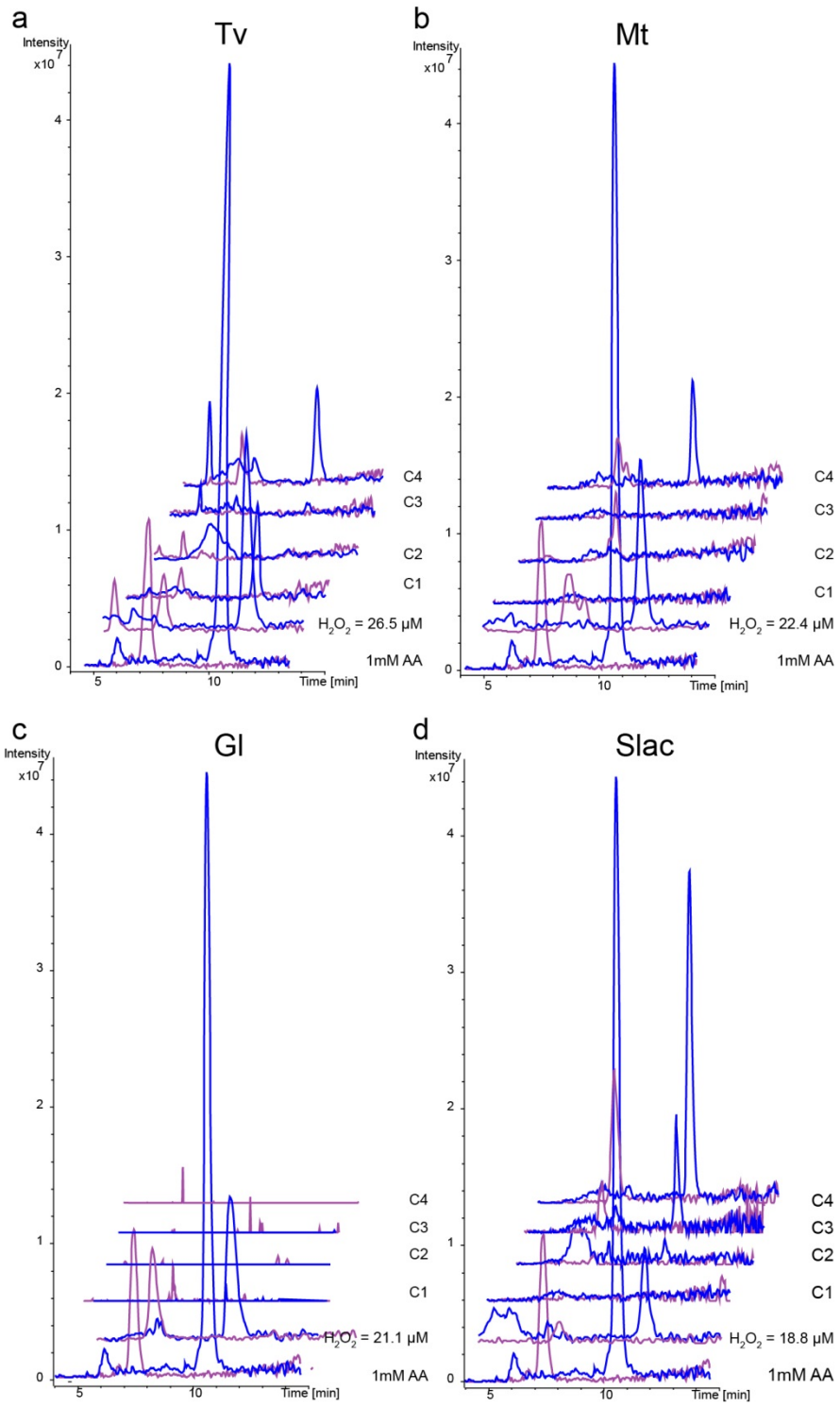

Fig. S7: LC-MS chromatograms showing results from control experiments of *Nc*LPMO9C reaction on PASC incubated with laccase oxidized organosolv lignin supernatant. The naming of control experiment is in accordance with Table S3. The four different panels show control experiments with the four different laccases, namely Panel a: Tv laccase, panel b: Mt laccase, panel c: Gl laccase and panel d: Slac laccase. The

two major peaks in the chromatogram for the positive control reaction (1 mM AA) represent DP2ox (violet trace) and DP3ox (blue trace). For comparison, the cleaned supernatant reactions of each laccase reaction incubated with *Nc*LPMO9C, PASC and 50 µM ascorbic acid from Fig. 4 in the main text are also included here (second lowest set of traces). The results show that except for the reactions containing Tv laccase oxidized supernatant, catalase addition results in no product formation by *Nc*LPMO9C (control C1). The reaction with Tv laccase and catalase shows reduced product formation compared to the reaction without catalase. The control experiments with uncleaned laccase supernatants (controls C2-C4) all show reduced product formation compared to the experiments with cleaned laccase supernatants.